Studies in Fuzziness and Soft Computing

S. R. Kannan
Mark Last
Tzung-Pei Hong
Chun-Hao Chen *Editors*

Fuzzy Mathematical Analysis and Advances in Computational Mathematics

Springer

Studies in Fuzziness and Soft Computing

Volume 419

Series Editor

Janusz Kacprzyk, Systems Research Institute, Polish Academy of Sciences, Warsaw, Poland

The series "Studies in Fuzziness and Soft Computing" contains publications on various topics in the area of soft computing, which include fuzzy sets, rough sets, neural networks, evolutionary computation, probabilistic and evidential reasoning, multi-valued logic, and related fields. The publications within "Studies in Fuzziness and Soft Computing" are primarily monographs and edited volumes. They cover significant recent developments in the field, both of a foundational and applicable character. An important feature of the series is its short publication time and world-wide distribution. This permits a rapid and broad dissemination of research results.

Indexed by SCOPUS, DBLP, WTI Frankfurt eG, zbMATH, SCImago.

All books published in the series are submitted for consideration in Web of Science.

More information about this series at https://link.springer.com/bookseries/2941

S. R. Kannan · Mark Last · Tzung-Pei Hong ·
Chun-Hao Chen
Editors

Fuzzy Mathematical Analysis and Advances in Computational Mathematics

Springer

Editors
S. R. Kannan (Deceased)
Kalapet, India

Tzung-Pei Hong
Department of Computer Science
and Information Engineering
National University of Kaohsiung
Kaohsiung, Taiwan

Mark Last
Department of Software and Information
Systems Engineering
Ben-Gurion University of the Negev
Beersheba, Israel

Chun-Hao Chen
Department of Information and Finance
Mangment
National Taipei University of Technology
Taipei, Taiwan

ISSN 1434-9922 ISSN 1860-0808 (electronic)
Studies in Fuzziness and Soft Computing
ISBN 978-981-19-0470-7 ISBN 978-981-19-0471-4 (eBook)
https://doi.org/10.1007/978-981-19-0471-4

© The Editor(s) (if applicable) and The Author(s), under exclusive license to Springer Nature Singapore Pte Ltd. 2022
This work is subject to copyright. All rights are solely and exclusively licensed by the Publisher, whether the whole or part of the material is concerned, specifically the rights of translation, reprinting, reuse of illustrations, recitation, broadcasting, reproduction on microfilms or in any other physical way, and transmission or information storage and retrieval, electronic adaptation, computer software, or by similar or dissimilar methodology now known or hereafter developed.
The use of general descriptive names, registered names, trademarks, service marks, etc. in this publication does not imply, even in the absence of a specific statement, that such names are exempt from the relevant protective laws and regulations and therefore free for general use.
The publisher, the authors and the editors are safe to assume that the advice and information in this book are believed to be true and accurate at the date of publication. Neither the publisher nor the authors or the editors give a warranty, expressed or implied, with respect to the material contained herein or for any errors or omissions that may have been made. The publisher remains neutral with regard to jurisdictional claims in published maps and institutional affiliations.

This Springer imprint is published by the registered company Springer Nature Singapore Pte Ltd.
The registered company address is: 152 Beach Road, #21-01/04 Gateway East, Singapore 189721, Singapore

Preface

The edited volume includes papers in the fields of fuzzy mathematical analysis and advances in computational mathematics, which can provide valuable solutions to complex problems. They have been applied in multiple areas such as high-dimensional data analysis, medical diagnosis, computer vision, hand-written character recognition, pattern recognition, machine intelligence, weather forecasting, network optimization, and VLSI design. The volume covers ongoing research in fuzzy and computational mathematical analysis and brings forward its recent applications to important real-world problems in various fields. The book includes selected high-quality papers from the International Conference on Fuzzy Mathematical Analysis and Advances in Computational Mathematics (FMAACM 2020), which was initially scheduled in 2020, but was held at Pondicherry, India, on February 25–26, 2021, due to the impact of COVID-19, as well as some invited papers from distinguished scholars. In the editing process of the volume, we are very sorrowful about the demise of the main editor, Prof. S. R. Kannan, in the COVID-19 spread. He is such an excellent scholar and a close friend of ours. Therefore, we try our best to finish this volume in memory of Prof. Kannan.

All the submitted papers were extended from the conference presentation and reviewed based on their originality, significance, relevance, and clarity of presentation. There are a total of eighteen articles included. The first paper devises the essential notion on bipolar complex Pythagorean fuzzy sets, which are an extension of complex Pythagorean fuzzy sets to deal with ambiguous and inexact information on real-life problems. The second paper solves fuzzy linear programming problems by modifying the two operations of subtraction and division for trapezoidal fuzzy numbers. The third paper proposes a generalized quadratic fuzzy method for solving fuzzy transportation problems without altering them to classical transportation problems. The fourth paper also solves the fuzzy transportation problem but uses a new ranking technique for handling the nonagonal fuzzy numbers. The fifth paper then defines a new type of interval-valued intuitionistic fuzzy numbers and discusses its impact on existing ranking functions.

The sixth paper is an application of fuzzy sets. It adopts a fuzzy clustering method to analyze the skin melanoma image. Next, the seventh paper establishes the fuzzy

chromatic number and the fuzzy index number of a quadruple layered fuzzy graph from a simple fuzzy cycle graph and verifies its boundary. The eighth paper discusses the d_2-coloring number of a central graph, a middle graph, and a total graph. The ninth paper proposes an improved accuracy function on the collection of trapezoidal intuitionistic fuzzy numbers and makes comparisons with existing functions. The tenth paper establishes a new distance measure based on two soft sets with two parameters and investigates some of their features.

The several subsequent papers then focus on the advances in computational mathematics. The eleventh paper conducts an automated sleep-stage classification using machine learning approaches. It can properly investigate irregularities during sleep based on a single channel of electroencephalography signal. The twelfth paper compares the finite mixtures of several non-normal distributions for model-based clustering approaches. The thirteenth paper discusses a single-server retrial queueing model with multiple working vacations and starting failure. The fourteenth paper then examines a classical queueing model with heterogeneous servers. The fifteenth paper calculates the Revan and hyper-Revan indices for the hexagonal-derived networks, which are helpful in chemical and pharmaceutical sciences.

The sixteenth paper then analyzes the impacts of the magnetic parameter, radiation parameter, and chemical reaction parameter along with Dufour and Soret effects in two nanofluids over a vertical rotating cone. The seventeenth paper introduces a fuzzy interactive controller with a least-squares-delay-based adaptive algorithm for adaptive feedback cancelation in hearing aids. The last paper elucidates the method of retrieving the correct parameter with the aid of relative weights of codewords and fuzzy logic.

At last, we are grateful to all the authors for their contributions and the referees for their vision and efforts. Appreciation is also given to Prof. Rajeswari Seshadri, Dr. Rajesh Kumar Mohapatra, and Dr. Esha Kashyap in Pondicherry University to provide us with the article information when we took over the editing job after Prof. Kannan. We would also like to thank Mr. Aninda Bose, the executive editor, and Mrs. Shalini Selvam, the project coordinator in Springer Nature, for their tremendous help to realize the volume. We hope the volume can bring some exciting ideas and recent advances in fuzzy mathematical analysis and advances in computational mathematics.

Kaohsiung, Taiwan — Tzung-Pei Hong
Beersheba, Israel — Mark Last
Taipei, Taiwan — Chun-Hao Chen

Contents

Bipolar Complex Pythagorean Fuzzy Graphs 1
R. Nandhini and D. Amsaveni

Modified Operations of Trapezoidal Fuzzy Numbers for Solving Fuzzy Linear Programming Problems 33
M. Mohamed Salih Mukthar and S. Ramathilagam

An Innovative Method for Finding Optimal Solution Fully Solved by Using Generalized Quadratic Fuzzy Transportation Problems 43
M. Venkatachalapathy, S. Muthuperumal, and R. Rajasekar

A New Ranking Method for Solving Nanogonal Fuzzy Transportation Problem 55
R. Saravanan and M. Valliathal

Novel Arithmetic Operations on IVIFNs and Their Properties on Ranking Functions 67
M. Edwin Antony Raj, Geetha Sivaraman, and P. Vishnukumar

Fuzzy Clustering Technique for Segmentation on Skin Cancer Dermoscopic Images 81
M. Kavitha, A. Senthil Arumugam, and Tzung-Pei Hong

A Study on Fuzzy Coloring in Quadruple Layered Fuzzy Graph 91
L. Jethruth Emelda Mary and R. Kiruthikaswari

On d_2-Coloring of Certain Families of Graphs 99
C. Natarajan, S. Venkatesh, P. Rajadurai, and S. Shanmugavelan

Improved Solution to a Decision-Making Problem Involving TraIFNs Data with TOPSIS Method 111
P. Vishnukumar, Geetha Sivaraman, and M. Edwin Antony Raj

A New Distance and Similarity Measure on Soft Parameter Sets and Their Applications to MCDM Problem 127
S. Vijayabalaji, A. Ramesh, and P. Balaji

Automated Accurate Sleep Stage Classification System Using Machine Learning Techniques with EEG Signals 137
Santosh Kumar Satapathy and D. Loganathan

On Comparative Study of Clustering Using Finite Mixture of Non-Gaussian Distributions 163
R. Deepana and C. Kiruthika

***M/G/1* Retrial Queueing System with Working Vacation and Starting Failure** 181
P. Rajadurai, R. Madhumidha, M. Sundararaman, and D. Narasimhan

Analysis of $MAP/PH_1, PH_2/2$ Queue with Working Breakdown, Starting Failure, and Bernoulli Vacation 189
G. Ayyappan and R. Gowthami

Results on Revan and Hyper Revan Indices of Some HEX Derived Networks 209
D. Narasimhan, R. Vignesh, and Kalyani Desikan

Dufour and Soret Effects on MHD Flow of Cu-Water and Al_2O_3-Water Nanofluid Flow Over a Permeable Rotating Cone 221
K. Padmaja and B. Rushi Kumar

Adaptive Feedback Cancelation in Hearing Aids Using Least Squares Delay-Based Fuzzy Interactive Controller 237
G. Jayanthi and Latha Parthiban

Retrieval of Erroneous Information by Adopting a Novel Way Using Fuzzy Logic 255
A. Neeraja and B. Amudhambigai

Author Index 267

Editors and Contributors

About the Editors

S. R. Kannan received his Ph.D. from Indian Institute of Technology, Madras, India and PDF at DISI, University of Genova, Genova, Italy. He has received post doctoral fellowship from National Cheng Kung University, Taiwan. Presently Dr. S.R. Kannan is working as Professor in Department of Mathematics, Pondicherry University (A Central University of India), India. He had been awarded a grant in the framework of a joint agreement between the Direzione Generale per la Cooperazione allo Sviluppo of the Italian Ministry of Foreign Affairs and the ICTP Programme for Training and Research in Italian Laboratories. He had been invited by Director General, National Agriculture Research Center, Tsukuba, Japan, for joint research work on remote sensing data to estimate rice yield. He has joint collaborative research projects with NSC Taiwan and MOST Israel. He has received number of research grants from Indian funding agencies UGC India, CSIR India, DST India and research grants from foreign funding agencies NSC Taiwan, MOST Israel, ICTP Italy, External Affair Ministry Italy, NARC Japan, etc. He has been served as editorial board member for many scientific journals.

Mark Last is a Full Professor and the Head of the Data Engineering Program at the Department of Software and Information Systems Engineering, Ben-Gurion University of the Negev, Israel. Prof. Last obtained his Ph.D. degree from Tel Aviv University, Israel in 2000. Prior to starting his appointment at Ben-Gurion University in March 2001, Mark Last was a Visiting Assistant Professor at the Department of Computer Science and Engineering, University of South Florida, Tampa, FL, USA (1999-2001). Between the years 2018-2020, Prof. Last has served as the Founding Director of the Data Science Research Center at Ben-Gurion University. He has published over 200 peer-reviewed papers and 12 books on data mining, text mining, software engineering, and cyber security. Prof. Last is a Senior Member of the IEEE Computer Society and a Professional Member of the Association for Computing Machinery (ACM). He currently serves as an Editorial Board Member of Data Mining

and Knowledge Discovery (DAMI) and Machine Learning Journal (MLJ). Previously, he has served as an Associate Editor of IEEE Transactions on Systems, Man, and Cybernetics - Part C (2004 – 2012), Pattern Analysis and Applications (2007-2016), and IEEE Transactions on Cybernetics (2013-2019). His main research interests are focused on data mining, cross-lingual text mining, soft computing, cyber intelligence, and medical informatics.

Tzung-Pei Hong received his B.S. degree in chemical engineering from National Taiwan University in 1985, and his Ph.D. degree in computer science and information engineering from National Chiao-Tung University in 1992. He served at the Department of Computer Science in Chung-Hua Polytechnic Institute from 1992 to 1994, and at the Department of Information Management in I-Shou University from 1994 to 2001. He was in charge of the whole computerization and library planning for National University of Kaohsiung in Preparation from 1997 to 2000 and served as the first director of the library and computer center in National University of Kaohsiung from 2000 to 2001, as the Dean of Academic Affairs from 2003 to 2006, as the Administrative Vice President from 2007 to 2008, and as the Academic Vice President in 2010. He is currently a distinguished and chair professor at the Department of Computer Science and Information Engineering and at the Department of Electrical Engineering, and the director of AI Research Center in National University of Kaohsiung, Taiwan. He is also a joint professor at the Department of Computer Science and Engineering, National Sun Yat-sen University, Taiwan. He got the first national flexible wage award from Ministry of Education in Taiwan. He has published more than 600 research papers in international/national journals and conferences and has planned more than fifty information systems. He is also the board member of more than forty journals and the program committee member of more than five hundred conferences. His current research interests include knowledge engineering, data mining, soft computing, management information systems.

Chun-Hao Chen is an associate professor at Department of Information and Finance Management at National Taipei University of Technology, Taipei, Taiwan. Dr. Chen received his Ph.D. degree with major in computer science and information engineering from National Cheng Kung University, Taiwan, in 2008. After that, he joined Department of Computer Science and Information Engineering of National University of Kaohsiung at Kaohsiung City, Taiwan, as a postdoctoral fellow during 2009. During February 2010 to July 2013, August 2013 to July 2017 and August 2017 to Jounary 2020, he served as an assistant, associate and professor of Department of Computer Science and Information Engineering at Tankang University, respectively. He has a wide variety of research interests covering data mining, time series, machine learning, evolutionary algorithms, and fuzzy theory. Research topics cover portfolio selection, trading strategy, business data analysis, time series pattern discovery, etc. He has published more than 120 research papers in referred journals (40 SCI papers) and international conferences (more than 75 papers, including IEEE CEC, Fuzz-IEEE, IEEE SMC, IEEE ICKII, PAKDD, and ACIIDS, etc). His google scholar citation is 882 (h-index: 15). He serves as the associate editor of the International

Journal of Data Science and Pattern Recognition, and IEEE Access (SCI). He is also a member of IEEE.

Contributors

D. Amsaveni Department of Mathematics, Sri Sarada College for Women, Salem, Tamil Nadu, India

B. Amudhambigai Department of Mathematics, Sri Sarada College for Women, Salem, Tamil Nadu, India

G. Ayyappan Department of Mathematics, Pondicherry Engineering College, Puducherry, India

P. Balaji Department of Mathematics, MEASI Academy of Architecture, Chennai, Tamil Nadu, India

R. Deepana Department of Mathematics, Hindustan University, Chennai, India

Kalyani Desikan Division of Mathematics, School of Advanced Sciences, Vellore Institute of Technology, Chennai, Tamil Nadu, India

M. Edwin Antony Raj Department of Mathematics, K. Ramakrishnan College of Engineering, Samayapuram, Tiruchy, Tamilnadu, India

R. Gowthami Department of Mathematics, Pondicherry Engineering College, Puducherry, India

Tzung-Pei Hong Department of Computer Science and Information Engineering, AI Research Center, National University of Kaohsiung, Kaohsiung City, Taiwan

G. Jayanthi Department of Electrical and Electronics Engineering, Dr. M.G.R. Educational and Research Institute, Chennai, India

L. Jethruth Emelda Mary PG and Research Department of Mathematics, St. Joseph's College of Arts and Science (Autonomous), Cuddalore, Tamil Nadu, India

M. Kavitha Manonmaniam Sundaranar University, Abhishekapatti, Tirunelveli, Tamilnadu, India

C. Kiruthika Department of Statistics, Pondicherry University, Puducherry, India

R. Kiruthikaswari PG and Research Department of Mathematics, St. Joseph's College of Arts and Science (Autonomous), Cuddalore, Tamil Nadu, India

D. Loganathan Pondicherry Engineering College, Puducherry, India

R. Madhumidha Department of Mathematics, Srinivasa Ramanujan Centre, SASTRA Deemed University, Kumbakonam, Tamil Nadu, India

M. Mohamed Salih Mukthar PG and Research Department of Mathematics, C. Abdul Hakeem College (Autonomous), Melvisharam, India

S. Muthuperumal K. Ramakrishnan College of Engineering (Autonomous), Samayapuram, Trichirappalli, Tamil Nadu, India

R. Nandhini Department of Mathematics, Sri Sarada College for Women, Salem, Tamil Nadu, India

D. Narasimhan Department of Mathematics, Srinivasa Ramanujan Centre, SASTRA Deemed University, Kumbakonam, Tamil Nadu, India

C. Natarajan Department of Mathematics, Srinivasa Ramanujan Centre, SASTRA Deemed University, Kumbakonam, Tamil Nadu, India

A. Neeraja Department of Mathematics, Sri Sarada College for Women, Salem, Tamil Nadu, India

K. Padmaja Department of Mathematics, School of Advanced Sciences, VIT, Vellore, Tamil Nadu, India

Latha Parthiban Department of Computer Science, Pondicherry University CC, Pondicherry, India

P. Rajadurai Department of Mathematics, Srinivasa Ramanujan Centre, SASTRA Deemed University, Kumbakonam, Tamil Nadu, India

R. Rajasekar K. Ramakrishnan College of Engineering (Autonomous), Samayapuram, Trichirappalli, Tamil Nadu, India

S. Ramathilagam Department of Mathematics, Periyar Arts College, Cuddalore, India

A. Ramesh Department of Mathematics, C. Abdul Hakeem College of Engineering and Technology, Melvisharam, Tamil Nadu, India

B. Rushi Kumar Department of Mathematics, School of Advanced Sciences, VIT, Vellore, Tamil Nadu, India

R. Saravanan NIFT-TEA College of Knitwear Fashion, Tirupur, India

Santosh Kumar Satapathy Pondicherry Engineering College, Puducherry, India

A. Senthil Arumugam Sri Ram Nallamani Yadhava College of Arts and Science, Tenkasi, Tamilnadu, India

S. Shanmugavelan Department of Mathematics, Srinivasa Ramanujan Centre, SASTRA Deemed University, Kumbakonam, Tamil Nadu, India

Geetha Sivaraman Department of Mathematics, St. Joseph's College (Autonomous), Tiruchirappalli, Tamil Nadu, India

M. Sundararaman Department of Mathematics, Srinivasa Ramanujan Centre, SASTRA Deemed University, Kumbakonam, Tamil Nadu, India

M. Valliathal Chikkaiah Naicker College, Erode, India

M. Venkatachalapathy K. Ramakrishnan College of Engineering (Autonomous), Samayapuram, Trichirappalli, Tamil Nadu, India

S. Venkatesh Department of Mathematics, Srinivasa Ramanujan Centre, SASTRA Deemed University, Kumbakonam, Tamil Nadu, India

R. Vignesh Division of Mathematics, School of Advanced Sciences, Vellore Institute of Technology, Chennai, Tamil Nadu, India

S. Vijayabalaji Department of Mathematics, University College of Engineering Panruti (A Constituent College of Anna University Chennai), Panruti, Tamil Nadu, India

P. Vishnukumar Department of Mathematics, St. Joseph's College (Autonomous), Tiruchirappalli, Tamil Nadu, India

Bipolar Complex Pythagorean Fuzzy Graphs

R. Nandhini and D. Amsaveni

Abstract The innovative approach of this article is to devise the key notion on bipolar complex Pythagorean fuzzy set ($\mathcal{BCPFS}$), which is an extension of complex Pythagorean fuzzy set dealt with ambiguous and inexact information on problems of real life. Next, bipolar complex Pythagorean fuzzy graphs ($\mathcal{BCPFGS}$) and their operations (i.e.,) ring sum, join and the union are elucidated with relevant examples. Finally, the concepts of complete $\mathcal{BCPFG}$, edge regular $\mathcal{BCPFG}$ and totally edge regular $\mathcal{BCPFGS}$ are developed, and few significant characteristics are examined.

Keywords Bipolar complex Pythagorean fuzzy set · Bipolar complex Pythagorean fuzzy graph · Regular bipolar complex Pythagorean fuzzy graph · Edge regular bipolar complex Pythagorean fuzzy graph · Totally edge regular bipolar complex Pythagorean fuzzy graph

Mathematics Subject Classification 54A40 · 03E72 · 05C72

1 Introduction

American cybernetician, Lofti Asker. Zadeh [35], pioneered the fuzzy set-theoretical notion, which is the most powerful tool for solving the unforeseeable factors associated with real-life situations in different disciplines such as medicine, spatial, automation, robotics and artificial intelligence. After two decades, the intuitionistic fuzzy set ($\mathcal{IFS}$) was philosophized by Atanassov [8]. Now, it is being applied in several areas like a computer network, pattern recognition, biological and natural sciences. In the meantime, the concept of intuitionistic fuzzy points and intuitionistic fuzzy topological spaces was substantiated by Coker [11, 12]. The combination of fuzzy sets and complex numbers was detailed by Buckley [10] and Nguyen et al. [20]. A few years later, Ramot et al. [24] developed the novel concept of a complex fuzzy set ($\mathcal{CFS}$), which was an extension of the unit circle in a complex plane. Subsequently,

R. Nandhini (✉) · D. Amsaveni
Department of Mathematics, Sri Sarada College for Women, Salem, Tamil Nadu, India

© The Author(s), under exclusive license to Springer Nature Singapore Pte Ltd. 2022

S. R. Kannan et al. (eds.), *Fuzzy Mathematical Analysis and Advances in Computational Mathematics*, Studies in Fuzziness and Soft Computing 419,
https://doi.org/10.1007/978-981-19-0471-4_1

the review of $\mathcal{CFS}$ was systematically studied by Yazdanbakhsh and Dick [34]. The complex intuitionistic fuzzy sets ($\mathcal{CIFS}$) and their operations on Attanassov $\mathcal{CIFS}$ were discovered by Alkouri [6, 7]. Then, these $\mathcal{CFS}$ and $\mathcal{CIFS}$ have been widely applied by mathematicians in decision-making and complex problems. Moreover, Zhang [36, 37] and Lee [17] proposed a concept of the bipolar fuzzy set ($\mathcal{BFS}$), which played a significant role in the extension of membership ranges from [0, 1] to [−1, 1], and it was applied by Gulistan [15]. Next, the view of edge regular concepts on $\mathcal{FGS}, \mathcal{IFGS}, \mathcal{BFGS}$ was described [2, 16, 22, 23] . Following that, the bipolar intuitionistic fuzzy graph ($\mathcal{BIFG}$) was well characterized by Ezhilmaran and Sankar in [14]. More recently, the applications of complex intuitionistic fuzzy graphs ($\mathcal{CIFGS}$) were put forward in cellular networking systems by Yaqoob et al. [33]. Further, the Pythagorean fuzzy set ($\mathcal{PFS}$) and complex Pythagorean fuzzy sets ($\mathcal{CPFSS}$) were well devised by Peng [21], Dick et al. [13], Luqman [18] and Yager [29, 30, 31, 32] in 2013 and Ullah et al. [27]. The representation of $\mathcal{PFS}$ has more capability than $\mathcal{IFS}$ which weaken the condition $\mu + \nu \leq 1$ with $\mu^2 + \nu^2 \leq 1$. Currently, the complexity arising in the ambiguous situation of the relation between the objects can be solved by using an effective dynamic model called graph theory in the networking system. Rosenfeld [25] provided the solution for vague information by applying the significant graph-theoretical theme known as fuzzy graphs ($\mathcal{FGS}$). Later, its comments were detailed by Bhattacharya [9]. Besides these, the $\mathcal{FGS}$ were further developed into $\mathcal{CFGS}$ by thirunavukarasu et al. [26]. Also, the idea on the energy of Pythagorean fuzzy graphs ($\mathcal{PFGS}$) [28] and complex Pythagorean fuzzy graphs ($\mathcal{CPFGS}$) [1, 3, 4] was well acquainted by Akram and Naz [5], and it is being applied practically, which motivated us to frame the bipolar complex Pythagorean fuzzy set ($\mathcal{BCPFS}$) and an imaginative concept called bipolar complex Pythagorean fuzzy graphs ($\mathcal{BCPFGS}$). Subsequently, several operations like complement, join, union and ring sum of the $\mathcal{BCPFGS}$ are derived, and certain examples are also explained. In addition, the notions of $\mathcal{RBCPFGS}$ and $\mathcal{TRBCPFGS}$ are defined, and some of its significant characterizations are analyzed in detail. Finally, $\mathcal{ERBCPFGS}$ and $\mathcal{TERBCPFGS}$ are established, also few of their properties are investigated.

2 Preliminaries

This section comprises necessary fundamental ideas related to this research paper.

Definition 2.1 [17, 36] Let X be a non-empty set. A bipolar fuzzy set B in X is an object having the form $B = \{(x, \mu^P(x), \mu^N(x)) : x \in X\}$, where $\mu^P : X \to [0, 1]$, $\mu^N : X \to [-1, 0]$, are the mappings.

Definition 2.2 [1] A complex Pythagorean fuzzy graph on a non-empty set Y is a pair $G = (C, D)$, where C is a complex Pythagorean fuzzy set on Y and D is a complex Pythagorean fuzzy relation on Y such that:

$$\mu_D(rs)e^{i\alpha_D(rs)} \leq (\mu_c(r) \wedge \mu_c(s))e^{i(\alpha_C(r)\wedge\alpha_C(s))},$$

$$\nu_D(rs)e^{i\beta_D(rs)} \leq (\mu_c(r) \vee \mu_c(s))e^{i(\alpha_C(r)\vee\beta_C(s))}; \quad 0 \leq \mu_D^2(rs) + \nu_D^2(rs) \leq 1$$

and $0 \leq \alpha_D^2(rs) + \beta_D^2(rs) \leq 2\pi$ for all $r, s \in Y$. we call C and D the complex Pythagorean fuzzy vertex set and the complex Pythagorean fuzzy edge set of G.

Definition 2.3 [19] A bipolar complex intuitionistic fuzzy set (in brief BCIF set) $\mathcal{E}$ defined on a universe of discourse χ, which is defined as an object of the form $\mathcal{E} = \left\{\left(\xi, \mu_E^+(\xi)e^{i\alpha_E(\xi)}, \mu_E^-(\xi)e^{i\beta_E(\xi)}, \nu_E^+(\xi)e^{i\gamma_E(\xi)}, \nu_E^-(\xi)e^{i\delta_E(\xi)}\right), : \xi \in \chi\right\}$,

where $i = \sqrt{-1}$, $\mu_E^+, \nu_E^+ : X \to [0, 1]$, $\mu_E^-, \nu_E^- : X \to [-1, 0]$, $\alpha_E, \beta_E, \gamma_E, \delta_E \in [0, 2\pi]$ and $0 \leq \mu_E^+ + \nu_E^+ \leq 1$. $-1 \leq \mu_E^- + \nu_E^- \leq 0$.

3 Bipolar Complex Pythagorean Fuzzy Graphs

Definition 3.1 A bipolar complex Pythagorean fuzzy set (in brief $\mathcal{BCPF}set$) $\mathcal{P}$ is defined on a universe of discourse χ, which is defined as an object of the form $\mathcal{P} = \left(\xi, \mu_P^+(\xi)e^{i\alpha_P(\xi)}, \mu_P^-(\xi)e^{i\beta_P(\xi)}, \nu_P^+(\xi)e^{i\gamma_P(\xi)}, \nu_P^-(\xi)e^{i\delta_P(\xi)}\right) : \xi \in \chi$ where $i = \sqrt{-1}$, $\mu_P^+, \nu_P^+ : X \to [0, 1]$, $\mu_P^-, \nu_P^- : X \to [-1, 0]$, $\alpha_P, \beta_P, \gamma_P, \delta_P \in [0, 2\pi]$ and $0 \leq {\mu_P^+}^2 + {\nu_P^+}^2 \leq 1$, $-1 \leq -\left[{\mu_P^-}^2 + {\nu_P^-}^2\right] \leq 0$ and $0 \leq \alpha_P^2(\xi) + \beta_P^2(\xi) \leq 2\pi, 0 \leq \gamma_P^2(\xi) + \delta_P^2(\xi) \leq 2\pi$.

Definition 3.2 For any three $\mathcal{BCPF}$ sets

$$\mathcal{P} = \left\{\left(\xi, \mu_P^+(\xi)e^{i\alpha_P(\xi)}, \mu_P^-(\xi)e^{i\beta_P(\xi)}, \nu_P^+(\xi)e^{i\gamma_P(\xi)}, \nu_P^-(\xi)e^{i\delta_P(\xi)}\right), : \xi \in \chi\right\},$$

$$\mathcal{Q} = \left\{\left(\xi, \mu_Q^+(\xi)e^{i\alpha_Q(\xi)}, \mu_Q^-(\xi)e^{i\beta_Q(\xi)}, \nu_Q^+(\xi)e^{i\gamma_Q(\xi)}, \nu_Q^-(\xi)e^{i\delta_Q(\xi)}\right), : \xi \in \chi\right\},$$

$\mathcal{R} = \left\{\left(\xi, \mu_R^+(\xi)e^{i\alpha_R(\xi)}, \mu_R^-(\xi)e^{i\beta_R(\xi)}, \nu_R^+(\xi)e^{i\gamma_R(\xi)}, \nu_R^-(\xi)e^{i\delta_R(\xi)}\right), : \xi \in \chi\right\}$ in χ, then.

1. $\mathcal{P} \subseteq \mathcal{Q}$ iff $\mu_P^+(\xi) \leq \mu_Q^+(\xi)$, $\mu_P^-(\xi) \geq \mu_Q^-(\xi)$, $\nu_P^+(\xi) \leq \nu_Q^+(\xi)$, $\nu_P^-(\xi) \geq \nu_Q^-(\xi)$ for amplitude terms and $\alpha_P(\xi) \leq \alpha_Q(\xi), \beta_P(\xi) \geq \beta_Q(\xi), \gamma_P(\xi) \leq \gamma_Q(\xi), \delta_P(\xi) \geq \delta_Q(\xi)$ for phase terms $\forall \xi$ in χ;
2. $\mathcal{P} = \mathcal{Q}$ iff $\mu_P^+(\xi) = \mu_Q^+(\xi), \mu_P^-(\xi) = \mu_Q^-(\xi), \nu_P^+(\xi) = \nu_Q^+(\xi), \nu_P^-(\xi) = \nu_Q^-(\xi)$ for amplitude terms and $\alpha_P = \alpha_Q, \beta_P = \beta_Q, \gamma_P = \gamma_Q, \delta_P = \delta_Q$;
3. $\overline{\mathcal{P}} = \left\{\left(\xi, \nu_P^+(\xi)e^{i\gamma_P(\xi)}, \nu_P^-(\xi)e^{i\delta_P(\xi)}, \mu_P^+(\xi)e^{i\alpha_P(\xi)}, \mu_P^-(\xi)e^{i\beta_P(\xi)}\right) : \xi \in \chi\right\}$.

Remark 3.1 The set of the form $(\mu_P^+(\xi)e^{i\alpha_P(\xi)}, \mu_P^-(\xi)e^{i\beta_P(\xi)}, \nu_P^+(\xi)e^{i\gamma_P(\xi)}, \nu_P^-(\xi)e^{i\delta_P(\xi)})$ is called the bipolar complex Pythagorean fuzzy number $\mathcal{BCPFN}$.

Example 3.1 Let us consider a fixed set χ contains one single element ξ, then $\mathcal{BCPFN}$ is defined as $\mu_P^+(\xi) = 0.2, \alpha_P(\xi) = 0.5(2\pi), \mu_P^-(\xi) = -0.5, \beta_P(\xi) = 0.5(2\pi), \nu_P^+(\xi) = 0.6, \gamma_P(\xi) = 0.3(2\pi), \nu_P^-(\xi) = -0.4, \delta_P(\xi) = 0.6(2\pi)$.

Definition 3.3 Let $\mathcal{P}_1 = \{(\xi, \mu_{P_1}^+(\xi)e^{i\alpha_{P_1}(\xi)}, \mu_{P_1}^-(\xi)e^{i\beta_{P_1}(\xi)}, \nu_{P_1}^+(\xi)e^{i\gamma_{P_1}(\xi)}, \nu_{P_1}^-(\xi)e^{i\delta_{P_1}(\xi)}), : \xi \in \chi\}$, and $\mathcal{P}_2 = \{(\xi, \mu_{P_2}^+(\xi)e^{i\alpha_{P_2}(\xi)}, \mu_{P_2}^-(\xi)e^{i\beta_{P_2}(\xi)}, \nu_{P_2}^+(\xi)e^{i\gamma_{P_2}(\xi)}, \nu_{P_2}^-(\xi)e^{i\delta_{P_2}(\xi)}), : \xi \in \chi\}$, be any two $\mathcal{BCPF}$ sets in χ. Then $\mathcal{P}_1 \cup \mathcal{P}_2$ and $\mathcal{P}_1 \cap \mathcal{P}_2$ are defined as follows.

1. $\mathcal{P}_1 \cup \mathcal{P}_2 = \Big\{\Big(\xi, \max\{\mu_{P_1}^+(\xi), \mu_{P_2}^+(\xi)\}\mathrm{e}^{i\max\{\alpha_{P_1}(\xi),\alpha_{P_2}(\xi)\}}, \min\{\mu_{P_1}^-(\xi), \mu_{P_2}^-(\xi)\}$
$\mathrm{e}^{i\min\{\beta_{P_1}(\xi),\beta_{P_2}(\xi)\}}, \min\{\nu_{P_1}^+(\xi), \nu_{P_2}^+(\xi)\}\mathrm{e}^{i\min\{\gamma_{P_1}(\xi),\gamma_{P_2}(\xi)\}},$
$\max\{\nu_{P_1}^-(\xi), \nu_{P_2}^-(\xi)\}\ \mathrm{e}^{i\max\{\delta_{P_1}(\xi),\delta_{P_2}(\xi)\}}\Big) : \xi \in \chi\Big\},$

2. $\mathcal{P}_1 \cap \mathcal{P}_2 = \Big\{\Big(\xi,\ \min\{\mu_{P_1}^+(\xi), \mu_{P_2}^+(\xi)\}\mathrm{e}^{i\min\{\alpha_{P_1}(\xi),\alpha_{P_2}(\xi)\}}, \max\{\mu_{P_1}^-(\xi), \mu_{P_2}^-(\xi)\}\ ,$
$\mathrm{e}^{i\max\{\beta_{P_1}(\xi),\beta_{P_2}(\xi)\}}, \max\{\nu_{P_1}^+(\xi), \nu_{P_2}^+(\xi)\}\mathrm{e}^{i\max\{\gamma_{P_1}(\xi),\gamma_{P_2}(\xi)\}},$
$\min\{\nu_{P_1}^-(\xi), \nu_{P_2}^-(\xi)\}\ e^{i\min\{\delta_{P_1}(\xi),\delta_{P_2}(\xi)\}}\Big), : \xi \in \chi\Big\}.$

Definition 3.4 Let $\mathcal{Q}$ be a $\mathcal{BCPF}set$ in $\chi \times \chi$. Then $\mathcal{Q}$ is a bipolar complex Pythagorean fuzzy relation in χ and is defined by

$$\mathcal{Q} = \{(\xi\eta, \mu_Q^+(\xi\eta)e^{i\alpha_Q(\xi\eta)}, \mu_Q^-(\xi\eta)e^{i\beta_Q(\xi\eta)}, \nu_Q^+(\xi\eta)e^{i\gamma_Q(\xi\eta)}, \nu_Q^-(\xi\eta)e^{i\delta_Q(\xi\eta)}), : \xi\eta \in \chi \times \chi\},$$

where $\mu_Q^+, \nu_Q^+ : \chi \times \chi \to [0, 1]$ and $\mu_Q^-, \nu_Q^- : \chi \times \chi \to [-1, 0]$ give the positive membership, positive non-membership, negative membership, negative non-membership function of $\mathcal{Q}$, respectively, $0 \le \mu_P^{+^2}(\xi\eta) + \nu_P^{+^2}(\xi\eta) \le 1$, $-1 \le -\big[\mu_P^{-\,2}(\xi\eta) + \nu_P^{-\,2}(\xi\eta)\big] \le 0$ and $0 \le \alpha_P^2(\xi\eta) + \beta_P^2(\xi\eta) \le 2\pi, 0 \le \gamma_P^2(\xi\eta) + \delta_P^2(\xi\eta) \le 2\pi, \forall \xi\eta \in \chi \times \chi$.

Definition 3.5 A bipolar complex Pythagorean fuzzy graph in brief $\mathcal{BCPFG}$ on an underlying set χ is an ordered pair $\mathcal{G} = (\mathcal{P}, \mathcal{Q})$, where $\mathcal{P}$ is a $\mathcal{BCPF}set$ on χ and $\mathcal{Q}$ is a bipolar complex Pythagorean fuzzy relation on χ which satisfies

1. $\mu_Q^+(\xi\eta)\mathrm{e}^{i\alpha_Q(\xi\eta)} \le \min\{\mu_P^+(\xi), \mu_P^+(\eta)\}\mathrm{e}^{i\min\{\alpha_P(\xi),\alpha_P(\eta)\}}$
2. $\mu_Q^-(\xi\eta)\mathrm{e}^{i\beta_Q(\xi\eta)} \ge \max\{\mu_P^-(\xi), \mu_P^-(\eta)\}e^{i\max\{\beta_P(\xi),\beta_P(\eta)\}}$
3. $\nu_Q^+(\xi\eta)\mathrm{e}^{i\gamma_Q(\xi\eta)} \le \max\{\nu_P^+(\xi), \nu_P^+(\eta)\}\mathrm{e}^{i\max\{\gamma_P(\xi),\gamma_P(\eta)\}}$
4. $\nu_Q^-(\xi\eta)\mathrm{e}^{i\delta_Q(\xi\eta)} \ge \min\{\nu_P^-(\xi), \nu_P^-(\eta)\}\mathrm{e}^{i\min\{\delta_P(\xi),\delta_P(\eta)\}}$

$\forall \xi, \eta \in \chi$ with $0 \le \mu_P^{+^2} + \nu_P^{+^2} \le 1$, $-1 \le -\big[\mu_P^{-\,2} + \nu_P^{-\,2}\big] \le 0$ and $0 \le \alpha_P^2(\xi\eta) + \beta_P^2(\xi\eta) \le 2\pi, 0 \le \gamma_P^2(\xi\eta) + \delta_P^2(\xi\eta) \le 2\pi,\ \forall \xi,\ \eta \in \chi$. Here, we take $\mathcal{P}$ and $\mathcal{Q}$ as the $\mathcal{BCPF}$ vertax set and $\mathcal{BCPF}$ edge set of $\mathcal{G}$, respectively.

Definition 3.6 Let $\mathcal{P} = \{(\xi, \mu_P^+(\xi)e^{i\alpha_P(\xi)}, \mu_P^-(\xi)e^{i\beta_P(\xi)}, \nu_P^+(\xi)e^{i\gamma_P(\xi)}, \nu_P^-(\xi)e^{i\delta_P(\xi)}) : \xi \in P\}$. and $Q = \{(\xi\eta, \mu_Q^+(\xi\eta)e^{i\alpha_Q(\xi\eta)}, \mu_Q^-(\xi\eta)e^{i\beta_Q(\xi\eta)}, \nu_Q^+(\xi\eta)e^{i\gamma_Q(\xi\eta)}, \nu_Q^-(\xi\eta)e^{i\delta_Q(\xi\eta)}) : \xi\eta \in Q\}$ be the vertex and the edge set of a $\mathcal{BCPFG}$. Then the order of a $\mathcal{BCPFG}$ is defined as

$$\mathcal{O}(\mathcal{G}) = \Big(\sum_{\xi_i \in P} \mu_P^+(\xi_i)e^{i\sum_{\xi_i\in P}\alpha_P(\xi_i)}, \sum_{\xi_i \in P} \mu_P^-(\xi_i)e^{i\sum_{\xi_i\in P}\beta_P(\xi_i)}, \sum_{\xi_i \in P} \nu_P^+(\xi_i)e^{i\sum_{\xi_i\in P}\gamma_P(\xi_i)}, \sum_{\xi_i \in P} \nu_P^-(\xi_i)e^{i\sum_{\xi_i\in P}\delta_P(\xi_i)}\Big).$$

Definition 3.7 Let $\mathcal{O}(\mathcal{G}) = (\mathcal{P}, \mathcal{Q})$ be a $\mathcal{BCPFG}$. The size of a $\mathcal{BCPFG}$ is symbolized and defined by

$$\mathcal{S}(\mathcal{G}) = \Big(\sum_{\xi_i\eta_i \in Q} \mu_Q^+(\xi_i\eta_i)e^{\sum_{\xi_i\eta_i\in Q}\alpha_Q(\xi_i\eta_i)}, \sum_{\xi_i\eta_i \in Q} \mu_Q^-(\xi_i\eta_i)e^{\sum_{\xi_i\eta_i\in Q}\beta_Q(\xi_i\eta_i)}, \sum_{\xi_i\eta_i \in Q} \nu_Q^+(\xi_i\eta_i)e^{\sum\limits_{\xi_i\eta_i\in Q}\gamma_Q(\xi_i\eta_i)}, \sum_{\xi_i\eta_i \in Q} \nu_Q^-(\xi_i\eta_i)e^{\sum\limits_{\xi_i\eta_i\in Q}\delta_Q(\xi_i\eta_i)}\Big).$$

Definition 3.8 Let $\mathcal{G} = (\mathcal{P}, \mathcal{Q})$ be a $\mathcal{BCPFG}$. Then the degree of a vertex $\xi \in \mathcal{P}$ in $\mathcal{BCPFGG}$ symbolized as

$$deg_{\mathcal{G}}(\xi) = \big(deg\mu^+e^{i\alpha}(\xi), deg\mu^-e^{i\beta}(\xi), deg\nu^+e^{i\gamma}(\xi), deg\nu^-e^{i\delta}(\xi)\big),$$

where

$$\deg\, \mu^+e^{i\alpha}(\xi) = \sum_{\xi,\eta\neq\xi\in P} \mu_Q^+(\xi\eta)e^{i\sum\limits_{\xi,\eta\neq\xi\in P}\alpha_Q(\xi\eta)}, \ \deg\, \mu^-e^{i\beta}(\xi) = \sum_{\xi,\eta\neq\xi\in P} \mu_Q^-(\xi\eta)e^{i\sum\limits_{\xi,\eta\neq\xi\in P}\beta_Q(\xi\eta)},$$

$$\deg\, \nu^+e^{i\gamma}(\xi) = \sum_{\xi,\eta\neq\xi\in P} \nu_Q^+(\xi\eta)e^{i\sum\limits_{\xi,\eta\neq\xi\in P}\gamma_Q(\xi\eta)}, \ \deg\, \nu^-e^{i\delta}(\xi) = \sum_{\xi,\eta\neq\xi\in P} \nu_Q^-(\xi\eta)e^{i\sum\limits_{\xi,\eta\neq\xi\in P}\delta_Q(\xi\eta)}$$

Example 3.2 Let us consider a graph $G^* = (P, Q)$, where $P = \{a, b, c, d\}$ and $Q = \{\text{ab}, \text{bc}, \text{cd}, \text{da}\}$ are the vertex and edge set of G, respectively. Let $\mathcal{G} = (\mathcal{P}, \mathcal{Q})$ be a $\mathcal{BCPFG}$ on $\mathcal{P}$ as shown in Fig. 1 defined by.

$$\mathcal{P}\Big(\Big\langle \frac{a}{0.5e^{i2\pi(0.8)}, -0.7e^{i2\pi(0.9)}, 0.6e^{i2\pi(0.6)}, -0.4e^{i2\pi(0.3)}}, \frac{b}{0.8e^{i2\pi(0.7)}, -0.5e^{i2\pi(0.8)}, 0.3e^{i2\pi(0.4)}, -0.4e^{i2\pi(0.6)}}, \frac{c}{0.7e^{i2\pi(0.7)}, -0.4e^{i2\pi(0.6)}, 0.4e^{i2\pi(0.5)}, -0.3e^{i2\pi(0.3)}}, \frac{d}{0.4e^{i2\pi(0.6)}, -0.5e^{i2\pi(0.4)}, 0.3e^{i2\pi(0.5)}, -0.6e^{i2\pi(0.7)}}, \Big\rangle\Big)$$

$$\mathcal{Q} = \Big(\Big\langle \frac{\text{ab}}{0.5e^{i2\pi(0.6)}, -0.4e^{i2\pi(0.9)}, 0.5e^{i2\pi(0.5)}, -0.3e^{i2\pi(0.3)}}, \frac{\text{bc}}{0.6e^{i2\pi(0.6)}, -0.2e^{i2\pi(0.8)}, 0.3e^{i2\pi(0.5)}, -0.3e^{i2\pi(0.3)}},$$

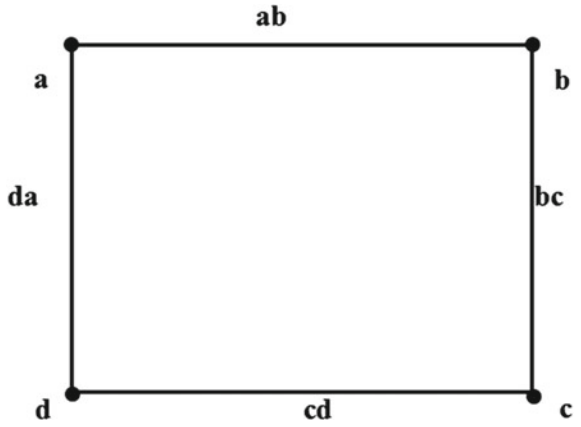

Fig. 1 Bipolar complex Pythagorean fuzzy graph

$$\frac{\text{cd}}{0.4\text{e}^{i2\pi(0.5)}, -0.3\text{e}^{i2\pi(0.6)}, 0.3\text{e}^{i2\pi(0.4)}, -0.5\text{e}^{i2\pi(0.3)}},$$
$$\frac{\text{da}}{0.3\text{e}^{i2\pi(0.5)}, -0.4\text{e}^{i2\pi(0.9)}, 0.5\text{e}^{i2\pi(0.6)}, -0.5\text{e}^{i2\pi(0.3)}}, \Big\rangle\Big).$$

(i) Order of a $\mathcal{BCPFG}, \mathcal{O}(\mathcal{G}) = (2.4e^{i2\pi(2.8)}, -2.1e^{i2\pi(2.1)}, 1.6e^{i2\pi(2)}, -1.7e^{i2\pi(1.9)})$

(ii) degree of a vertex in a $\mathcal{BCPFG}$,

$$\deg(a) = \left(0.8\text{e}^{i2\pi(1.2)}, -0.8\text{e}^{i2\pi(1.8)}, 1.0\text{e}^{i2\pi(1.1)}, -0.8\text{e}^{i2\pi(0.6)}\right),$$

$$\deg(b) = \left(1.1\text{e}^{i2\pi(1.2)}, -0.6\text{e}^{i2\pi(1.7)}, 0.8\text{e}^{i2\pi(1.0)}, -0.6\text{e}^{i2\pi(0.6)}\right),$$

$$\deg(c) = \left(1.0\text{e}^{i2\pi(1.1)}, -0.5\text{e}^{i2\pi(1.4)}, 0.6\text{e}^{i2\pi(0.9)}, -0.8\text{e}^{i2\pi(0.6)}\right),$$

$$\deg(d) = \left(0.7\text{e}^{i2\pi(1.0)}, -0.7\text{e}^{i2\pi(1.5)}, 0.8\text{e}^{i2\pi(1.0)}, -1.0\text{e}^{i2\pi(0.6)}\right),$$

(iii) The size of a $\mathcal{BCPFG}$,

$$\mathcal{S}(\mathcal{G}) = \left(1.8\text{e}^{i2\pi(2.2)}, -1.3\text{e}^{i2\pi(3.2)}, 1.6\text{e}^{i2\pi(2)}, -1.6\text{e}^{i2\pi(1.2)}\right).$$

Remark 3.2 For any $\mathcal{BCPF}$ set $(\mu_P^+(\xi)\text{e}^{i\alpha_P(\xi)}, \mu_P^-(\xi)\text{e}^{i\beta_P(\xi)}, \nu_P^+(\xi)\text{e}^{i\gamma_P(\xi)}, \nu_P^-(\xi)\text{e}^{i\delta_P(\xi)})$. If $\alpha_E = \beta_E = \gamma_E = \delta_E = 0$ and 2π, then $\mathcal{BCPF}$ set is $\mathcal{BIF}$ set.

Thus, $\mathcal{BCPFG}$ is $\mathcal{BIFG}$.

Definition 3.9 The complement of a$\mathcal{BCPFG}, \mathcal{G} = (\mathcal{P}, \mathcal{Q})$ on an underlying graph G^* is a $\mathcal{BCPFG}, \overline{\mathcal{G}} = \left(\overline{\mathcal{P}}, \overline{\mathcal{Q}}\right)$, where

1. $\overline{\mu_P^+}(\xi)\mathrm{e}^{i\alpha_{\overline{P}}(\xi)} = \mu_P^+(\xi)\mathrm{e}^{i\alpha_P(\xi)}, \overline{\mu_P^-}(\xi)\mathrm{e}^{i\beta_{\overline{P}}(\xi)} = \mu_P^-(\xi)\mathrm{e}^{i\beta_P(\xi)}, \overline{\nu_P^+}(\xi)\mathrm{e}^{i\gamma_{\overline{P}}(\xi)}$
$= \nu_P^+(\xi)\mathrm{e}^{i\gamma_P(\xi)}, \overline{\nu_P^-}(\xi)\mathrm{e}^{i\delta_{\overline{P}}(\xi)} = \nu_P^-(\xi)\mathrm{e}^{i\delta_P(\xi)}.$

2. $\overline{\dot{\mu}_Q^+}(\xi\eta)\mathrm{e}^{i\alpha_{\bar{Q}}(\xi\eta)}$

$$= \begin{cases} \min\left\{\mu_P^+(\xi), \mu_P^+(\eta)\right\}\mathrm{e}^{i\min\{\alpha_P(\xi),\alpha_P(\eta)\}} & \text{if } \mu_Q^+(\xi\eta)\mathrm{e}^{i\alpha_Q(\xi\eta)} = 0 \\ \min\left\{\mu_P^+(\xi), \mu_P^+(\eta)\right\}\mathrm{e}^{i\min\{\alpha_P(\xi),\alpha_P(\eta)\}} - \mu_Q^+(\xi\eta)\mathrm{e}^{i\alpha_Q(\xi\eta)} & \text{if } 0 < \mu_Q^+(\xi\eta)\mathrm{e}^{i\alpha_Q(\xi\eta)} \le 1, \end{cases}$$

$\overline{\mu_Q^-}(\xi\eta)e^{i\beta_{\bar{Q}}(\xi\eta)}$

$$= \begin{cases} \max\left\{\mu_P^-(\xi), \mu_P^-(\eta)\right\}e^{i\max\{\beta_P(\xi),\beta_P(\eta)\}} & \text{if } \mu_Q^-(\xi\eta)e^{i\beta_Q(\xi\eta)} = 0 \\ \max\left\{\mu_P^-(\xi), \mu_P^-(\eta)\right\}e^{i\max\{\beta_P(\xi),\beta_P(\eta)\}} - \mu_Q^-(\xi\eta)e^{i\beta_Q(\xi\eta)} & \text{if } -1 < \mu_Q^-(\xi\eta)e^{i\beta_Q(\xi\eta)} \le 0 \end{cases}$$

$\overline{\nu_Q^+}(\xi\eta)e^{i\gamma_{\bar{Q}}(\xi\eta)}$

$$= \begin{cases} \max\left\{\nu_P^+(\xi), \nu_P^+(\eta)\right\}e^{i\max\{\gamma_P(\xi),\gamma_P(\eta)\}} & \text{if } \nu_Q^+(\xi\eta)e^{i\gamma_Q(\xi\eta)} = 0 \\ \max\left\{\nu_P^+(\xi), \nu_P^+(\eta)\right\}e^{i\max\{\gamma_P(\xi),\gamma_P(\eta)\}} - \nu_Q^+(\xi\eta)e^{i\gamma_Q(\xi\eta)} & \text{if } 0 < \nu_Q^+(\xi\eta)e^{i\gamma_Q(\xi\eta)} \le 1 \end{cases}$$

$\overline{\nu_Q^-}(\xi\eta)e^{i\delta_{\bar{Q}}(\xi\eta)}$

$$= \begin{cases} \min\left\{\nu_P^-(\xi), \nu_P^-(\eta)\right\}e^{i\min\{\delta_P(\xi),\delta_P(\eta)\}} & \text{if } \nu_Q^-(\xi\eta)e^{i\delta_Q(\xi\eta)} = 0 \\ \min\left\{\nu_P^-(\xi), \nu_P^-(\eta)\right\}e^{i\min\{\delta_P(\xi),\delta_P(\eta)\}} & \text{if } -1 < \nu_Q^-(\xi\eta)e^{i\delta_Q(\xi\eta)} \le 0 \end{cases}.$$

Proposition 3.1 Let $\overline{\mathcal{G}}$ be the $\mathcal{BCPFG}$ and its complement is $\mathcal{G}$ (i.e) $\overline{\overline{\mathcal{G}}} = \mathcal{G}$.

Example 3.3 Let us assume a graph $G^* = (P, Q)$, where $P = \{a, b, c, d, e, f\}$ and $Q = \{\text{ab, bc, bd, de, and df}\}$ are the vertex and edge set of G. Let $\mathcal{G} = (\mathcal{P}, \mathcal{Q})$ be a $\mathcal{BCPFG}$ on $\mathcal{P}$ as shown in Fig. 2 defined by

$$\mathcal{P} = \left\{\left\langle \frac{a}{0.9\mathrm{e}^{i2\pi(0.7)}, -0.6\mathrm{e}^{i2\pi(0.6)}, 0.2\mathrm{e}^{i2\pi(0.4)}, -0.5\mathrm{e}^{i2\pi(0.5)}}, \right.\right.$$
$$\frac{b}{0.7\mathrm{e}^{i2\pi(0.8)}, -0.8\mathrm{e}^{i2\pi(0.9)}, 0.4\mathrm{e}^{i2\pi(0.6)}, -0.5\mathrm{e}^{i2\pi(0.3)}},$$
$$\left.\left.\frac{c}{0.5\mathrm{e}^{i2\pi(0.6)}, -0.4\mathrm{e}^{i2\pi(0.5)}, 0.6\mathrm{e}^{i2\pi(0.3)}, -0.3\mathrm{e}^{i2\pi(0.7)}}, \right.\right.$$

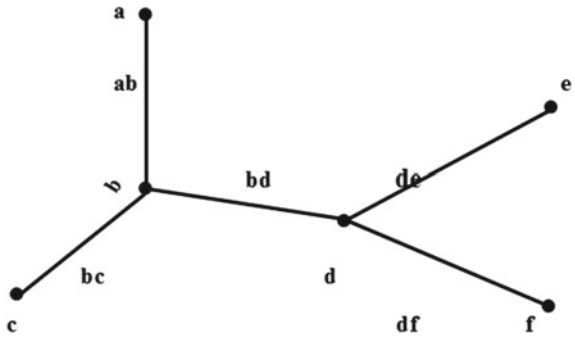

Fig. 2 $\mathcal{BCPFG}$

$$\frac{d}{0.7e^{i2\pi(0.9)}, -0.6e^{i2\pi(0.6)}, 0.4e^{i2\pi(0.5)}, -0.5e^{i2\pi(0.3)}},$$
$$\frac{e}{0.7e^{i2\pi(0.6)}, -0.9e^{i2\pi(0.7)}, 0.4e^{i2\pi(0.3)}, -0.2e^{i2\pi(0.5)}},$$
$$\left.\frac{f}{0.8e^{i2\pi(0.6)}, -0.9e^{i2\pi(0.3)}, 0.5e^{i2\pi(0.2)}, -0.2e^{i2\pi(0.5)}}\right\rangle\Bigg\},$$

$$\mathcal{Q} = \Bigg\{\Bigg\langle\frac{ab}{0.6e^{i2\pi(0.3)}, -0.4e^{i2\pi(0.9)}, 0.2e^{i2\pi(0.5)}, -0.4e^{i2\pi(0.3)}},$$
$$\frac{bc}{0.3e^{i2\pi(0.4)}, -0.2e^{i2\pi(0.9)}, 0.4e^{i2\pi(0.3)}, -0.3e^{i2\pi(0.3)}},$$
$$\frac{bd}{0.4e^{i2\pi(0.7)}, -0.4e^{i2\pi(0.9)}, 0.3e^{i2\pi(0.6)}, -0.3e^{i2\pi(0.3)}},$$
$$\frac{de}{0.4e^{i2\pi(0.5)}, -0.5e^{i2\pi(0.7)}, 0.3e^{i2\pi(0.3)}, -0.4e^{i2\pi(0.3)}},$$
$$\left.\frac{df}{0.5e^{i2\pi(0.5)}, -0.4e^{i2\pi(0.8)}, 0.2e^{i2\pi(0.4)}, -0.3e^{i2\pi(0.3)}}\right\rangle\Bigg\}.$$

Then its complement is shown in Fig. 3.

Definition 3.10 Let $\mathcal{G}_1 = (\mathcal{P}_1, \mathcal{Q}_1)$ and $\mathcal{G}_2 = (\mathcal{P}_2, \mathcal{Q}_2)$ be two $\mathcal{BCPFG}s$ of the graphs $G_1^* = (P_1, Q_1)$, $G_2^* = (P_2, Q_2)$, respectively. Then the union $\mathcal{G}_1 \cup \mathcal{G}_2 = (\mathcal{P}_1 \cup \mathcal{P}_2, \mathcal{Q}_1 \cup \mathcal{Q}_2)$ of two $\mathcal{BCPFG}s$ is defined as follows:

1. $\mu^+_{P_1\cup P_2}(\xi)e^{i\alpha_{P_1\cup P_2}(\xi)} = \mu^+_{P_1}(\xi)e^{i\alpha_{P_1}(\xi)}$

$$\mu^-_{P_1\cup P_2}(\xi)e^{i\beta_{P_1\cup P_2}(\xi)} = \mu^-_{P_1}(\xi)e^{i\beta_{P_1}(\xi)}$$

$$\nu^+_{P_1\cup P_2}(\xi)e^{i\gamma_{P_1\cup P_2}(\xi)} = \nu^+_{P_1}(\xi)e^{i\gamma_{P_1}(\xi)}$$

$\nu^-_{P_1\cup P_2}(\xi)e^{i\delta_{P_1\cup P_2}(\xi)} = \nu^-_{P_1}(\xi)e^{i\delta_{P_1}(\xi)}$ for $\xi \in P_1$ and $\xi \notin P_2$.

2. $\mu^+_{P_1\cup P_2}(\xi)e^{i\alpha_{P_1\cup P_2}(\xi)} = \mu^+_{P_2}(\xi)e^{i\alpha_{P_2}(\xi)}$

$$\mu^-_{P_1\cup P_2}(\xi)e^{i\beta_{P_1\cup P_2}(\xi)} = \mu^-_{P_2}(\xi)e^{i\beta_{P_2}(\xi)}$$

$$\nu^+_{P_1\cup P_2}(\xi)e^{i\gamma_{P_1\cup P_2}(\xi)} = \nu^+_{P_2}(\xi)e^{i\gamma_{P_2}(\xi)}$$

$\nu^-_{P_1\cup P_2}(\xi)e^{i\delta_{P_1\cup P_2}(\xi)} = \nu^-_{P_2}(\xi)e^{i\delta_{P_2}(\xi)}$ for $\xi \notin P_1$ and $\xi \in P_2$.

3. $\mu^+_{P_1\cup P_2}(\xi)e^{i\alpha_{P_1\cup P_2}(\xi)} = \max\{\mu^+_{P_1}(\xi), \mu^+_{P_2}(\xi)\}e^{i\max\{\alpha_{P_1}(\xi),\alpha_{P_2}(\xi)\}}$

$$\mu^-_{P_1\cup P_2}(\xi)e^{i\beta_{P_1\cup P_2}(\xi)} = \min\{\mu^-_{P_1}(\xi), \mu^-_{P_2}(\xi)\}e^{i\min\{\beta_{P_1}(\xi),\beta_{P_2}(\xi)\}}$$

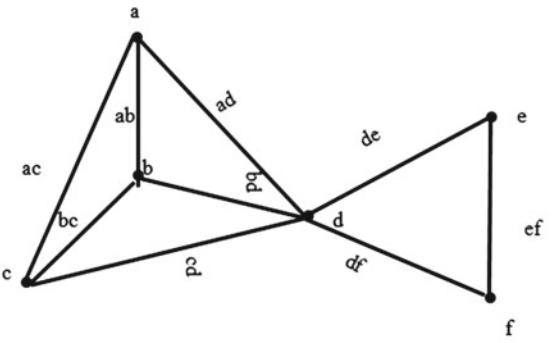

$a(0.9e^{i2\pi(0.7)}, -0.6e^{i2\pi(0.6)}, 0.2e^{i2\pi(0.4)}, -0.5e^{i2\pi(0.5)})$ $ad(0.7e^{i2\pi(0.7)}, -0.6e^{i2\pi(0.6)}, 0.4e^{i2\pi(0.5)}, -0.5e^{i2\pi(0.3)})$

$b(0.7e^{i2\pi(0.8)}, -0.8e^{i2\pi(0.9)}, 0.4e^{i2\pi(0.6)}, -0.5e^{i2\pi(0.3)})$ $de(0.3e^{i2\pi(0.1)}, -0.1e^{i2\pi(0)}, 0.1e^{i2\pi(0.2)}, -0.1e^{i2\pi(0)})$

$e(0.7e^{i2\pi(0.6)}, -0.9e^{i2\pi(0.7)}, 0.4e^{i2\pi(0.3)}, -0.2e^{i2\pi(0.5)})$ $(0.1e^{i2\pi(0.4)}, -0.2e^{i2\pi(0)}, 0.2e^{i2\pi(0.1)}, -0.1e^{i2\pi(0)})ab$

$(0.5e^{i2\pi(0.6)}, -0.4e^{i2\pi(0.6)}, 0.6e^{i2\pi(0.4)}, -0.5e^{i2\pi(0.7)})ac$ $ef(0.7e^{i2\pi(0.6)}, -0.9e^{i2\pi(0.7)}, 0.5e^{i2\pi(0.3)}, -0.2e^{i2\pi(0.5)})$

$(0.2e^{i2\pi(0.2)}, -0.2e^{i2\pi(0)}, 0.2e^{i2\pi(0.3)}, -0.2e^{i2\pi(0)})bc$ $d(0.7e^{i2\pi(0.9)}, -0.6e^{i2\pi(0.6)}, 0.4e^{i2\pi(0.5)}, -0.5e^{i2\pi(0.3)})$

$(0.5e^{i2\pi(0.6)}, -0.4e^{i2\pi(0.5)}, 0.6e^{i2\pi(0.3)}, -0.3e^{i2\pi(0.7)})c$ $ef(0.7e^{i2\pi(0.6)}, -0.9e^{i2\pi(0.7)}, 0.5e^{i2\pi(0.3)}, -0.2e^{i2\pi(0.5)})$

$f(0.8e^{i2\pi(0.6)}, -0.9e^{i2\pi(0.3)}, 0.5e^{i2\pi(0.2)}, -0.2e^{i2\pi(0.5)})$ $df(0.2e^{i2\pi(0.1)}, -0.2e^{i2\pi(0)}, 0.3e^{i2\pi(0.1)}, -0.2e^{i2\pi(0)})$

$cd(0.5e^{i2\pi(0.6)}, -0.4e^{i2\pi(0.6)}, 0.6e^{i2\pi(0.5)}, -0.5e^{i2\pi(0.3)})$ $bd(0.3e^{i2\pi(0.1)}, -0.2e^{i2\pi(0)}, 0.1e^{i2\pi(0)}, -0.2e^{i2\pi(0)})$

Fig. 3 Complement of $\mathcal{BCPFG}$ is $\overline{\mathcal{G}}$ and its values are given

$$\nu^{+}_{P_1\cup P_2}(\xi)e^{i\gamma_{P_1\cup P_2}(\xi)} = \max\left\{\nu^{+}_{P_1}(\xi), \nu^{+}_{P_2}(\xi)\right\}e^{i\max\left\{\gamma_{P_1}(\xi),\gamma_{P_2}(\xi)\right\}}$$

$$\nu^{-}_{P_1\cup P_2}(\xi)e^{i\delta_{P_1\cup P_2}(\xi)} = \min\left\{\nu^{-}_{P_1}(\xi), \nu^{-}_{P_2}(\xi)\right\}e^{i\min\left\{\delta_{P_1}(\xi),\delta_{P_2}(\xi)\right\}} \text{ for } \xi \in P_1 \cap P_2.$$

4. $$\mu^{+}_{Q_1\cup Q_2}(\xi\eta)e^{i\alpha_{Q_1\cup B_2}(\xi\eta)} = \mu^{+}_{Q_1}(\xi\eta)e^{i\alpha_{Q_1}(\xi\eta)}$$

$$\mu^{-}_{Q_1\cup Q_2}(\xi\eta)e^{i\beta_{Q_1\cup Q_2}(\xi\eta)} = \mu^{-}_{Q_1}(\xi\eta)e^{i\beta_{Q_1}(\xi\eta)}$$

$$\nu^{+}_{Q_1\cup Q_2}(\xi\eta)e^{i\gamma_{Q_1\cup Q_2}(\xi\eta)} = \nu^{+}_{Q_1}(\xi\eta)e^{i\gamma_{Q_1}(\xi\eta)}$$

$$\nu^{-}_{Q_1\cup Q_2}(\xi\eta)e^{i\delta_{Q_1\cup Q_2}(\xi\eta)} = \nu^{-}_{Q_1}(\xi\eta)e^{i\delta_{Q_1}(\xi\eta)} \text{ for } \xi\eta \in Q_1 \text{ and } \xi\eta \notin Q_2.$$

5. $$\mu^{+}_{Q_1\cup Q_2}(\xi\eta)e^{i\alpha_{Q_1\cup Q_2}(\xi\eta)} = \mu^{+}_{Q_2}(\xi\eta)e^{i\alpha_{Q_2}(\xi\eta)}$$

$$\mu^{-}_{Q_1\cup Q_2}(\xi\eta)e^{i\beta_{Q_1\cup Q_2}(\xi\eta)} = \mu^{-}_{Q_2}(\xi\eta)e^{i\beta_{Q_2}(\xi\eta)}$$

$$\nu^{+}_{Q_1\cup Q_2}(\xi\eta)e^{i\gamma_{Q_1\cup Q_2}(\xi\eta)} = \nu^{+}_{Q_2}(\xi\eta)e^{i\gamma_{Q_2}(\xi\eta)}$$

$\nu^{-}_{Q_1\cup Q_2}(\xi\eta)e^{i\delta_{Q_1\cup Q_2}(\xi\eta)} = \nu^{-}_{Q_2}(\xi\eta)e^{i\delta_{Q_2}(\xi\eta)}$ for $\xi\eta \in Q_2$ and $\xi\eta \notin Q_1$.

6. $\mu^{+}_{Q_1\cup Q_2}(\xi\eta)e^{i\alpha_{Q_1\cup Q_2}(\xi\eta)} = \max\{\mu^{+}_{Q_1}(\xi\eta), \mu^{+}_{Q_2}(\xi\eta)\}e^{i\max\{\alpha_{Q_1}(\xi\eta),\alpha_{Q_2}(\xi\eta)\}}$

$$\mu^{-}_{Q_1\cup Q_2}(\xi\eta)e^{i\beta_{Q_1\cup Q_2}(\xi\eta)} = \min\{\mu^{-}_{Q_1}(\xi\eta), \mu^{-}_{Q_2}(\xi\eta)\}e^{i\min\{\beta_{Q_1}(\xi\eta),\beta_{Q_2}(\xi\eta)\}}$$

$\nu^{+}_{Q_1\cup Q_2}(\xi\eta)e^{i\gamma_{Q_1\cup B_2}(\xi\eta)} = \max\{\nu^{+}_{Q_1}(\xi\eta), \nu^{+}_{Q_2}(\xi\eta)\}e^{i\max\{\gamma_{Q_1}(\xi\eta),\gamma_{Q_2}(\xi\eta)\}}$
$\nu^{-}_{Q_1\cup Q_2}(\xi\eta)e^{i\delta_{Q_1\cup Q_2}(\xi\eta)} = \min\{\nu^{-}_{Q_1}(\xi\eta), \nu^{-}_{Q_2}(\xi\eta)\}e^{i\min\{\delta_{Q_1}(\xi\eta),\delta_{Q_2}(\xi\eta)\}}$ for $\xi\eta \in Q_1 \cap Q_2$.

Proposition 3.2 For any two crisp graphs G^{*}_{i}, where $i = 1, 2$ of the $\mathcal{BCPFG}s$, $\mathcal{G}_i$, and if $P_1 \cap P_2 = \phi$. Then, its union $\mathcal{G}_1 \cup \mathcal{G}_2 = (\mathcal{P}_1 \cup \mathcal{P}_2, \mathcal{Q}_1 \cup \mathcal{Q}_2)$ individually is a $\mathcal{BCPFG}$ of G^{*} iff $\mathcal{G}_i$s are $\mathcal{BCPFG}s$ of G^{*}_{i}'s.

Example 3.4 Let us assume two $\mathcal{BCPFG}s$ in Fig. 4, then its union $\mathcal{G}_1 \cup \mathcal{G}_2$ is a $\mathcal{BCPFG}$ given in Fig. 5.

Definition 3.11 Let $\mathcal{G}_i = (\mathcal{P}_i, \mathcal{Q}_i)$, where $i = 1, 2$, let $\mathcal{P}_1$ and $\mathcal{P}_2$ be two $\mathcal{BCPF}$ subsets of $P_1 \& P_2$, and $\mathcal{Q}_1 \& \mathcal{Q}_2$ be two correspondingly $\mathcal{BCPF}$ subsets of Q_1 and Q_2. Then the ring sum of two $\mathcal{BCPFG}s$ is defined by $\mathcal{G}_1 \oplus \mathcal{G}_2 = (\mathcal{P}_1 \oplus \mathcal{P}_2, \mathcal{Q}_1 \oplus \mathcal{Q}_2)$.

1. $\mu^{+}_{P_1\oplus P_2}(x)e^{i\alpha_{P_1\oplus P_2}(\xi)} = \mu^{+}_{P_1\cup P_2}(\xi)e^{i\alpha_{P_1\cup P_2}(\xi)}$

$$\mu^{-}_{P_1\oplus P_2}(x)e^{i\beta_{P_1\oplus P_2}(\xi)} = \mu^{-}_{P_1\cup P_2}(\xi)e^{i\beta_{P_1\cup P_2}(\xi)}$$

$$\nu^{+}_{P_1\oplus P_2}(x)e^{i\gamma_{P_1\oplus P_2}(\xi)} = \nu^{+}_{P_1\cup P_2}(\xi)e^{i\gamma_{P_1\cup P_2}(\xi)}$$

$\nu^{-}_{P_1\oplus P_2}(x)e^{i\delta_{P_1\oplus P_2}(\xi)} = \nu^{-}_{P_1\cup P_2}(\xi)e^{i\delta_{P_1\cup P_2}(\xi)}$ for $\xi \in P_1 \cup P_2$,

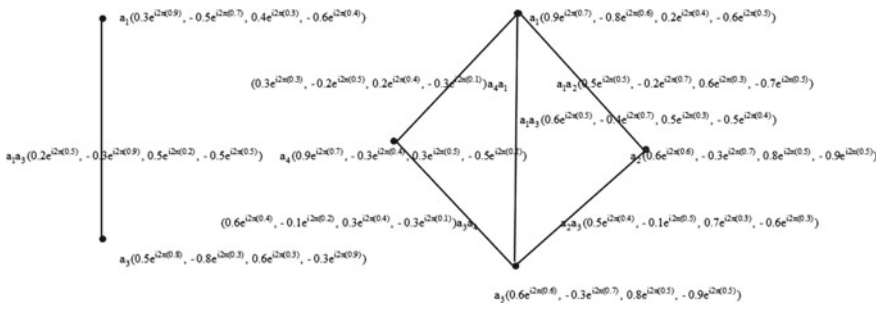

Fig. 4 $\mathcal{G}_1$ and $\mathcal{G}_2$

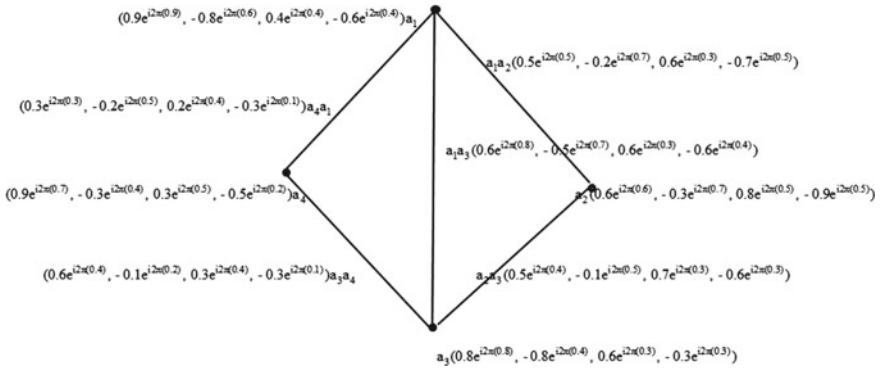

Fig. 5 $\mathcal{G}_1 \cup \mathcal{G}_2$

2. $\mu^+_{Q_1\oplus Q_2}(\xi\eta)\mathrm{e}^{i\alpha_{Q_1\oplus Q_2}(\xi\eta)} = \mu^+_{Q_1}(\xi\eta)\mathrm{e}^{i\alpha_{Q_1}(\xi\eta)}$

$$\mu^-_{Q_1\oplus Q_2}(\xi\eta)\mathrm{e}^{i\beta_{Q_1\oplus Q_2}(\xi\eta)} = \mu^-_{Q_1}(\xi\eta)\mathrm{e}^{i\beta_{Q_1}(\xi\eta)}$$

$$\nu^+_{Q_1\oplus Q_2}(\xi\eta)e^{i\gamma_{Q_1\oplus Q_2}(\xi\eta)} = \nu^+_{Q_1}(\xi\eta)e^{i\gamma_{Q_1}(\xi\eta)}$$

$\nu^-_{Q_1\oplus Q_2}(\xi\eta)e^{i\delta_{Q_1\oplus Q_2}(\xi\eta)} = \nu^-_{Q_1}(\xi\eta)e^{i\delta_{Q_1}(\xi\eta)}$ for $\xi\eta \in Q_1$ and $\xi\eta \notin Q_2$.

3. $\mu^+_{Q_1\oplus Q_2}(\xi\eta)e^{i\alpha_{Q_1\oplus Q_2}(\xi\eta)} = \mu^+_{Q_2}(\xi\eta)e^{i\alpha_{Q_2}(\xi\eta)}$

$$\mu^-_{Q_1\oplus Q_2}(\xi\eta)e^{i\beta_{Q_1\oplus Q_2}(\xi\eta)} = \mu^-_{Q_2}(\xi\eta)e^{i\beta_{Q_2}(\xi\eta)}$$

$$\nu^+_{Q_1\oplus Q_2}(\xi\eta)e^{i\gamma_{Q_1\oplus Q_2}(\xi\eta)} = \nu^+_{Q_2}(\xi\eta)e^{i\gamma_{Q_2}(\xi\eta)}$$

$\nu^-_{Q_1\oplus Q_2}(\xi\eta)e^{i\delta_{Q_1\oplus Q_2}(\xi\eta)} = \nu^-_{Q_2}(\xi\eta)e^{i\delta_{Q_2}(\xi\eta)}$ for $\xi\eta \in Q_2$ and $\xi\eta \notin Q_1$.

4. $\mu^+_{Q_1\oplus Q_2}(\xi\eta)e^{i\alpha_{Q_1\oplus Q_2}(\xi\eta)} = 0$, $\mu^-_{Q_1\oplus Q_2}(\xi\eta)e^{i\beta_{Q_1\oplus Q_2}(\xi\eta)} = 0$

$\nu^+_{Q_1\oplus Q_2}(\xi\eta)e^{i\gamma_{Q_1\oplus Q_2}(\xi\eta)} = 0$, $\nu^-_{Q_1\oplus Q_2}(\xi\eta)e^{i\delta_{Q_1\oplus Q_2}(\xi\eta)} = 0$ for $\xi\eta \in Q_1 \cap Q_2$.

Example 3.5 Let $\mathcal{G}_1$ and $\mathcal{G}_2$ be the two $\mathcal{BCPFG}s$ in Figs. 6 and 7, and their ring sum $\mathcal{G}_1 \oplus \mathcal{G}_2$ is also $\mathcal{BCPFG}$ as shown in Fig. 8.

Definition 3.12 Let $\mathcal{G}_i = (\mathcal{P}_i, \mathcal{Q}_i)$, where $i = 1, 2$ be the $\mathcal{BCPFG}s$ of G^*_1 and G^*_1 correspondingly. Then the join $\mathcal{G}_1 + \mathcal{G}_2 = (\mathcal{P}_1 + \mathcal{P}_2, \mathcal{Q}_1 + \mathcal{Q}_2)$ of two $\mathcal{BCPFG}s$ are defined as follows:

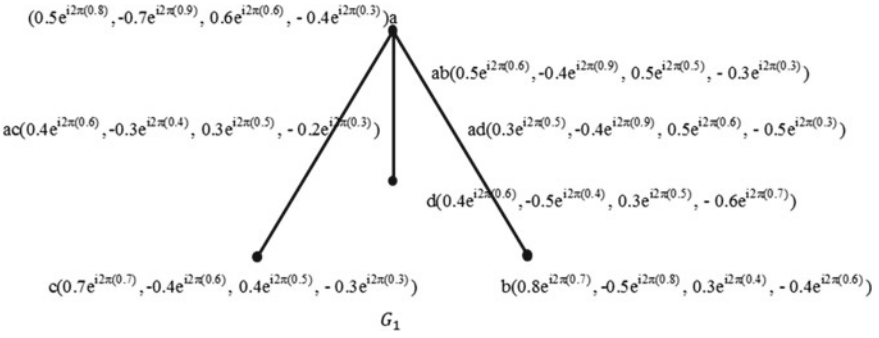

Fig. 6 $\mathcal{BCPFG}, \mathcal{G}_1$

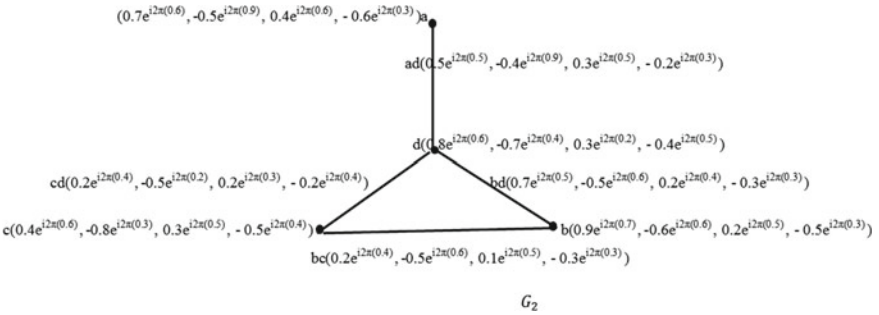

Fig. 7 $\mathcal{BCPFG}, \mathcal{G}_2$

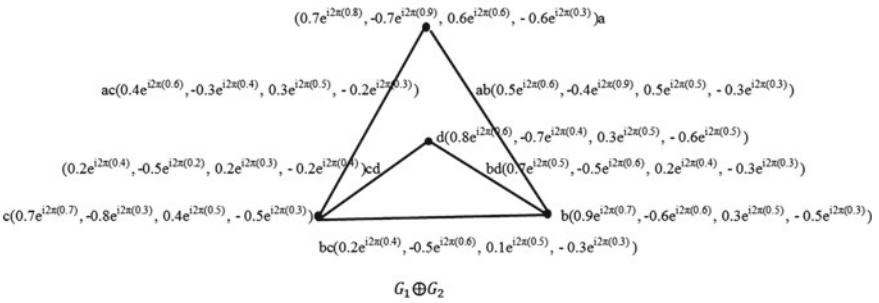

Fig. 8 Ring sum $\mathcal{G}_1 \oplus \mathcal{G}_2$ of $\mathcal{BCPFG}s$

1. $\mu^+_{P_1+P_2}(\xi)e^{i\alpha_{P_1+P_2}(\xi)} = \mu^+_{P_1\cup P_2}(\xi)e^{i\alpha_{P_1\cup P_2}(\xi)}$.

$$\mu^-_{P_1+P_2}(\xi)e^{i\beta_{P_1+P_2}(\xi)} = \mu^-_{P_1\cup P_2}(\xi)e^{i\beta_{P_1\cup P_2}(\xi)}$$

$$\nu^+_{P_1+P_2}(\xi)e^{i\gamma_{P_1+P_2}(\xi)} = \nu^+_{P_1\cup P_2}(\xi)e^{i\gamma_{P_1\cup P_2}(\xi)}$$

$$\nu^{-}_{P_1+P_2}(\xi)e^{i\delta_{P_1+P_2}(\xi)} = \nu^{-}_{P_1\cup P_2}(\xi)e^{i\delta_{P_1\cup P_2}(\xi)} \text{ for } \xi \in P_1 \cup P_2,$$

2. $$\mu^{+}_{Q_1+Q_2}(\xi\eta)e^{i\alpha_{Q_1+Q_2}(\xi\eta)} = \mu^{+}_{Q_1\cup Q_2}(\xi\eta)e^{i\alpha_{Q_1\cup Q_2}(\xi\eta)}$$

$$\mu^{-}_{Q_1+Q_2}(\xi\eta)e^{i\beta_{Q_1+Q_2}(\xi\eta)} = \mu^{-}_{Q_1\cup Q_2}(\xi\eta)e^{i\beta_{Q_1\cup Q_2}(\xi\eta)}$$

$$\nu^{+}_{Q_1+Q_2}(\xi\eta)e^{i\gamma_{Q_1+Q_2}(\xi\eta)} = \nu^{+}_{Q_1\cup Q_2}(\xi\eta)e^{i\gamma_{Q_1\cup Q_2}(\xi\eta)}$$

$$\nu^{-}_{Q_1+Q_2}(\xi\eta)e^{i\delta_{Q_1+Q_2}(\xi\eta)} = \nu^{-}_{Q_1\cup Q_2}(\xi\eta)e^{i\delta_{Q_1\cup Q_2}(\xi\eta)} \text{ for } \xi\eta \in Q_1 \cap Q_2.$$

3. $$\mu^{+}_{Q_1+Q_2}(\xi\eta)e^{i\alpha_{Q_1+Q_2}(\xi\eta)} = \min\left\{\mu^{+}_{P_1}(\xi), \mu^{+}_{P_2}(\eta)\right\}e^{i\min\left\{\alpha_{P_1}(\xi),\alpha_{P_2}(\eta)\right\}}$$

$$\mu^{-}_{Q_1+Q_2}(\xi\eta)e^{i\beta_{Q_1+Q_2}(\xi\eta)} = \max\left\{\mu^{-}_{P_1}(\xi), \mu^{-}_{P_2}(\eta)\right\}e^{i\max\left\{\beta_{P_1}(\xi),\beta_{P_2}(\eta)\right\}}$$

$$\nu^{+}_{Q_1+Q_2}(\xi\eta)e^{i\gamma_{Q_1+Q_2}(\xi\eta)} = \min\left\{\nu^{+}_{P_1}(\xi), \nu^{+}_{P_2}(\eta)\right\}e^{i\min\left\{\gamma_{P_1}(\xi),\gamma_{P_2}(\eta)\right\}}$$

$$\nu^{-}_{Q_1+Q_2}(\xi\eta)e^{i\delta_{Q_1+Q_2}(\xi\eta)} = \max\left\{\nu^{-}_{P_1}(\xi), \nu^{-}_{P_2}(\eta)\right\}e^{i\max\left\{\delta_{P_1}(\xi),\delta_{P_2}(\eta)\right\}}$$

if $\xi\eta \in Q'$, where Q' is the set of all edges joining the point of P_1 and P_2, for $\xi\eta \in Q_2$ and $\xi\eta \notin Q_1$.

Proposition 3.3 If $\mathcal{G}_1$ and $\mathcal{G}_2$ are the two $\mathcal{BCPFG}s$, then their join $\mathcal{G}_1 + \mathcal{G}_2$ is also a $\mathcal{BCPFG}$.

Proposition 3.4 Let $\mathcal{G}_i = (\mathcal{P}_i, \mathcal{Q}_i)$, where $i = 1, 2$ be the two $\mathcal{BCPFG}s$ of the graphs G_1^* and G_2^* and let $P_1 \cap P_2 = \phi$. Then, join $\mathcal{G}_1 + \mathcal{G}_2 = (\mathcal{P}_1 + \mathcal{P}_2, \mathcal{Q}_1 + \mathcal{Q}_2)$ individually is a $\mathcal{BCPFG}$ of G^* iff $\mathcal{G}_1$ and $\mathcal{G}_2$ are $\mathcal{BCPFG}s$ of G_1^* and G_2^*.

Definition 3.13 The total degree of a vertex $\xi \in \mathcal{P}$ in $\mathcal{BCPFG}, \mathcal{G}$ symbolized as $T\deg_{\mathcal{G}}(\xi) = \left(T\deg\mu^{+}e^{i\alpha}(\xi), T\deg\mu^{-}e^{i\beta}(\xi), T\deg\nu^{+}e^{i\gamma}(\xi), T\deg\nu^{-}e^{i\delta}(\xi)\right)$

where $T\deg\mu^{+}e^{i\alpha}(\xi) = \sum_{\xi,\eta\neq\xi\in P}\mu^{+}_{Q}(\xi\eta)e^{i\sum_{\xi,\eta\neq\xi\in P}\alpha_Q(\xi\eta)} + \mu^{+}_{P}(\xi)e^{i\alpha_P(\xi)}$,

$T\deg\mu^{-}e^{i\beta}(\xi) = \sum_{\xi,\eta\neq\xi\in P}\mu^{-}_{Q}(\xi\eta)e^{i\sum_{\xi,\eta\neq\xi\in P}\beta_Q(\xi\eta)} + \mu^{-}_{P}(\xi)e^{i\beta_P(\xi)}$,

$T\deg\nu^{+}e^{i\gamma}(\xi) = \sum_{\xi,\eta\neq\xi\in P}\nu^{+}_{Q}(\xi\eta)e^{i\sum_{\xi,\eta\neq\xi\in P}\gamma_Q(\xi\eta)} + \nu^{+}_{P}(\xi)e^{i\gamma_P(\xi)}$,

$T\deg\nu^{-}e^{i\delta}(\xi) = \sum_{\xi,\eta\neq\xi\in P}\nu^{-}_{Q}(\xi\eta)e^{i\sum_{\xi,\eta\neq\xi\in P}\delta_Q(\xi\eta)} + \nu^{-}_{P}(\xi)e^{i\delta_P(\xi)}$.

Example 3.6 For any two $\mathcal{BCPFG}s$, $\mathcal{G}_1$ and $\mathcal{G}_2$ are shown in Fig. 9, and then its join is a $\mathcal{BCPFG}$ as shown in Fig. 10.

Definition 3.14 Let $\mathcal{G}_1 = (\mathcal{P}_1, \mathcal{Q}_1)$ and $\mathcal{G}_2 = (\mathcal{P}_2, \mathcal{Q}_2)$ be the two $\mathcal{BCPFG}s$. If $\xi \in P_1 \cup P_2$, then to consider three cases.

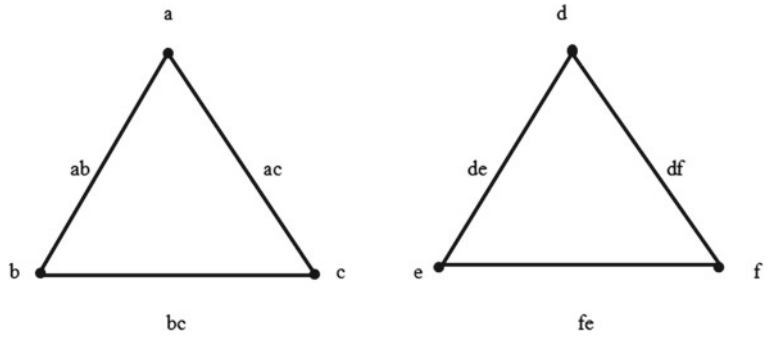

Fig. 9 $\mathcal{BCPFG}s$, $\mathcal{G}_1$ and $\mathcal{G}_2$

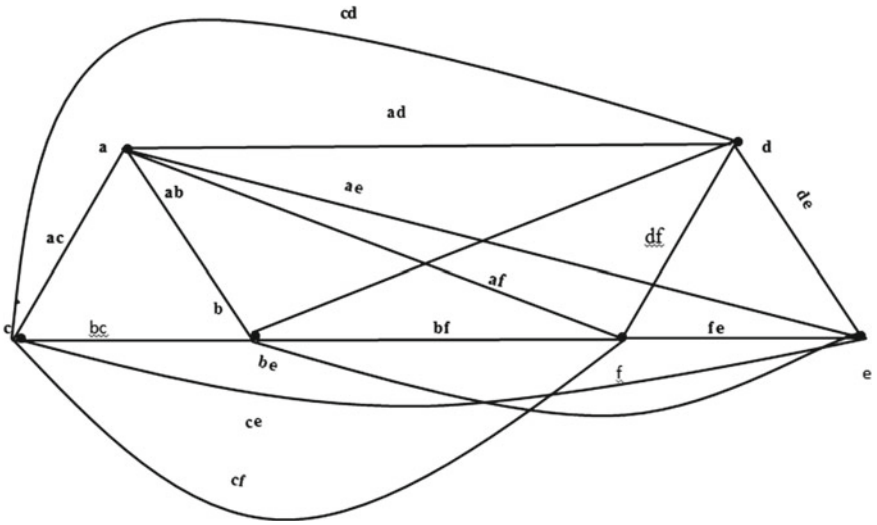

Fig. 10 Join $\mathcal{G}_1 + \mathcal{G}_2$ of two $\mathcal{BCPFG}s$

Case I: If $\xi \in P_1 - P_2$ or $P_2 - P_1$, then there is no edge incident at $\xi \in$. $Q_1 \cap Q_2$. Hence, for $\xi \in P_1 - P_2$,

$$\deg_{\mathcal{G}_1 \cup \mathcal{G}_2} \mu^+ e^{i\alpha}(\xi) = \sum_{\xi\eta \in Q_1} \mu^+_{Q_1}(\xi\eta) e^{i \sum\limits_{\xi\eta \in Q_1} \alpha_{Q_1}(\xi\eta)} = \deg_{\mathcal{G}_1} \mu^+ e^{i\alpha}(\xi),$$

$$\deg_{\mathcal{G}_1 \cup \mathcal{G}_2} \mu^- e^{i\beta}(\xi) = \sum_{\xi\eta \in Q_1} \mu^-_{Q_1}(\xi\eta) e^{i \sum\limits_{\xi\eta \in Q_1} \beta_{Q_1}(\xi\eta)} = \deg_{\mathcal{G}_1} \mu^- e^{i\beta}(\xi),$$

$$\deg_{\mathcal{G}_1 \cup \mathcal{G}_2} \nu^+ e^{i\gamma}(\xi) = \sum_{\xi\eta \in Q_1} \nu^+_{Q_1}(\xi\eta) e^{i \sum\limits_{\xi\eta \in Q_1} \gamma_{Q_1}(\xi\eta)} = \deg_{\mathcal{G}_1} \nu^+ e^{i\gamma}(\xi),$$

$$\deg_{\mathcal{G}_1 \cup \mathcal{G}_2} \nu^- e^{i\delta}(\xi) = \sum_{\xi\eta \in Q_1} \nu^-_{Q_1}(\xi\eta) e^{i \sum\limits_{\xi\eta \in Q_1} \delta_{Q_1}(\xi\eta)} = \deg_{\mathcal{G}_1} \nu^- e^{i\delta}(\xi).$$

$$T\deg_{\mathcal{G}_1\cup\mathcal{G}_2}(\xi) = \big(T\deg_{\mathcal{G}_1}\mu^+e^{i\alpha}(\xi), T\deg_{\mathcal{G}_1}\mu^-e^{i\beta}(\xi), T\deg_{\mathcal{G}_1}\nu^+e^{i\gamma}(\xi), T\deg_{\mathcal{G}_1}\nu^-e^{i\delta}(\xi)\big)$$

For $\xi \in P_2 - P_1$,

$$\deg_{\mathcal{G}_1\cup\mathcal{G}_2}\mu^+e^{i\alpha}(\xi) = \sum_{\xi\eta\in Q_2}\mu^+_{\mathcal{Q}_2}(\xi\eta)e^{i\sum\limits_{\xi\eta\in Q_2}\alpha_{\mathcal{Q}_2}(\xi\eta)} = \deg_{\mathcal{G}_2}\mu^+e^{i\alpha}(\xi),$$

$$\deg_{\mathcal{G}_1\cup\mathcal{G}_2}\mu^-e^{i\beta}(\xi) = \sum_{\xi\eta\in Q_2}\mu^-_{\mathcal{Q}_2}(\xi\eta)e^{i\sum\limits_{\xi\eta\in Q_2}\beta_{\mathcal{Q}_2}(\xi\eta)} = \deg_{\mathcal{G}_2}\mu^-e^{i\beta}(\xi),$$

$$\deg_{\mathcal{G}_1\cup\mathcal{G}_2}\nu^+e^{i\gamma}(\xi) = \sum_{\xi\eta\in Q_2}\nu^+_{\mathcal{Q}_2}(\xi\eta)e^{i\sum\limits_{\xi\eta\in Q_2}\gamma_{\mathcal{Q}_2}(\xi\eta)} = \deg_{\mathcal{G}_2}\nu^+e^{i\gamma}(\xi),$$

$$\deg_{\mathcal{G}_1\cup\mathcal{G}_2}\nu^-e^{i\delta}(\xi) = \sum_{\xi\eta\in Q_2}\nu^-_{\mathcal{Q}_2}(\xi\eta)e^{i\sum\limits_{\xi\eta\in Q_2}\delta_{\mathcal{Q}_2}(\xi\eta)} = \deg_{\mathcal{G}_2}\nu^-e^{i\delta}(\xi),$$

$$T\deg_{\mathcal{G}_1\cup\mathcal{G}_2}(\xi) = \big(T\deg_{\mathcal{G}_2}\mu^+e^{i\alpha}(\xi), T\deg_{\mathcal{G}_2}\mu^-e^{i\beta}(\xi), T\deg_{\mathcal{G}_2}\nu^+e^{i\gamma}(\xi), T\deg_{\mathcal{G}_2}\nu^-e^{i\delta}(\xi)\big).$$

Case II: If $\xi \in P_2 - P_1$ and no edge incident at $\xi \in Q_1 \cap Q_2$., then, hence, any edge incident at ξ, is either $\xi \in Q_1 - Q_2$ or $Q_2 - Q_1$.

$$\begin{aligned}\deg_{\mathcal{G}_1\cup\mathcal{G}_2}\mu^+e^{i\alpha}(\xi) &= \sum_{\xi\eta\in Q_1\cup Q_2}\big(\mu^+_{\mathcal{Q}_1}\cup\mu^+_{\mathcal{Q}_2}\big)(\xi\eta)e^{i\sum\limits_{\xi\eta\in Q_1\cup Q_2}\left(\alpha_{\mathcal{Q}_1}\cup\alpha_{\mathcal{Q}_2}\right)(\xi\eta)}\\ &= \sum_{\xi\eta\in Q_1}\mu^+_{\mathcal{Q}_1}(\xi\eta)e^{i\sum\limits_{\xi\eta\in Q_1}\alpha_{\mathcal{Q}_1}(\xi\eta)} + \sum_{\xi\eta\in Q_2}\mu^+_{\mathcal{Q}_2}(\xi\eta)e^{i\sum\limits_{\xi\eta\in Q_2}\alpha_{\mathcal{Q}_2}(\xi\eta)}\\ &= \deg_{\mathcal{G}_1}\mu^+e^{i\alpha}(\xi) + \deg_{\mathcal{G}_2}\mu^+e^{i\alpha}(\xi)\end{aligned}$$

$$\begin{aligned}\deg_{\mathcal{G}_1\cup\mathcal{G}_2}\mu^+e^{i\beta}(\xi) &= \sum_{\xi\eta\in Q_1\cup Q_2}\big(\mu^-_{\mathcal{Q}_1}\cup\mu^-_{\mathcal{Q}_2}\big)(\xi\eta)e^{i\sum\limits_{\xi\eta\in Q_1\cup Q_2}\left(\beta_{\mathcal{Q}_1}\cup\beta_{\mathcal{Q}_2}\right)(\xi\eta)}\\ &= \sum_{\xi\eta\in Q_1}\mu^-_{\mathcal{Q}_1}(\xi\eta)e^{i\sum\limits_{\xi\eta\in Q_1}\beta_{\mathcal{Q}_1}(\xi\eta)} + \sum_{\xi\eta\in Q_2}\mu^-_{\mathcal{Q}_2}(\xi\eta)e^{i\sum\limits_{\xi\eta\in Q_2}\beta_{\mathcal{Q}_2}(\xi\eta)}\\ &= \deg_{\mathcal{G}_1}\mu^-e^{i\beta}(\xi) + \deg_{\mathcal{G}_2}\mu^+e^{i\beta}(\xi)\end{aligned}$$

$|||^{ly}$ we have for $\deg_{\mathcal{G}_1\cup\mathcal{G}_2}\nu^+e^{i\gamma}(\xi) = \deg_{\mathcal{G}_1}\nu^+e^{i\gamma}(\xi) + \deg_{\mathcal{G}_2}\nu^+e^{i\gamma}(\xi)$

$$\deg_{\mathcal{G}_1\cup\mathcal{G}_2}\nu^-e^{i\delta}(\xi) = \deg_{\mathcal{G}_1}\nu^-e^{i\delta}(\xi) + \deg_{\mathcal{G}_2}\nu^-e^{i\delta}(\xi)$$

$$
\begin{aligned}
&T\deg_{\mathcal{G}_1\cup\mathcal{G}_2}(\xi)\\
&\quad=\big(T\deg_{\mathcal{G}_1\cup\mathcal{G}_2}\mu^+e^{i\alpha}(\xi),\,T\deg_{\mathcal{G}_1\cup\mathcal{G}_2}\mu^-e^{i\beta}(\xi),\\
&\quad T\deg_{\mathcal{G}_1\cup\mathcal{G}_2}\nu^+e^{i\gamma}(\xi),\,T\deg_{\mathcal{G}_1\cup\mathcal{G}_2}\nu^-e^{i\delta}(\xi)\big);
\end{aligned}
$$

$$
\begin{aligned}
T\deg_{\mathcal{G}_1\cup\mathcal{G}_2}\mu^+e^{i\alpha}(\xi) &= \sum_{\xi\eta\in Q_1\cup Q_2},\big(\mu^+_{\mathcal{Q}_1}\cup\mu^+_{\mathcal{Q}_2}\big)(\xi\eta)e^{\,i\sum\limits_{\xi\eta\in Q_1\cup Q_2}(\alpha_{\mathcal{Q}_1}\cup\alpha_{\mathcal{Q}_2})(\xi\eta)}\\
&\quad-\min\big\{\mu^+_{\mathcal{P}_1}(\xi),\mu^+_{\mathcal{P}_2}(\xi)\big\}e^{i\min\{\alpha_{\mathcal{P}_1}(\xi),\alpha_{\mathcal{P}_2}(\xi)\}}\\
&=\deg_{\mathcal{G}_1}\mu^+e^{i\alpha}(\xi)+\deg_{\mathcal{G}_2}\mu^+e^{i\alpha}(\xi)\\
&\quad-\min\big\{\mu^+_{\mathcal{P}_1}(\xi),\mu^+_{\mathcal{P}_2}(\xi)\big\}e^{i\min\{\alpha_{\mathcal{P}_1}(\xi),\alpha_{\mathcal{P}_2}(\xi)\}}\\
&=T\deg_{\mathcal{G}_1}\mu^+e^{i\alpha}(\xi)+T\deg_{\mathcal{G}_2}\mu^+e^{i\alpha}(\xi)\\
&\quad-\min\big\{\mu_{\mathcal{P}_1}(\xi)\big\},\mu_{\mathcal{P}_2}(\xi)e^{i\min\{\alpha_{\mathcal{P}_1}(\xi),\alpha_{\mathcal{P}_2}(\xi)\}}.
\end{aligned}
$$

$$
\begin{aligned}
&T\deg_{\mathcal{G}_1\cup\mathcal{G}_2}\mu^-e^{i\beta}(\xi)\\
&=T\deg_{\mathcal{G}_1}\mu^-e^{i\beta}(\xi)+T\deg_{\mathcal{G}_2}\mu^-e^{i\beta}(\xi)-\max\left\{\mu_{\mathcal{P}_1}(\xi),\mu_{\mathcal{P}_2}(\xi)e^{\,i\min\left\{\beta_{\mathcal{P}_1}(\xi),\beta_{\mathcal{P}_2}(\xi)\right\}}\right\}
\end{aligned}
$$

$$
\begin{aligned}
|||^{l\gamma}T\deg_{\mathcal{G}_1\cup\mathcal{G}_2}\nu^+e^{i\gamma}(\xi) &= T\deg_{\mathcal{G}_1}\nu^+e^{i\gamma}(\xi)\\
&\quad+T\deg_{\mathcal{G}_2}\nu^+e^{i\gamma}(\xi)\\
&\quad-\max\left\{\nu_{\mathcal{P}_1}(\xi),\nu_{\mathcal{P}_2}(\xi)e^{\,i\max\{\gamma_{\mathcal{P}_1}(\xi),\gamma_{\mathcal{P}_2}(\xi)\}}\right\}
\end{aligned}
$$

$$
\begin{aligned}
T\deg_{\mathcal{G}_1\cup\mathcal{G}_2}\nu^-e^{i\delta}(\xi) &= T\deg_{\mathcal{G}_1}\nu^-e^{i\delta}(\xi)+T\deg_{\mathcal{G}_2}\nu^-e^{i\delta}(\xi)\\
&\quad-\min\left\{\nu_{\mathcal{P}_1}(\xi),\nu_{\mathcal{P}_2}(\xi)e^{\,i\min\{\delta_{\mathcal{P}_1}(\xi),\delta_{\mathcal{P}_2}(\xi)\}}\right\}.
\end{aligned}
$$

Case III: If $\xi\in P_1\cap P_2$ and, some edges incident at $\xi\in Q_1\cap Q_2$.

$$
\begin{aligned}
\deg_{\mathcal{G}_1\cup\mathcal{G}_2}\mu^+e^{i\alpha}(\xi) &= \sum_{\xi\eta\in Q_1\cup Q_2}\big(\mu^+_{\mathcal{Q}_1}\cup\mu^+_{\mathcal{Q}_2}\big)(\xi\eta)e^{\,i\sum\limits_{\xi\eta\in Q_1\cup Q_2}(\alpha_{\mathcal{Q}_1}\cup\alpha_{\mathcal{Q}_2})(\xi\eta)}\\
&=\sum_{\xi\eta\in Q_1-Q_2}\mu^+_{\mathcal{Q}_1}(\xi\eta)e^{\,i\sum\limits_{\xi\eta\in Q_1-Q_2}\alpha_{\mathcal{Q}_1}(\xi\eta)}\\
&\quad+\sum_{\xi\eta\in Q_2-Q_1}\mu^+_{\mathcal{Q}_2}(\xi\eta)e^{\,i\sum\limits_{\xi\eta\in Q_2-Q_1}\alpha_{\mathcal{Q}_2}(\xi\eta)}\\
&\quad+\sum_{\xi\eta\in Q_1\cap Q_2}\max\{\mu^+_{\mathcal{Q}_1},\mu^+_{\mathcal{Q}_2})(\xi\eta)\}e^{\,i\sum\limits_{\xi\eta\in Q_1\cap Q_2}\max\{\alpha_{\mathcal{Q}_1},\alpha_{\mathcal{Q}_2}\}(\xi\eta)}\\
&=\sum_{\xi\eta\in Q_1-Q_2}\mu^+_{\mathcal{Q}_1}(\xi\eta)e^{\,i\sum\limits_{\xi\eta\in Q_1-Q_2}\alpha_{\mathcal{Q}_1}(\xi\eta)}
\end{aligned}
$$

$$
\begin{aligned}
&+ \sum_{\xi\eta \in Q_2 - Q_1} \mu^+_{Q_2}(\xi\eta) e^{i \sum\limits_{\xi\eta \in Q_2 - Q_1} \alpha_{Q_2}(\xi\eta)} \\
&+ \sum_{\xi\eta \in Q_1 \cap Q_2} \max\{\mu^+_{Q_1}, \mu^+_{Q_2})(\xi\eta)\} e^{i \sum\limits_{\xi\eta \in Q_1 \cap Q_2} \max\{\alpha_{Q_1}, \alpha_{Q_2}\}(\xi\eta)} \\
&+ \sum_{\xi\eta \in Q_1 \cap Q_2} \min\{\mu^+_{Q_1}, \mu^+_{Q_2})(\xi\eta)\} e^{i \sum\limits_{\xi\eta \in Q_1 \cap Q_2} \min\{\alpha_{Q_1}, \alpha_{Q_2}\}(\xi\eta)} \\
&- \sum_{\xi\eta \in Q_1 \cap Q_2} \min\left\{\mu^+_{Q_1}, \mu^+_{Q_2}(\xi\eta)\right\} e^{i \sum\limits_{\xi\eta \in Q_1 \cap Q_2} \min\{\alpha_{Q_1}, \alpha_{Q_2}\}(\xi\eta)} \\
&= \sum_{\xi\eta \in Q_1} \mu^+_{Q_1}(\xi\eta) e^{i \sum\limits_{\xi\eta \in Q_1} \alpha_{Q_1}(\xi\eta)} \\
&+ \sum_{\xi\eta \in Q_2} \mu^+_{Q_2}(\xi\eta) e^{i \sum\limits_{\xi\eta \in Q_2} \alpha_{Q_2}(\xi\eta)} \\
&- \sum_{\xi\eta \in Q_1 \cap Q_2} \min\left\{\mu^+_{Q_1}, \mu^+_{Q_2}(\xi\eta)\right\} e^{i \sum\limits_{\xi\eta \in Q_1 \cap Q_2} \min\{\alpha_{Q_1}, \alpha_{Q_2}\}(\xi\eta)} \\
&= \deg_{\mathcal{G}_1} \mu^+ e^{i\alpha}(\xi) + \deg_{\mathcal{G}_2} \mu^+ e^{i\alpha}(\xi) \\
&- \sum_{\xi\eta \in Q_1 \cap Q_2} \min\left\{\mu^+_{Q_1}, \mu^+_{Q_2}(\xi\eta)\right\} \\
&\qquad e^{i \sum\limits_{\xi\eta \in Q_1 \cap Q_2} \min\{\alpha_{Q_1}, \alpha_{Q_2}\}(\xi\eta)}.
\end{aligned}
$$

$$
\begin{aligned}
\deg_{\mathcal{G}_1 \cup \mathcal{G}_2} \mu^- e^{i\beta}(\xi) &= \deg_{\mathcal{G}_1} \mu^- e^{i\beta}(\xi) + \deg_{\mathcal{G}_2} \mu^- e^{i\beta}(\xi) \\
&- \sum_{\xi\eta \in Q_1 \cap Q_2} \max\left\{\mu^-_{Q_1}, \mu^-_{Q_2}(\xi\eta)\right\} \\
&\qquad e^{i \sum\limits_{\xi\eta \in Q_1 \cap Q_2} \max\{\beta_{Q_1}, \beta_{Q_2}\}(\xi\eta)}.
\end{aligned}
$$

$$
\begin{aligned}
\deg_{\mathcal{G}_1 \cup \mathcal{G}_2} \nu^+ e^{i\gamma}(\xi) &= \deg_{\mathcal{G}_1} \nu^+ e^{i\gamma}(\xi) + \deg_{\mathcal{G}_2} \nu^+ e^{i\gamma}(\xi) \\
&- \sum_{\xi\eta \in Q_1 \cap Q_2} \max\left\{\nu^+_{Q_1}, \nu^+_{Q_2}(\xi\eta)\right\} \\
&\qquad e^{i \sum\limits_{\xi\eta \in Q_1 \cap Q_2} \max\{\gamma_{Q_1}, \gamma_{Q_2}\}(\xi\eta)}.
\end{aligned}
$$

$$
\begin{aligned}
\deg_{\mathcal{G}_1 \cup \mathcal{G}_2} \nu^- e^{i\delta}(\xi) &= \deg_{\mathcal{G}_1} \nu^- e^{i\delta}(\xi) + \deg_{\mathcal{G}_2} \nu^- e^{i\delta}(\xi) \\
&- \sum_{\xi\eta \in Q_1 \cap Q_2} \min\left\{\nu^-_{Q_1}, \nu^-_{Q_2}(\xi\eta)\right\}
\end{aligned}
$$

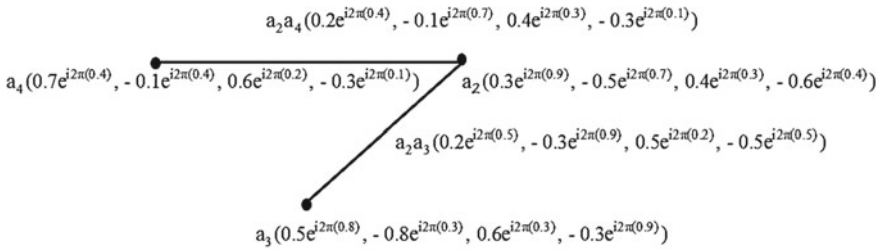

Fig. 11 $\mathcal{BCPFG}$, $\mathcal{G}_1$

$$e^{i\sum\limits_{\xi\eta\in Q_1\cap Q_2}\min\{\delta_{\mathcal{Q}_1},\delta_{\mathcal{Q}_2}\}(\xi\eta)}.$$

$$\begin{aligned}T\deg_{\mathcal{G}_1\cup\mathcal{G}_2}\mu^+e^{i\alpha}(\xi) &= T\deg_{\mathcal{G}_1}\mu^+e^{i\alpha}(\xi)+T\deg_{\mathcal{G}_2}\mu^+e^{i\alpha}(\xi)\\ &\quad-\sum_{\xi\eta\in Q_1\cap Q_2}\min\{\mu^+_{\mathcal{Q}_1},\mu^+_{\mathcal{Q}_2}(\xi\eta)\}e^{i\sum\limits_{\xi\eta\in Q_1\cap Q_2}\min\{\alpha_{\mathcal{Q}_1},\alpha_{\mathcal{Q}_2}\}(\xi\eta)}\\ &\quad-\min\{\mu^+_{\mathcal{P}_1}(\xi),\mu^+_{\mathcal{P}_2}(\xi)\}e^{i\min\{\alpha_{\mathcal{P}_1},\alpha_{\mathcal{P}_2}\}},\end{aligned}$$

$$\begin{aligned}T\deg_{\mathcal{G}_1\cup\mathcal{G}_2}\mu^-e^{i\beta}(\xi) &= T\deg_{\mathcal{G}_1}\mu^-e^{i\beta}(\xi)+T\deg_{\mathcal{G}_2}\mu^-e^{i\beta}(\xi)\\ &\quad-\sum_{\xi\eta\in Q_1\cap Q_2}\max\{\mu^-_{\mathcal{Q}_1},\mu^-_{\mathcal{Q}_2}(\xi\eta)\}e^{i\sum\limits_{\xi\eta\in Q_1\cap Q_2}\max\{\beta_{\mathcal{Q}_1},\beta_{\mathcal{Q}_2}\}(\xi\eta)}\\ &\quad-\max\{\mu^-_{\mathcal{P}_1}(\xi),\mu^-_{\mathcal{P}_2}(\xi)\}e^{i\max\{\beta_{\mathcal{P}_1},\beta_{\mathcal{P}_2}\}},\end{aligned}$$

$$-\sum_{\xi\eta\in Q_1\cap Q_2}\max\{\mu^-_{\mathcal{Q}_1},\mu^-_{\mathcal{Q}_2}(\xi\eta)\}e^{i\sum\limits_{\xi\eta\in Q_1\cap Q_2}\max\{\beta_{\mathcal{Q}_1},\beta_{\mathcal{Q}_2}\}(\xi\eta)}-\max\{\mu^-_{\mathcal{P}_1}(\xi),\mu^-_{\mathcal{P}_2}(\xi)\}e^{i\max\{\beta_{\mathcal{P}_1},\beta_{\mathcal{P}_2}\}},$$

$$\begin{aligned}T\deg_{\mathcal{G}_1\cup\mathcal{G}_2}\nu^+e^{i\gamma}(\xi) &= T\deg_{\mathcal{G}_1}\nu^+e^{i\gamma}(\xi)+T\deg_{\mathcal{G}_2}\nu^+e^{i\gamma}(\xi)\\ &\quad-\sum_{\xi\eta\in Q_1\cap Q_2}\max\{\nu^+_{\mathcal{Q}_1},\nu^+_{\mathcal{Q}_2}(\xi\eta)\}e^{i\sum\limits_{\xi\eta\in Q_1\cap Q_2}\max\{\gamma_{\mathcal{Q}_1},\gamma_{\mathcal{Q}_2}\}(\xi\eta)}\\ &\quad-\max\{\nu^+_{\mathcal{P}_1}(\xi),\nu^+_{\mathcal{P}_2}(\xi)\}e^{i\max\{\gamma_{\mathcal{P}_1},\gamma_{\mathcal{P}_2}\}},\end{aligned}$$

$$\begin{aligned}T\deg_{\mathcal{G}_1\cup\mathcal{G}_2}\nu^-e^{i\delta}(\xi) &= T\deg_{\mathcal{G}_1}\nu^-e^{i\delta}(\xi)+T\deg_{\mathcal{G}_2}\nu^-e^{i\delta}(\xi)\\ &\quad-\sum_{\xi\eta\in Q_1\cap Q_2}\min\{\nu^-_{\mathcal{Q}_1},\nu^-_{\mathcal{Q}_2}(\xi\eta)\}e^{i\sum\limits_{\xi\eta\in Q_1\cap Q_2}\min\{\delta_{\mathcal{Q}_1},\delta_{\mathcal{Q}_2}\}(\xi\eta)}\\ &\quad-\min\{\nu^+_{\mathcal{P}_1}(\xi),\nu^+_{\mathcal{P}_2}(\xi)\}e^{i\max\{\delta_{\mathcal{P}_1},\delta_{\mathcal{P}_2}\}}\end{aligned}$$

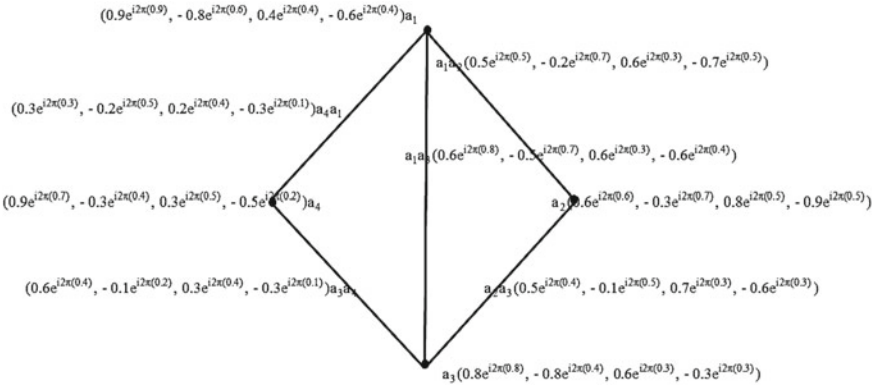

Fig. 12 $\mathcal{BCPFG}$, $\mathcal{G}_2$

Example 3.7 Consider two $\mathcal{BCPFG}s$, $\mathcal{G}_1 = (\mathcal{P}_1, \mathcal{Q}_1)$ and $\mathcal{G}_2 = (\mathcal{P}_2, \mathcal{Q}_2)$ on $\mathcal{P}_1 = \{a_2, a_3, a_4\}$, $\mathcal{P}_2 = \{a_1, a_2, a_3, a_4\}$ and $\mathcal{Q}_1$ & $\mathcal{Q}_2$ independently, as shown in Figs. 11 and 12.

Case I: $\because a_1 \in P_2$ but $a_1 \notin P_1$. Thus, $\deg_{\mathcal{G}_1\cup\mathcal{G}_2} \mu^+e^{i\alpha}(a_1) = \deg_{\mathcal{G}_2} \mu^+e^{i\alpha}(a_1) = 0.8e^{i2\pi(0.8)}$ $\deg_{\mathcal{G}_1\cup\mathcal{G}_2} \mu^-e^{i\beta}(a_1) = \deg_{\mathcal{G}_2} \mu^-e^{i\beta}(a_1) = -0.4e^{i2\pi(1.2)}$, $\deg_{\mathcal{G}_1\cup\mathcal{G}_2} \nu^+e^{i\gamma}(a_1) = \deg_{\mathcal{G}_2} \nu^+e^{i\gamma}(a_1) = 0.8e^{i2\pi(0.7)}$, $\deg_{\mathcal{G}_1\cup\mathcal{G}_2} \nu^-e^{i\delta}(a_1) = \deg_{\mathcal{G}_2} \nu^-e^{i\delta}(a_1) = -1.0e^{i2\pi(0.6)}$

$$\therefore \deg_{\mathcal{G}_1\cup\mathcal{G}_2}(a_1) = \deg_{\mathcal{G}_2}(a_1) = \left(0.8e^{i2\pi(0.8)}, -0.4e^{i2\pi(1.2)}, 0.8e^{i2\pi(0.7)}, -1.0e^{i2\pi(0.6)}\right)$$

$$\therefore T\deg_{\mathcal{G}_1\cup\mathcal{G}_2}(a_1) = \left(T\deg_{\mathcal{G}_2} \mu^+e^{i\alpha}(a_1), T\deg_{\mathcal{G}_2} \mu^-e^{i\beta}(a_1), T\deg_{\mathcal{G}_2} \nu^+e^{i\gamma}(a_1), T\deg_{\mathcal{G}_2} \nu^-e^{i\delta}(a_1)\right),$$

$$= \left(1.7e^{i2\pi(1.7)}, -1.2e^{i2\pi(1.8)}, 1.2e^{i2\pi(1.1)} - 1.6e^{i2\pi(1.0)}\right).$$

Case II: Choose $a_4 \in P_1 \cap P_2$, and it lies in $Q_1 \cap Q_2$ with no edges incidence

$$\therefore \deg_{\mathcal{G}_1\cup\mathcal{G}_2}(a_4) = \deg_{\mathcal{G}_1}(a_4) + \deg_{\mathcal{G}_2}(a_4) = \left(1.1e^{i2\pi(1.1)}, -0.4e^{i2\pi(1.4)}, 0.9e^{i2\pi(1.1)}, -0.9e^{i2\pi(0.3)}\right)$$

$$T\deg_{\mathcal{G}_1}(a_4) = \left(0.9e^{i2\pi(0.8)}, -0.2e^{i2\pi(1.1)}, 1.0e^{i2\pi(0.5)}, -0.6e^{i2\pi(0.2)}\right);$$

$$Tdeg_{\mathcal{G}_2}(a_4) = \left(1.8e^{i2\pi(1.4)}, -0.6e^{i2\pi(1.1)}, 0.8e^{i2\pi(1.3)}, -1.1e^{i2\pi(0.4)}\right)$$

$$\therefore T\deg_{\mathcal{G}_1\cup\mathcal{G}_2}(a_4) = \left(2.0e^{i2\pi(1.8)}, -0.7e^{i2\pi(1.8)}, 1.2e^{i2\pi(1.3)}, -1.2e^{i2\pi(0.5)}\right).$$

Case III: $\because a_2 \in P_1 \cap P_2$ and $a_2a_3 \in Q_1 \cap Q_2$.

Then $\deg_{\mathcal{G}_1}(a_2) = \left(0.4e^{i2\pi(0.9)}, -0.4e^{i2\pi(1.6)}, 0.9e^{i2\pi(0.5)}, -0.8e^{i2\pi(0.6)}\right)$

$$\deg_{\mathcal{G}_2}(a_2) = \left(1.0e^{i2\pi(0.9)}, -0.3e^{i2\pi(1.2)}, 1.3e^{i2\pi(0.6)}, -1.3e^{i2\pi(0.8)}\right)$$

$$\therefore \deg_{\mathcal{G}_1\cup\mathcal{G}_2}(a_1) = \left(1.2e^{i2\pi(1.4)}, -0.6e^{i2\pi(1.9)}, 1.5e^{i2\pi(0.8)}, -1.5e^{i2\pi(1.1)}\right)$$

$$\therefore T\deg_{\mathcal{G}_1}(a_1) = \left(0.7e^{i2\pi(1.8)}, -0.9e^{i2\pi(2.3)}, 1.3e^{i2\pi(0.8)}, -141e^{i2\pi(1.0)}\right)$$

$$T\deg_{\mathcal{G}_2}(a_1) = \left(1.3e^{i2\pi(1.8)}, -0.8e^{i2\pi(1.9)}, 1.7e^{i2\pi(0.9)}, -1.9e^{i2\pi(1.2)}\right)$$

$$\therefore T\deg_{\mathcal{G}_1\cup\mathcal{G}_2}(a_1) = \left(1.5e^{i2\pi(2.2)}, -1.3e^{i2\pi(2.6)}, 1.5e^{i2\pi(0.9)}, -1.8e^{i2\pi(1.5)}\right).$$

Definition 3.15 Let $\mathcal{G}_1$ and $\mathcal{G}_2$ be two $\mathcal{BCPFG}s$. If any vertex $\xi \in P_1 \oplus P_2$, then it considers two cases. Case I: If either $\xi \in P_1 - P_2$ or $\xi \in P_2 - P_1$.

Case II: If $\xi \in P_1 \cap P_2$. Then any edge incident at ξ is either $\xi \in Q_1 - Q_2$ or $\xi \in Q_2 - Q_1$. For both cases

$$\begin{aligned}
&\left(\deg_{\mathcal{G}_1\oplus\mathcal{G}_2}\mu^+e^{i\alpha}(\xi), \deg_{\mathcal{G}_1\oplus\mathcal{G}_2}\mu^-e^{i\beta}(\xi), \deg_{\mathcal{G}_1\oplus\mathcal{G}_2}\nu^+e^{i\gamma}(\xi), \deg_{\mathcal{G}_1\oplus}\nu^-e^{i\delta}(\xi)\right)\\
&= \left(\deg_{\mathcal{G}_1\cup\mathcal{G}_2}\mu^+e^{i\alpha}(\xi), \deg_{\mathcal{G}_1\cup\mathcal{G}_2}\mu^-e^{i\beta}(\xi), \deg_{\mathcal{G}_1\cup\mathcal{G}_2}\nu^+e^{i\gamma}(\xi), \deg_{\mathcal{G}_1\cup\mathcal{G}_2}\nu^-e^{i\delta}(\xi)\right)\\
&\quad\left(T\deg_{\mathcal{G}_1\oplus\mathcal{G}_2}\mu^+e^{i\alpha}(\xi), T\deg_{\mathcal{G}_1\oplus\mathcal{G}_2}\mu^-e^{i\beta}(\xi), T\deg_{\mathcal{G}_1\oplus\mathcal{G}_2}\nu^+e^{i\gamma}(\xi), T\deg_{\mathcal{G}_1\oplus\mathcal{G}_2}\nu^-e^{i\delta}(\xi)\right)\\
&\quad= T\deg_{\mathcal{G}_1\cup\mathcal{G}_2}\mu^+e^{i\alpha}(\xi), T\deg_{\mathcal{G}_1\cup\mathcal{G}_2}\mu^-e^{i\beta}(\xi), T\deg_{\mathcal{G}_1\cup\mathcal{G}_2}\nu^+e^{i\gamma}(\xi), T\deg_{\mathcal{G}_1\cup\mathcal{G}_2}\nu^-e^{i\delta}(\xi)
\end{aligned}$$

Definition 3.16 Let $\mathcal{G}_1$ and $\mathcal{G}_2$ be two $\mathcal{BCPFG}s$. If any vertex $\xi \in P_1 + P_2$, then

$$\begin{aligned}
\deg_{\mathcal{G}_1+\mathcal{G}_2}\mu^+e^{i\alpha}(\xi) &= \sum_{\xi\eta\in Q_1\cup Q_2}\left(\mu^+_{\mathcal{Q}_1}\cup\mu^+_{\mathcal{Q}_2}\right)(\xi\eta)e^{i\sum\limits_{\xi\eta\in Q_1\cup Q_2}\left(\alpha_{\mathcal{Q}_1}\cup\alpha_{\mathcal{Q}_2}\right)(\xi\eta)}\\
&\quad+\sum_{\xi\eta\in Q'}\min\left\{\mu^+_{\mathcal{P}_1}(\xi), \mu^+_{\mathcal{P}_2}(\xi)\right\}e^{i\sum\limits_{\xi\eta\in Q'}\min\left\{\alpha_{\mathcal{P}_1}(\xi),\alpha_{\mathcal{P}_2}(\eta)\right\}}
\end{aligned}$$

$$\begin{aligned}
\deg_{\mathcal{G}_1+\mathcal{G}_2}\mu^-e^{i\beta}(\xi) &= \sum_{\xi\eta\in Q_1\cup Q_2}\left(\mu^-_{\mathcal{Q}_1}\cup\mu^-_{\mathcal{Q}_2}\right)(\xi\eta)e^{i\sum\limits_{\xi\eta\in Q_1\cup Q_2}\left(\beta_{\mathcal{Q}_1}\cup\beta_{\mathcal{Q}_2}\right)(\xi\eta)}\\
&\quad+\sum_{\xi\eta\in Q'}\max\left\{\mu^-_{\mathcal{P}_1}(\xi), \mu^-_{\mathcal{P}_2}(\xi)\right\}e^{i\sum\limits_{\xi\eta\in Q'}\max\left\{\beta_{\mathcal{P}_1}(\xi),\beta_{\mathcal{P}_2}(\eta)\right\}}
\end{aligned}$$

$$\begin{aligned}
\deg_{\mathcal{G}_1+\mathcal{G}_2}\nu^+e^{i\gamma}(\xi) &= \sum_{\xi\eta\in Q_1\cup Q_2}\left(\nu^+_{\mathcal{Q}_1}\cup\nu^+_{\mathcal{Q}_2}\right)(\xi\eta)e^{i\sum\limits_{\xi\eta\in Q_1\cup Q_2}\left(\gamma_{\mathcal{Q}_1}\cup\gamma_{\mathcal{Q}_2}\right)(\xi\eta)}\\
&\quad+\sum_{\xi\eta\in Q'}\min\left\{\nu^+_{\mathcal{P}_1}(\xi), \nu^+_{\mathcal{P}_2}(\xi)\right\}e^{i\sum\limits_{\xi\eta\in Q'}\min\left\{\gamma_{\mathcal{P}_1}(\xi),\gamma_{\mathcal{P}_2}(\eta)\right\}}
\end{aligned}$$

$$\deg_{\mathcal{G}_1+\mathcal{G}_2}\nu^-e^{i\delta}(\xi) = \sum_{\xi\eta\in Q_1\cup Q_2}\left(\nu^-_{\mathcal{Q}_1}\cup\nu^-_{\mathcal{Q}_2}\right)(\xi\eta)e^{i\sum\limits_{\xi\eta\in Q_1\cup Q_2}\left(\delta_{\mathcal{Q}_1}\cup\gamma_{\mathcal{Q}_2}\right)(\xi\eta)}$$

$$+\sum_{\xi\eta\in Q'}\max\left\{\nu^-_{\mathcal{P}_1}(\xi),\nu^-_{\mathcal{P}_2}(\xi)\right\}e^{i\sum\limits_{\xi\eta\in Q'}\max\left\{\delta_{\mathcal{P}_1}(\xi),\delta_{\mathcal{P}_2}(\eta)\right\}}$$

$$T\deg_{\mathcal{G}_1+\mathcal{G}_2}\mu^+e^{i\alpha}(\xi)=\sum_{\xi\eta\in Q_1\cup Q_2}\left(\mu^+_{\mathcal{Q}_1}\cup\mu^+_{\mathcal{Q}_2}\right)(\xi\eta)e^{i\sum\limits_{\xi\eta\in Q_1\cup Q_2}\left(\alpha_{\mathcal{Q}_1}\cup\alpha_{\mathcal{Q}_2}\right)(\xi\eta)}$$
$$+\sum_{\xi\eta\in Q'}\min\left\{\mu^+_{\mathcal{P}_1}(\xi),\mu^+_{\mathcal{P}_2}(\xi)\right\}e^{i\sum\limits_{\xi\eta\in Q'}\min\left\{\alpha_{\mathcal{P}_1}(\xi),\alpha_{\mathcal{P}_2}(\xi)\right\}}$$
$$+\max\left\{\mu^+_{\mathcal{P}_1}(\xi),\mu^+_{\mathcal{P}_2}(\eta)\right\}e^{i\max\left\{\alpha_{\mathcal{P}_1}(\xi),\alpha_{\mathcal{P}_2}(\eta)\right\}}$$

$$T\deg_{\mathcal{G}_1+\mathcal{G}_2}\mu^-e^{i\beta}(\xi)=\sum_{\xi\eta\in Q_1\cup Q_2}\left(\mu^-_{\mathcal{Q}_1}\cup\mu^-_{\mathcal{Q}_2}\right)(\xi\eta)e^{i\sum\limits_{\xi\eta\in Q_1\cup Q_2}\left(\beta_{\mathcal{Q}_1}\cup\beta_{\mathcal{Q}_2}\right)(\xi\eta)}$$
$$+\sum_{\xi\eta\in Q'}\max\left\{\mu^-_{\mathcal{P}_1}(\xi),\mu^-_{\mathcal{P}_2}(\xi)\right\}e^{i\sum\limits_{\xi\eta\in Q'}\max\left\{\beta_{\mathcal{P}_1}(\xi),\beta_{\mathcal{P}_2}(\xi)\right\}}$$
$$+\min\left\{\mu^-_{\mathcal{P}_1}(\xi),\mu^-_{\mathcal{P}_2}(\eta)\right\}e^{i\min\left\{\beta_{\mathcal{P}_1}(\xi),\beta_{\mathcal{P}_2}(\eta)\right\}}$$

$$T\deg_{\mathcal{G}_1+\mathcal{G}_2}\nu^+e^{i\gamma}(\xi)=\sum_{\xi\eta\in Q_1\cup Q_2}\left(\nu^+_{\mathcal{Q}_1}\cup\nu^+_{\mathcal{Q}_2}\right)(\xi\eta)e^{i\sum\limits_{\xi\eta\in Q_1\cup Q_2}\left(\gamma_{\mathcal{Q}_1}\cup\gamma_{\mathcal{Q}_2}\right)(\xi\eta)}$$
$$+\sum_{\xi\eta\in Q'}\min\left\{\nu^+_{\mathcal{P}_1}(\xi),\nu^+_{\mathcal{P}_2}(\xi)\right\}e^{i\sum\limits_{\xi\eta\in Q'}\min\left\{\gamma_{\mathcal{P}_1}(\xi),\gamma_{\mathcal{P}_2}(\xi)\right\}}$$
$$+\max\left\{\nu^+_{\mathcal{P}_1}(\xi),\nu^+_{\mathcal{P}_2}(\eta)\right\}e^{i\max\left\{\gamma_{\mathcal{P}_1}(\xi),\gamma_{\mathcal{P}_2}(\eta)\right\}}$$

$$T\deg_{\mathcal{G}_1+\mathcal{G}_2}\nu^-e^{i\delta}(\xi)=\sum_{\xi\eta\in Q_1\cup Q_2}\left(\nu^-_{\mathcal{Q}_1}\cup\nu^-_{\mathcal{Q}_2}\right)(\xi\eta)e^{i\sum\limits_{\xi\eta\in Q_1\cup Q_2}\left(\delta_{\mathcal{Q}_1}\cup\delta_{\mathcal{Q}_2}\right)(\xi\eta)}$$
$$+\sum_{\xi\eta\in Q'}\max\left\{\nu^-_{\mathcal{P}_1}(\xi),\mu^-_{\mathcal{P}_2}(\xi)\right\}e^{i\sum\limits_{\xi\eta\in Q'}\max\left\{\delta_{\mathcal{P}_1}(\xi),\delta_{\mathcal{P}_2}(\xi)\right\}}$$
$$+\min\left\{\nu^-_{\mathcal{P}_1}(\xi),\nu^-_{\mathcal{P}_2}(\eta)\right\}e^{i\min\left\{\delta_{\mathcal{P}_1}(\xi),\delta_{\mathcal{P}_2}(\eta)\right\}}$$

4 Regular and Edge Regular Bipolar Complex Pythagorean Fuzzy Graphs

In this section, the concepts of $\mathcal{RBCPFG}$, $\mathcal{TRBCPFG}$, $\mathcal{ERBCPFG}$ and $\mathcal{TERBCPFG}$ s are defined, and several characterizations are discussed.

Definition 4.1 Let $\mathcal{G} = (\mathcal{P}, \mathcal{Q})$ be a $\mathcal{BCPFG}$ of G^*. Then $\mathcal{G}$ is said to be $(\xi_1, \xi_2, \xi_3, \xi_4)$ regular $\mathcal{BCPFG}(inshort\mathcal{RBCPFG})$ if each vertex has the same degree-$(\xi_1, \xi_2, \xi_3, \xi_4)$.

$$(i.e.)\ \deg_{\mathcal{G}(\xi_i)} = \left(\deg \mu^+ e^{i\alpha}(\xi), \deg \mu^- e^{i\beta}(\xi), \deg \nu^+ e^{i\gamma}(\xi), \deg \nu^+ e^{i\delta}(\xi)\right)$$
$$= (\xi_1, \xi_2, \xi_3, \xi_4) \forall \xi \in P,$$

where $\deg \mu^+ e^{i\alpha}(\xi) = \sum_{\xi,\eta \neq \xi \in P} \mu^+_{\mathcal{Q}}(\xi\eta) e^{i \sum_{\xi,\eta \neq \xi \in P} \alpha_{\mathcal{Q}}(\xi\eta)} = \xi_1,$

$$\deg \mu^- e^{i\beta}(\xi) = \sum_{\xi,\eta \neq \xi \in P} \mu^-_{\mathcal{Q}}(\xi\eta) e^{i \sum_{\xi,\eta \neq \xi \in P} \beta_{\mathcal{Q}}(\xi\eta)} = \xi_2,$$

$$\deg \nu^+ e^{i\gamma}(\xi) = \sum_{\xi,\eta \neq \xi \in P} \nu^+_{\mathcal{Q}}(\xi\eta) e^{i \sum_{\xi,\eta \neq \xi \in P} \gamma_{\mathcal{Q}}(\xi\eta)} = \xi_3,$$

$$\deg \nu^- e^{i\delta}(\xi) = \sum_{\xi,\eta \neq \xi \in P} \nu^-_{\mathcal{Q}}(\xi\eta) e^{i \sum_{\xi,\eta \neq \xi \in P} \delta_{\mathcal{Q}}(\xi\eta)} = \xi_4, \mathcal{G} \text{ is called regular of degree-}$$

$(\xi_1, \xi_2, \xi_3, \xi_4)$.

Definition 4.2 Let $\mathcal{G} = (\mathcal{P}, \mathcal{Q})$ be a $\mathcal{BCPFG}$. Then $\mathcal{G}$ is said to be totally regular $\mathcal{TRBCPFG}$ (in short $\mathcal{TRBCPFG}$) if every vertex has the same total degree-$(\tau_1, \tau_2, \tau_3, \tau_4)$ $(i.e.)$

$$T \deg_{\mathcal{G}}(\xi_i) = \left(T \deg \mu^+ e^{i\alpha}(\xi), T \deg \mu^- e^{i\beta}(\xi), T \deg \nu^+ e^{i\gamma}(\xi), T \deg \nu^+ e^{i\delta}(\xi)\right)$$
$$= (\tau_1, \tau_2, \tau_3, \tau_4) \forall \xi_i \in P,$$

where

$$T \deg \mu^+ e^{i\alpha}(\xi) = \sum_{\xi,\eta \neq \xi \in P} \mu^+_{\mathcal{Q}}(\xi\eta) e^{i \sum_{\xi,\eta \neq \xi \in P} \alpha_{\mathcal{Q}}(\xi\eta)} + \mu^+_{\mathcal{P}}(\xi) e^{i\alpha_{\mathcal{P}}(\xi)} = \tau_1,$$

$$T \deg \mu^- e^{i\beta}(\xi) = \sum_{\xi,\eta \neq \xi \in P} \mu^-_{\mathcal{Q}}(\xi\eta) e^{i \sum_{\xi,\eta \neq \xi \in P} \beta_{\mathcal{Q}}(\xi\eta)} + \mu^-_{\mathcal{P}}(\xi) e^{i\beta_{\mathcal{P}}(\xi)} = \tau_2,$$

$$T \deg \nu^+ e^{i\gamma}(\xi) = \sum_{\xi,\eta \neq \xi \in P} \nu^+_{\mathcal{Q}}(\xi\eta) e^{i \sum_{\xi,\eta \neq \xi \in P} \gamma_{\mathcal{Q}}(\xi\eta)} + \nu^+_{\mathcal{P}}(\xi) e^{i\gamma_{\mathcal{P}}(\xi)} = \tau_3,$$

$$T \deg \nu^- e^{i\delta}(\xi) = \sum_{\xi,\eta \neq \xi \in P} \nu^-_{\mathcal{Q}}(\xi\eta) e^{i \sum_{\xi,\eta \neq \xi \in P} \delta_{\mathcal{Q}}(\xi\eta)} + \nu^-_{\mathcal{P}}(\xi) e^{i\delta_{\mathcal{P}}(\xi)} = \tau_4,$$

$\mathcal{G}$ is called totally regular of degree-$(\tau_1, \tau_2, \tau_3, \tau_4)$.

Remark 4.1 There is no relationship between $(\xi_1, \xi_2, \xi_3, \xi_4)$-$\mathcal{RBCPFG}$ and $(\tau_1, \tau_2, \tau_3, \tau_4)$-$\mathcal{TRBCPFG}$.

Proposition 4.1 For a $(\xi_1, \xi_2, \xi_3, \xi_4)$-$\mathcal{RBCPFG}$. Then $\mathfrak{S}(\mathcal{G}) = \left(\frac{n\xi_1}{2}, \frac{n\xi_2}{2}, \frac{n\xi_3}{2}, \frac{n\xi_4}{2}\right)$, where $|P| = n$.

Proposition 4.2 Let $\mathcal{G} = (\mathcal{P}, \mathcal{Q})$ be a $(\tau_1, \tau_2, \tau_3, \tau_4)$-$\mathcal{TRBCPFG}$. Then, $2\mathfrak{S}(\mathcal{G}) + \mathfrak{O}(\mathcal{G}) = (n\tau_1, n\tau_2, n\tau_3, n\tau_4)$, where $|P| = n$.

Proposition 4.3 Let $\mathcal{G} = (\mathcal{P}, \mathcal{Q})$ be a $(\xi_1, \xi_2, \xi_3, \xi_4)$-$\mathcal{RBCPFG}$ and $(\tau_1, \tau_2, \tau_3, \tau_4)$-$\mathcal{TRBCPFG}$. Then, $\mathcal{O}(\mathcal{G}) = n\{(\tau_1, \tau_2, \tau_3, \tau_4) - (\xi_1, \xi_2, \xi_3, \xi_4)\}$.

Definition 4.3 *A $\mathcal{BCPFG}, \mathcal{G} = (\mathcal{P}, \mathcal{Q})$ is complete $\mathcal{BCPFG}$* if

$$\mu_{\mathcal{Q}}^{+}(\xi\eta)e^{i\alpha_{\mathcal{Q}}(\xi\eta)} = \min\left\{\mu_{P}^{+}(\xi), \mu_{P}^{+}(\eta)\right\}e^{i\min\{\alpha_P(\xi),\alpha_P(\eta)\}}$$

$$\mu_{\mathcal{Q}}^{-}(\xi\eta)e^{i\beta_{\mathcal{Q}}(\xi\eta)} = \min\left\{\mu_{P}^{-}(\xi), \mu_{P}^{-}(\eta)\right\}e^{i\max\{\beta_P(\xi),\beta_P(\eta)\}}$$

$$\nu_{\mathcal{Q}}^{+}(\xi\eta)e^{i\gamma_{\mathcal{Q}}(\xi\eta)} = \max\left\{\nu_{P}^{+}(\xi), \nu_{P}^{+}(\eta)\right\}e^{i\max\{\gamma_P(\xi),\gamma_P(\eta)\}}$$

$$\nu_{\mathcal{Q}}^{-}(\xi\eta)e^{i\delta_{\mathcal{Q}}(\xi\eta)} = \min\left\{\nu_{P}^{-}(\xi), \nu_{P}^{-}(\eta)\right\}e^{i\min\{\delta_P(\xi),\delta_P(\eta)\}}.$$

Remark 4.2 Every complete $\mathcal{BCPFG}$ is a $\mathcal{TRBCPFG}$.

Proposition 4.4 Let $\mathcal{G} = (\mathcal{P}, \mathcal{Q})$ be a $\mathcal{BCPFG}$ of a graph G^*. Then $\mathcal{Q} = \left(\mu_{\mathcal{Q}}^{+}(\xi)e^{i\alpha_{\mathcal{Q}}}, \mu_{\mathcal{Q}}^{-}e^{i\beta_{\mathcal{Q}}}, \nu_{\mathcal{Q}}^{+}e^{i\gamma_{\mathcal{Q}}}, \nu_{\mathcal{Q}}^{-}e^{i\delta_{\mathcal{Q}}}\right)$ is a constant mapping iff the equivalent statement as follows (i) $\mathcal{G}$ is a $n\mathcal{RBCPFG}$. (ii) $\mathcal{G}$ is a $\mathcal{TRBCPFG}$.

Example 4.1 Consider a $\mathcal{BCPFG}, \mathcal{G} = (\mathcal{P}, \mathcal{Q})$ on $P = \{a_1, a_2, a_3, a_4, a_5, a_6\}$ and $\mathcal{Q} = \{a_1a_2, a_2a_3, a_2a_5, a_1a_3, a_3a_4, a_1a_6, a_4a_5, a_4a_6, a_5a_6\}$ is defined as in Fig. 13.

Proposition 4.5 If a $\mathcal{BCPFG}$, $\mathcal{G}$ is an $\mathcal{RBCPFG}$ and also $\mathcal{TRBCPFG}$, then $\mathcal{P} = \left(\mu_{\mathcal{P}}^{+}(\xi)e^{i\alpha_{\mathcal{P}}}, \mu_{\mathcal{P}}^{-}e^{i\beta_{\mathcal{P}}}, \nu_{\mathcal{P}}^{+}e^{i\gamma_{\mathcal{P}}}, \nu_{\mathcal{P}}^{-}e^{i\delta_{\mathcal{P}}}\right)$ is a constant function.

Proposition 4.6 Let $\mathcal{G}_1 = (\mathcal{P}_1, \mathcal{Q}_1)$ and $\mathcal{G}_2 = (\mathcal{P}_2, \mathcal{Q}_2)$ be two $\mathcal{BCPFG}$s and $\mathcal{G}_1 \cong \mathcal{G}_2$: (i) If $\mathcal{G}_1$ is $\mathcal{RBCPFG}$, then $\mathcal{G}_2$ is $\mathcal{RBCPFG}$.

(ii) If $\mathcal{G}_1$ is $\mathcal{TRBCPFG}$, then $\mathcal{G}_2$ is $\mathcal{TRBCPFG}$.

Example 4.2 Consider a $\mathcal{BCPFG}, \mathcal{G} = (\mathcal{P}, \mathcal{Q})$ on $P = \{a_1, a_2, a_3, a_4, a_5, a_6\}$ and $\mathcal{Q} = \{a_1a_2, a_2a_3, a_2a_5, a_1a_3, a_3a_4, a_1a_6, a_4a_5, a_4a_6, a_5a_6\}$ is defined as in Fig. 14.

Definition 4.4 Let $\mathcal{G} = (\mathcal{P}, \mathcal{Q})$ be a $\mathcal{BCPFG}$ on G^*. Then the degree of an edge $\xi_i\xi_j \in \mathcal{Q}$ is in G^* is defined by

$$(i.e.)\ \deg_{\mathcal{G}}(\xi_i\xi_j) = \left(\deg_{\mathcal{G}} \mu^{+}e^{i\alpha}(\xi_i\xi_j), \deg_{\mathcal{G}} \mu^{-}e^{i\beta}(\xi_i\xi_j), \deg_{\mathcal{G}} \nu^{+}e^{i\gamma}(\xi_i\xi_j), \deg_{\mathcal{G}} \nu^{+}e^{i\delta}(\xi_i\xi_j)\right)\forall \xi \in P,$$

where

$$\deg \mu^{+}e^{i\alpha}(\xi_i\xi_j) = \deg \mu^{+}e^{i\alpha}(\xi_i) + \deg \mu^{+}e^{i\alpha}(\xi_j) - 2\mu_{\mathcal{Q}}^{+}(\xi_i\xi_j)e^{i2\alpha_{\mathcal{Q}}(\xi_i\xi_j)}$$

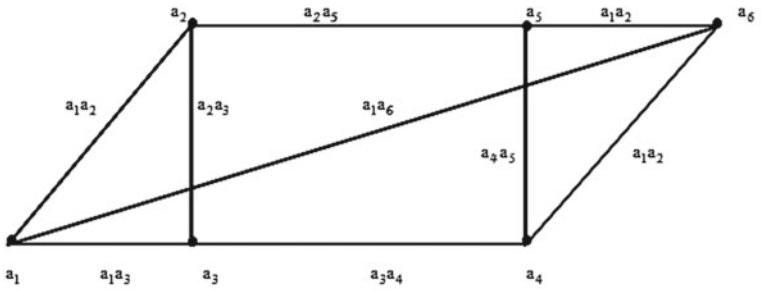

$a_1(0.5e^{i2\pi(0.5)}, -0.4e^{i2\pi(0.1)}, 0.6e^{i2\pi(0.1)}, -0.1e^{i2\pi(0.1)})$ $a_1a_3(0.3e^{i2\pi(0.1)}, -0.3e^{i2\pi(0.2)}, 0.2e^{i2\pi(0.1)}, -0.3e^{i2\pi(0.2)})$

$a_2(0.6e^{i2\pi(0.7)}, -0.7e^{i2\pi(0.2)}, 0.3e^{i2\pi(0.1)}, -0.1e^{i2\pi(0.1)})$ $a_3a_4(0.2e^{i2\pi(0.2)}, -0.3e^{i2\pi(0.3)}, 0.3e^{i2\pi(0.1)}, -0.1e^{i2\pi(0.1)})$

$a_3(0.4e^{i2\pi(0.7)}, -0.7e^{i2\pi(0.1)}, 0.6e^{i2\pi(0.5)}, -0.1e^{i2\pi(0.1)})$ $a_1a_6(0.2e^{i2\pi(0.2)}, -0.2e^{i2\pi(0.2)}, 0.4e^{i2\pi(0.4)}, -0.1e^{i2\pi(0.1)})$

$a_4(0.8e^{i2\pi(0.4)}, -0.6e^{i2\pi(0.1)}, 0.3e^{i2\pi(0.1)}, -0.3e^{i2\pi(0.1)})$ $a_4a_5(0.2e^{i2\pi(0.2)}, -0.2e^{i2\pi(0.2)}, 0.4e^{i2\pi(0.4)}, -0.1e^{i2\pi(0.1)})$

$a_5(0.7e^{i2\pi(0.3)}, -0.6e^{i2\pi(0.1)}, 0.4e^{i2\pi(0.1)}, -0.5e^{i2\pi(0.1)})$ $a_4a_6(0.3e^{i2\pi(0.1)}, -0.3e^{i2\pi(0.2)}, 0.2e^{i2\pi(0.1)}, -0.3e^{i2\pi(0.2)})$

$a_6(0.7e^{i2\pi(0.3)}, -0.8e^{i2\pi(0.2)}, 0.4e^{i2\pi(0.1)}, -0.5e^{i2\pi(0.1)})$ $a_5a_6(0.2e^{i2\pi(0.2)}, -0.3e^{i2\pi(0.3)}, 0.3e^{i2\pi(0.1)}, -0.1e^{i2\pi(0.1)})$

$a_2a_5(0.3e^{i2\pi(0.1)}, -0.3e^{i2\pi(0.2)}, 0.2e^{i2\pi(0.1)}, -0.3e^{i2\pi(0.2)})$ $a_1a_2(0.2e^{i2\pi(0.2)}, -0.3e^{i2\pi(0.3)}, 0.3e^{i2\pi(0.1)}, -0.1e^{i2\pi(0.1)})$

$(0.2e^{i2\pi(0.2)}, -0.2e^{i2\pi(0.2)}, 0.4e^{i2\pi(0.4)}, -0.1e^{i2\pi(0.1)})a_2a_3$

Fig. 13 $\mathcal{RBCPFG}$

$$= \sum_{\xi_i,\xi_k \in Q \quad k\neq j} \mu^{+}_{Q}(\xi_i\xi_k) e^{\,i \sum\limits_{\xi_i,\xi_k \in Qk\neq j} \alpha_{Q}(\xi_i\xi_k)} + \sum_{\xi_j,\xi_k \in Qk\neq i} \mu^{+}_{Q}(\xi_j\xi_k) e^{\,i \sum\limits_{\xi_j,\xi_k \in Qk\neq i} \alpha_{Q}(\xi_j\xi_k)}$$

(or)

$$\deg \mu^{-} e^{i\beta}(\xi_i\xi_j) = \deg \mu^{-} e^{i\beta}(\xi_i) + \deg \mu^{-} e^{i\beta}(\xi_j) - 2\mu^{-}_{Q}(\xi_i\xi_j) e^{i2\beta_{Q}(\xi_i\xi_j)}$$

$$= \sum_{\xi_i,\xi_k \in Qk\neq j} \mu^{-}_{Q}(\xi_i\xi_k) e^{\,i \sum\limits_{\xi_i,\xi_k \in Qk\neq j} \beta_{Q}(\xi_i\xi_k)} + \sum_{\xi_j,\xi_k \in Qk\neq i} \mu^{-}_{Q}(\xi_j\xi_k) e^{\,i \sum\limits_{\xi_j,\xi_k \in Qk\neq i} \beta_{Q}(\xi_j\xi_k)}$$

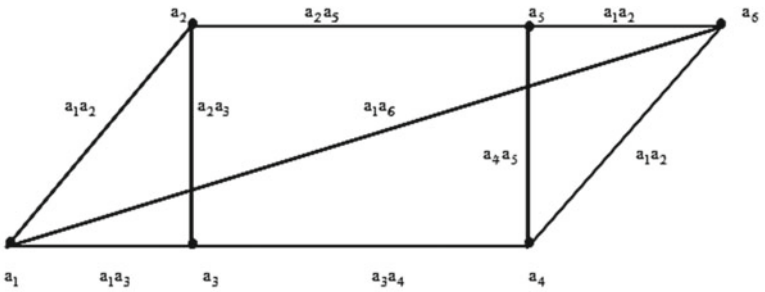

$a_1(0.5e^{i2\pi(0.5)}, -0.4e^{i2\pi(0.1)}, 0.6e^{i2\pi(0.1)}, -0.1e^{i2\pi(0.1)})$ $a_1a_3(0.3e^{i2\pi(0.1)}, -0.3e^{i2\pi(0.2)}, 0.2e^{i2\pi(0.1)}, -0.3e^{i2\pi(0.2)})$

$a_2(0.6e^{i2\pi(0.7)}, -0.7e^{i2\pi(0.2)}, 0.3e^{i2\pi(0.1)}, -0.1e^{i2\pi(0.1)})$ $a_3a_4(0.2e^{i2\pi(0.2)}, -0.3e^{i2\pi(0.3)}, 0.3e^{i2\pi(0.1)}, -0.1e^{i2\pi(0.1)})$

$a_3(0.4e^{i2\pi(0.7)}, -0.7e^{i2\pi(0.1)}, 0.6e^{i2\pi(0.5)}, -0.1e^{i2\pi(0.1)})$ $a_1a_6(0.2e^{i2\pi(0.2)}, -0.2e^{i2\pi(0.2)}, 0.4e^{i2\pi(0.4)}, -0.1e^{i2\pi(0.1)})$

$a_4(0.8e^{i2\pi(0.4)}, -0.6e^{i2\pi(0.1)}, 0.3e^{i2\pi(0.1)}, -0.3e^{i2\pi(0.1)})$ $a_4a_5(0.2e^{i2\pi(0.2)}, -0.2e^{i2\pi(0.2)}, 0.4e^{i2\pi(0.4)}, -0.1e^{i2\pi(0.1)})$

$a_5(0.7e^{i2\pi(0.3)}, -0.6e^{i2\pi(0.1)}, 0.4e^{i2\pi(0.1)}, -0.5e^{i2\pi(0.1)})$ $a_4a_6(0.3e^{i2\pi(0.1)}, -0.3e^{i2\pi(0.2)}, 0.2e^{i2\pi(0.1)}, -0.3e^{i2\pi(0.2)})$

$a_6(0.7e^{i2\pi(0.3)}, -0.8e^{i2\pi(0.2)}, 0.4e^{i2\pi(0.1)}, -0.5e^{i2\pi(0.1)})$ $a_5a_6(0.2e^{i2\pi(0.2)}, -0.3e^{i2\pi(0.3)}, 0.3e^{i2\pi(0.1)}, -0.1e^{i2\pi(0.1)})$

$a_2a_5(0.3e^{i2\pi(0.1)}, -0.3e^{i2\pi(0.2)}, 0.2e^{i2\pi(0.1)}, -0.3e^{i2\pi(0.2)})$ $a_1a_2(0.2e^{i2\pi(0.2)}, -0.3e^{i2\pi(0.3)}, 0.3e^{i2\pi(0.1)}, -0.1e^{i2\pi(0.1)})$

$(0.2e^{i2\pi(0.2)}, -0.2e^{i2\pi(0.2)}, 0.4e^{i2\pi(0.4)}, -0.1e^{i2\pi(0.1)})a_2a_3$

Fig. 14 $\mathcal{TRBCPFG}$

$$\begin{aligned}\deg \nu^{+}e^{i\gamma}\left(\xi_i\xi_j\right) &= \deg \nu^{+}e^{i\gamma}(\xi_i) + \deg \nu^{+}e^{i\gamma}\left(\xi_j\right) - 2\nu^{+}_{\mathcal{Q}}\left(\xi_i\xi_j\right)e^{i2\gamma_{\mathcal{Q}}(\xi_i\xi_j)} \\ &= \sum_{\xi_i,\xi_k\in Qk\neq j} \nu^{+}_{\mathcal{Q}}(\xi_i\xi_k)e^{\,i\sum\limits_{\xi_i,\xi_k\in Qk\neq j}\gamma_{\mathcal{Q}}(\xi_i\xi_k)} \\ &\quad + \sum_{\xi_j,\xi_k\in Qk\neq i} \nu^{+}_{\mathcal{Q}}\left(\xi_j\xi_k\right)e^{\,i\sum\limits_{\xi_j,\xi_k\in Qk\neq i}\gamma_{\mathcal{Q}}\left(\xi_j\xi_k\right)}\end{aligned}$$

$$\begin{aligned}&\deg \nu^{-}e^{i\delta}\left(\xi_i\xi_j\right) = \deg \nu^{-}e^{i\delta}(\xi_i) + \deg \nu^{-}e^{i\delta}\left(\xi_j\right) - 2\nu^{-}_{\mathcal{Q}}\left(\xi_i\xi_j\right)e^{i2\delta_{\mathcal{Q}}\left(\xi_i\xi_j\right)} \\ &= \sum_{\xi_i,\xi_k\in Qk\neq j} \nu^{-}_{\mathcal{Q}}(\xi_i\xi_k)e^{\,i\sum\limits_{\xi_i,\xi_k\in Qk\neq j}\delta_{\mathcal{Q}}(\xi_i\xi_k)} + \sum_{\xi_j,\xi_k\in Qk\neq i} \nu^{-}_{\mathcal{Q}}\left(\xi_j\xi_k\right)e^{\,i\sum\limits_{\xi_j,\xi_k\in Qk\neq i}\delta_{\mathcal{Q}}\left(\xi_j\xi_k\right)}.\end{aligned}$$

Definition 4.5 Let $\mathcal{G} = (\mathcal{P}, \mathcal{Q})$ be a $\mathcal{BCPFG}$. Then (i) the minimum edge degree of a $\mathcal{BCPFG}$, $\mathcal{G}$ is $\delta_{\mathcal{Q}_\mathcal{G}} = \left(\delta_\mathcal{G}\mu^{+}, \delta_\mathcal{G}\mu^{-}, \delta_\mathcal{G}\nu^{+}, \delta_\mathcal{G}\nu^{-}\right)$ where $\delta_\mathcal{G}\mu^{+} = \min\left\{\deg \mu^{+}e^{i\alpha}\left(\xi_i\xi_j\right) : \xi_i\xi_j \in Q\right\}, \delta_\mathcal{G}\mu^{-} = \max\left\{\deg \mu^{-}e^{i\beta}\left(\xi_i\xi_j\right) : \xi_i\xi_j \in Q\right\}$,

$$\delta_{\mathcal{G}}\nu^{+} = \max\{\deg \nu^{+}e^{i\gamma}(\xi_i\xi_j) : \xi_i\xi_j \in Q\}, \delta_{\mathcal{G}}\nu^{-} = \min\{\deg \nu^{-}e^{i\delta}(\xi_i\xi_j) : \xi_i\xi_j Q$$

(ii) the maximum edge degree of a $\mathcal{BCPFG}$, $\mathcal{G}$ is $\Delta_{Q_{\mathcal{G}}} = (\Delta_{\mathcal{G}}\mu^{+}, \Delta_{\mathcal{G}}\mu^{-}, \Delta_{\mathcal{G}}\nu^{+}, \Delta_{\mathcal{G}}\nu^{-})$ where

$\Delta_{\mathcal{G}}\mu^{+} = \max\{\deg \mu^{+}e^{i\alpha}(\xi_i\xi_j) : \xi_i\xi_j \in Q\}$, $\Delta_{\mathcal{G}}\mu^{-} = \min\{\deg \mu^{-}e^{i\beta}(\xi_i\xi_j) : \xi_i\xi_j \in Q\}$, $\Delta_{\mathcal{G}}\nu^{+} = \min\{\deg \nu^{+}e^{i\gamma}(\xi_i\xi_j) : \xi_i\xi_j \in Q\}$, $\Delta_{\mathcal{G}}\nu^{-} = \max\{\deg \nu^{-}e^{i\delta}(\xi_i\xi_j) : \xi_i\xi_j \in Q\}$.

Definition 4.6 Let $\mathcal{G} = (\mathcal{P}, \mathcal{Q})$ be a $\mathcal{BCPFG}$. Then, $\mathcal{G}$ is edge regular if every edge has the same degree (i.e.,)

$$\deg_{\mathcal{G}}(\xi_i\xi_j) = (\deg_{\mathcal{G}} \mu^{+}e^{i\alpha}(\xi_i\xi_j), \deg_{\mathcal{G}} \mu^{-}e^{i\beta}(\xi_i\xi_j), \deg_{\mathcal{G}} \nu^{+}e^{i\gamma}(\xi_i\xi_j), \deg_{\mathcal{G}} \nu^{-}e^{i\delta}(\xi_i\xi_j)) \quad \text{for all } \xi_i\xi_j \in Q, \text{ where}$$

$$= (\eta_1, \eta_2, \eta_3, \eta_4)$$

$$\deg_{\mathcal{G}} \mu^{+}e^{i\alpha}(\xi\xi_j) = \sum_{\xi_i,\xi_k\in Q,k\neq j} \mu^{+}_{Q}(\xi_i\xi_k)e^{i\sum_{\xi_i,\xi_k\in Q,k\neq j}\alpha_{Q}(\xi_i\xi_k)} + \sum_{\xi_j,\xi_k\in Q,k\neq i} \mu^{+}_{Q}(\xi_j\xi_k)e^{i\sum_{\xi_j,\xi_k\in Q,k\neq i}\alpha_{Q}(\xi_j\xi_k)} = \eta_1$$

$$deg_{\mathcal{G}}\mu^{-}e^{i\beta}(\xi_i\xi_j) = \sum_{\xi_i,\xi_k\in Q,k\neq j} \mu^{-}_{Q}(\xi_i\xi_k)e^{i\sum_{\xi_i,\xi_k\in Q,k\neq j}\beta_{Q}(\xi_i\xi_k)} + \sum_{\xi_j,\xi_k\in Q,k\neq i} \mu^{-}_{Q}(\xi_j\xi_k)e^{i\sum_{\xi_j,\xi_k\in Q,k\neq i}\beta_{Q}(\xi_j\xi_k)} = \eta_2$$

$$\deg_{\mathcal{G}} \nu^{+}e^{i\gamma}(\xi_i\xi_j) = \sum_{\xi_i,\xi_k\in Q,k\neq j} \nu^{+}_{Q}(\xi_i\xi_k)e^{i\sum_{\xi_i,\xi_k\in Q,k\neq j}\gamma_{Q}(\xi_i\xi_k)} + \sum_{\xi_j,\xi_k\in Q,k\neq i} \nu^{+}_{Q}(\xi_j\xi_k)e^{i\sum_{\xi_j,\xi_k\in Q,k\neq i}\gamma_{Q}(\xi_j\xi_k)} = \eta_3$$

$$\deg_{\mathcal{G}} \nu^{+}e^{i\delta}(\xi_i\xi_j) = \sum_{\xi_i,\xi_k\in Q,k\neq j} \nu^{-}_{Q}(\xi_i\xi_k)e^{i\sum_{\xi_i,\xi_k\in Q,k\neq j}\delta_{Q}(\xi_i\xi_k)} + \sum_{\xi_j,\xi_k\in Q,k\neq i} \nu^{-}_{Q}(\xi_j\xi_k)e^{i\sum_{\xi_j,\xi_k\in Q,k\neq i}\delta_{Q}(\xi_j\xi_k)} = \eta_4 .$$

In $\mathcal{G}$, every edge has the degree $(\eta_1, \eta_2, \eta_3, \eta_4)$ is called edge regular of degree $(\eta_1, \eta_2, \eta_3, \eta_4)$ or $(\eta_1, \eta_2, \eta_3, \eta_4)$-$\mathcal{ERBCPFG}$.

Proposition 4.7 Let $\mathcal{G} = (\mathcal{P}, \mathcal{Q})$ be a $\mathcal{BCPFG}$ on a cycle $G^{*} = (P, Q)$. Then $\sum_{\xi_i\in P} \deg_{\mathcal{G}}(\xi_i) = \sum_{\xi_i\xi_j\in Q} \deg_{\mathcal{G}}(\xi_i\xi_j)$.

Proposition 4.8 For a regular graph G^* of the $\mathcal{BCPFG}$, $\mathcal{G} = (\mathcal{P}, \mathcal{Q})$, then $\sum_{\xi_i\xi_j \in Q} \deg_{\mathcal{G}}(\xi_i\xi_j) =$

$$\left(\sum_{\xi_i\xi_j \in Q} \deg_{\mathcal{G}^*}(\xi_i\xi_j)\,\mu^+(\xi_i\xi_j)e^{i\alpha}(\xi_i\xi_j), \sum_{\xi_i\xi_j \in Q} \deg_{\mathcal{G}^*}(\xi_i\xi_j)\mu^-(\xi_i\xi_j)e^{i\beta}(\xi_i\xi_j),\right.$$

$$\left.\sum_{\xi_i\xi_j \in Q} \deg_{\mathcal{G}^*}(\xi_i\xi_j)\nu^+(\xi_i\xi_j)e^{i\gamma}(\xi_i\xi_j), \sum_{\xi_i\xi_j \in Q} \deg_{\mathcal{G}^*}(\xi_i\xi_j)\nu^+(\xi_i\xi_j)e^{i\delta}(\xi_i\xi_j)\right)$$

where $\deg_{G^*}(\xi_i\xi_j) = \deg_{G^*}(\xi_i) + \deg_{G^*}(\xi_j) - 2, \forall \xi_i\xi_j \in Q$.

Proposition 4.9 Let $\mathcal{G} = (\mathcal{P}, \mathcal{Q})$ be a $\mathcal{BCPFG}$ on G^*, and $\left(\mu^+_{\mathcal{Q}}(\xi)e^{i\alpha_{\mathcal{Q}}}, \mu^-_{\mathcal{Q}}e^{i\beta_{\mathcal{Q}}}, \nu^+_{\mathcal{Q}}e^{i\gamma}_{\mathcal{Q}}, \nu^-_{\mathcal{Q}}e^{i\delta_{\mathcal{Q}}}\right)$ is a constant mapping. Then $\mathcal{G}$ is an $\mathcal{ERBCPFG}$ iff G^* is an edge regular.

Definition 4.7 The total degree of an edge $\xi_i\xi_j \in Q$ in a $\mathcal{BCPFG}, \mathcal{G} = (\mathcal{P}, \mathcal{Q})$ is defined by $(i.e.)T\deg_{\mathcal{G}}(\xi_i\xi_j) = T\deg_{\mathcal{G}}\mu^+e^{i\alpha}(\xi\xi_j)$, $Tdeg_{\mathcal{G}}\mu^-e^{i\beta}(\xi_i\xi_j), Tdeg_{\mathcal{G}}\nu^+e^{i\gamma}(\xi_i\xi_j), Tdeg_{\mathcal{G}}\nu^+e^{i\delta}(\xi_i\xi_j))$ where

$$T\deg\mu^+e^{i\alpha}(\xi_i\xi_j) = \deg\mu^+e^{i\alpha}(\xi_i) + \deg\mu^+e^{i\alpha}(\xi_j)\mu^+_{\mathcal{Q}}(\xi_i\xi_j)e^{i\alpha_{\mathcal{Q}}(\xi_i\xi_j)}$$

$$= \sum_{\xi_i,\xi_k\in Q,k\neq j} \mu^+_{\mathcal{Q}}(\xi_i\xi_k)e^{i\sum\limits_{\xi_i,\xi_k\in Q,k\neq j}\alpha_{\mathcal{Q}}(\xi_i\xi_k)}$$

$$+ \sum_{\xi_j,\xi_k\in Q,k\neq i} \mu^+_{\mathcal{Q}}(\xi_j\xi_k)e^{i\sum\limits_{\xi_j,\xi_k\in Q,k\neq i}\alpha_{\mathcal{Q}}(\xi_j\xi_k)} + \mu^+_{\mathcal{Q}}(\xi_j\xi_k)e^{\alpha_{\mathcal{Q}}(\xi_j\xi_k)}$$

$$T\deg\mu^-e^{i\beta}(\xi_i\xi_j) = \deg\mu^-e^{i\beta}(\xi_i) + \deg\mu^-e^{i\beta}(\xi_j) - \mu_{\mathcal{Q}^-}(\xi_i\xi_j)e^{i\beta_{\mathcal{Q}}(\xi_i\xi_j)}$$

$$= \sum_{\xi_i,\xi_k\in Q,k\neq j} \mu^-_{\mathcal{Q}}(\xi_i\xi_k)e^{i\sum\limits_{\xi_i,\xi_k\in Q,k\neq j}\beta_{\mathcal{Q}}(\xi_i\xi_k)}$$

$$+ \sum_{\xi_j,\xi_k\in Q,k\neq i} \mu^-_{\mathcal{Q}}(\xi_j\xi_k)e^{i\sum\limits_{\xi_j,\xi_k\in Q,k\neq i}\beta_{\mathcal{Q}}(\xi_j\xi_k)} + \mu^-_{\mathcal{Q}}(\xi_i\xi_k)e^{i\beta_{\mathcal{Q}}(\xi_j\xi_k)}$$

$$T\deg\nu^+e^{i\gamma}(\xi_i\xi_j) = \deg\nu^+e^{i\gamma}(\xi_i) + \deg\nu^+e^{i\gamma}(\xi_j) - \nu^+_{\mathcal{Q}}(\xi_i\xi_j)e^{i\gamma_{\mathcal{Q}}(\xi_i\xi_j)}$$

$$= \sum_{\xi_i,\xi_k\in Q,k\neq j} \nu^+_{\mathcal{Q}}(\xi_i\xi_k)e^{i\sum\limits_{\xi_i,\xi_k\in Q,k\neq j}\gamma_{\mathcal{Q}}(\xi_i\xi_k)}$$

$$+ \sum_{\xi_j,\xi_k\in Q,k\neq i} \nu^+_{\mathcal{Q}}(\xi_j\xi_k)e^{i\sum\limits_{\xi_j,\xi_k\in Q,k\neq i}\gamma_{\mathcal{Q}}(\xi_j\xi_k)} + \nu^+_{\mathcal{Q}}(\xi_i\xi_k)e^{i\gamma_{\mathcal{Q}}(\xi_j\xi_k)}$$

$$T\deg\nu^-e^{i\delta}(\xi_i\xi_j) = \deg\nu^-e^{i\delta}(\xi_i) + \deg\nu^-e^{i\delta}(\xi_j) - \nu^-_{\mathcal{Q}}(\xi_i\xi_j)e^{i\delta_{\mathcal{Q}}(\xi_i\xi_j)}$$

$$= \sum_{\xi_i,\xi_k\in Q,k\neq j} \nu^-_{\mathcal{Q}}(\xi_i\xi_k)e^{i\sum\limits_{\xi_i,\xi_k\in Q,k\neq j}\delta_{\mathcal{Q}}(\xi_i\xi_k)}$$

$$+\sum_{\xi_j,\xi_k\in Q,k\neq i}\nu_Q^-\big(\xi_j\xi_k\big)e^{i\sum\limits_{\xi_j,\xi_k\in Q,k\neq i}\delta_Q\left(\xi_j\xi_k\right)}+\nu_Q^-(\xi_i\xi_k)e^{i\delta_Q\left(\xi_j\xi_k\right)}.$$

Definition 4.8 A $\mathcal{BCPFG},\mathcal{G}$ on G^* is said to totally edge regular (in short $\mathcal{TERBCPFG}$) if every edge has the same total degree. If every edge has a total degree $(\rho_1,\rho_2,\rho_3,\rho_4)$ (i.e.,) $\deg_{\mathcal{G}}\big(\xi_i\xi_j\big)=(\rho_1,\rho_2,\rho_3,\rho_4)$ for all $\xi_i\xi_j\in Q$, where

$$\begin{aligned}T\deg_{\mathcal{G}}\mu^+e^{i\alpha}\big(\xi\xi_j\big)&=\sum_{\xi_i,\xi_k\in Q,k\neq j}\mu_Q^+(\xi_i\xi_k)e^{i\sum\limits_{\xi_i,\xi_k\in Q,k\neq j}\alpha_Q\left(\xi_i\xi_k\right)}\\&+\sum_{\xi_j,\xi_k\in Q,k\neq i}\mu_Q^+\big(\xi_j\xi_k\big)e^{i\sum\limits_{\xi_j,\xi_k\in Q,k\neq i}\alpha_Q\left(\xi_j\xi_k\right)}\\&+\mu_Q^+\big(\xi_j\xi_k\big)e^{\alpha_Q\left(\xi_j\xi_k\right)}=\rho_1,\end{aligned}$$

$$\begin{aligned}T\deg\mu^-e^{i\beta}\big(\xi_i\xi_j\big)&=\sum_{\xi_i,\xi_k\in Q,k\neq j}\mu_Q^-(\xi_i\xi_k)e^{i\sum\limits_{\xi_i,\xi_k\in Q,k\neq j}\beta_Q\left(\xi_i\xi_k\right)}\\&+\sum_{\xi_j,\xi_k\in Q,k\neq i}\mu_Q^-\big(\xi_j\xi_k\big)e^{i\sum\limits_{\xi_j,\xi_k\in Q,k\neq i}\beta_Q\left(\xi_j\xi_k\right)}\\&+\mu_Q^-(\xi_i\xi_k)e^{i\beta_Q\left(\xi_j\xi_k\right)}=\rho_2,\end{aligned}$$

$$\begin{aligned}T\deg\nu^+e^{i\gamma}\big(\xi_i\xi_j\big)&=\sum_{\xi_i,\xi_k\in Q,k\neq j}\nu_Q^+(\xi_i\xi_k)e^{i\sum\limits_{\xi_i,\xi_k\in Q,k\neq j}\gamma_Q\left(\xi_i\xi_k\right)}\\&+\sum_{\xi_j,\xi_k\in Q,k\neq i}\nu_Q^+\big(\xi_j\xi_k\big)e^{i\sum\limits_{\xi_j,\xi_k\in Q,k\neq i}\gamma_Q\left(\xi_j\xi_k\right)}\\&+\nu_Q^+(\xi_i\xi_k)e^{i\gamma_Q\left(\xi_j\xi_k\right)}=\rho_3\end{aligned}$$

$$\begin{aligned}T\deg\nu^-e^{i\delta}\big(\xi_i\xi_j\big)&=\sum_{\xi_i,\xi_k\in Q,k\neq j}\nu_Q^-(\xi_i\xi_k)e^{i\sum\limits_{\xi_i,\xi_k\in Q,k\neq j}\delta_Q\left(\xi_i\xi_k\right)}\\&+\sum_{\xi_j,\xi_k\in Q,k\neq i}\nu_Q^-\big(\xi_j\xi_k\big)e^{i\sum\limits_{\xi_j,\xi_k\in Q,k\neq i}\delta_Q\left(\xi_j\xi_k\right)}\\&+\nu_Q^-(\xi_i\xi_k)e^{i\delta_Q\left(\xi_j\xi_k\right)}=\rho_4.\end{aligned}$$

Thus, $\mathcal{G}$ is totally edge regular of degree $(\rho_1,\rho_2,\rho_3,\rho_4)$ or $(\rho_1,\rho_2,\rho_3,\rho_4)$-$\mathcal{TERBCPFG}$.

Proposition 4.10 Let $\mathcal{G} = (\mathcal{P}, \mathcal{Q})$ be a $\mathcal{BCPFG}$. Then $\left(\mu_{\mathcal{Q}}^{+}(\xi)e^{i\alpha_{\mathcal{Q}}}, \mu_{\mathcal{Q}}^{-}e^{i\beta_{\mathcal{Q}}}, \nu_{\mathcal{Q}}^{+}e^{i\gamma_{\mathcal{Q}}}, \nu_{\mathcal{Q}}^{-}e^{i\delta_{\mathcal{Q}}}\right)$ is a constant mapping iff $\mathcal{G}$ is an $\mathcal{ERBCPFG} \Leftrightarrow \mathcal{G}$ is an $\mathcal{TERBCPFG}$.

5 Conclusion

In the complex modeling system, dynamical tools, such as graph theory and $\mathcal{BCPFG}$s, are being applied to solve the complex combinatorial network problems of incomplete information in cellular data, where $\mathcal{BCPFG}$s operate under the functions of the periodicity nature of exact information. The bipolar complex Pythagorean fuzzy paradigm has a vital scientific application in data science, big data analysis, complex neural networks and decision-making than Fs and IFs in the development of graph structure. The foremost intention of this study is to derive the innovative concept $\mathcal{BCPF}$ set and $\mathcal{BCPFG}$ and examined several features of it. Then, we developed some operations on $\mathcal{BCPFG}s$ as a complement, join, ring sum and union with certain specific examples. Also, proved that, $\overline{\overline{\mathcal{G}}} = \mathcal{G}$ and $\sum_{\xi_i \in P} \deg_{\mathcal{G}}(\xi_i) = \sum_{\xi_i \xi_j \in Q} \deg_{\mathcal{G}}(\xi_i \xi_j)$. Finally, we also established the notions of $\mathcal{RBCPFG}s$, $\mathcal{ERBCPFG}s$, $\mathcal{TRBCPFG}s$ and $\mathcal{TERBCPFG}s$ and investigated its essential characterizations. The bipolar complex Pythagorean fuzzy hypergraphs, bipolar fuzzy neutrosophic complex Pythagorean graphs, bipolar complex Pythagorean fuzzy digital structure and its advanced properties will be studied shortly.

References

1. Akram, M., Sumera, N.: A novel decision-making approach under a complex Pythagorean fuzzy environment. Math. Comput. Appl. **24**(3), 1–33 (2019). https://doi.org/10.3390/mca24030073
2. Akram, M., Dudek, W.A.: Regular bipolar fuzzy graphs. Neural Comput. Appl. **21**(1), 197–205 (2012). https://doi.org/10.1007/s00521-011-0772-6
3. Akram, M., et al.: Pythagorean Dombi fuzzy graphs. Complex Intell. Syst. **6**, 29–54 (2020). https://doi.org/10.1007/s40747-019-0109-0
4. Akram, M., Dar, J.M., Naz, S.: Certain graphs under Pythagorean fuzzy environment. Complex Intell. Syst. **5**(2), 127–144 (2019). https://doi.org/10.1007/s40747-018-0089-5
5. Akram, M., Naz, S., Davvaz, B.: Simplified interval-valued Pythagorean fuzzy graphs with the application. Complex Intell. Syst. **5**(2), 229–253 (2019). https://doi.org/10.1007/s40747-019-0106-3
6. Alkouri, A.S., Salleh, A.R.: Complex intuitionistic fuzzy sets. In: AIP Conference Proceedings, vol. 1482(1). American Institute of Physics (2012). https://doi.org/10.1063/1.4757515
7. Alkouri, A.U.M, Salleh, A.R.: Complex Atanassov's intuitionistic fuzzy relation. Abstract Appl. Anal. (2013). https://doi.org/10.1155/2013/287382
8. Atanassov, K.T.: Intuitionistic fuzzy sets. Fuzzy Sets Syst. **20**, 87–96 (1986). https://doi.org/10.1016/S0165-0114(86)80034-3

9. Bhattacharya, P.: Some remarks on fuzzy graphs. Pattern Recognit. Lett. **6**, 297–302 (1987). https://doi.org/10.1016/0167-8655(87)90012-2
10. Buckley, J.J.: Fuzzy complex numbers. Fuzzy Sets Syst. **33**(3), 333–345 (1989). https://doi.org/10.1016/0165-0114(89)90122-X
11. Coker, D.: An introduction to intuitionistic fuzzy topological spaces. Fuzzy Sets Syst. **88**(1), 81–89 (1997). https://doi.org/10.1016/S0165-0114(96)00076-0
12. Coker, D., D. M.: On intuitionistic fuzzy points. Notes IFS **1**(2), 79–84 (1995)
13. Dick, S., Yager, R.R., Yazdanbakhsh, O.: On Pythagorean and complex fuzzy set operations. IEEE Trans. Fuzzy Syst. **24**(5), 1009–1021 (2015). https://doi.org/10.1109/TFUZZ.2015.2500273
14. Ezhilmaran, D., Sanker, K.: Morphism of bipolar intuitionistic fuzzy graphs. J. Discrete Math. Sci. Crypt. **18**(5), 605–621 (2015). https://doi.org/10.1080/09720529.2015.1013673
15. Gulistan, M.: Complex bipolar fuzzy sets: an application in a transport's company. J. Intell. Fuzzy Syst. **40**, 3981–3997 (2021). https://doi.org/10.3233/JIFS-200234
16. Karunambigai, M.G., Kasilingam, P., Shanmugam, S.: Edge regular intuitionistic fuzzy graph. Adv. Fuzzy Sets Syst. **20**(1), 25–46 (2015). https://doi.org/10.17654/AFSSSep2015_025_046
17. Lee, K.M.: Bipolar-valued fuzzy sets and their operations. In: Proceedings International Conference on Intelligent Technologies, Thailand (2000)
18. Luqman, A., et al.: A study on hypergraph representations of complex fuzzy information. Symmetry **11**, 1381 (2019). https://doi.org/10.3390/sym11111381
19. Nandhini, R., Amsaveni, D.: On bipolar complex intuitionistic fuzzy graphs. TWMS J. Appl. Eng. Math. **12**(1), 92–106 (2022)
20. Nguyen, H.T., Kandel, A., Kreinovich, V.: Complex fuzzy sets: towards new foundations. In: Proceedings of the Ninth IEEE International Conference on Fuzzy Systems, San Antonio, TX, USA (2000). https://doi.org/10.1109/FUZZY.2000.839195
21. Peng, X., Yang, Y.: Some results for Pythagorean fuzzy sets. Int. J. Intell. Syst. **30**(11), 1133–1160 (2015). https://doi.org/10.1002/int.21738
22. Radha, K., Kumaravel, N.: On edge regular fuzzy graphs. Int. J. Math. Arch. **5**(9), 100–112 (2014)
23. Radha, K., Kumaravel, N.: On edge regular bipolar fuzzy graphs. Ann. Pure Appl. Math. **10**(2), 129–139 (2015)
24. Ramot, D., et al.: Complex fuzzy sets. IEEE Trans. Fuzzy Syst. **10**(2), 171–186 (2002). https://doi.org/10.1109/91.995119
25. Rosenfeld, A.: Fuzzy graphs. In Zadeh, L.A., Fu, K.S., Shimura (eds.) Fuzzy Sets and Their Applications, pp. 77–95. Academic Press, New York (1975). https://doi.org/10.1016/B978-0-12-775260-0.50008-6
26. Thirunavukarasu, P., Suresh, R., Viswanathan, K.K.: Energy of a complex fuzzy graph. Int. J. Math. Sci. Eng. Appl. **10**(1), 243–248 (2016)
27. Ullah, K., et al.: On some distance measures of complex Pythagorean fuzzy sets and their applications in pattern recognition. Complex Intell. Syst. **6**(1), 15–27 (2020). https://doi.org/10.1007/s40747-019-0103-6
28. Verma, R., Merigo, J.M., Sahni, M.: Pythagorean fuzzy graphs: some results. s.l.: arXiv preprint. https://arxiv.org/abs/1806.06721 (2018)
29. Yager, R.R.: Pythagorean fuzzy subsets. s.l. In: 2013 Joint IFSA World Congress and NAFIPS Annual Meeting (IFSA/NAFIPS), IEEE (2013). https://doi.org/10.1109/IFSA-NAFIPS.2013.6608375
30. Yager, R.R.: Pythagorean membership grades in multicriteria decision making. IEEE Trans. Fuzzy Syst. **22**(4), 958–965 (2013). https://doi.org/10.1109/TFUZZ.2013.2278989
31. Yager, R.R.: Properties and applications of Pythagorean fuzzy sets. In: Angelov, P., Sotirov, S. (ed.) Imprecision and Uncertainty in Information Representation and Processing, Studies in Fuzziness and Soft Computing, pp. 119–136. Springer, Cham (2016). https://doi.org/10.1007/978-3-319-26302-1_9
32. Yager, R.R., Abbasov, M.A.: Pythagorean membership grades, complex numbers, and decision-making. Int. J. Intell. Syst. **28**(5), 436–452 (2013). https://doi.org/10.1002/int.21584

33. Yaqoob, N., et al.: Complex intuitionistic fuzzy graphs with application in cellular network provider companies. Mathematics **7**(1) (2019). https://doi.org/10.3390/math7010035
34. Yazdanbakhsh, O., Dick, S.: A systematic review of complex fuzzy sets and logic. Fuzzy Sets Syst. 338, 1–22 (2018). https://doi.org/10.1016/j.fss.2017.01.010
35. Zadeh, L.A.: Fuzzy sets. Inf. Control **8**, 338–353 (1965). https://doi.org/10.1016/S0019-9958(65)90241-X
36. Zhang, W.: Bipolar fuzzy sets and relations: a computational framework for cognitive modeling and multiagent decision analysis. In: Proceedings of IEEE Conference (1994). https://doi.org/10.1109/IJCF.1994.375115
37. Zhang, W.: Bipolar fuzzy sets. In: 1998 IEEE International Conference on Fuzzy Systems Proceedings. IEEE World Congress on Computational Intelligence, vol. 1, pp. 835–840 (1998). https://doi.org/10.1109/FUZZY.1998.687599

Modified Operations of Trapezoidal Fuzzy Numbers for Solving Fuzzy Linear Programming Problems

M. Mohamed Salih Mukthar and S. Ramathilagam

Abstract In the standard fuzzy subtraction and division of trapezoidal fuzzy numbers, some difficulties arise while getting the solution of fuzzy linear equations and solving the fully fuzzy linear programming problems. In this paper, we have modified both operations subtraction and division of trapezoidal fuzzy numbers, derived the sufficient conditions of both operations and verified by using some examples. Also, these new operations provide the exact inverses of the addition and multiplication operators.

Keywords Fuzzy numbers · Trapezoidal fuzzy numbers · Fuzzy arithmetic operations

1 Introduction

The arithmetic behaviors of fuzzy numbers in the domain of combinatory are described by Kauffman and Gupta [1] and their explanations based on the α-cut approach. Das et al. [2] were explained the standard arithmetic operations of trapezoidal fuzzy numbers. Vahidi and Rezvani [3] were discussed some nonlinear arithmetic operations on trapezoidal fuzzy numbers. The generalized concept of fuzzy linear programming was first proposed by Tanaka et al. [4, 5]. The first formulation of fuzzy linear programming was proposed by Zimmermann [6]. The fuzzy linear programming problems containing all the parameters and variables are represented by fuzzy numbers are referred as fully fuzzy linear programming problems. Buckley and Feuring [7] introduced a method to find the solution of fully fuzzy linear programming problems with all the parameters and variables as fuzzy numbers by changing the objective function into a multi objective function fuzzy linear programming problem.

M. Mohamed Salih Mukthar (✉)
PG and Research Department of Mathematics, C. Abdul Hakeem College (Autonomous), Melvisharam 632509, India
e-mail: salih.mat@cahc.edu.in

S. Ramathilagam
Department of Mathematics, Periyar Arts College, Cuddalore 607001, India

© The Author(s), under exclusive license to Springer Nature Singapore Pte Ltd. 2022

S. R. Kannan et al. (eds.), *Fuzzy Mathematical Analysis and Advances in Computational Mathematics*, Studies in Fuzziness and Soft Computing 419,
https://doi.org/10.1007/978-981-19-0471-4_2

In this paper, Sect. 2 deals with the preliminary concepts, Sects. 3 and 4 explain the existed standard operations of trapezoidal fuzzy operations and their disadvantages, respectively. Sections 5 and 6 describe the modified operations subtraction and division of trapezoidal fuzzy numbers and their applications respectively.

2 Preliminaries

First let us discuss the following basic terminologies and notions from [2, 3, 8].

Definition 2.1 A fuzzy number $\tilde{X}$ is a fuzzy set on the real line $\boldsymbol{R}$ which satisfies the following conditions:

(i) $\tilde{X}$ is normal
(ii) $\alpha_{\tilde{X}}$ is a closed interval for every $\alpha \epsilon (0, 1]$
(iii) The support of $\tilde{X}$ is bounded.

Definition 2.2 A fuzzy number $\tilde{T} = (a, b, c, d)$ is said to be a trapezoidal fuzzy number if its membership function is defined as follows: $\mu_{\tilde{T}}(x) = \begin{cases} \frac{x-a}{b-a}, & a \le x \le b \\ 1, & b \le x \le c \\ \frac{x-d}{c-d}, & c \le x \le d \\ 0, & \text{else} \end{cases}$

Definition 2.3 A trapezoidal fuzzy number $\tilde{T} = (a, b, c, d)$ is said to be nonpositive (nonnegative) if $a \le 0$ ($a \ge 0$).

Definition 2.4 Let $\widetilde{T}_1 = (a, b, c, d)$ and $\widetilde{T}_2 = (e, f, g, h)$ be two arbitrary trapezoidal fuzzy numbers. Then we say that $\widetilde{T}_1 < \widetilde{T}_2$ if and only if $(b - a) < (f - e)$ or $b < f$ and $b - a = f - e$ or $b = f$, $b - a = f - e$ and $\frac{b+c}{2} < \frac{f+g}{2}$ or $b = f$, $b - a = f - e$, $\frac{b+c}{2} = \frac{f+g}{2}$ and $d - c < h - g$.

3 Arithmetic Operations of Trapezoidal Fuzzy Numbers

In this section, we discuss the existed standard fuzzy arithmetic operations from [2, 3].

3.1 Addition

Let $\widetilde{T}_1 = (a, b, c, d)$ and $\widetilde{T}_2 = (e, f, g, h)$ be two arbitrary trapezoidal fuzzy numbers.

Then the addition of trapezoidal fuzzy numbers $\widetilde{T_1}$ and $\widetilde{T_2}$ [3] is defined as

$$\widetilde{T_1} + \widetilde{T_2} = (a, b, c, d) + (e, f, g, h) = (a + e, b + f, c + g, d + h)$$

3.2 Subtraction

Let $\widetilde{T_1} = (a, b, c, d)$ and $\widetilde{T_2} = (e, f, g, h)$ be two arbitrary trapezoidal fuzzy numbers.

Then the subtraction of trapezoidal fuzzy numbers $\widetilde{T_1}$and$\widetilde{T_2}$ [3] is defined as

$$\widetilde{T_1} - \widetilde{T_2} = (a, b, c, d) - (e, f, g, h) = (a - h, b - g, c - f, d - e)$$

3.3 Multiplication

Let $\widetilde{T_1} = (a, b, c, d)$ and $\widetilde{T_2} = (e, f, g, h)$ be two arbitrary trapezoidal fuzzy numbers.

Then the multiplication of trapezoidal fuzzy numbers $\widetilde{T_1}$ and $\widetilde{T_2}$ [3] is defined as

$$\widetilde{T_1} \times \widetilde{T_2} = (a, b, c, d) \times (e, f, g, h) = (w, x, y, z),$$

where $w = \min(ae, af, be, bf)$, $x = \max(ae, af, be, bf)$,

$y = \min(cg, ch, dg, dh)$, $\quad z = \max(cg, ch, dg, dh)$

3.4 Division

Let $\widetilde{T_1} = (a, b, c, d)$ and $\widetilde{T_2} = (e, f, g, h)$ be two arbitrary trapezoidal fuzzy numbers.

Then the division of trapezoidal fuzzy numbers $\widetilde{T_1}$ and $\widetilde{T_2}$ [3] is defined as

$$\widetilde{T_1}/\widetilde{T_2} = (a, b, c, d)/(e, f, g, h) = (a, b, c, d) \times (1/h, 1/g, 1/f, 1/e) = (w, x, y, z),$$

where $w = \min(a/h, a/g, b/h, b/g)$, $x = \max(a/h, a/g, b/h, b/g)$,

$y = \min(c/f, c/e, d/f, d/e)$, $z = \max(c/f, c/e, d/f, d/e)$, provided $\widetilde{T_2}$ is nonzero.

4 Disadvantages of the Operations (Subtraction and Division) of Trapezoidal Fuzzy Numbers

In the above operations of subtraction and division of trapezoidal fuzzy numbers, if $\widetilde{T_1}$ is any trapezoidal fuzzy number, then $\widetilde{T_1} - \widetilde{T_1} \neq 0$ and $\widetilde{T_1}/\widetilde{T_1} \neq 1$, where $0 = (0, 0, 0, 0)$ and $1 = (1, 1, 1, 1)$.

If $\widetilde{T_1}$, $\widetilde{T_2}$ and $\widetilde{T_3}$ are trapezoidal fuzzy numbers, then the solution of fuzzy linear equation $\widetilde{T_1} + \widetilde{T_2} = \widetilde{T_3}$ does not imply $\widetilde{T_2} = \widetilde{T_3} - \widetilde{T_1}$.

If $\widetilde{T_1}$, $\widetilde{T_2}$ and $\widetilde{T_3}$ are trapezoidal fuzzy numbers, then the solution of fuzzy linear equation $\widetilde{T_1} \times \widetilde{T_2} = \widetilde{T_3}$ does not imply $\widetilde{T_2} = \widetilde{T_3}/\widetilde{T_1}$.

Thus, the addition and subtraction as well as multiplication and division of trapezoidal fuzzy numbers are not reciprocal equations. Therefore, it is not possible to solve inverse problems using the above fuzzy arithmetic operations.

5 Modified Operations of Subtraction and Division of Trapezoidal Fuzzy Numbers

In this paper, our aim is to develop the new operations of subtraction and division of trapezoidal fuzzy numbers to rectify the above disadvantages and to obtain that addition and subtraction are the inverse operations and multiplication and division are the inverse operations.

5.1 Subtraction

Let $\widetilde{T_1} = (a, b, c, d)$ and $\widetilde{T_2} = (e, f, g, h)$ be two arbitrary trapezoidal fuzzy numbers. Then the subtraction of trapezoidal fuzzy numbers $\widetilde{T_1}$ and $\widetilde{T_2}$ is defined as

$$\widetilde{T_1} - \widetilde{T_2} = (a, b, c, d) - (e, f, g, h) = (a - e, b - f, c - g, d - h).$$

For example, $(4, 6, 8, 9) - (2, 3, 5, 4) = (2, 3, 3, 5)$

$$(7, 9, 11, 13) - (7, 9, 11, 13) = (0, 0, 0, 0)$$

5.2 Notation

Let $\tilde{A} = (a, b, c, d)$ and $\tilde{B} = (e, f, g, h)$ be two arbitrary trapezoidal fuzzy numbers.

$$D\left(\tilde{A}\right) = \frac{d-a}{2}, D\left(\tilde{B}\right) = \frac{h-e}{2}, M\left(\tilde{A}\right) = \frac{d+a}{2}, M\left(\tilde{B}\right) = \frac{h+e}{2}$$

Theorem 5.3 Let $\widetilde{T}_1 = (a, b, c, d)$ and $\widetilde{T}_2 = (e, f, g, h)$ be two arbitrary trapezoidal fuzzy numbers.

(i) If $\widetilde{T}_1 \geq \widetilde{T}_2$, then the modified subtraction (5.1) exists only if $D(\widetilde{T}_1) \geq D(\widetilde{T}_2)$
(ii) If $\widetilde{T}_1 \leq \widetilde{T}_2$, then the modified subtraction (5.1) exists only if $D(\widetilde{T}_1) \leq D(\widetilde{T}_2)$

Proof

Case (i) $\widetilde{T}_1 \geq \widetilde{T}_2$.

For obtaining the condition for $\widetilde{T}_1 - \widetilde{T}_2 = (w, x, y, z)$, let us assume that $w \leq x \leq y \leq z$.
Then $w \leq z$.
This is possible only if $(a - e) \leq (d - h)$

$$\Rightarrow (a-d) \leq (e-h)$$
$$\Rightarrow \left(M(\widetilde{T}_1) - D(\widetilde{T}_1)\right) - \left(M(\widetilde{T}_1) + D(\widetilde{T}_1)\right) \leq \left(M(\widetilde{T}_2) - D(\widetilde{T}_2)\right) - \left(M(\widetilde{T}_2) + D(\widetilde{T}_2)\right)$$
$$\Rightarrow -2D(\widetilde{T}_1) \leq -2D(\widetilde{T}_2)$$
$$\Rightarrow D(\widetilde{T}_1) \geq D(\widetilde{T}_2)$$

Case (ii) $\widetilde{T}_1 \leq \widetilde{T}_2$.

To find the condition for $\widetilde{T}_1 - \widetilde{T}_2 = (w, x, y, z)$, let us assume that $w \leq x \leq y \leq z$.
Then $w \leq z$.
This is possible only if $-(a - e) \leq -(d - h)$

$$\Rightarrow (a-e) \geq (d-h)$$
$$\Rightarrow (a-d) \geq (e-h)$$
$$\Rightarrow \left(M(\widetilde{T}_1) - D(\widetilde{T}_1)\right) - \left(M(\widetilde{T}_1) + D(\widetilde{T}_1)\right) \geq \left(M(\widetilde{T}_2) - D(\widetilde{T}_2)\right) - \left(M(\widetilde{T}_2) + D(\widetilde{T}_2)\right)$$
$$\Rightarrow -2D(\widetilde{T}_1) \geq -2D(\widetilde{T}_2)$$
$$\Rightarrow D(\widetilde{T}_1) \leq D(\widetilde{T}_2)$$

Hence, the theorem is proved.

5.3 Division

Let $\widetilde{T}_1 = (a, b, c, d)$ and $\widetilde{T}_2 = (e, f, g, h) \neq (0, 0, 0, 0)$ be two arbitrary trapezoidal fuzzy numbers. Then the division of trapezoidal fuzzy numbers $\widetilde{T}_1$ and $\widetilde{T}_2$ is defined as

$$\widetilde{T}_1/\widetilde{T}_2 = (a, b, c, d)/(e, f, g, h) = (a/e, b/f, c/g, d/h).$$

For example, $(4, 6, 10, 15)/(2, 3, 5, 5) = (2, 2, 2, 3)$
$(4, 7, 8, 9)/(4, 7, 8, 9) = (1, 1, 1, 1)$

Theorem 5.5 Let $\widetilde{T}_1 = (a, b, c, d)$ and $\widetilde{T}_2 = (e, f, g, h) \neq (0, 0, 0, 0)$ be two arbitrary trapezoidal fuzzy numbers.

(i) If $\widetilde{T}_1 \geq \widetilde{T}_2$, then the modified division (5.4) exists only if $\frac{M(\widetilde{T}_1)}{D(\widetilde{T}_1)} \leq \frac{M(\widetilde{T}_2)}{D(\widetilde{T}_2)}$

(ii) If $\widetilde{T}_1 \leq \widetilde{T}_2$, then the modified division (5.4) exists only if $\frac{M(\widetilde{T}_1)}{D(\widetilde{T}_1)} \geq \frac{M(\widetilde{T}_2)}{D(\widetilde{T}_2)}$

Proof

Case (i) $\widetilde{T}_1 \geq \widetilde{T}_2$.

For computing the condition of $\widetilde{T}_1/\widetilde{T}_2 = (w, x, y, z)$, let us assume that $w \leq x \leq y \leq z$.

Then $w \leq z$.

This is possible only if $\frac{a}{e} \leq \frac{d}{h}$

$$\Rightarrow ah \leq ed$$
$$\Rightarrow \big(M(\widetilde{T}_1) - D(\widetilde{T}_1)\big)\big(M(\widetilde{T}_2) + D(\widetilde{T}_2)\big) \leq \big(M(\widetilde{T}_2) - D(\widetilde{T}_2)\big)\big(M(\widetilde{T}_1) + D(\widetilde{T}_1)\big)$$
$$\Rightarrow 2M(\widetilde{T}_1)D(\widetilde{T}_2) \leq 2D(\widetilde{T}_1)M(\widetilde{T}_2)$$
$$\Rightarrow \frac{M(\widetilde{T}_1)}{D(\widetilde{T}_1)} \leq \frac{M(\widetilde{T}_2)}{D(\widetilde{T}_2)}$$

Case (ii) $\widetilde{T}_1 \leq \widetilde{T}_2$.

To obtain the condition of $\widetilde{T}_1/\widetilde{T}_2 = (w, x, y, z)$, let us assume that $w \leq x \leq y \leq z$.

Then $w \leq z$.

This is possible only if $\frac{1}{\frac{a}{e}} \leq \frac{1}{\frac{d}{h}}$

$$\Rightarrow \frac{a}{e} \geq \frac{d}{h}$$
$$\Rightarrow ah \geq ed$$
$$\Rightarrow \big(M(\widetilde{T}_1) - D(\widetilde{T}_1)\big)\big(M(\widetilde{T}_2) + D(\widetilde{T}_2)\big) \geq \big(M(\widetilde{T}_2) - D(\widetilde{T}_2)\big)\big(M(\widetilde{T}_1) + D(\widetilde{T}_1)\big)$$
$$\Rightarrow 2M(\widetilde{T}_1)D(\widetilde{T}_2) \geq 2D(\widetilde{T}_1)M(\widetilde{T}_2)$$
$$\Rightarrow \frac{M(\widetilde{T}_1)}{D(\widetilde{T}_1)} \geq \frac{M(\widetilde{T}_2)}{D(\widetilde{T}_2)}$$

Hence, the theorem is proved.

6 Application of the Modified Operations (for Solving Fully Fuzzy Linear Programming Problem)

In this section, we solve the fully fuzzy linear programming problem using the modified operations subtraction and division of trapezoidal fuzzy numbers.

Consider the following fully fuzzy linear programming problem:

Maximize $Z = (2, 5, 7, 8)\widetilde{x_1} + (4, 6, 8, 9)\widetilde{x_2}$.

Subject to $(1, 2, 3, 4)\widetilde{x_1} + (2, 3, 4, 5)\widetilde{x_2} \leq (3, 4, 5, 6)$

$$(3, 4, 5, 6)\widetilde{x_1} + (4, 5, 6, 7)\widetilde{x_2} \leq (6, 7, 8, 9)$$
$$\widetilde{x_1}, \widetilde{x_2} \geq 0$$

Solution:

We solve this problem by using Simplex method [9].

Introducing slack variables (trapezoidal fuzzy numbers) for $\leq$ constraints, the given problem becomes

Maximize $Z = (2, 5, 7, 8)\widetilde{x_1} + (4, 6, 8, 9)\widetilde{x_2} + (0, 0, 0, 0)\widetilde{s_1} + (0, 0, 0, 0)\widetilde{s_2}$.

Subject to $(1, 2, 3, 4)\widetilde{x_1} + (2, 3, 4, 5)\widetilde{x_2} + (1, 1, 1, 1)\widetilde{s_1} = (3, 4, 5, 6)$

$$(3, 4, 5, 6)\widetilde{x_1} + (4, 5, 6, 7)\widetilde{x_2} + (1, 1, 1, 1)\widetilde{s_2} = (6, 7, 8, 9)$$
$$\widetilde{x_1}, \widetilde{x_2}, \widetilde{s_1}, \widetilde{s_2} \geq 0$$

Iteration 1.

CB_i	C_j	(2, 5, 7, 8)	(4, 6, 8, 9)	(0, 0, 0, 0)	(0, 0, 0, 0)	Solution
	Basic variable	$\widetilde{x_1}$	$\widetilde{x_2}$	$\widetilde{s_1}$	$\widetilde{s_2}$	
(0, 0, 0, 0)	$\widetilde{s_1}$	(1, 2, 3, 4)	(**2**, **3**, **4**, **5**)	(1, 1, 1, 1)	(0, 0, 0, 0)	(3, 4, 5, 6)
(0, 0, 0, 0)	$\widetilde{s_2}$	(3, 4, 5, 6)	(4, 5, 6, 7)	(0, 0, 0, 0)	(1, 1, 1, 1)	(6, 7, 8, 9)
Z_j		(0, 0, 0, 0)	(0, 0, 0, 0)	(0, 0, 0, 0)	(0, 0, 0, 0)	(0, 0, 0, 0)
$C_j - Z_j$		(2, 5, 7, 8)	(4, 6, 8, 9)	(0, 0, 0, 0)	(0, 0, 0, 0)	

In this iteration 1, some $C_j - Z_j$'s are positive. Hence optimality condition is not satisfied. So, we go for next iteration with the key element = (2, 3, 4, 5).

Iteration 2.

CB_i	C_j	(2, 5, 7, 8)	(4, 6, 8, 9)	(0, 0, 0, 0)	(0, 0, 0, 0)	Solution
	Basic variable	$\widetilde{x_1}$	$\widetilde{x_2}$	$\widetilde{s_1}$	$\widetilde{s_2}$	
(4, 6, 8, 9)	$\widetilde{x_2}$	(0.5, 0.67, 0.75, 0.8)	(1, 1, 1, 1)	(0.2, 0.25, 0.3, 0.5)	(0, 0, 0, 0)	(1.2, 1.25, 1.3, 1.5)
(0, 0, 0, 0)	$\widetilde{s_2}$	(**0.4**, **0.5**, **0.7**, **1**)	(0, 0, 0, 0)	(−2, −1.67, −1.5, −1.4)	(1, 1, 1, 1)	(0, 0.3, 0.5, 0.6)
Z_j		(2, 4.02, 6.24, 7.2)	(4, 6, 8, 9)	(1.8, 1.8, 2, 2)	(0, 0, 0, 0)	(6, 9, 9.6, 11.25)
$C_j - Z_j$		(0, 0.76, 0.8, 0.98)	(0, 0, 0, 0)	(−2, −2, −1.8, −1.8)	(0, 0, 0, 0)	

In this iteration 2, one $C_j - Z_j$ is positive. Hence, optimality condition is not satisfied. So, we go for next iteration with the key element = (0.4, 0.5, 0.7, 1).

Iteration 3.

CB_i	C_j	(2, 5, 7, 8)	(4, 6, 8, 9)	(0, 0, 0, 0)	(0, 0, 0, 0)	Solution
	Basic variable	$\widetilde{x_1}$	$\widetilde{x_2}$	$\widetilde{s_1}$	$\widetilde{s_2}$	
(4, 6, 8, 9)	$\widetilde{x_2}$	(0, 0, 0, 0)	(1, 1, 1, 1)	(1.04, 1.3, 1.5, 1.84)	(−1.34, −1.25, −1.07, −0.8)	(−3.15, 0.76, 1.02, 1.2)
(2, 5, 7, 8)	$\widetilde{x_1}$	(1, 1, 1, 1)	(0, 0, 0, 0)	(−5, −3.34, −2.1, −1.4)	(1, 1.4, 2, 2.5)	(0, 0.6, 0.6, 0.7)
Z_j		(2, 5, 7, 8)	(4, 6, 8, 9)	(−20.84, −9, 2.2, 9.88)	(−6.04, 2, 4.37, 13.6)	(−18.9, 7.56, 12.36, 16.4)
$C_j - Z_j$		(0, 0, 0, 0)	(0, 0, 0, 0)	(−9.88, −2.2, 9, 20.84)	(−13.6, −4.37, −2, 6.04)	

In this iteration 3, all $C_j - Z_j$'s are non-positive. Hence optimality condition is satisfied.

Thus, we get the optimal solution of the given problem is Z = (−18.9, 7.56, 12.36, 16.4),

when $\widetilde{x_1} = (0, 0.6, 0.6, 0.7)$ and $\widetilde{x_2} = (-3.15, 0.76, 1.02, 1.2)$.

7 Conclusion

The main objective of this paper is to introduce modified operations subtraction and division of trapezoidal fuzzy numbers. The advantage of these operations is to obtain the inverse operations of addition and multiplication operators. These operations may be helpful to solve the fully fuzzy linear programming problems.

Ethical Approval

This article does not contain any studies with human participants or animals performed by any of the authors.

References

1. Kauffmann, A., Gupta, M.M.: Introduction to Fuzzy Arithmetic: Theory and Applications. Van Nostrand Reinhold, New York (1991)
2. Das, S.K., Mandal, T., Edalatpanah, S.A.: A mathematical model for solving fully fuzzy linear programming problem with trapezoidal fuzzy numbers. Appl. Intell. **46**(3), 509–519 (2016)
3. Vahid, J., Rezvani, S.: Arithmetic operations on trapezoidal fuzzy numbers. Nonlinear Anal. Appl. **2013**, 1–8 (2013)
4. Tanaka, H., Okuda, T., Asai, K.: On fuzzy mathematical programming. J. Cybern. **3**, 37–46 (1974)
5. Tanaka, H., Asai, K.: Fuzzy linear programming problems with fuzzy numbers. Fuzzy Sets Syst. **13**, 1–10 (1984)
6. Zimmermann, H.J.: Fuzzy programming and linear programming with several objective functions. Fuzzy Sets Syst. **1**, 45–55 (1978)
7. Buckley, J., Feuring, T.: Evolutionary algorithm solution to fuzzy problems: fuzzy linear programming. Fuzzy Sets Syst. **109**, 35–53 (2000)
8. Klir, G.J., Yuan, B.: Fuzzy sets and fuzzy logic: theory and applications. Prentice-Hall, PTR, New Jersey (1995)
9. Mahdavi–Amiri, N., Nasseri, S.H.: Duality results and a dual Simplex method for linear programming problems with trapezoidal fuzzy variables. Fuzzy Sets Syst. **158**, 1961–1978 (2007)

An Innovative Method for Finding Optimal Solution Fully Solved by Using Generalized Quadratic Fuzzy Transportation Problems

M. Venkatachalapathy, S. Muthuperumal, and R. Rajasekar

Abstract A transportation model is an appropriate case for the linear programming problem. This paper focuses on solving fuzzy transportation problems by assuming that a decision maker is only uncertain about the precise values of the transportation cost and not about the supply and demand of the product. In this method transportation, costs are represented by generalized quadratic fuzzy numbers. It deals with transporting the bearings of alien article from sources to destinations in which both the capacity (tons) absolute and requirements (tons) are accepted as generalized quadratic fuzzy numbers. In this paper, an appropriate type of optimal solution of Band-Aid for application was produced from GQFVAM and GQFMODI method.

Keywords Transportation problem (TP) · Generalized quadratic fuzzy number (GQFN) · Generalized quadratic fuzzy Vogel's method (GQFVAM) · Generalized quadratic fuzzy modified distribution method (GQFMODI)

1 Introduction

In life's most of the parts, data retrieved for choice making are especially known. The traditional transportation issue (TP) manages dispatching items from sources to objections at least expense. Dantzig and Thapa [1], one of the earliest and most significant implementations of linear programming problem is transportation problem. Gass [2] provided a methodology to solve the transportation problems. In 1965, Zadeh [3] had delivered the idea of fuzzy set concept to deal with such problems. In 1987, Dubois and Prade [4] represented fuzzy range as fuzzy subset for the proper line. Fuzzy numbers help us to deliver the numerical model of a semantic variable or fuzzy conditions. Abbasbandy and Hajjari [5] made a novel strategy by ranking trapezoidal fuzzy numbers based totally on the left and perfect spreads. Venkatachalapathy and Edward Samuel [6] evaluated a choice technique for fixing fuzzy transportation hassle for using ranking functions. Kaur and Kumar [7] proposed the

M. Venkatachalapathy (✉) · S. Muthuperumal · R. Rajasekar
K. Ramakrishnan College of Engineering (Autonomous), Samayapuram, Trichirappalli, Tamil Nadu 621112, India

© The Author(s), under exclusive license to Springer Nature Singapore Pte Ltd. 2022

S. R. Kannan et al. (eds.), *Fuzzy Mathematical Analysis and Advances in Computational Mathematics*, Studies in Fuzziness and Soft Computing 419,
https://doi.org/10.1007/978-981-19-0471-4_3

weighted distance fuzzy numbers. In actual life, surprising conditions crop up, and it will give the uncertainty in making judgements and a lack of evidence among others. Vimala et al. [8] introduced OFSTF method, an optimal solution for transportation problem. Zimmermann [9] confirmed that options received through the fuzzy linear programming technique are continually efficient. Stephan Dinagar and Christoper Raj [10] presented a method for solving generalized quadrilateral fuzzy numbers using transportation problems. Muthuperumal et al. [11] proposed a new manner of algorithmic way to deal with the settle unbalanced triangular fuzzy transportation issues. Amaravathy et al. [12] presented a comparative study on MDMA method with OFSTF method in transportation problem. Venkatachalapathy M et al. [13] developed a learning about fixing the octagonal fuzzy numbers proposed a modified Vogel's approximation method. Venkatachalapathy M et al. [14] presented a method for solving generalized quadratic fuzzy number, which is an algorithm for acquiring optimal solution. Amaliah and Fatichah [15] presented an initial basic feasible solution (IBFS). Öztürk et al. [16] developed fuzzy neural network controller as a continuous controller utilizing PSO. Kuncan et al. [17] presented fuzzy logic-based ball on plate, balancing real-time system control by image processing. Karakoç et al. [18] used the fuzzy logic controller for the aircraft height control Otomatik Kontrol Ulusal Toplantısı. Ramesh Babu and Rama Bhupal Reddy [19] developed a method for solving feasibility of fuzzy new method in finding initial basic feasible solution for fuzzy transportation problems. Mathur and Srivastava [20] developed an innovative approach to optimize transportation problems through generalized trapezoidal numbers in a fuzzy environment. Doğan H et al. [21] developed H.M.: PID and fuzzy logic approach to vehicle and Kaplan K et al. [22] proposed in H.M.: prediction of bearing using fuzzy logic. Edward Samuel A and Venkatachalapathy M, [23] proposed a new procedure for solving trapezoidal fuzzy transportation problems. This paper focuses on enhancing the given balanced generalized quadratic fuzzy transportation problem to reap the preliminary primary viable solution.

The proposed method is a new technique, which is very easy to understand, comprehend, and useful for solving the unbalanced generalized quadratic fuzzy transportation problems. Section 2 provides preliminaries and arithmetic operations. Section 3 explains the use of potential algorithms in the generalized quadratic fuzzy Vogel's approximation method and generalized quadratic fuzzy modified distribution method approaches. In Sect. 4, the numerical examples are presented, and Sect. 5 concludes the discussion and provide the main results.

2 Preliminaries

2.1 Formulation of Generalized Quadratic Fuzzy Transportation Method

The objective is to minimize the total fuzzy cost of distributing the units. All the parameters of the model are included in this parameter Table 1.

Therefore, formulating a generalized quadratic fuzzy transportation problem requires only filling of a generalized quadratic fuzzy cost boundary table in the organization of Table 1.

The general formulations of Fuzzy linear programming problem are given below:

$$\text{Min } Z = \sum_{i=1}^{m}\sum_{j=1}^{n} \tilde{c}_{ij}x_{ij}$$

subject to

$$\sum_{j=1}^{n} x_{ij} = \tilde{s}_i,\ i = 1, 2, \ldots, m$$

$$\sum_{i=1}^{m} x_{ij} = \tilde{d}_j,\ j = 1, 2, \ldots, n$$

$$x_{ij} \geq 0,\ i = 1, 2, \ldots, m,\ j = 1, 2, \ldots, n$$

$$\text{and} \quad \sum_{i=1}^{m} \tilde{s}_i = \sum_{j=1}^{n} \tilde{d}_j, \quad \text{(balanced condition)}.$$

The balanced condition and the sufficient condition are essential for the presence of an achievable result for the transportation issues.

Table 1 Parameter table for the quadratic fuzzy transportation problem

	Fuzzy cost per unit distributed						
	Destination						
	1	2	3	.	.	n	Supply (s_i)
1	$\tilde{c}_{11}$	$\tilde{c}_{12}$	$\tilde{c}_{13}$	.	.	$\tilde{c}_{1n}$	$\tilde{s}_1$
2	$\tilde{c}_{21}$	$\tilde{c}_{22}$	$\tilde{c}_{23}$	.	.	$\tilde{c}_{2n}$	$\tilde{s}_2$
3	$\tilde{c}_{31}$	$\tilde{c}_{32}$	$\tilde{c}_{33}$	.	.	$\tilde{c}_{3n}$	$\tilde{s}_3$
.	.	.	.	.	.	.	
.	.	.	.	.	.	.	
M	$\tilde{c}_{m1}$	$\tilde{c}_{m2}$	$\tilde{c}_{m3}$	.	.	$\tilde{c}_{mn}$	$\tilde{s}_m$
Demand (d_j)	$\tilde{d}_1$	$\tilde{d}_2$	$\tilde{d}_3$			$\tilde{d}_n$	

2.2 Definition: Fuzzy Set

The fuzzy set $\widetilde{A}$ is defined by $\widetilde{A} = \left\{(x, \mu_{\widetilde{A}}(x) : x \in A \text{ and } \mu_{\widetilde{A}}(x) \in [0, 1]\right\}$, $\mu_{\widetilde{A}}(x)$ is called the membership function.

2.3 Definition: Fuzzy Number

A real piecewise quadratic fuzzy number $\widetilde{A} = (p_1, p_2, p_3, p_4, p_5)$ is a fuzzy subset from the real line $\Re$ with the membership function $\mu_{\widetilde{A}}(x)$ satisfying the following conditions:

(i) $\mu_{\widetilde{A}}(x)$ is a continuous mapping from $\Re$ to the closed interval [0,1].
(ii) $\mu_{\widetilde{A}}(x) = 0$ for every $\widetilde{A} \in (-\infty, p_1]$.
(iii) $\mu_{\widetilde{A}}(x)$ is strictly increasing and continuous on $[p_1, p_2]$.
(iv) $\mu_{\widetilde{A}}(x)$ is strictly increasing and continuous on $[p_2, p_3]$.
(v) $\mu_{\widetilde{A}}(x)$ is a strictly decreasing and continuous on $[p_3, p_4]$.
(vi) $\mu_{\widetilde{A}}(x)$ is a strictly decreasing and continuous on $[p_4, p_5]$.
(vii) $\mu_{\widetilde{A}}(x) = 0$ for every $\widetilde{A} \in [p_5, \infty)$.

The membership values assigned to distinct values are represented diagrammatically below $\left\{\frac{0}{p_1}, \frac{0.5}{p_2}, \frac{1}{p_3}, \frac{0.5}{p_4}, \frac{0}{p_5}\right\}$ (Fig. 1).

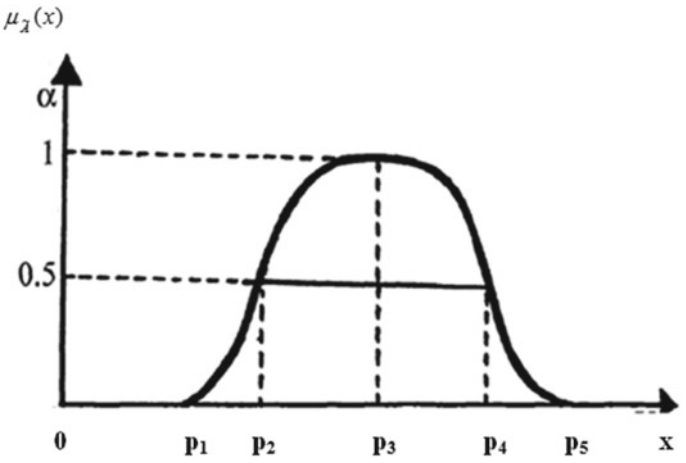

Fig. 1 Membership function of generalized quadratic fuzzy number

2.4 The Requirements Assumption [1]

Each source has a fixed quadratic fuzzy supply of units; as a whole, this flexibility should be disseminated to the objections. (let $\tilde{s}_i$ denote the number of units being supplied by source i, for $i = 1, 2, \ldots, m$). Essentially, every objective has a fixed quadratic fuzzy demand for units, whereas the whole interest must be received from the sources (let $\tilde{d}_j$ denote the number of units being received by destination j, for $j = 1, 2, \ldots, n$).

2.5 The Feasible Solutions Property [1]

A transportation problem will have feasible solutions only if $\sum_{i=1}^{m} \tilde{s}_i = \sum_{j=1}^{n} \tilde{d}_j$. In some genuine issues, the provisions really speak about the most extreme sums (as opposed to fixed add up) that are to be conveyed. Likewise, in different cases, the requests speak about the most extreme sums (as opposed to fixed add up) that are to be received. It is conceivable to reformulate the issue, so that they can be made to fit into this model by presenting a spurious objective or dummy source to take up the leeway between the real sums and greatest sums being dispersed.

2.6 Fuzzy Optimal Solution [1]

A feasible solution is optimal if total fuzzy transportation cost is minimized.

2.7 Non-Degenerate BFS [1]

A feasible solution of m by n is the basic feasible solution of non-degenerate if,

(i) Total number of positive allocations is $m + n - 1$.
(ii) These allocations must be in independent positions.

2.8 Rank of the Transportation Problem [1]

The rank of the system is exactly $m + n - 1$. Moreover, every condition is a direct blend of the other $m + n - 1$ conditions, so any one condition might be called excess and might be disposed of on the off chance that it is helpful to do as such.

2.9 Number of Basic Variables [1]

There are exactly $m + n - 1$ piecewise quadratic fuzzy number of basic variables x_{ij}.

2.10 Integrality Property of Basic Variables [1]

All the essential factors have fuzzy whole number qualities if the rows and columns of absolute fuzzy supplies $\tilde{s}_i$, and fuzzy demands $\tilde{d}_j$ are integers.

3 Piecewise Quadratic Fuzzy Numbers

3.1 Definition

A piecewise quadratic fuzzy number $\widetilde{A}$ is essentially a fuzzy number indicated as $\widetilde{A} = (p_1, p_2, p_3, p_4, p_5)$ and is denoted by the membership function as

$$\mu_{\widetilde{A}}(x) = \begin{cases} \frac{1}{2(p_2-p_1)^2}(x-p_1)^2 & \text{for } p_1 \le x \le p_2 \\ \frac{1}{2(p_3-p_2)^2}(x-p_3)^2 + 1 & \text{for } p_2 \le x \le p_3 \\ \frac{1}{2(p_4-p_3)^2}(x-p_3)^2 + 1 & \text{for } p_3 \le x \le p_4 \\ \frac{1}{2(p_5-p_4)^2}(x-p_5)^2 & \text{for } p_4 \le x \le p_5 \\ 0 & \text{otherwise} \end{cases}$$

The piecewise quadratic fuzzy number is a bell-shaped curve symmetric about the line $x = p_3$, and it possess a supporting interval $[p_1, p_5]$. Moreover, $p_3 = \frac{1}{2}(p_1 + p_5)$ and $p_3 - p_2 = p_4 - p_3$. The α-cut for $\alpha = \frac{1}{2}$ between the points (p_2, p_4) and they are called cross-over points. The interval of confidence at level α is given to be $A_\alpha = \{p_1 + (p_3 - p_1)\alpha, p_5 - (p_5 - (p_5 - p_3)\alpha\}$.

3.2 Arithmetic Operations

In this part, arithmetic operations of two generalized quadratic fuzzy numbers are taken, Let $\widetilde{A} = (p_1, p_2, p_3, p_4, p_5)$ and $\widetilde{B} = (q_1, q_2, q_3, q_4, q_5)$. There are two piecewise quadratic fuzzy numbers.

(i). **Addition**

$$\widetilde{A} + \widetilde{B} = (p_1 + q_1, p_2 + q_2, p_3 + q_3, p_4 + q_4, p_5 + q_5)$$

(ii). **Subtraction**

$$\widetilde{A} - \widetilde{B} = (p_1 - q_5, p_2 - q_4, p_3 - q_3, p_4 - q_2, p_5 - q_1)$$

(iii). **Scalar Multiplication**

$$\lambda\widetilde{A} = (\lambda p_1, \lambda p_2, \lambda p_3, \lambda p_4, \lambda p_5) \text{ for } \lambda > 0$$
$$\lambda\widetilde{A} = (\lambda p_5, \lambda p_4, \lambda p_3, \lambda p_2, \lambda p_1) \text{ for } \lambda < 0$$

(iv). **Multiplication**

$$\widetilde{A} \otimes \widetilde{B} = \begin{pmatrix} \frac{1}{2}(p_5q_1 + p_1q_5), \frac{1}{2}(p_4q_2 + p_2q_4), p_3q_3, \\ \frac{1}{2}(p_2q_2 + p_4q_4), \frac{1}{2}(p_1q_1 + p_5q_5) \end{pmatrix}$$

4 Algorithms for Optimal Method

4.1 Algorithm for Generalized Quadratic Fuzzy Vogel's Approximation Method

STEP 4.1.1: Check if fuzzy transportation problem is balanced or unbalanced. When unbalanced, add dummy (row or column) as required.

STEP 4.1.2: Calculate penalties for each and every row or column using the ability to differentiate between the lowest cost and the corresponding most available cost in that row/column. If there are two lesser costs, then the penalty will be zero.

STEP 4.1.3: Choose the row/column that has the maximum penalty and allocation in the field having the least value in the chosen row/column. If two or greater equal penalties exists, select one location (row/column) which has minimal unit cost. If there is also a tie, pick out one of the region where most allocations can be made.

STEP 4.1.4: Remove the row/column which has the capacity (tons) and requirements (tons).

STEP 4.1.5: Repeat steps (4.1.2) and (4.1.3) till the desires are satisfied.

STEP 4.1.6: Obtain the IBFS.

4.2 Algorithm for Generalized Quadratic Fuzzy Modified Distribution Method

STEP 4.2.1: Determine an IBFS for the use of GQFVAM.
STEP 4.2.2: Determine, and use, dual variables $\tilde{u}_i$ and $\tilde{v}_j$ using $\tilde{u}_i + \tilde{v}_j = \tilde{c}_{ij}$.
STEP 4.2.3: Calculate the cost of the possibility using $\tilde{d}_{ij} = \tilde{c}_{ij} - \tilde{u}_i - \tilde{v}_j$.
STEP 4.2.4: Test each and every sign and all the possibility value.

(a) If the possibility costs of all the non-allocated cells are either excessive quality or zero; then, the given solution is the optimal solution.
(b) If one or more non-allocated cell has a terrible possibility price, then the given solution is no longer the most dependable reply, and transportation costs are possible in the similar way.

STEP 4.2.5: Choose the unoccupied box as the box to be filled in with the corresponding solution with the minimum negative opportunity cost.
STEP 4.2.6: For the non-allocated cell chosen in the preceding step, draw a closed path or loop.
STEP 4.2.7: Assign appropriate (+) and (−) signs on the nook determinants of the closed route to the unoccupied cells with a (+) sign determined at the unit.
STEP 4.2.8: Determine the maximum unit variety to be shipped to that unoccupied cell. The minimal value on the closed route with absolutely horrible function means the rate of units that can be delivered to the cell to get in. Then, add this quantity to all the cells on the corner cost of the closed route marked with (+) sign, and subtract it from these cells marked with (−) signs. In this way, an unoccupied cell transforms into an involved cell.
STEP 4.2.9: Repeat the entire procedure until it obtains an optimal solution.

5 Numerical Example

National oil industry has three refineries (R1, R2, R3) located throughout a state. Oil production at each plant is as follow: plant1 (P1), plant2 (P2), plant3 (P3). Every day, the oil must fulfill the needs of its three distribution refineries. Transportation cost per ton capacities and requirements are given below. Determine the optimal solution of generalized quadratic fuzzy numbers (Table 2).

The given problem is an unbalanced problem. Because, sum of the capacity (tons) is not equal to the sum of the requirements (tons). The maximum of the total capacity and requirements is 147, 149, 150, 151, and 153. Hence, it is called as an unbalanced generalized quadratic fuzzy transportation model. So, it must be converted into a balanced one.

Table 2 Identification of capacity (tons in fuzzy) requirements (tons in fuzzy)

	Plant 1	Plant 2	Plant 3	Capacity (tons)
Refineries 1	(3, 5, 6, 7, 9)	(7, 9, 10, 11, 13)	(11, 13, 14, 15, 17)	(47, 49, 50, 51, 53)
Refineries 2	(9, 11, 12, 13, 15)	(16, 18, 19, 20, 22)	(18, 20, 21, 22, 24)	(47, 49, 50, 51, 53)
Refineries 3	(12, 14, 15, 16, 18)	(11, 13, 14, 15, 17)	(14, 16, 17, 18, 20)	(47, 49, 50, 51, 53)
Requirement (tons)	(27, 29, 30, 31, 33)	(37, 39, 40, 41, 43)	(52, 54, 55, 56, 58)	

Sum of the capacities are more than the sum of the requirements by (7, 19, 25, 31, 43) units. So, a dummy column is to be introduced with a requirements (tons) of (7, 19, 25, 31, 43) units to absorb the excess capacity (tons), since it is balanced.

Let us use the GQFVAM procedure to explain the above algorithm. Penalties are calculated, and a cell is selected for the allocation according to the least cost along the row or column that has earned the highest penalty allocation. Penalty is proportional to the difference (least value of the cells) (least value of the cells remaining). Calculate for each row and column to measure the penalties which is the difference between the first two least cell values. Repeat the process from step 4.1.3 to step 4.1.6 until an initial solution is found out from the table.

The initial basic feasible solution (IBFS) allocation of the generalized quadratic fuzzy transportation problems is as follows (Table 3):

The total cost of the solution is obtained by adding the products of the cost of transportation per unit given in every basic cell, and the corresponding number of units allocated to it.

The IBFS of generalized quadratic fuzzy transportation costs are

$$\begin{aligned}&(7, 19, 25, 31, 43)(0, 0, 0, 0, 0) + (27, 29, 30, 31, 33)(9, 11, 12, 13, 15)\\ &\quad + (37, 39, 40, 41, 43)(7, 9, 10, 11, 13) + (14, 18, 20, 22, 26)(18, 20, 21, 22, 24)\\ &\quad + (4, 18, 25, 32, 46)(14, 16, 17, 18, 20) + (4, 8, 10, 12, 16)(11, 13, 14, 15, 17)\\ &= (1628, 1732, 1745, 1758, 1862).\end{aligned}$$

Table 3 IBFS of generalized quadratic fuzzy transportation

	P1	P2	P3	P4
R1	(3, 5, 6, 7, 9)	(37, 39, 40, 41, 43) (7, 9, 10, 11, 13)	(4, 8, 10, 12, 16) (11, 13, 14, 15, 17)	(0, 0, 0, 0, 0)
R2	(27, 29, 30, 31, 33) (9, 11, 12, 13, 15)	(16, 18, 19, 20, 22)	(14, 18, 20, 22, 26) (18, 20, 21, 22, 24)	(0, 0, 0, 0, 0)
R3	(12, 14, 15, 16, 18)	(11, 13, 14, 15, 17)	(4, 18, 25, 32, 46) (14, 16, 17, 18, 20)	(7, 19, 25, 31, 43) (0, 0, 0, 0, 0)

Table 4 IBFS of generalized quadratic fuzzy transportation

	$\tilde{v}_1$	$\tilde{v}_2$	$\tilde{v}_3$	$\tilde{v}_4$
$\tilde{u}_1$	(3, 5, 6, 7, 9)	(37, 39, 40, 41, 43) (7, 9, 10, 11, 13)	(4, 8, 10, 12, 16) (11, 13, 14, 15, 17)	(0, 0, 0, 0, 0)
$\tilde{u}_2$	(27, 29, 30, 31, 33) (9, 11, 12, 13, 15)	(16, 18, 19, 20, 22)	(14, 18, 20, 22, 26) (18, 20, 21, 22, 24)	(0, 0, 0, 0, 0)
$\tilde{u}_3$	(12, 14, 15, 16, 18)	(11, 13, 14, 15, 17)	(4, 18, 25, 32, 46) (14, 16, 17, 18, 20)	(7, 19, 25, 31, 43) (0, 0, 0, 0, 0)

Table 5 Optimal solution of generalized quadratic fuzzy transportation

	P1	P2	P3	P4
R1	(2, 4, 5, 6, 8) (3, 5, 6, 7, 9)	(37, 39, 40, 41, 43) (7, 9, 10, 11, 13)	(−4, 2, 5, 8, 14) (11, 13, 14, 15, 17)	(0, 0, 0, 0, 0)
R2	(19, 23, 25, 27, 31) (9, 11, 12, 13, 15)	(16, 18, 19, 20, 22)	(18, 20, 21, 22, 24)	(16, 22, 25, 28, 34) (0, 0, 0, 0, 0)
R3	(12, 14, 15, 16, 18)	(11, 13, 14, 15, 17)	(20, 40, 50, 60, 80) (14, 16, 17, 18, 20)	(0, 0, 0, 0, 0)

Using algorithm for GQFMODI method

The GQFMODI is an efficient approach to check the optimality of the preliminary possible solution (Table 4).

Since the number of basic cells and the solution are non-degenerate, we calculate $\tilde{u}_i$ and $\tilde{v}_j$ using $\tilde{u}_i + \tilde{v}_j = \tilde{c}_{ij}$ for all occupied basic cells. Arbitrarily, start with some $\tilde{u}_i$ or $\tilde{v}_j$ as zero. At this stage, all $\tilde{u}_i$ and $\tilde{v}_j$ values will be known. Compute the cell evaluations $\tilde{d}_{ij} = \tilde{c}_{ij} - \tilde{u}_i - \tilde{v}_j$ for unoccupied cells. If all cell projections are positive or zero, then the current feasible basic solution is optimal. The current solution is not optimal when every cell evaluation is negative. Continue the cycle before they reach optimum solution (Table 5).

The optimum solution of generalized quadratic fuzzy transportation cost is

$$
\begin{aligned}
&= (2, 4, 5, 6, 8)(3, 5, 6, 7, 9) + (37, 39, 40, 41, 43)(7, 9, 10, 11, 13) \\
&\quad + (-4, 2, 5, 8, 14)(11, 13, 14, 15, 17) + (19, 23, 25, 27, 31)(9, 11, 12, 13, 15) \\
&\quad + (16, 22, 25, 28, 34)(0, 0, 0, 0, 0) + (20, 40, 50, 60, 80)(14, 16, 17, 18, 20) \\
&= (1497, 1633, 1650, 1667, 1803)
\end{aligned}
$$

6 Results Comparison

See Table 6.

Table 6 Comparison of IBFS and optimal

Methods	Fuzzy IBFS/optimal solution
GFNWCM	(1680, 1800, 1815, 1830, 1950)
GFLCM	(1777, 1873, 1885, 1897, 1993)
GFVAM	(1628, 1732, 1745, 1758, 1862)
GFVAM	(1497, 1633, 1650, 1667,1803)

7 Conclusion

This paper proposes a generalized quadratic fuzzy VAM method for solving fuzzy transportation problems without altering them to classical transportation problems. To illustrate the proposed technique, the most useful solution of generalized quadratic MODI need to be acquired. To get the optimum solution of transportation problems described via the utilization of piecewise quadratic fuzzy quantity, a unique method is proposed to showcase the works successfully. For further research, this strategy can be utilized to take care of the practical problems in the field of Hungarian technique, mobile sales reps problems, scheduling, and critical way strategy. It can also be utilized in the trapezoidal fuzzy and quadratic fuzzy numbers for the expense of fuzzy flexibility and fuzzy interest issues to get advanced arrangement of the transportation models.

Compliance with Ethical Standards Conflicts of Interest

The authors proclaim that there are no irreconcilable circumstances with respect to the distribution of this paper. All the authors have equivalent commitments. All the authors read and approved the final manuscript. The authors would like to thank the editor and anonymous referees. Any funding does not support this research.

This article doesn't contain any investigations with human members or creatures performed by any of the writers.

All referred investigation is featured in the Literature Review.

Acknowledgments The authors would like to thank to the editor-in-chief and the anonymous reviewers for their suggestions that have led to an improvement in both the quality and clarity of the paper

References

1. Dantzig, G.B., Thapa, M.N.: Springer: Linear Programming: 2: Theory and Extensions. Princeton University Press, New Jersey (1963)
2. Gass SI (1990) On solving the transportation problem. J. Oper. Res. Soc. **41**(4), 291–297
3. Zadeh, L.A.: Fuzzy sets. Inform. Control **8**, 338–353 (1965)
4. Dubois, D., Prade, H.: Fuzzy set and systems theory and application. Academic Press, New York (1980)

5. Abbasbandy, S., Hajjari, T.: A new approach for the ranking of trapezoidal fuzzy numbers. Comput. Math. Appl. **57**, 413–419 (2009)
6. Venkatachalapathy, M., Edward Samuel, A.: An alternative method for solving Fuzzy transportation problems using ranking functions. Int. J. Appl. Math. Sci. **9**(1), 61–68 (2016)
7. Kaur, A., Kumar, A.: A new approach for solving fuzzy transportation problems using generalized trapezoidal fuzzy numbers. Appl. Soft Comput. 1–34 (2011)
8. Vimala, S., Thiagarajan, K., Amaravathy, A.: OFSTF method—an optimal solution for transportation problem. Indian J. Sci. Technol. **9**(48), 1–3 (2016)
9. Zimmermann, H.J.: Fuzzy programming and linear programming with several objective functions. Fuzzy Sets Syst. **1**, 45–55 (1978)
10. Stephan Dinagar, D., Christoper Raj, B.: A method for solving fully Fuzzy transportation problem with generalized quadrilateral Fuzzy numbers. Malaya J. Matematik **S**(1), 24–27 (2019)
11. Muthuperumal, S., Titus, P., Venkatachalapathy, M.: An algorithmic approach to solve unbalanced triangular Fuzzy transportation problems. In: Soft Computing, Springer-Verlag GmbH Germany, part of Springer Nature (2020)
12. Amaravathy, A., Seerengasamy, V., Vimala, S.: Comparative study on MDMA Method with OFSTF method in transportation problem. Int. J. Comput. Organ. Trends (IJCOT) **6**(6), 50–55 (2016)
13. Venkatachalapathy, M., Jayaraja, A., Samuel, A.E.: A study on solving octagonal Fuzzy numbers using the modified Vogel's approximation method. Int. J. Pure Appl. Math. **118**(6), 201–207 (2018)
14. Venkatachalapathy, M., Pandiarajan, R., Ganeshkumar, S.: A special type of solving transportation problems using generalized quadratic fuzzy number. Int. J. Sci. Technol. Res. **9**(2), 6344–6348 (2020)
15. Amaliah, B., Fatichah, C., Suryani, E.: Total opportunity cost matrix—minimal total: a new approach to determine initial basic feasible solution of a transportation problem. Egypt. Inform. J. **20**, 131–141 (2019)
16. Öztürk, S., Karakuzu, C., Kuncan, M., Erdil, A.: Fuzzy neural network controller as a real time controller using PSO. Akademik Platform Mühendislik ve Fen Bilimleri Dergisi **5**(1), 15–22 (2017)
17. Kuncan, M., Kaplan, K., Acar, F., Kundakçi, I.M., Ertunç, H.M.: Fuzzy logic based ball on plate balancing system real time control by image processing. Int. J. Nat. Eng. Sci. **10**(3), 28–32 (2016)
18. Karakoç, H., Erin, K., Çağıran, R., Kuncan, M., Kaplan, K., Ertunç, H.M.: The Performance Comparison of PD Controller and Fuzzy Logic Controller for the Aircraft Height Control Otomatik Kontrol Ulusal Toplantısı, TOK'2015, pp. 10–12 (2015)
19. Ramesh Babu, A., Rama Bhupal Reddy, B.: Feasibility of fuzzy new method in finding initial basic feasible solution for a fuzzy transportation problem. J. Comput. Math. Sci. **10**(1), 43–54 (2019)
20. Mathur, N., Srivastava, P.K.: An inventive approach to optimize fuzzy transportation problem. Int. J. Math. Eng. Manage. Sci. **5**(5), 985–994 (2020)
21. Doğan, H., Kaplan, K., Kuncan, M., Ertunç, H.M.: PID and fuzzy logic approach to vehicle suspension system control. Otomatik Kontrol Ulusal Toplantısı 10–12 (2015)
22. Kaplan, K., Kuncan, M., Ertunc, H.M.: Prediction of bearing fault size by using model of adaptive neuro-fuzzy inference system. In: 2015 23nd Signal Processing and Communications Applications Conference (SIU) IEEE, pp. 1925–1928 (2015)
23. Edward Samuel A, Venkatachalapathy M (2012) A new procedure for solving the generalized trapezoidal Fuzzy transportation problem. Adv Fuzzy Sets Syst **12**(2), 111–125

A New Ranking Method for Solving Nanogonal Fuzzy Transportation Problem

R. Saravanan and M. Valliathal

Abstract Transportation problem plays a vital role in decision-making problems. A fuzzy transportation problem is a transportation problem in which the transportation costs, supply, and demand quantities are fuzzy quantities. In this paper, a new ranking technique is proposed for ranking the nanogonal fuzzy numbers. Using the proposed ranking procedure, the fuzzy transportation problem is transformed into crisp transportation problem. An optimal solution of fuzzy transportation problem is obtained by using proposed ranking method only which is illustrated with example.

Keywords Nanogonal fuzzy number · Fuzzy transportation problem · Robust ranking method · Proposed ranking method

1 Introduction

Transportation problem is the special case of linear programming problem. The aim of transportation problem is to minimize the cost of distributing goods from a various origins to various destinations. The methods for solving the transportation problem are available only when the demand and supply quantities are exactly known. In some situation, the quantities of the problem does not know exactly. This distrustful situation is called uncertainty. When uncertainty exists, there steer has been fuzziness. A fuzzy transportation problem is a transportation problem in which the transportation costs, supply, and demand quantities are fuzzy quantities. Decisions made by the decision makers only after ranking the fuzzy numbers. Ranking of fuzzy numbers plays an important role in decision-making problems.

Zadeh [1] was first to introduce the concept of fuzzy sets to deal with imprecision, vagueness in real-life situations. Bellmann and Zadeh [2] expressed the concept of decision-making in fuzzy environment. Zimmermann [3] showed that solutions

R. Saravanan (✉)
NIFT-TEA College of Knitwear Fashion, Tirupur, India

M. Valliathal
Chikkaiah Naicker College, Erode, India

© The Author(s), under exclusive license to Springer Nature Singapore Pte Ltd. 2022

S. R. Kannan et al. (eds.), *Fuzzy Mathematical Analysis and Advances in Computational Mathematics*, Studies in Fuzziness and Soft Computing 419,
https://doi.org/10.1007/978-981-19-0471-4_4

obtained by fuzzy linear programming are always efficient. Chanas and Kuchta [4] discussed the concept of the optimal solution of the transportation problem with fuzzy cost coefficients. Chanas and Kuchta [5] solved fuzzy integer transportation problem. Liu and Kao [6] found solution of fuzzy transportation problems based on extension principle. Chanas et al. [7] discussed a fuzzy approach for solving the transportation problem. Basirzadeh [8] approached a new technique for solving fuzzy transportation problem.

Pandian and Natarajan [9] approached a new method called a fuzzy zero point method for finding optimal solution of fuzzy transportation problems. Solaiappan and Jeyaraman [10] investigated the fuzzy transportation problem by using zero termination method. Gani and Razak [11] analyzed two-stage fuzzy transportation problem. Annie Christi and Malini [12] solved the octagonal fuzzy transportation problem using best candidate method and centroid method. Renuka and Jenita Nancy [13] solved nanogonal fuzzy transportation problem using Russell's method. Sudha et al. [14] found the optimal solution of fuzzy transportation problem using nonagonal fuzzy number.

Singh and Thakur [15] calculated a new method for solving fuzzy transportation problem using dodecagonal fuzzy number. Sujatha et al. [16] solved a fuzzy transportation problem using zero point maximum allocation method. Malini and Kennedy [17] ordered an octagonal fuzzy numbers. Sudhakar and Navaneetha Kumar [18] developed a solution of multi-objective two-stage fuzzy transportation problem by using zero suffix method. Narayanamoorthy et al. [19] solved a fuzzy transportation problem using fuzzy Russell's method. Felix et al. [20] studied the arithmetic operations of nanogonal fuzzy number.

In this paper, a new ranking method is proposed for ranking the nanogonal fuzzy numbers. Using the two ranking technique, nanogonal fuzzy transportation problem can be converted in to crisp transportation problem. The optimal solution of nanogonal fuzzy transportation is obtained by using proposed ranking method.

2 Preliminaries

Definition 2.1 A fuzzy set is characterized by a membership function mapping element of a domain space or the universe of discourse X to the unit interval [0, 1]

$$(\text{i.e.})A = \{x, \mu_A(x)\ ;\ x \in X\}.\ \text{Here}\ \mu_A(x) = 1$$

Definition 2.2 A fuzzy set A of the universe of discourse X is called normal fuzzy set implying that there exist at least one $x \in X$ such that $\mu_A(x) = 1$.

Definition 2.3 The support of fuzzy set in the universal set X is the set that contains all the elements of X that have a non-zero membership grade in $\tilde{A}$.

$$(\text{i.e.})\text{Supp}\,(\tilde{A}) = \left\{x \in X/\mu_{\tilde{A}}(x) > 0\right\}$$

Definition 2.4 Given a fuzzy set A defined on X and any number $\alpha \in [0, 1]$ the α-cut, α_A is the crisp set $\alpha_A = \{x \in X/A(x) \geq \alpha, \alpha \in [0, 1]$.

Definition 2.5 A fuzzy set $\tilde{A}$ defined on the set of real numbers R is said to be fuzzy number if its membership function $\mu_A(x) : R \to [0, 1]$ has the following properties

(i) A must be a normal and convex fuzzy set
(ii) α_A must be a closed interval for every $\alpha \in (0, 1]$
(iii) The support of $\tilde{A}$ must be bounded

Definition 2.6 A fuzzy number $\tilde{A}$ is called triangular function is denoted by $\tilde{A} = (a_1, a_2, a_3)$ whose membership function is defined as follows:

$$\mu_{\tilde{A}}(x) = \begin{cases} 0 & x < a_1 \\ \frac{x-a_1}{a_2-a_1} & a_1 \leq x \leq a_2 \\ \frac{a_3-x}{a_3-a_2} & a_2 \leq x \leq a_3 \\ 0 & x > a_3 \end{cases}$$

Definition 2.7 A fuzzy number $\tilde{A}$ is called trapezoidal function is denoted by $\tilde{A} = (a_1, a_2, a_3, a_4)$ whose membership function is defined as follows:

$$\mu_{\tilde{A}}(x) = \begin{cases} 0 & x < a_1 \\ \frac{x-a_1}{a_2-a_1} & a_1 \leq x \leq a_2 \\ 1 & a_2 \leq x \leq a_3 \\ \frac{a_4-x}{a_4-a_3} & a_3 \leq x \leq a_4 \\ 0 & x > a_3 \end{cases}$$

Definition 2.8 A nanogonal fuzzy number is denoted by $\tilde{A}$ is defined to be the ordered 6-tuple $\tilde{A} = \left(f_1(r), g_1(s), h_1(t), \overline{f}_1(r), \overline{g}_1(s), \overline{h}_1(t)\right)$ for $r \in [0, k_1]$, $s \in [k_1, k_2]$ and $t \in [k_2, 1]$ where

(i) $f_1(r)$ is a bounded left continuous non-decreasing function over $[0, k_1]$, $[0 \leq k_1 \leq k_2]$
(ii) $g_1(s)$ is a bounded left continuous non-decreasing function over $[k_1, k_2]$,$[k_1 \leq k_2 \leq 1]$
(iii) $\overline{f}_1(r)$ is a bounded left continuous non-increasing function over $[0, k_1]$, $[0 \leq k_1 \leq k_2]$
(iv) $\overline{g}_1(s)$ is a bounded left continuous non-increasing function over $[k_1, k_2]$,$[k_1 \leq k_2 \leq 1]$

3 Nanogonal Fuzzy Number

A fuzzy number $\tilde{A}$ is a nanogonal fuzzy number defined by $\tilde{A} = (a_1, a_2, a_3, a_4, a_5, a_6, a_7, a_8, a_9)$ where $a_1, a_2, a_3, a_4, a_5, a_6, a_7, a_8, a_9$ are real

numbers, and its membership function is given by

$$\mu_{\tilde{A}}(x) = \begin{cases} 0 & x < a_1 \\ k_1\left(\frac{x-a_1}{a_1-a_2}\right) & a_1 \le x \le a_2 \\ k_1 & a_2 \le x \le a_3 \\ k_1 + (1-k_1)\left(\frac{x-a_3}{a_4-a_3}\right) & a_3 \le x \le a_4 \\ k_1 + (1-k_1)\left(\frac{x-a_4}{a_5-a_4}\right) & a_4 \le x \le a_5 \\ k_1 + (1-k_1)\left(\frac{a_6-x}{a_6-a_5}\right) & a_5 \le x \le a_6 \\ k_1 + (1-k_1)\left(\frac{a_7-x}{a_7-a_6}\right) & a_6 \le x \le a_7 \\ k_1 & a_7 \le x \le a_8 \\ k_1\left(\frac{a_9-x}{a_9-a_8}\right) & a_8 \le x \le a_9 \\ 0 & x > a_9 \end{cases} \quad \text{where } 0 < k_1 < 1$$

3.1 Arithmetic Operations on Nanogonal Fuzzy Number

Let $\tilde{A}_{NFN} = (a_1, a_2, a_3, a_4, a_5, a_6, a_7, a_8, a_9)$ and $B_{NFN} = (b_1, b_2, b_3, b_4, b_5, b_6, b_7, b_8, b_9)$ be two nanogonal fuzzy numbers; then, the addition, subtraction, and scalar multiplication can be defined as

$$\begin{aligned} \tilde{A}_{\text{NFN}} + \tilde{B}_{\text{NFN}} &= [a_1 + b_1, a_2 + b_2, a_3 + b_3, a_4 + b_4, a_5 + b_5, \\ &\quad a_6 + b_6, a_7 + b_7, a_8 + b_8, a_9 + b_9] \\ \tilde{A}_{\text{NFN}} - \tilde{B}_{\text{NFN}} &= [a_1 - b_9, a_2 - b_8, a_3 - b_7, a_4 - b_6, a_5 - b_5, \\ &\quad a_6 - b_4, a_7 - b_3, a_8 - b_2, a_9 - b_1] \\ \lambda\tilde{A}_{\text{NFN}} &= [\lambda a_1, \lambda a_2, \lambda a_3, \lambda a_4, \lambda a_5, \lambda a_6, \lambda a_7, \lambda a_8, \lambda a_9] \\ \lambda\tilde{B}_{\text{NFN}} &= [\lambda b_1, \lambda b_2, \lambda b_3, \lambda b_4, \lambda b_5, \lambda b_6, \lambda b_7, \lambda b_8, \lambda b_9] \end{aligned}$$

3.2 Measure of Fuzzy Number

The measure of $\tilde{A}_\omega$ is a measure is a function $M_o : R_\omega(I) \to R^+$ which assign a non-negative real numbers $M_o^{NFN}\left(\tilde{A}_\omega\right)$ that expresses the measure of

$$M_o^{\text{NFN}}\left(\tilde{A}_\omega\right) = \frac{1}{2}\int_\alpha^{k_1} \left(f_1(r) + \overline{f}_1(r)\right) \mathrm{d}r$$

$$+\frac{1}{2}\int_{k_1}^{\omega}\left(g_1(s)+\overline{g}_1(s)\right)\mathrm{d}s \text{ where } 0\le\alpha<1$$

4 Proposed Ranking Method

Let $\tilde{A}$ be a normal nanogonal fuzzy number. The measure of $\tilde{A}$ is calculated as follows:

$$M_o^{\mathrm{NFN}}\left(\tilde{A}_\omega\right)=\frac{1}{2}\int_0^{k_1}\left(f_1(r)+\overline{f}_1(r)\right)\mathrm{d}r+\frac{1}{2}\int_{k_1}^{1}\left(g_1(s)+\overline{g}_1(s)\right)\mathrm{d}s$$

$$M_o^{\mathrm{NFN}}(\tilde{A})=\frac{1}{4}\{(a_1+a_2+a_8+a_9)\,k_1+(a_3+a_4+2a_5+a_6+a_7)\,(1-k_1)\}$$

$$, \qquad \text{where } 0<k_1<1$$

5 Robust Ranking Method for Nanogonal Fuzzy Number

Robust ranking technique for nanogonal fuzzy number is defined as follows. If ã is a fuzzy number, then the robust ranking is defined by $\Re(\tilde{a})=\int_0^1(0.5)\left(a_\alpha^L,a_\alpha^U\right)d\alpha$ where

$$\left(a_\alpha^L,a_\alpha^U\right)=\begin{bmatrix}(a_2-a_1)\,\alpha+a_1,\ a_4-(a_4-a_3)\,\alpha,\ (a_6-a_5)\,\alpha\\ +a_5,\ a_7-(a_7-a_6)\,\alpha,\\ (a_7-a_6)\,\alpha+a_6,\ a_9-(a_9-a_8)\alpha\end{bmatrix} \tag{5.1}$$

6 Fuzzy Transportation Problem

The mathematical form of fuzzy transportation problem is as follows:

$$\text{Minimize } Z=\sum_{i=1}^{m}\sum_{j=1}^{n}\tilde{c}_{ij}\tilde{x}_{ij}$$

Subject to the constraints

$$\sum_{j=1}^{n} \tilde{x}_{ij} = \tilde{a}_i \qquad i = 1, 2, ...m$$

$$\sum_{i=1}^{m} \tilde{x}_{ij} = \tilde{b}_j \qquad j = 1, 2....n$$

where $\tilde{x}_{ij} \geq 0$ for all i and j

where $\tilde{a}_i$ is the fuzzy availability of the product at the ith source; $\tilde{b}_j$ is the fuzzy demand of the product at the jth destination; $\tilde{c}_{ij}$ is the fuzzy transporting cost of one unit of the product from the ith source to the jth destination, and $\tilde{x}_{ij}$ is the amount of units of the product that should be transported from the ith source to jth destination.

Generally, the transportation problem is displayed in the following tabular form:

7 Numerical Example

Let us consider the following fuzzy nanogonal transportation problem. The problem has three sources and three destinations. The cost, supply, and demand are taken as a nanogonal fuzzy numbers. The objective of the given problem is to minimize the transportation cost (Table 2).

The mathematical formulation of the given fuzzy transportation problem is

$$\begin{aligned}\text{Minimize } \tilde{Z}^* = {} & \Re\,(1, 2, 3, 4, 5, 6, 7, 8, 9) + \Re(2, 4, 6, 8, 10, 12, 14, 16, 18) \\ & + \Re(1, 3, 5, 7, 9, 11, 13, 15, 17) \\ & + \Re(3, 6, 9, 12, 15, 18, 21, 24, 27) + \Re(2, 5, 8, 9, 10, 11, 14, 17, 18) \\ & + \Re(3, 4, 5, 6, 7, 8, 9, 10, 11) \\ & + \Re(7, 8, 9, 10, 11, 12, 13, 14, 15) + \Re(5, 6, 7, 8, 9, 10, 11, 12, 13) \\ & + \Re + (4, 6, 8, 10, 12, 14, 16, 18, 20) \\ & + \Re(6, 8, 10, 12, 14, 16, 18, 20, 22) + \Re(9, 10, 11, 12, 13, 14, 15, 16, 17) \\ & + \Re(5, 7, 9, 11, 13, 15, 17, 19, 21) \\ & + \Re(1, 4, 7, 10, 13, 16, 19, 22, 25) + \Re(2, 4, 6, 8, 10, 12, 14, 16, 18) \\ & + \Re(10, 11, 12, 13, 14, 15, 16, 17, 18)\end{aligned}$$

7.1 Ranking of Nanogonal Fuzzy Number Using Proposed Method

To find the optimum transportation cost, first to convert the nanogonal fuzzy cost into crisp cost using our ranking method. Take the value of $k_1 = 0.5$. Using our proposed ranking method, the transformed (crisp cost) transportation table is given below.

7.2 Crisp Transportation Problem of the Corresponding Nanogonal Fuzzy Transportation Problem

The crisp transportation problem of the corresponding nanogonal fuzzy transportation problem is given in Table 3

Here, total supply = total demand. The given transportation problem is balanced transportation problem. Initial basic feasible solution is obtained by using Vogel's approximation method. After that we are applying the modified distribution method to the given problem; the optimum solution is obtained. The optimum transportation allocation table is given in Table 4.

The optimum (minimum) transportation cost is

$$16.25 \times 6.25 + 1.25 \times 8.5 + 1.25 \times 11.25 + 11.25 \times 8.75 + 16.25 \times 16.25 = 488.73 \text{ units}$$

8 Ranking of Nanogonal Fuzzy Number Using Robust Ranking Method

Using robust ranking method (5.1), the nanogonal fuzzy cost (in Table 1) is converted into crisp cost. The transformed cost is given in Table 5.

Table 1 Fuzzy transportation problem

	Destination					
Source		1	2	…	n	Fuzzy supply
	1	$\tilde{c}_{11}$	$\tilde{c}_{12}$	…	$\tilde{c}_{1n}$	$\tilde{a}_1$
	2	$\tilde{c}_{21}$	$\tilde{c}_{22}$	…	$\tilde{c}_{2n}$	$\tilde{a}_2$
	…	…	…		…	…
	m	$\tilde{c}_{m1}$	$\tilde{c}_{m2}$	…	$\tilde{c}_{mn}$	$\tilde{a}_m$
	Fuzzy demand	$\tilde{b}_1$	$\tilde{b}_2$		$\tilde{b}_n$	

Table 2 Nanogonal fuzzy transportation problem

	D_1	D_2	D_3	Fuzzy Supply
S_1	(1, 2, 3, 4, 5, 6, 7, 8, 9)	(2, 4, 6, 8, 10, 12, 14, 16, 18)	(1, 3, 5, 7, 9, 11, 13, 15, 17)	(3, 6, 9, 12, 15, 18, 21, 24, 27)
S_2	(2, 5, 8, 9, 10, 11, 14, 17, 18)	(3, 4, 5, 6, 7, 8, 9, 10, 11)	(7, 8, 9, 10, 11, 12, 13, 14, 15)	(5, 6, 7, 8, 9, 10, 11, 12, 13)
S_3	(4, 6, 8, 10, 12, 14, 16, 18, 20)	(6, 8, 10, 12, 14, 16, 18, 20, 22)	(9, 10, 11, 12, 13, 14, 15, 16, 17)	(5, 7, 9, 11, 13, 15, 17, 19, 21)
Fuzzy demand	(1, 4, 7, 10, 13, 16, 19, 22, 25)	(2, 4, 6, 8, 10, 12, 14, 16, 18)	(10, 11, 12, 13, 14, 15, 16, 17, 18)	

Table 3 Crisp transportation problem of the corresponding nanogonal fuzzy transportation problem is given in Table 3

	D_1	D_2	D_3	Supply
S_1	6.25	12.5	11.25	18.75
S_2	13	8.75	13.75	11.25
S_3	15	17.5	16.25	16.25
Demand	16.25	12.5	17.5	

Table 4 Optimum transportation allocation table for proposed ranking method

	D_1		D_2		D_3	
S_1	**16.25**		**1.25**		**1.25**	
		6.25		8.5		11.25
S_2			**11.25**			
	13			8.75		13.75
S_3		15		17.5	**16.25**	
						16.25

Table 5 Crisp transportation problem of the corresponding nanogonal fuzzy transportation problem

	D_1	D_2	D_3	Supply
S_1	16	32	29	48
S_2	32.5	22	34	28
S_3	38	44	40	41
Demand	42	32	43	

Here, total supply = total demand. The given transportation problem is balanced transportation problem. Initial basic feasible solution is obtained by using Vogel's approximation method. After that we are applying the modified distribution method

Table 6 Optimum transportation allocation table for Robust ranking method

	D_1		D_2		D_3	
S_1	**42**		**4**		**2**	
		16		32		29
S_2			**28**			
	32.5			22		3.75
S_3		38		44	**41**	
						40

Table 7 Solution is attained by using two ranking technique

Methods	Optimal solution
Existing method (Robust ranking)	3114
Proposed method	488.73

to the given problem; the optimum solution is obtained. The optimum transportation allocation table is given in Table 6.

The optimum (minimum) transportation cost is

$$42 \times 16 + 4 \times 32 + 4 \times 29 + 28 \times 22 + 41 \times 40 = 3114$$

The solution is attained by using two ranking technique is listed in Table 7.

From the above results, we conclude that the optimum solution of the problem is attained with the help of proposed method is minimum than that of the existing method.

9 Merit of Proposed Method

The created ranking strategy is easy to ascertain and easy to get, meanwhile the results acquired from this transportation ranking technique are precise than existing strategy.

10 Conclusion

Ranking of fuzzy number plays an important role in decision-making problems. Fuzzy numbers must be ranked before an action is taken by a decision maker. Mapping function has applied to convert a fuzzy number to a crisp number by ranking methods. The ranking method presented here is a new flexible one of the nonagonal fuzzy numbers. The proposed ranking method is simple and easy to calculate the rank

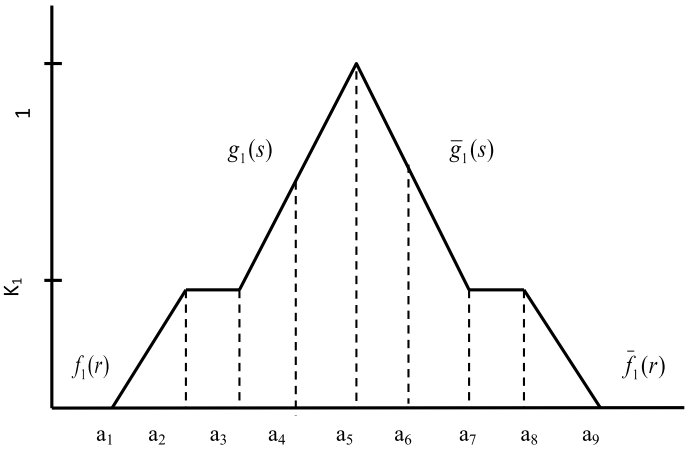

Fig. 1 Graphical representation of nanogonal fuzzy number

of fuzzy numbers which also gives optimum solution to the given problem. This ranking method is used to rank the all the nanogonal fuzzy numbers. The advantage of the proposed model is illustrated by examples. In future, this method is applied to assigning jobs to suitable persons in a real-life problem.

References

1. Zadeh, L.A.: Fuzzy Sets. Inf. Control **8**, 338–353 (1965)
2. Bellman, R.E., Zadeh, L.A.: Decision-making in a fuzzy environment. Manage. Sci. **17**(4), 141–164 (1970)
3. Zimmermann, H.J.: Fuzzy programming and linear programming with several objective functions. Fuzzy Sets Syst. **1**, 45–55 (1978)
4. Chanas, S., Kuchta, D.: A concept of the optimal solution of the transportation problem with fuzzy cost coefficients. Fuzzy Sets Syst. **82**, 299–305 (1996)
5. Chanas, S., Kuchta, D.: Fuzzy integer transportation problem. Fuzzy Sets Syst. **98**, 291–298 (1998)
6. Liu, S.T., and.Kao C,: Solving fuzzy transportation problems based on extension principle. Eur. J. Oper. Res. **153**, 661–674 (2004)
7. Chanas, S., Kolodziejczyk, W., Machaj, A.: A fuzzy approach to the transportation problem. Fuzzy Sets Syst. **13**, 211–221 (1984)
8. Basirzadeh, H.: An approach for solving fuzzy transportation problem. Appl. Math. Sci. **5**(32), 1549–1566 (2011)
9. Pandian, P., Natarajan, G.: A new algorithm for finding a fuzzy optimal solution for fuzzy transportation problem. Appl. Math. Sci. **4**(2), 79–90 (2010)
10. Solaiappan, S., Jeyaraman, K.: On trapezoidal fuzzy transportation problem using zero termination method. Int. J. Math. Res. **5**(4), 351–359 (2013)
11. Nagoor Gani, A., Abdul Razak, K.: Two stage fuzzy transportation problem. J. Phys. Sci. **10**, 63–69 (2006)
12. Annie Christi, M.S., Malini, D.: An approach to solve transportation problems with octagonal fuzzy numbers using best candidates method and different ranking techniques. Int. J. Comput. Appl. **6**(1), 71–85 (2016)

13. Renuka, S., Nancy, J.: Solving a transportation problem using nanogonal fuzzy number with Robust ranking and Russell's method. Int. J. Eng. Technol. Comput. Res. **5**(5), 100–104 (2017)
14. Sudha, L., Shanmugapriya, R., Rama, B.: Fuzzy transportation problem using nanogonal fuzzy number. J. Appl. Sci. Comput. **6**(3), 1100–1105 (2019)
15. Singh, J.P., Thakur, N.I.: An approach for solving a fuzzy transportation problem using dodecagonal fuzzy number. Int. J. Math. Arch. **6**(4), 105–112 (2015)
16. Sujatha, L., Vinothini, P., Jothilakshmi, R.: Solving fuzzy transportation problem using zero point maximum allocation method. Int. J. Current Adv. Res. **7**(1), 173–178 (2018)
17. Malini, S.U., Kennedy, F.C.: An approach for solving fuzzy transportation problem using octagonal fuzzy numbers. Appl. Math. Sci. **7**(54), 2661–2673 (2013)
18. Sudhakar, V.J., Navaneetha Kumar, V.: Solving the multi objective two stage fuzzy transportation problem by zero suffix method. J. Math. Res. **2**(4), 135–140 (2010)
19. Narayanamoorthy, S., Saranya, S., Maheswari, S.: A method for solving fuzzy transportation problem (FTP) using fuzzy Russell's method. Int. J. Intel. Syst. Appl. **2**, 71–75 (2013)
20. Felix, A., Christopher, S., Victor Devadoss, A.: A nonagonal fuzzy number and its arithmetic operation. Int. J. Math. Appl. **3**(2), 185–195 (2015)

Novel Arithmetic Operations on IVIFNs and Their Properties on Ranking Functions

M. Edwin Antony Raj, Geetha Sivaraman, and P. Vishnukumar

Abstract In this paper, a new type of IVIFN is defined from TraIFN. Some operations are defined by using the concept of arithmetic operations on intervals. Later, the main theme of the paper is elaborated on that is how the operation defined over the new type of IVIFNs has an impact on existing ranking functions. It is a seed for several developments in the field of MCDM, fuzzy multi-objective LPP, and in various fields of fuzzy theory. Finally, an application of one of the ranking methods is discussed.

1 Introduction

When there is ambiguity in IFN modeling, IVIFNs are frequently used to represent a range of IFNs that are erratic from the most pessimistic to the most idealistic assessment. IVIFNs are a breakthrough that allows us to avoid such prohibitive complexity. In the past, fuzzy set theory was applied to fuzzy decision-making and fuzzy multi-objective LPPs.

IFS theory has recently gained popularity among researchers, who have applied it to the field of fuzzy theory. IFS is frequently mentioned as another way to acknowledge a fuzzy set, particularly in cases, where existing information is insufficient to define an uncertain theory using a standard fuzzy set. Interval arithmetic is proposed by Dwyer [1]. Ganesan and Veeramani [2] and Moor [3] developed the same concept. Atanassov was the first to introduce operators over IVIFSs [4]. Xu introduced methods for aggregating IVIF data and their application to decision-making [5]. Wei and Wang developed some geometric aggregation operators based on IVIFNs and their application to group decision-making [6]. Based on some operational laws of IVIFNs, Xu and Chen [7] invented some IVIF arithmetic aggregation operators, such

M. Edwin Antony Raj (✉)
Department of Mathematics, K. Ramakrishnan College of Engineering, Samayapuram, Tiruchy, Tamilnadu, India

G. Sivaraman · P. Vishnukumar
Department of Mathematics, St. Joseph's College (Autonomous), Tiruchy, Tamilnadu, India

© The Author(s), under exclusive license to Springer Nature Singapore Pte Ltd. 2022

S. R. Kannan et al. (eds.), *Fuzzy Mathematical Analysis and Advances in Computational Mathematics*, Studies in Fuzziness and Soft Computing 419,
https://doi.org/10.1007/978-981-19-0471-4_5

as IIFWA, IIFOWA, and IIFHA. Based on the IVIF-weighted geometric (IIFWG) operator, Xu and Chen [7] developed some IVIF geometric aggregation operators, such as IIFOWG operator and the IIFHG operator. Some results on generalized IVIFSs have introduced by Bhowmik and Pal [8]. Interval-valued intuitionistic hesitant fuzzy aggregation operators and their application in-group decision-making are proposed by Zhang [9]. New operations over interval-valued intuitionistic hesitant fuzzy set are introduced by Zhang [10].

Many researchers introduced ranking functions and then apply them into MCDM problems. Xu [5] introduced score and accuracy functions. Ye [11] introduced the novel accuracy function. Nayagam et al. [12] discovered the new novel accuracy and general accuracy functions. Liu [13] introduced the general accuracy function. Joshi [1] introduced the accuracy function.

This paper coordinates as in the following way: After the introduction, elementary definitions are discussed in the preliminaries. A new type of IVIFNs is defined, and operations over the new type of IVIFNs are discussed in Sect. 3. How the ranking functions are acted over the operations defined on the new type of IVIFNs are discussed in Sect. 4. Section 5 contains numerical examples. Section 6 explains how to use the existing method. Section 7 contains the conclusion and future scope of the proposed concept.

2 Preliminaries

Definition 2.0.1 (Atanassov and Gargov [14]) Let $D[0, 1]$ be the set of all closed subintervals of [0, 1]. An expression of an IVIFS in a given set $X(\neq \emptyset)$ is given by $P = \{x, \mu_P(x), \gamma_P(x) : x \in X\}$ where $\mu_P\ X \to D[0, 1]\ \gamma_P : X \to D[0, 1][0, 1]$ where $0 < \sup_x \mu_P(x) + \sup_x \gamma_P(x) \leq 1$. An IVIFN is denoted by $P = ([p, q][r, s])$.

Definition 2.0.2 (Xu [5]) The complement P^c of $P = \{\cdot\mu_P(x), \gamma_P(x) : x \in X\}$ is defined by $p^c = \{x, \gamma_p(x), \mu_p(x) : x \in X\}$.

Definition 2.0.3 (Xu [5]) Let $P = ([p, q], [r, s])$ be an IVIFN. The score function S is defined by

$$S(P) = \frac{p + q - r - s}{2}$$

Definition 2.0.4 (Xu [5]) Let $P = ([p, q], [r, s])$ be an IVIFN. The accuracy function H is defined by

$$H(P) = \frac{p + q + r + s}{2}$$

Definition 2.0.5 (Ye [11]) Let $P = ([p, q], [r, s])$ be an IVIFN. The novel accuracy function M is defined by

$$M(P) = p + q - 1 + \frac{r+s}{2}$$

Definition 2.0.6 (Nayagam et al. [15]) Let $P = ([p, q], [r, s])$ be an IVIFN. The new novel accuracy function L is defined by

$$L(P) = \frac{p - s(1-q) + q - r(1-p)}{2}$$

Definition 2.0.7 (Nayagam and Sivaraman [12]) Let $P = ([p, q], [r, s]$ be an IVIFN. The general accuracy function LG is defined by

$$LG(P) = \frac{(p+q)(1-\delta) + \delta(2-(r+s))}{2}$$

Definition 2.0.8 (Liu [13]) Let $P = ([p, q], [r, s])$ be an IVIFN. The general accuracy function A is defined by

$$A(P) = \frac{p + q + \delta_1(1-p-r) + \delta_2(1-q-s)}{2}$$

Definition 2.0.9 (Joshi and Kumar [1]) Let $P = ([p, q], [r, s])$ be an IVIFN. The accuracy function T is defined by

$$T(P) = \frac{p(1-r) + q(1-s)}{2}$$

Definition 2.0.10 (Liu and Luo [13]) Let $P_j \in \text{IVIFS}(X)(j = 1, 2, \ldots, n)$. Then, the weighted arithmetic average (WAA) operators are defined as follows:

$$F_w(P_1, \quad P_2, \quad \ldots, \quad P_n) = \sum_{j=1}^{n} w_j P_j$$

$$= \left[1 - \prod_{j=1}^{n} \left(1 - \mu_{P_j}^{-}(x)\right)^{w_i}, 1 - \prod_{j=1}^{n} \left(1 - \mu_{P_j}^{+}(x)\right)^{w_j}\right]$$

$$\left[\prod_{j=1}^{n} \left(v_{P_j}^{-}(x)\right)^{w_j}, \prod_{j=1}^{n} \left(v_{P_j}^{+}(x)\right)^{w_j}\right]$$

Definition 2.0.11 (Nayagam and Sivaraman [12]) Let $P = ([p, q, r, s], [t, u, v, w])$ where $t \geq r$ and $u \geq s$(or) $v \leq p$ and $w \leq q$ be a TrIFN on new type (TraIFN).

3 A New Type of IVIFN

Definition 3.0.1 Let $P = ([p, q], [r, s])$ be an IVIFN, where p, q, r, and $s \in R^+$ A new type of IVIFN is defined by $P = \{x, \mu_P(x), \gamma_P(x) : x \in X\}$ where μ_P: $R^+ \to [0, 1]$, γ_P: $R^+ \to [0, 1]$ by choosing the choice of non- membership function as $r \geq q$ or $(s \leq p)$.The graphical representations of the new type of IVIFN are given in Fig. 1a, b.

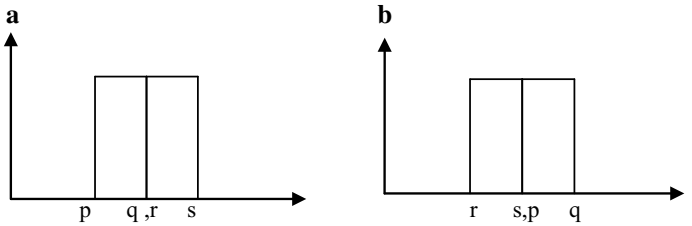

Fig. 1 Graphical representation of new type of IVIFNs

Note 3.0.2 In this paper, we take $r \geq q$. The results discussed thorough out this paper are also true for $s \leq p$.

3.1 Operations on New Type of IVIFNs

Let $P = ([p_1, q_1], [r_1, s_1])$ and $Q = ([p_2, q_2], [r_2, s_2])$ where $p_1, q_1, r_1, s_1, p_2, q_2, r_2$ and $s_2 \in R^+$ are two IVIFNs of new type. Then, by the usual arithmetic operations on interval, we can define the following operations:

1. $P + Q = ([p_1 + p_2, q_1 + q_2],[r_1 + r_2, s_1 + s_2])$

2. $P.Q = ([p_1 p_2, q_1 q_2],[r_1 r_2, s_1 s_2])$

3. $\lambda P = ([\lambda p, \lambda q], [\lambda_r, \lambda_s]), \lambda > 0$

4. $P \cup Q = \begin{cases} ([p_2, q_2], [r_2, s_2]) = Q & \text{if} P \leq Q \\ ([p_1, q_1], [r_1, s_1]) = P & \text{if } P \geq Q \end{cases}$

5. $P \cap Q = \begin{cases} ([p_1, q_1], [r_1, s_1]) = P & \text{if} P \leq Q \\ ([p_2, q_2], [r_2, s_2]) = Q & \text{if } P \geq Q \end{cases}$

Theorem 3.1.1 The operations defined on addition, multiplication, and scalar multiplication are again an IVIFN on new type.

Proof Since by the definition 3.0.1, $r \geq q$,

1. $r_1 \geq q_1, r_2 \geq q_2, \Rightarrow r_1 + r_2 \geq q_1 + q_2$
   $\therefore P + Q = ([p_1 + p_2, q_1 + q_2], [r_1 + r_2, s_1 + s_2])$ is again an IVIFN on new type.
2. $r_1 \geq q_1, r_2 \geq q_2, \Rightarrow r_1.r_2 \geq q_1.q_2$
   $\therefore P \cdot Q = ([p_1 p_2, q_1 q_2], [r_1 r_2, s_1 s_2])$ is again an IVIFN on new type.
3. Since, $\lambda > 0, \lambda r \geq \lambda q, \therefore \lambda P = ([\lambda p, \lambda q], [\lambda r, \lambda s])$ is again an IVIFN on new type. Therefore, the operations are well defined.

Example 3.1.2 Let $P = ([0.2, 0.4], [0.5, 0.6])$ and $Q = ([0.3, 0.5], [0.5, 0.5])$ be two IVIFNs. Then,

1. $P + Q = ([0.5, 0.9], [1.0, 1.1])$
2. $P \cdot Q = ([0.06, 0.2], [0.25, 0.3])$
3. $\lambda P = ([0.4, 0.8], [1.0, 1.2])$ taking $\lambda = 2$

Clearly, addition, multiplication, and scalar multiplication are again IVIFNs on new type.

4 Operations on Ranking Functions

Based on the operations discussed above, let us see how some of them play a role in ranking functions on IVIFN on new type.

Remark 4.0.1 Operation on score function [5]

1. $$S(P + Q) = \frac{p_1 + p_2 + q_1 + q_2 - [r_1 + r_2 + s_1 + s_2]}{2} = \frac{p_1 + q_1 - r_1 - s_1 + p_2 + q_2 - r_2 - s_2}{2} = S(P) + S(Q)$$

2. $$S(\lambda P) = \frac{\lambda p + \lambda q - \lambda r - \lambda s}{2} = \lambda \left[\frac{p + q - r - s}{2} \right] = \lambda S(P)$$

3. $$S\left(P^c\right) = \frac{r + s - p - q}{2} = -\left[\frac{p + q - r - s}{2} \right] = -S(P)$$

Remark 4.0.2 Operation on accuracy function [7]

1. $H(P+Q) = \dfrac{p_1+p_2+q_1+q_2+r_1+r_2+s_1+s_2}{2}$
$= \dfrac{p_1+q_1+r_1+s_1+p_2+q_2+r_2+s_2}{2}$
$= H(P)+H(Q)$

2. $H(\lambda P) = \dfrac{\lambda p+\lambda q+\lambda r+\lambda s}{2} = \lambda\left[\dfrac{p+q+r+s}{2}\right] = \lambda H(P)$

3. $H\left(P^c\right) = \dfrac{r+s+p+q}{2} = \left[\dfrac{p+q+r+s}{2}\right] = H(P)$

Remark 4.0.3 Operation on novel accuracy function [11].

1. $M(P+Q) = p_1+p_2+q_1+q_2-1+\dfrac{r_1+r_2+s_1+s_2}{2}$
$= p_1+q_1-1+\dfrac{r_1+s_1}{2}+p_2+q_2-1+\dfrac{r_2+s_2}{2}+1$
$= M(P)+M(Q)+1$

2. $M(\lambda P) = \lambda p+\lambda q-1+\dfrac{\lambda r+\lambda s}{2} = \lambda p+\lambda q-1+\dfrac{\lambda r+\lambda s}{2}+\lambda-\lambda$
$= \lambda\left[p+q-1+\dfrac{r+s}{2}\right]+\lambda-1$
$= \lambda M(P)+\lambda-1$

3. $M\left(P^c\right) = r+s-1+\dfrac{p+q}{2} = \dfrac{1}{2}\left[p+q-1+\dfrac{4(r+s)}{2}\right]-\dfrac{1}{2}$
$= \dfrac{1}{2}\left[p+q-1+\dfrac{r+s}{2}\right]+\dfrac{3(r+s)}{4}-\dfrac{1}{2} = \dfrac{1}{2}M(P)+\dfrac{3(r+s)-2}{4}$
$= \dfrac{1}{2}\left[M(P)+\dfrac{3(r+s)-2}{2}\right]$

Remark 4.0.4 Operation on new novel accuracy function [15]

1. $L(P+Q)$
$= \dfrac{p_1+p_2+q_1+q_2-(s_1+s_2)[1-(q_1+q_2)]-(r_1+r_2)[1-(p_1+p_2)]}{2}$
$= \dfrac{p_1+q_1-s_1[1-q_1]-r_1[1-p_1]}{2}+\dfrac{p_2+q_2-s_2[1-q_2]-r_2[1-p_2]}{2}$
$+\dfrac{s_1q_2+q_1s_2+p_1r_2+p_2r_1}{2}$

$$= L(P) + L(Q) + \frac{s_1q_2 + q_1s_2 + p_1r_2 + p_2r_1}{2}$$

2. $$L(\lambda P) = \frac{\lambda p - \lambda s(1-\lambda q) + \lambda q - \lambda r(1-\lambda p)}{2}$$
$$= \frac{\lambda p - \lambda s(1-\lambda q+q-q) + \lambda q - \lambda r(1-\lambda p+p-p)}{2}$$
$$= \lambda\left[\frac{p - s(1-q) + q - r(1-p)}{2}\right] + \frac{\lambda[\lambda qs - qs + \lambda pr - pr]}{2}$$
$$= \lambda L(P) + \frac{\lambda(\lambda-1)}{2}(pr+qs)$$

3. $$L\left(P^c\right) = \frac{r - q(1-s) + s - p(1-r)}{2}$$
$$= \frac{r - q(1-s) + s - p(1-r) + p + q - p - q + r + s - r - s}{2}$$
$$= L(P) - [p + q - r - s]$$
$$= L(P) - 2S(P)(\text{or})L(P) + 2S\left(P^c\right)$$

Remark 4.0.5 Operation on general accuracy function [12]

1. $$LG(P+Q) = \frac{(1-\delta)[p_1+p_2+q_1+q_2]+\delta[2-(r_1+r_2+s_1+s_2)]}{2}$$
$$= \frac{(1-\delta)[p_1+p_2+q_1+q_2]+\delta[2+2-(r_1+r_2+s_1+s_2)-2]}{2}$$
$$= \frac{(1-\delta)[p_1+q_1]+(1-\delta)[p_2+q_2]+\delta[2-(r_1+s_1)]}{2}$$
$$+ \frac{\delta[2-(r_2+s_2)]-2\delta}{2}$$
$$= LG(P) + LG(Q) - \delta$$

Note 4.0.6 $LG(P+Q) = \frac{p_1+p_2+q_1+q_2}{2}$ if $\delta = 0$

2. $$\text{LG}(\lambda P) = \frac{(\lambda p + \lambda q)(1-\delta) + \delta(2-(\lambda r + \lambda s))}{2}$$
$$= \frac{\lambda(p+q)(1-\delta) + \delta(2\lambda - 2\lambda + 2 - (\lambda r + \lambda s))}{2}$$
$$= \lambda\left[\frac{(p+q)(1-\delta) + \delta(2-(r+s))}{2}\right] + \delta(1-\lambda)$$
$$= \lambda LG(P) + \delta(1-\lambda)$$

Note 4.0.7 $\text{LG}(\lambda P) = \lambda\frac{p+q}{2}$ if $\delta = 0$

3. $$\text{LG}\left(P^c\right) = \frac{(r+s)(1-\delta) + \delta(2-(p+q))}{2}$$

$$= \frac{(r+s)(1-\delta)+\delta(2-(p+q))+p+q-p-q}{2}$$
$$= \frac{(p+q)(1-\delta)+\delta(2-(r+s))}{2} + \frac{r+s-(p+q)}{2}$$
$$= \mathrm{LG}(P) - S(P)(\mathrm{or})\mathrm{LG}(P) + S\left(P^c\right).$$

Remark 4.0.8 Operation on general accuracy function [13]

1. $\tilde{A}(P+Q) = \frac{p_1+p_2+q_1+q_2+\delta_1[1-p_1-p_2-r_1-r_2]}{2}$
$$+ \frac{\delta_2[1-q_1-q_2-s_1-s_2]}{2}$$
$$= \frac{p_1+p_2+q_1+q_2+\delta_1[1+1-1-p_1-p_2-r_1-r_2]}{2}$$
$$+ \frac{\delta_2[1+1-1-q_1-q_2-s_1-s_2]}{2}$$
$$= \tilde{A}(P) + \tilde{A}(Q) - \frac{(\delta_1+\delta_2)}{2}$$

Note 4.0.8 $\tilde{A}(P+Q) = \frac{p_1+p_2+q_1+q_2}{2}$ if $\delta_1 = \delta_2 = 0$

2. $\tilde{A}(\lambda P) = \frac{\lambda p+\lambda q+\delta_1(1-\lambda p-\lambda r)+\delta_2(1-\lambda q-\lambda s)}{2}$
$$= \frac{\lambda p+\lambda q+\delta_1(\lambda-\lambda+1-\lambda p-\lambda r)+\delta_2(\lambda-\lambda+1-\lambda q-\lambda s)}{2}$$
$$= \lambda\left[\frac{p+q+\delta_1(1-p-r)+\delta_2(1-q-s)}{2}\right] + \frac{(1-\lambda)(\delta_1+\delta_2)}{2}$$
$$= \lambda\tilde{A}(P) + \frac{(1-\lambda)(\delta_1+\delta_2)}{2}$$

Note 4.0.9 $\tilde{A}(\lambda P) = \lambda\frac{p+q}{2}$ if $\delta_1 = \delta_2 = 0$

3. $\tilde{A}\left(P^c\right) = \frac{r+s+\delta_1(1-r-p)+\delta_2(1-s-q)}{2}$
$$= \frac{r+s+\delta_1(1-r-p)+\delta_2(1-s-q)+p+q-p-q}{2}$$
$$= \frac{p+q+\delta_1(1-p-r)+\delta_2(1-q-s)}{2} + \frac{r+s-p-q}{2}$$
$$= \widetilde{A}(P) - S(P) \quad \text{or} \quad \widetilde{A}(P) + S\left(P^c\right).$$

Remark 4.0.11 Operation on accuracy function [1]

1. $T(P+Q) = \frac{(p_1+p_2)(1-r_1-r_2)+(q_1+q_2)(1-s_1-s_2)}{2}$
$$= \frac{p_1(1-r_1)+q_1(1-s_1)+p_2(1-r_2)+q_2(1-s_2)}{2}$$

$$- \frac{p_1r_2 - p_2r_1 - q_1s_2 - q_2s_1}{2}$$
$$= T(P) + T(Q) - \frac{1}{2}(p_1r_2 + p_2r_1 + q_1s_2 + q_2s_1)$$

2. $T(\lambda P) = \dfrac{\lambda p(1-\lambda r) + \lambda q(1-\lambda s)}{2}$
$$= \frac{\lambda p(1-\lambda r + r - r) + \lambda q(1-\lambda s + s - s)}{2}$$
$$= \lambda T(P) + \frac{\lambda(1-\lambda)[pr + qs]}{2}$$

3. $T\left(P^c\right) = \dfrac{r(1-p) + s(1-q) + p - p + q - q}{2}$
$$= \frac{p(1-r) + q(1-s) + r + s - p - q}{2}$$
$$= \frac{p(1-r) + q(1-s)}{2} + \frac{r + s - p - q}{2}$$
$$= T(P) - S(P)(\text{or})T(P) + S\left(P^c\right)$$

Remark 4.0.12 Let * be any ranking function then,

1. $*(P \cup Q) = \begin{cases} *(P) & \text{if } P \geq Q \\ *(Q) & \text{if } P \leq Q \end{cases}$

2. $*(P \cap Q) = \begin{cases} *(P) & \text{if } P \leq Q \\ *(Q) & \text{if } P \geq Q \end{cases}$

Then, Table 1 shows the overall view of operation on ranking functions.

5 Numerical Example

Example 5.0.1 Let $P = ([0.1, 0.1], [0.2, 0.3])$ and $Q = ([0.1, 0.2], [0.3, 0.4])$ be two IVIFNs on new type. Then,

1. $P + Q = ([0.2, 0.3], [0.5, 0.7])$
2. $\lambda P = ([0.2, 0.2], [0.4, 0.6])$ taking $\lambda = 2$
3. $P^c = ([0.2, 0.3], [0.1, 0.1])$

Let us consider * be any ranking function. From Table 2, we can verify the above results.

Table 1 Overall view of operation on ranking functions

Ranking function	Addition	Multiplication	Complement
Score function [5]	$S(P+Q)=S(P)+S(Q)$	$S(\lambda P)=\lambda S(P)$	$S(P^c)=-S(P)$
Accuracy function [5]	$H(P+Q)=H(P)+H(Q)$	$H(\lambda P)=\lambda H(P)$	$H(P^c)=H(P)$
Novel accuracy function [11]	$M(P+Q)=$ $M(P)+M(Q)+1$	$M(\lambda P)=\lambda M(P)+\lambda-1$	$M(P^c)=$ $\frac{1}{2}\left[M(P)+\frac{3(r+s)-2}{2}\right]$
New novel accuracy function [12]	$L(P+Q)=L(P)+L(Q)+$ $\frac{s_1q_2+q_1s_2+p_1r_2+p_2r_1}{2}$	$L(\lambda P)=$ $\lambda L(P)+\frac{\lambda(\lambda-1)}{2}(pr+qs)$	$L(P^c)=$ $L(P)-2S(P)$ (or)$L(P)+2S(P^c)$
General accuracy function [12]	$LG(P+Q)=$ $LG(P)+LG(Q)-\delta$	$LG(\lambda P)=\lambda LG(P)+(1-\lambda)$	$LG(P^c)=LG(P)-$ $S(P)$(or)$LG(P)+$ $S(P^c)$
General accuracy function [13]	$\tilde{A}(P+Q)=$ $\tilde{A}(P)+\tilde{A}(Q)-\frac{(\delta_1+\delta_2)}{2}$	$\tilde{A}(\lambda P)=$ $\lambda\left[\frac{p+q+\delta_1(1-p-r)+\delta_2(1-q-s)}{2}\right]+$ $\frac{(1-\lambda)(\delta_1+\delta_2)}{2}$	$\tilde{A}(P^c)=$ $\tilde{A}(P)-S(P)$ or $\tilde{A}(P)+S(P^c)$
Accuracy function [1]	$T(P+Q)=T(P)+T(Q)-$ $\frac{1}{2}(p_1r_2+p_2r_1+q_1s_2+q_2s_1)$	$T(\lambda P)=$ $\lambda T(P)+\frac{\lambda(1-\lambda)[pr+qs]}{2}$	$T(P^c)=$ $T(P)-S(P)$(or) $T(P)+S(P^c)$

Table. 2 Verification

$*$ Ranking function	$*(P+Q)$	$*(\lambda P)$	$*(P^C)$	$*(P)$	$*(Q)$
Score function [5]	−0.35	−0.3	0.15	−0.15	−0.2
Accuracy function [5]	0.85	0.7	0.35	0.35	0.5
Novel accuracy function [11]	0.1	−0.1	−0.4	−0.55	−0.35
New novel accuracy function [12]	−0.195	−0.2	0.175	−0.125	−0.145
General accuracy function [12] Taking ($\delta=0.5$)	0.325	0.35	0.575	0.425	0.4
general accuracy function [4] Taking ($\delta1=\delta2=0.5$)	0.325	0.35	0.575	0.425	0.4
accuracy function [16]	0.095	0.1	0.225	0.075	0.095

6 Application of the Existing Ranking Function in MCDM Problem

Analytically speaking, the MCDM problem about m alternatives with n criteria can be represented by

$$\begin{array}{c} \\ A_1 \\ A_2 \\ \vdots \\ A_m \end{array} \begin{array}{c} \begin{array}{cccc} C_1 & C_2 & \cdots & C_n \end{array} \\ \begin{pmatrix} A_{11} & A_{12} & \cdots & A_{1n} \\ A_{21} & A_{22} & & A_{2n} \\ \vdots & \vdots & \ddots & \vdots \\ A_{m1} & A_{m2} & \cdots & A_{mn} \end{pmatrix} \end{array}$$

where $A = \{A_1, A_2, \ldots, A_m\}$ be the set of alternatives and $C = \{C_1, C_2, \ldots, C_n\}$ be set of criteria, and the weight of the criterion $C_j (j = 1, 2, \ldots, n)$ is $\omega_j \quad \omega_j \in [0, 1]$, and $\sum_j^n \omega_j = 1; \quad A_{ij} (i = 1, 2, \ldots, m; j = 1, 2, \ldots, n)$ is the assessment of alternatives A_i under the criteria C_j collected from the experts, represented by an IVIFN. In arbitrary, the decision process can be summarized as follows:

6.1 Algorithm

1. After collecting data from the experts form DM.
2. Calculate the WAA values of P_i by definition 2.0.10 for $P_i (i = 1, 2, \ldots, m)$ and denote the aggregating values of P_i by β_i.
3. Calculate the accuracy value by using any of the ranking function in the preliminaries. Here, we take general accuracy function $\mathrm{LG}(\beta_i)(i = 1, 2, \ldots, m)$ by the definition 2.0.7.
4. Rank the alternatives P_i and select the best one based on the values of $\mathrm{LG}(\beta_i)(i = 1, 2, \ldots, m)$.

Example 6.1.1 After completing a bachelor's degree, a student must choose between three courses offered by three different institutions: MBA in X, MCA in Y, or M.Tech in Z. In order to do so, he must select the best college (X, Y, or Z) as well as the appropriate discipline based on a set of criteria. Table 3 shows the decision matrix for the college and discipline based on the criteria.

Table. 3 Decision matrix based on requirements

	Transportation/fees	Ranking/stipend	Teaching/placement
MBA in X	([0.5, 0.7], [0.7, 0.8])	([0.6, 0.8], [0.8, 1])	([0.4, 0.6], [0.8, 1])
MCA in Y	([0.2, 0.4], [0.6, 0.8])	([0.2, 0.4], [0.4, 0.6])	([0.6, 0.8], [0.8, 1])
M.Tech in Z	([0.6, 0.8], [0.9, 1])	([0.6, 0.8], [0.9, 1])	([0.4, 0.6], [0.6, 0.8])

step (i): See Table 3.

step (ii): Let the weights of C_1, C_2, and C_3 as 0.25, 0.35, and 0.40. Then, the WAA values of P_i by definition 2.0.10 are

$$\beta_1 = ([0.5026, 0.7079], [0.7737, 0.9457])$$
$$\beta_2 = ([0.3937, 0.6134], [0.5410, 0.7909])$$
$$\beta_3 = ([0.5296, 0.7361], [0.7653, 0.9146])$$

step (iii): By using general accuracy function defined by Lakshmana et al 2.0.7

$$\mathrm{LG}(\beta_1) = 1.5865, \mathrm{LG}(\beta_2) = 1.4022, \mathrm{LG}(\beta_3) = 1.6044$$

step (iv): Therefore, the order of priority is $P_3 > P_1 > P_2$.
Thus, studying M.Tech in the institution Z is very suitable for the student [17, 18]

7 Conclusion and Future Scope

In this paper, a new type of IVIFNs is defined. Also, by using the concept of arithmetic operation on interval, some operations are defined. Later, the main theme of the paper is elaborated that is how the operation defined over the new type of IVIFNs makes an impact on existing ranking functions. It is a seed of several development in the field of fuzzy MCDM, fuzzy multi-objective LPP, and in various fields of fuzzy theory. We are working on the applications of the proposed method in different domains. We may come across practical problems in a real-life situation like offering two things simultaneously. For example, if one may want to buy a TV in a popular brand like Samsung, Micromax, LG, Sony based on some criteria at the same time, he may want to buy a DTH in a popular brand like Tata Sky, Airtel, Sun Direct based on some criteria. In this case, decision maker has to combine these two MCDM problems into a single MCDM problem. For that our proposed method will be used to combine two simultaneous MCDM problems into single MCDM problem. We are working on these types of problems. In future, we will find the best solution.

References

1. Joshi, D., Kumar, S.: Improved accuracy function for interval valued intuitionistic fuzzy sets and its application to multi-attributes group decision making. Cybern. Syst. (2018). https://doi.org/10.1080/01969722.2017.1412890
2. Ganesan, K., Veeramani, P.: On arithmetic operations of interval numbers. Uncertainty Fuzziness Knowl. Syst. **13**, 619–631 (2005)
3. Moore, R.E.: Interval Analysis. Printice Hall, Inc. Englewood & Cliffs, N.J. (1966)

4. Atanassov, K.: Operators over interval-valued intuitionistic fuzzy sets. Fuzzy Sets Syst. **64**(2), 159174 (1994)
5. Xu, Z.: Methods for aggregating interval-valued intuitionistic fuzzy information and their application to decision making. Control Decis. **22**(2), 215–219 (2007)
6. Wei, G.W., Wang, X.R.: Some geometric aggregation operators based on interval-valued intuitionistic fuzzy sets and their application to group decision making. In: Proceedings of the Conference on Computational Intelligence and Security, pp. 495–499 (2007)
7. Xu, Z.S., Chen, J.: On geometric aggregation over interval-valued intuitionistic fuzzy information. In: Fourth International Conference on Fuzzy Systems and Knowledge Discovery (FSKD), Haikou, China, pp. 466–471 (2007)
8. Bhowmikm, M., Pal, M.: Some results on generalized interval-valued intuitionistic fuzzy sets. Int. J. Fuzzy Syst. **14**(2) (2012)
9. Zhang, Z.: Interval-valued intuitionistic hesitant fuzzy aggregation operators and their application in group decision making. J. Appl. Math. (2013). https://doi.org/10.1155/2013/670285
10. Broumi, S., Smarandache, F.: New operations over interval valued intuitionistic hesitant fuzzy set. Math. Stat. **2**(2), 62–71 (2014)
11. Ye, J.: Multicriteria fuzzy decision-making method based on a novel accuracy function under interval- valued intuitionistic fuzzy environment. Expert Syst. Appl. **36**(3), 6899–6902 (2009)
12. Nayagam, V.L.G., Sivaraman, G.: Ranking of interval valued intuitionistic fuzzy sets. Appl. Soft Comput. **11**, 3368–3372 (2011)
13. Liu, B., Luo, M.-X.: Multicriteria decision making based on interval valued intuitionistic fuzzy sets with a new kind of accuracy function. In: Quantitative Logic and Soft Computing, Advances in Intelligent Systems and Computing, vol. 510 (2016)
14. Atanassov, K., Gargov, G.: Interval-valued intuitionistic fuzzy sets. Fuzzy Sets Syst. **31**, 343–349 (1989)
15. Nayagam, V.L.G., Muralikrishnan, S., Sivaraman, G.: Multicriteria decision-making method based on interval valued intuitionistic fuzzy sets. Expert Syst. Appl. **38**(3), 1464–1467 (2011)
16. Atanassov, K.: Operators over interval-valued intuitionistic fuzzy sets. Fuzzy Sets Syst. **64**(2), 159–174 (1994)
17. Broumi, S., Smarandache, F.: New operations over interval valued intuitionistic hesitant fuzzy set. Infinite Study **2**(2), 62–71 (2014)
18. Dymova, L., Sevastjanov, P.: The operations on interval-valued intuitionistic fuzzy values in the framework of Dempster–Shafer theory. Inf. Sci. **360**, 256–272 (2016)

Fuzzy Clustering Technique for Segmentation on Skin Cancer Dermoscopic Images

M. Kavitha, A. Senthil Arumugam, and Tzung-Pei Hong

Abstract Nowadays, the medical community requested the computational methods for medical image analysis. Segmentation acts as vital role for processing the medical images. In recent three decades, numerous people affected with skin cancer than any kind of cancer. Melanoma is the sort skin malignancy which has caused most of death rate. Melanoma is cured with a simple eradication if noticed early. Till now, the segmentation of the melanoma is significant tasks because of over or under segments. This chapter uses the fuzzy clustering method to analyze the skin melanoma image. Experiments show that this method can segregate various types of melanoma images successfully.

Index Terms K-means · Fuzzy C-means · Fuzzy clustering · Melanoma · Skin cancer

1 Introduction

Globally, skin disease is a primary malignancy apprehension once an unnatural weather change hits. Skin cancers are a significant health problem, influencing a huge part of the populace irrespective of skin colors [1]. The effect could be identified using dermoscopy to conclude whether the apparent spots on the skin are benign or malignant tumors. Computer-aided detection systems process digital images to find out the occurrence of cancer by construing clinical constraints, depending on an exact segmentation method to extract pertinent features. The skin malignancy

M. Kavitha (✉)
Manonmaniam Sundaranar University, Abhishekapatti, Tirunelveli, Tamilnadu, India

A. Senthil Arumugam
Sri Ram Nallamani Yadhava College of Arts and Science, Tenkasi, Tamilnadu, India

T.-P. Hong
Department of Computer Science and Information Engineering, AI Research Center, National University of Kaohsiung, Kaohsiung City, Taiwan
e-mail: tphong@nuk.edu.tw

© The Author(s), under exclusive license to Springer Nature Singapore Pte Ltd. 2022

S. R. Kannan et al. (eds.), *Fuzzy Mathematical Analysis and Advances in Computational Mathematics*, Studies in Fuzziness and Soft Computing 419,
https://doi.org/10.1007/978-981-19-0471-4_6

for individuals affected mostly is melanoma. It is also the most well-known and the utmost treatable and flat to be forestalled. Premature revelation is significant; however, moles will become dangerous once they show unusual effects, such as evolving size and shape. The dermoscopy finds out pigmented edifices [2] of the skin's layer noticeable. The horny layer is kept luminous by an oil submersion and a glowing light. A glass plate is put on the inspected skin territory. The skin lesions seen by the dermoscopy [3] typically show up a consistently earthy color or darkness. Varieties between the dark, earthy color, and the shadowy cobalt can be triggered by way of alterations of pigmentation in various skin layers [4]. The structures noticeable in a dermoscopy picture incorporate pigmented arrangement, dark spots, and earthy color globules [5]. This decreases the screening errors and gives more prominent separation between troublesome injuries, for example, pigmented Spitz nevi and little, clinically dubious sores. Be that as it may, it has been illustrated that dermoscopy [6] may really bring down the indicative precision in the hands of unpracticed dermatologists.

Owing to the absence of reproducibility in addition to partisanship of humanoid understanding, the advancement of mechanized picture investigation strategies is of foremost significance. The initial phase in the mechanized investigation of sore-skin images is to check the region of the sore fringes. The significance of fringe recognition for the investigation is two overlays. In the first place, the outskirt structure gives important data to an exact conclusion. Numerous clinical highlights, for example, asymmetry and fringe inconsistency, are determined from the outskirt. Subsequently, taking out of further significant clinical highlights such as atypical shade systems, gobbets, and cobalt-milky zones, basically relies on the precision of outskirt discovery. Various techniques [7] have been produced for fringe discovery in pigmented sore-skin pictures, more than for medical images. In any case, the late research has focused more on dermoscopy pictures.

2 Segmentation

In image processing, segmentation [8] holds a vital role. Moreover, it comes to be more domineering in dealing with medical images [9]. For example, to initialize and accelerate the recovery process of the pre-surgery and post-surgery, decisions that are taken based on the segmentation results are essential. Computer-aided detection of anomalous tissue growth is principally encouraged through the obligation of accomplishing extremely conceivable accurateness. Manual segregation of these abnormal tissues cannot be likened to the rapid-speed computing machines in the current days, which allows us to visually perceive the dimensions and positions of annoying tissues. In image analysis [10], both the supervised and unsupervised approaches [11] are commonly used. In supervised classification [12], adequate known pixels to produce illustrative parameters for each class of interest have been obtained; whereas in unsupervised clustering [13], pre-hand knowledge of classes is not required. Image segmentation [14] is commonly defined as grouping the neighboring pixels with

similar characteristics such as intensity, spatial topographies, semantic mean, and so on. Various systems use different cluster features for segregation [15]. Bezdek et al. proposed the famous fuzzy C-means (FCM) algorithm to assign an object to different clusters with membership values. Sarkar et al. introduced a hybrid technique named rough possibilities type FCM with the integration of random forest [16]. A novel multi-objective real-coded genetic FCM for segregation has also been designed [17]. A novel fast and robust FCM [18] have proposed by incorporating the local spatial and gray information. Despite segregating images by way of subtle texture and background, FCM may be incompetent to classify images with noises.

3 Review of FCM

FCM is an iterative clustering routine [19] that converges the optimal cluster segments by diminishing the sum squared error of the objective function $J_m(U, V)$ w.r.t. the association matrix U and the cluster centroids V. The function is defined as follows:

$$J_m(U, V) = \sum_{i=1}^{c} \sum_{k=1}^{n} (u_{ik})^m d^2(x_k, v_i) \tag{1}$$

where n denotes the pixel quantity of an image, $d^2(x_k, v_i)$ states the square of the Euclidean distance between the k-th pixel intensity (x_k) and the i-th centroid value (v_i), u_{ik} denotes the membership assessment the *k-th* pixel corresponding to the i-th cluster, and m represents the degree of fuzzification being either equal or greater than 1. Besides, the membership values satisfy the following constraint:

$$\sum_{i=1}^{c} u_{ik} = 1 \tag{2}$$

The repetitive working out of membership values and cluster centroids is accomplished through the following formulas:

$$u_{ik} = \frac{1}{\sum_{j=1}^{c} \left(\frac{d^2(x_k, v_i)}{d^2(x_k, v_j)} \right)^{\frac{1}{m-1}}} \text{ and} \tag{3}$$

$$v_i = \frac{\sum_{k=0}^{n} (u_{ik})^m x_k}{\sum_{k=0}^{n} (u_{ik})^m} \tag{4}$$

u_{ik} and v_i converge through several repetitions, with J_m being diminished as well. The minimization measure is designated based on associating the cluster centroids with their previous ones for the difference smaller than the given error threshold ϵ. The pseudocode of FCM with an image as its input is stated as follows.

FCM Algorithm

Procedure segmentation (Image I, Number of clusters c)

Initialization of the cluster centers V

Repeat

Derive the current membership matrix U according to Formula (3)

Derive the current membership matrix V according to Formula (4)

Till $\|V - V_{old}\| < \epsilon$

Return (U, V)

End procedure

In this procedure, an effective initialization technique named ordering-split was used with a good effect in [20].

4 Segmentation on Skin Cancer Images

This work is carried out with the fuzzy *c*-means clustering procedure. A skin lesion image has been given as the input. We assign the number of clusters [21] as 3 so that three centroids are selected randomly. We then initialize the fuzzy partition matrix and give an iteration threshold value. Next, the matrix of cluster centers is derived, and the Euclidean distance between each point and cluster center is calculated. The method then updates the fuzzy partition matrix. If the difference of the fuzzy partition matrix between new and previous iterations is less than ϵ, then the procedure stops; otherwise, the matrix of cluster centers is recalculated. The same procedure is repeated until the threshold condition is touched. The flowchart is shown in Fig. 1.

5 Experimental Result

In this method, the skin lesion image in the form of dermoscopy is given as the input. Two available datasets, ISBI 2017 and PH2, were used in the experiments. The former dataset was constructed for a challenge of skin lesion analysis toward melanoma detection. This informational collection is available for scientists, consisting of 8-bit RGB dermoscopic images with resolutions fluctuating in the ranges of 540–722 and 4499–6748. This informational index is a trifling port of the International Skin Imaging Collaboration (ISIC). The PH2 dataset was obtained from the research group of the Porto University, Hospital Pedro Hispano, Portugal. The FCM algorithm was

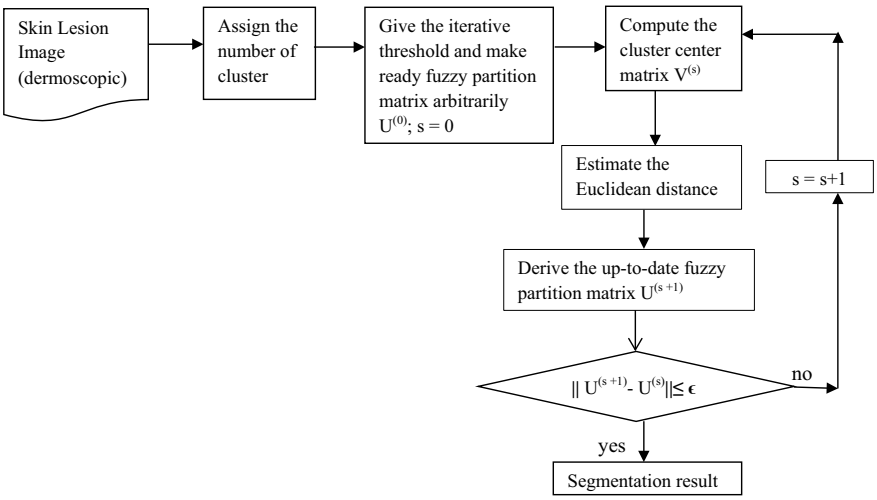
Skin Lesion Image (dermoscopic)
Assign the number of cluster
Give the iterative threshold and make ready fuzzy partition matrix arbitrarily $U^{(0)}$; s = 0
Compute the cluster center matrix $V^{(s)}$
Estimate the Euclidean distance
s = s+1
Derive the up-to-date fuzzy partition matrix $U^{(s+1)}$
$\| U^{(s+1)} - U^{(s)} \| \leq \epsilon$
no
yes
Segmentation result

Fig. 1 Flowchart for segmentation on skin cancer images using a fuzzy clustering method

experimented on the skin lesion images. FCM segregated the skin lesion properly even though the lesion has an irregular shape. Moreover, the blur lesion parts were segregated properly. The results are shown in Fig. 2.

Table 1 portrays the time taken to execute FCM for various skin lesion images. It takes only a few seconds for segregation from the dataset with hundreds of lesion images. FCM could be well applied to almost all the images and segregated the lesions properly even though they have irregular sizes and shapes. Here, for the sample, only a few different lesion images are discussed.

6 Conclusion

This chapter is focused on the analysis of skin lesion dermoscopic images. Segmentation has been carried out on the given lesion images. For the segmentation process, the fuzzy clustering method, FCM, has been applied. It is an unsupervised clustering method and is interesting as well as easy for implementation. FCM segregates skin lesions based on the number of clusters that has been defined in advance. The overall implementation of this method produces the outcome in few seconds. It segments images appropriately, even having irregular shapes of lesions. A novel hybrid segmentation method will be introduced as future enhancements for segmenting lesions more appropriately. Moreover, classification would have performed by mapping this resulting data with its corresponding ground truth data. Additionally, we may enrich this procedure with utmost latest optimization system for segmentation to improve the accuracy.

Fig. 2 Outputs

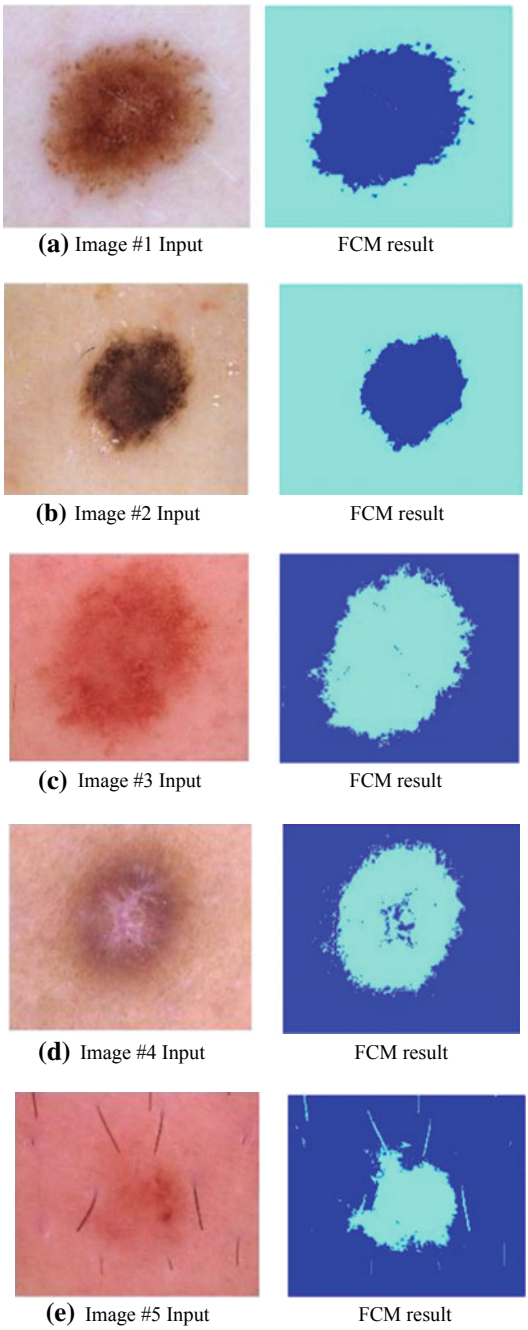

Fig. 2 (continued)

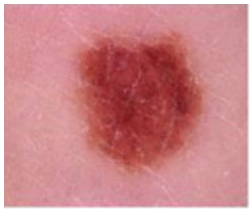

(f) Image #6 Input

FCM result

(g) Image #7 Input

FCM result

(h) Image #8 Input

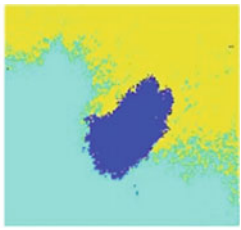

FCM result

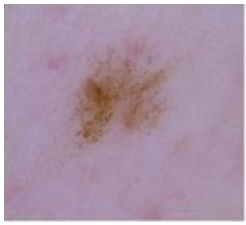

(i) Image #9 Input

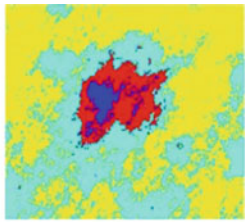

FCM result

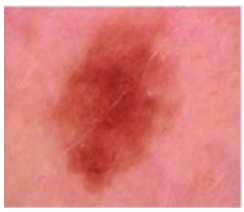

(j) Image #10 Input

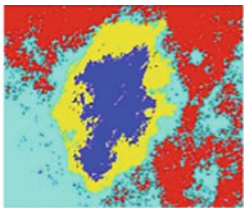

FCM result

Fig. 2 (continued)

(k) Image #11 Input

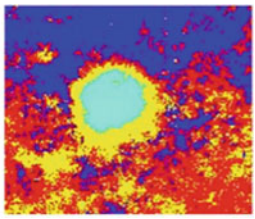

FCM result

Table 1 Time taken to execute (seconds)

Image	Seconds
Image-1	6.915
Image-2	9.0376
Image-3	10.765
Image-4	9.4325
Image-5	9.6519
Image-6	7.7674
Image-7	10.876
Image-8	12.767
Image-9	12.114
Image-10	14.462
Image-11	14.167

References

1. Kavitha, M., Senthil Arumugam, A., Saravana Kumar, V., Anathasivaprakasam, S.: An empirical study on image segmentation techniques for detection of skin cancer. J. Pharm. Res. Int. Sci. Domain Int. **33**(10), 71–81 (2021). https://doi.org/10.9734/jpri/2021/v33i1031235
2. Meskini, E.M.S., Helfroush, K.K., Sepaskhah, M.: A new algorithm for skin lesion border detection in dermoscopy images. J. Biomed. Phys. Eng. **8**, 117–126 (2018)
3. Kavitha, M., Senthil Arumugam, A., Saravana Kumar, V.: Enhanced clustering technique for segmentation on dermoscopic images. In: IEEE—4th International Conference on Intelligent Computing and Control Systems (ICICCS 2020), Madurai, TN, May, pp. 956–961 (2020). https://doi.org/10.1109/ICICCS48265.2020.9121102
4. Schaefer, G., Rajab, M.I., Emre Celebi, M., Iyatomi, H.: Colour and contrast enhancement for improved skin lesion segmentation. Comput. Med. Imaging Gr. **35**(2), 99–104 (2011). https://doi.org/10.1016/j.compmedimag.2010.08.004
5. Barata, C., Celebi, M.E., Marques, J.S.: A survey of feature extraction in dermoscopy image analysis of skin cancer. IEEE J. Biomed. Health Inform. **23**(3), 1096–1109 (2019). https://doi.org/10.1109/JBHI.2018.2845939
6. Mohanad, H.A., Ozok, Y.E., Rahebi, J., Abdullah, A.S.: Skin lesion segmentation method for dermoscopy images using artificial bee colony algorithm. Symmetry **10**(8), 347 (2018). https://doi.org/10.3390/sym10080347
7. Wang, N., Peng, Y., Wang, Y., Wang, M.: Skin lesion image segmentation based on adversarial networks. KSII Trans. Internet Inf. Syst. **12**(6), 2826 (2018). https://doi.org/10.3837/tiis.2018.06.021

8. Saravana Kumar, V., Naganathan, E.R.: Hyperspectral image segmentation based on particle swarm optimization with classical clustering methods. Adv. Nat. Appl. Sci. **9**(12), 45–53 (2015)
9. Suma, K.G., Saravanakumar, V.: A quantitative analysis of histogram equalization-based methods on fundus images for diabetic retinopathy detection. In: Springer Briefs in Forensic and Medical Bioinformatics, Computational Intelligence and Big Data Analytics, pp. 55–63 (2018). https://www.springer.com/us/book/9789811305436
10. Ananthsivaprakasam, Naganathan, E.R., Saravana Kumar, V., et al.: Wavelet based cervical image segmentation using morphological and statistical operations. J. Adv. Res. Dyn. Control Syst. **10-03** (2018). http://www.jardcs.org/abstract.php?archiveid=3838
11. Garcia-Escudero, L.A., Gordaliza, A.: Robustness properties of K-means and trimmed K-means. J. Am. Stat. Assoc. **94**(447), 956–969 (1999)
12. Suma, K.G., Saravanakumar, V.: Classification of abnormal blood vessels in diabetic retinopathy using neural network. In: Springer Briefs in Applied Sciences and Technology, Forensic and Medical Bioinformatics (2018). https://www.springer.com/in/book/9789811300585
13. Kavitha, M., Senthil Arumugam, A., Saravana Kumar, V.: Classical clustering technique for segmentation of skin cancer image. TEST Eng. Manage. Trade J. 5753–5758 (2020). http://testmagzine.biz/index.php/testmagzine/article/view/8412
14. Ananthasivaprakasam, S., Naganathan, E.R.: Segmentation and classification of cervical cytology images using morphological and statistical operations. ICTACT J. Image Video Process. **7**(3) (2017). https://doi.org/10.21917/ijivp.2017.0208
15. SaravanaKumar, V., Naganathan, E.R.: Hyperspectral image segmentation based on enhanced estimation of centroid with fast K-means. Int. Arab J. Inform. Technol. Jordon **15**(5), 904–911 (2018)
16. Sarkar, J., Saha, I., Maulik, U.: Rough possibilistic type-2 fuzzy C-means clustering for MR brain image segmentation. Appl. Soft Comput. **46**, 527–536 (2016). https://doi.org/10.1016/j.asoc.2016.01.040
17. Mukhopadhyay, A., Maulik, U.: Multiobjective approach to MR brain image segmentation. Appl. Soft Comput. **11**(1), 872–880 (2011). https://doi.org/10.1016/j.asoc.2010.01.007
18. Cai, W., Chen, S., Zhang, D.: Fast and robust fuzzy c-means clustering algorithms incorporating local information for image segmentation. Pattern Recogn. **40**(3), 825–838 (2007)
19. Koç, Y., Ölmez, T.: Improved fuzzy C-means and K-means algorithms for texture and boundary segmentation. In: 6th International Conference on Control Engineering & Information Technology (CEIT), Istanbul, Turkey, 2018, pp. 1–6 (2018). https://doi.org/10.1109/CEIT.2018.8751905
20. Sookpotharom, S.: Border detection of skin lesion images based on fuzzy C-means thresholding. Third Int. Conf. Genet. Evolut. Comput. Guilin **2009**, 777–780 (2009). https://doi.org/10.1109/WGEC.2009.96
21. Kovacs, F., Legany, C., Babos, A.: Cluster validity measurement techniques. In: Proceeding of 5th WSEAS International Conference on Artificial Intelligence, Knowledge Engineering & Database, pp. 388–393 (2006)

A Study on Fuzzy Coloring in Quadruple Layered Fuzzy Graph

L. Jethruth Emelda Mary and R. Kiruthikaswari

Abstract In this paper, we have discussed fuzzy vertex coloring, fuzzy edge coloring of a quadruple layered fuzzy graph of a simple fuzzy cycle graph and obtained some of the parameters such as fuzzy chromatic number and fuzzy index number for the same graph.

Keywords Quadruple layered fuzzy graph · Fuzzy vertex coloring · Fuzzy edge coloring

1 Introduction

In 1965, fuzzy relation concept was introduced by Zadeh [1]. Fuzzy graph coloring was developed by Munoz et al. [2]. The fuzzy vertex coloring (FVC) was first explained by authors Esclahchi and Onagh [3] in the year 2006. The degree of a vertex in some fuzzy graphs was discussed by Nagoorgani and Radha [4]. Different types of fuzzy graphs were defined by Nagoorgani and Malarvizhi [5] and discussed isomerism in fuzzy graphs. Pathianathan and Roseline [6] have defined double-layered fuzzy graph. In this paper, we discussed fuzzy edge coloring (FEC) and fuzzy vertex coloring (FVC) of a quadruple layered fuzzy graph of a simple fuzzy cycle graph.

2 Definitions

2.1 Quadruple Layered Fuzzy Graph

Let $G = (\sigma, \mu)$ be a fuzzy graph with the underlying crisp graph G^*: (σ^*, μ^*).

L. Jethruth Emelda Mary (✉) · R. Kiruthikaswari
PG and Research Department of Mathematics, St. Joseph's College of Arts and Science (Autonomous), Cuddalore, Tamil Nadu, India

© The Author(s), under exclusive license to Springer Nature Singapore Pte Ltd. 2022

S. R. Kannan et al. (eds.), *Fuzzy Mathematical Analysis and Advances in Computational Mathematics*, Studies in Fuzziness and Soft Computing 419,
https://doi.org/10.1007/978-981-19-0471-4_7

The pair $QL\ (G)$: (σ_{TL}, μ_{TL}) is defined as follows:
The vertex set of QL (G) is $\sigma^* \cup \mu^* \cup \mu^* = \{\sigma(u)$ if $u \in \sigma^* 2\sigma(u, v) = 0$

$$\mu_{\mathrm{QL}} = \begin{cases} \mu(uv) & \text{if } u, v \in \sigma^* \\ \mu(e_i) \wedge \mu(e_j) & \text{if the edge } e_i \text{ and } e_j \text{ have a node in common between them} \\ \sigma(u_i)) \wedge \mu(e_i) & \text{if } u_i \in \sigma^* \text{ and } e_i \in \mu^* \text{ each } e_i \text{ is incident with } u_i \text{ in clockwise direction.} \\ \sigma(u_i)) \wedge \mu(e_i) & \text{if } u_i \in \sigma^* \text{ and } e_i \in \mu^* \text{ each } e_i \text{ is incident with } u_i \text{ in anticlockwise direction.} \\ 0 & \text{otherwise} \end{cases}$$

By definition, $\mu_{\mathrm{QL}}(u, v) \leq \sigma_{\mathrm{QL}}(u) \wedge \sigma_{\mathrm{QL}}(v)$ for all u, v in $\sigma^* \cup \mu^*$. Here, μ_{QL} is a fuzzy relation on the fuzzy subset σ_{QL}. Hence, the pair QL(G): $(\sigma_{\mathrm{QL}}, \mu_{\mathrm{QL}})$ is defined as quadruple layered fuzzy graph (QLFG).

2.2 Definition

A family $\Gamma = \{\gamma_1, \gamma_2 \ldots \gamma_k\}$ of fuzzy sets on V is called k-fuzzy coloring of $\hat{G} = (V, \sigma, \mu)$.

If the following statements are true

(a) $\vee \Gamma = \sigma$
(b) $\gamma_i \wedge \gamma_j = 0$
(c) For every strong edge uv of $\hat{G}$, $\gamma_i(u) \wedge \gamma_i\ (v) = 0$ for $1 \leq i \leq k$.

2.3 Definition

A fuzzy graph G is k-fuzzy colorable if G has a proper k-fuzzy coloring. The fuzzy chromatic number $\chi^f\ (G)$ of a fuzzy graph G is the minimum k colors for which G is k-fuzzy colorable.

The above definition of k-fuzzy coloring was defined by the authors Eslahchi and Onagh [3] on the fuzzy set of vertices.

3 Fuzzy Vertex Coloring on Quadruple Layered Fuzzy Graph

Theorem: 3.1 *If $G_{\mathrm{QL}} = (\sigma_{\mathrm{QL}}, \mu_{\mathrm{QL}})$ is a QLFG of fuzzy cycle of order n, then fuzzy chromatic number is,*

$$\chi_{\mathrm{QLF}}(G) = \left\{ \begin{array}{l} 2, \text{if} n = 2k \\ 3, \text{if} n = 2k+1 \end{array} \right\}$$

Proof: This theorem can be proved in 2 cases,

1. **Case**

Here, we have considered the graph to be undirected, finite simple quadruple layered fuzzy graph. Let n be even. The vertex set V carries an even number of vertices. It is colored in two different colors C_1 and C_2 alternatively without affecting the concept of fuzzy proper coloring, and hence, it required two colors. Thus, a fuzzy chromatic number of $\chi_{\mathrm{QLF}}(G)$ is 2 if $n = 2$ k, $(k = 1, 2, 3\ldots)$.

2. **Case**

Suppose n is odd, the vertex set V consists of odd number of vertices; it is colored by two different colors C_1 and C_2, respectively, and the end vertex of V must be colored by a different color C_3. Hence, it required three colors,

Therefore, $\chi_{\mathrm{QLF}}(G)$=3, if $n = 2\,k + 1$.

Hence, $\chi_{\mathrm{QLF}}(G)$=2, if n is even and 3 if n is odd.

3.1 Example

The following diagrams show fuzzy chromatic number of $\chi_{\mathrm{QLF}}(G)$ of order $n = 5$ and $n = 8$ for $n = 5$. The fuzzy chromatic number is $\chi^{f}_{\mathrm{QLF}}(G) = 3$ (Figs. 1 and 2).

When $n = 8$, we have FCN for C_8 is $\chi^{f}_{\mathrm{QLF}}(G) = 2$ (Figs. 3 and 4).

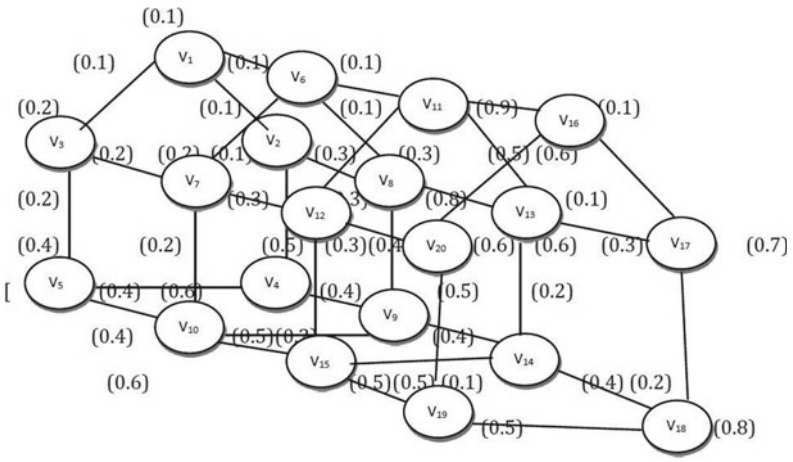

Fig. 1 $\chi^{f}_{\mathrm{QLF}}(C_5)$

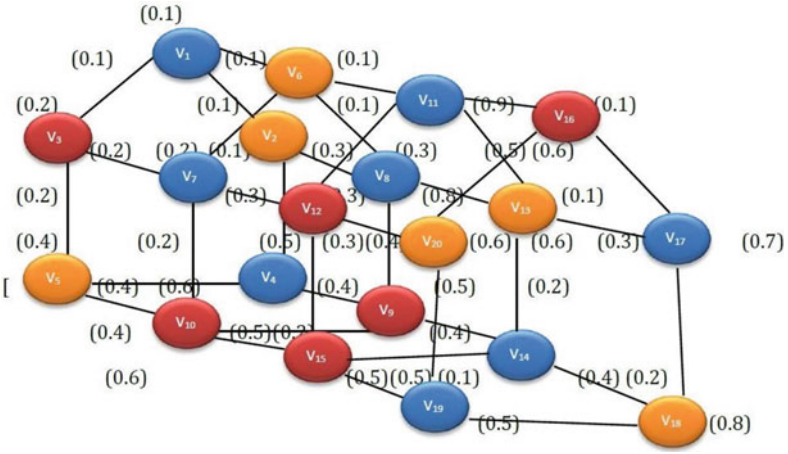

Fig. 2 $\chi^{f}_{\mathrm{QLF}}(\mathrm{C5}) = 3$

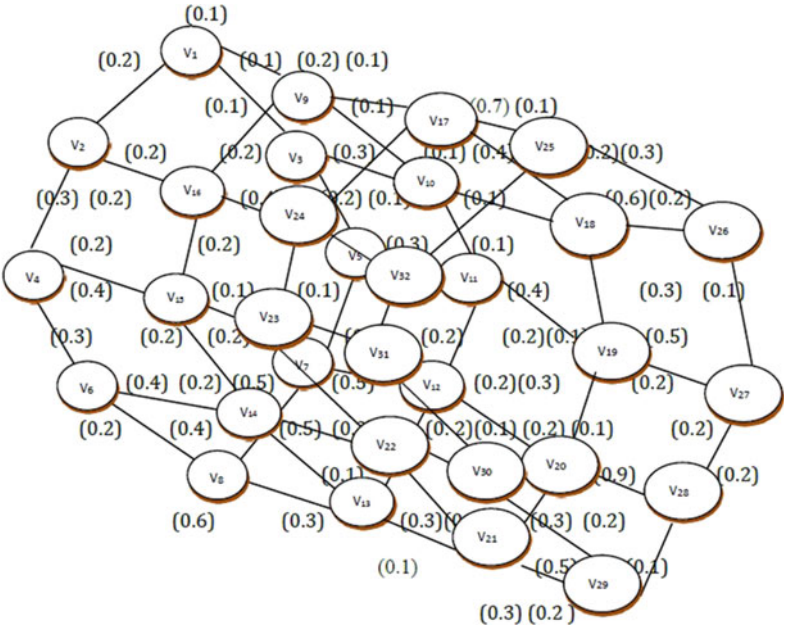

Fig. 3 $\chi^{f}_{\mathrm{QLF}}(\mathrm{C}_8)$

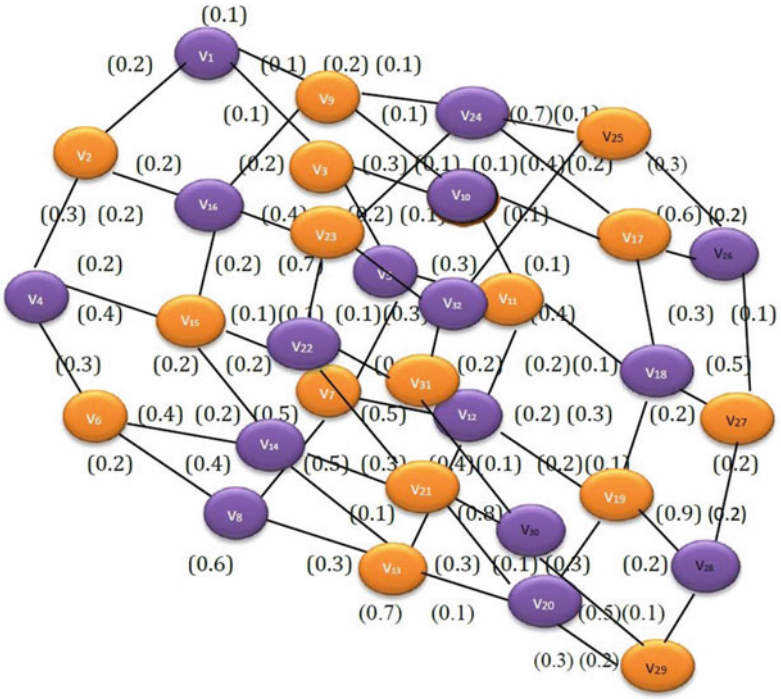

Fig. 4 $\chi^{f}_{\mathrm{QLF}}(C_8) = 2$

4 Fuzzy Edge Coloring of Quadruple Layered Fuzzy graph

Theorem: 4.1 *If GQL = (σ QL, μQL) is a QLFG of fuzzy cycle of size m where m* $= 2 + k$, *then* $\chi^{E}_{QLF}(G) = 4 \; \forall \; m > 2$ $(k = 1, 2, 3\ldots)$.

Proof: Suppose $E = \{1, 2, \ldots 2 + k\}$ is an edge set on QLF(G).

Let Γ'QL = {γ1,…., γ2 + k} be a family of quadruple layered fuzzy graph. The fuzzy set E is GQL = (σQL, μQL). Let us color the set of edges of E by three distinct colors C1, C2, and C3, and the last edge of E must be colored by C4 without changing the idea of quadruple layered fuzzy proper edge coloring. Finally, it is needed four colors.

Hence, $\chi^{E}_{\mathrm{QLF}}(G) = 4$, if $m = 2 + k$, for all $m > 2$ $(k = 1, 2, 3\ldots)$.

Example For $n = 4$.

The fuzzy index number of QLFG is 4 (Figs. 5 and 6).

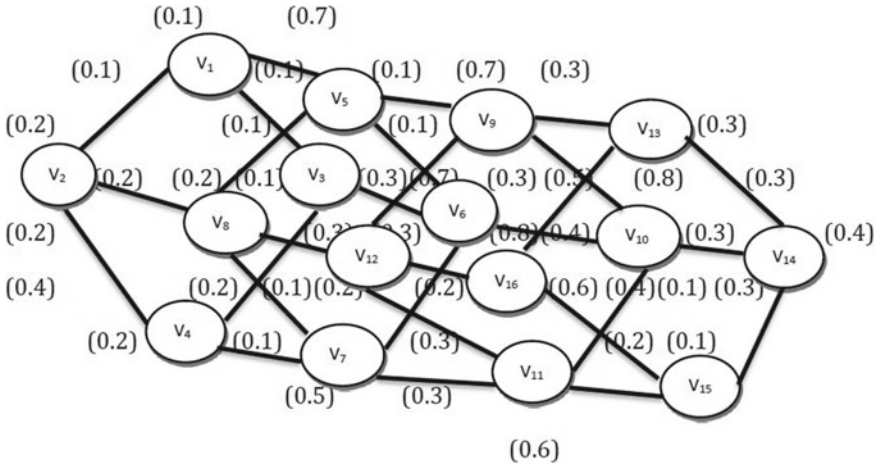

Fig. 5 $\chi^{f}_{\mathrm{QLF}}(C_4)$

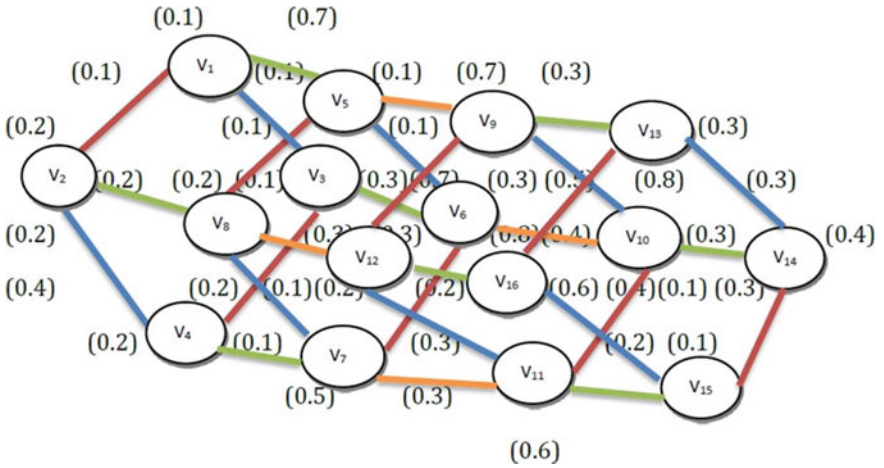

Fig. 6 $\chi^{f}_{\mathrm{QLF}}(C_4) = 4$

5 Conclusion

In this paper, we have established fuzzy chromatic number and fuzzy index number of QLFG of simple fuzzy cycle graph and verify its boundary. This wok can be extended for some other graphs such as fuzzy complete graph, fuzzy path graph of quadruple layered fuzzy graphs, and verify bounds for new parameters of dominator chromatic number of simple fuzzy graphs.

References

1. Zadeh, L.A.: Fuzzy set. Inf. Comput. **8**, 338–353 (1965)
2. Munoz, S., Ortuno, T., Ramirez, J., Yanez, J.: Coloring fuzzy graph. Omega **32**, 211–221 (2005)
3. Eslachi, C., Onagh, B.N.: Vertex strength of fuzzy graphs. Int. J. Math. Math. Sci. **2006**, 1–9 (2006)
4. Nagoorgani, A., Radha, K.: The degree of a vertex in some fuzzy graphs. Int. J. Algorithms Comput. Math. **2**(3), 107–116 (2009)
5. Nagoorgani, A., Malarvizhi, J.: Some aspects of total fuzzy graph. In: Proceedings of International Conference on Mathematical Methods and Computation, Tiruchirappalli, pp. 168–179 (2009)
6. Pathinathan, T., Jesintha Rosline, J.: Double layered fuzzy graph. Ann. Pure Appl. Math. **8**(1), 135–143 (2014)
7. Jethruth Emelda Mary, L., Kiruthikaswari, R.: A study on triple layered fuzzy graph 9(2020), E-ISSN:2278-179X, NO3, 390-400
8. Zadeh, L.A., Fu, K.S., Shimura, M. (eds.): Academic Press, New York (1975), p. 7

On d_2-Coloring of Certain Families of Graphs

C. Natarajan, S. Venkatesh, P. Rajadurai, and S. Shanmugavelan

Abstract Let $G = (V, E)$ be a connected graph. The d_2-coloring of G is an assignment of colors to the vertices of G such that the vertices which are at distance of two should not share the same color. The minimum number of colors required for such a coloring is called the d_2-coloring number and denoted by $\chi_{d_2}(G)$. In this chapter, we obtain the d_2-coloring number of a central graph, middle graph, and total graph of stars, paths, cycles, and we characterize the family of cactus graphs and block graphs for which $\chi_{d_2}(G) = \chi(G)$.

Keywords Central graph · Middle graph · Total graph · Cactus graph · Block graph · d_2-coloring

1 Introduction

A *proper vertex coloring* of a graph G is an assignment of colors to the vertices of G such that no two adjacent vertices receive the same color. The *chromatic number* $\chi(G)$ is the minimum number of colors required for a proper coloring of G. Niranjan and Srinivasa Rao [5] studied the k-distance chromatic number of trees and cycles. Dong and Xu [9] obtained some bounds on 2-distance coloring number of planar graphs with girth 5. For a detailed survey on distance-based coloring parameters, one may refer [4]. In [2], Benmedjdoub et al. studied 2-distance colorings of integer distance graphs. Yegnanarayanan and Parthiban [10] discussed vertex coloring of

C. Natarajan (✉) · S. Venkatesh · P. Rajadurai · S. Shanmugavelan
Department of Mathematics, Srinivasa Ramanujan Centre, SASTRA Deemed University, Kumbakonam, Tamil Nadu 612001, India
e-mail: natarajan_c@maths.sastra.edu

S. Venkatesh
e-mail: venkatesh_s@src.sastra.edu

P. Rajadurai
e-mail: rajadurai@src.sastra.edu

S. Shanmugavelan
e-mail: shanmugavelan@src.sastra.edu

© The Author(s), under exclusive license to Springer Nature Singapore Pte Ltd. 2022

S. R. Kannan et al. (eds.), *Fuzzy Mathematical Analysis and Advances in Computational Mathematics*, Studies in Fuzziness and Soft Computing 419,
https://doi.org/10.1007/978-981-19-0471-4_8

certain distance graphs. Hu and Wang [3] obtained 2-distance vertex-distinguishing total coloring of some well known of graphs such as paths, cycles, wheels, cartesian products of two paths, and cartesian product of a path and cycle. In [6], Selvakumar and Nithya introduced the concept of d_2-coloring of a graph. A d_2-coloring of G is an assignment of colors to the vertices of G such that the vertices which are at distance two should not share the same color. The minimum number of colors required for a d_2 coloring of G is called the d_2-coloring number and denoted by $\chi_{d_2}(G)$. Vernold et al. [8] found the achromatic number of central graph, middle graph, and total graph of star graph families. Venkatakrishnan and Swaminathan [7] found the color class domination number of central graph, middle graph, and total graph of complete graph, path, and cycle. In this sequel, we find the d_2-coloring number of central graph, middle graph, and total graph of stars, paths, and cycles. We recall some basic definitions to discuss further. For other graph theoretic terminologies not defined here, one may refer [1].

Definition 1 The central graph $C(G)$ of a graph G is a graph obtained by subdividing each edge of G exactly once and joining all the non-adjacent vertices of G.

Definition 2 Let $G = (V, E)$ be a graph. The middle graph of G denoted by $M(G)$ is defined as follows: The vertex set of $M(G)$ is $V(G) \cup E(G)$. Two vertices x, y in the vertex set of $M(G)$ are adjacent in $M(G)$ if one of the following holds:

(i) x, y are in $E(G)$ and x, y are adjacent in G
(ii) $x \in V(G)$, $y \in E(G)$ and y is incident at x in G.

Definition 3 Let $G = (V, E)$ be a graph. The total graph $T(G)$ of G is defined as follows: The vertex set of $T(G)$ is $V(G) \cup E(G)$. Two vertices x, y in the vertex set of $T(G)$ are adjacent in $T(G)$ if one of the following holds:

(i) $x, y \in V(G)$ and x is adjacent to y in G
(ii) $x, y \in E(G)$ and x is adjacent to y in G
(iii) $x \in V(G)$, $y \in E(G)$ and y is incident at x in G.

Observation In general, $\chi_{d_2}(G)$ and $\chi(G)$ are not comparable. To see this, consider the following graphs.

(i) For $G = K_n$, $\chi_{d_2}(K_n) = 1$ whereas $\chi(K_n) = n$.
(ii) For $G = K_{1,3}$, $\chi_{d_2}(K_{1,3}) = 3$ and $\chi(K_{1,3}) = 2$.
(iii) For $G = C_4$, $\chi_{d_2}(C_4) = 2 = \chi(C_4)$.

2 Main Results

2.1 d_2-Coloring of Star Graph Families

In this section, we find d_2-coloring number of star graph families such as central, middle, and total graphs of a star graph $K_{1,n}$.

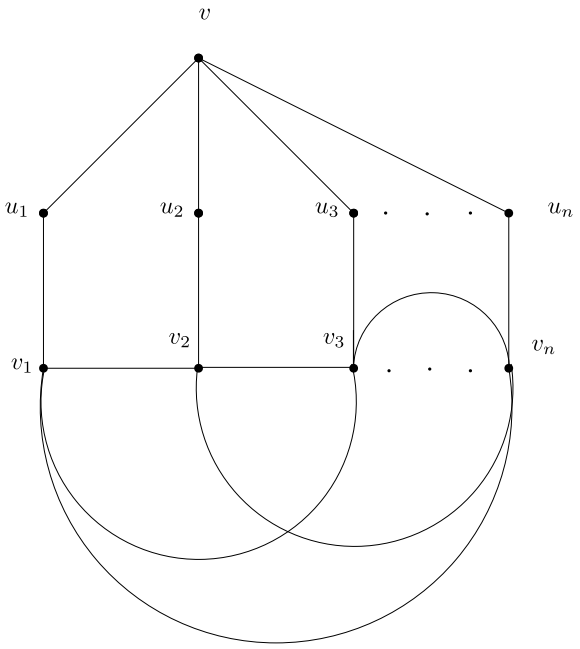

Fig. 1 Central graph $C(\lceil K_{1,n} \rceil)$ of a star graph $K_{1,n}$

Theorem 1 *For any star graph* $K_{1,n}$, $\chi_{d_2}\left[C(K_{1,n})\right] = n + 1$.

Proof Let v denotes the centre of $K_{1,n}$ and let $v_1, v_2, \ldots, v_n$ be leaves of $K_{1,n}$. Let u_i be the vertex subdividing the edge vv_i $(1 \leq i \leq n)$ in $C(K_{1,n})$. Let $V_1 = \{v_1, v_2, \ldots v_n\}$ and $V_2 = \{u_1, u_2, \ldots, u_n\}$ (Fig. 1).

As $d(v, v_i) = 2$ for all $1 \leq i \leq n$ in $C(K_{1,n})$, we need two colors c_1 and c_2; c_1 to be assigned to v and c_2 to each v_i $(1 \leq i \leq n)$. Further, since $d(v_i, u_j) = 2$ and $d(u_i, u_j) = 2$ for $i \neq j$ and $1 \leq i, j \leq n$, at least n colors other than c_2 are required to d_2-color the vertices of $N(v)$. Thus, we have $\chi_{d_2}\left[C(K_{1,n})\right] = n + 1$. □

Theorem 2 *For any star graph* $K_{1,n}$, $\chi_{d_2}\left[M(K_{1,n})\right] = 2$.

Proof Let $V(K_{1,n}) = \{v, v_1, v_2, \ldots, v_n\}$ where v is the central vertex of $K_{1,n}$ and $E(K_{1,n}) = \{e_1, e_2, \ldots, e_n\}$. By definition of middle graph, $V\left[M(K_{1,n})\right] = V(K_{1,n}) \cup E(K_{1,n})$.

It is clear that $E(K_{1,n}) \cup \{v\}$ induces a clique of order $n + 1$ in $M(K_{1,n})$. Therefore, we assign the color c_1 to every vertex e_i $(1 \leq i \leq n)$ and also to the vertex v. Since $V' = V(K_{1,n}) \setminus \{v\}$ is an independent set and $d(v_i, v_j) > 2$ in $M(K_{1,n})$ for $1 \leq i \leq n$, only one color, say c_2 is enough to d_2-color all vertices of V'. Hence, we get $\chi_{d_2}\left[M(K_{1,n})\right] = 2$. □

Theorem 3 *For any star graph* $K_{1,n}$, $\chi_{d_2}\left[T(K_{1,n})\right] = n + 1$.

Proof Let $V(K_{1,n}) = \{v_1, v_2, \ldots, v_n\}$ and $E(K_{1,n}) = \{e_1, e_2, \ldots, e_n\}$. By definition of total graph $V\left[T(K_{1,n})\right] = V(K_{1,n}) \cup E(K_{1,n})$ and the set $\{v\} \cup E(K_{1,n})$ induces a clique of order $n+1$ in $\left[T(K_{1,n})\right]$. Therefore, we assign the color c_1 to these vertices of $\{v\} \cup E(K_{1,n})$. Since $d(v_i, v_j) = 2$ for $i \neq j$ and $1 \leq i, j \leq n$, we require at least n colors other than c_1 to d_2 color the vertices $v_1, v_2, \ldots, v_n$. Thus, $\chi_{d_2}\left[T(K_{1,n})\right] = n+1$ (Figs. 2 and 3). □

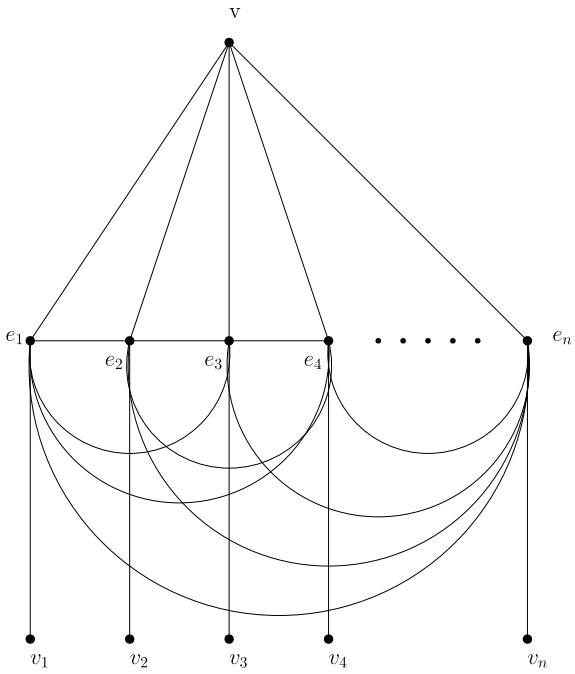

Fig. 2 Middle graph $M(\left[K_{1,n}\right])$ of a star graph $K_{1,n}$

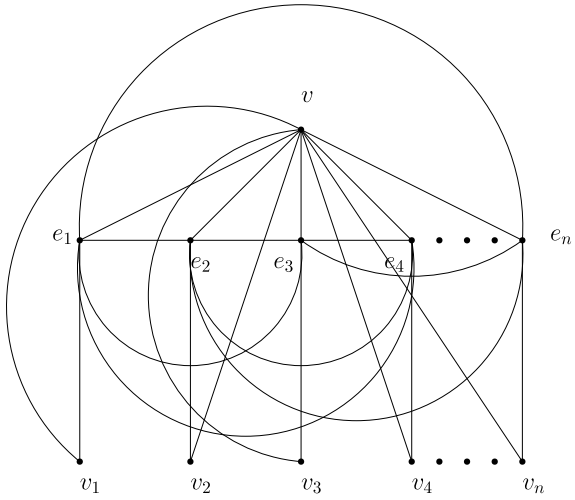

Fig. 3 Total graph $T(\left[K_{1,n}\right])$ of a star graph $K_{1,n}$

2.2 d_2-Coloring of $C(P_n)$, $M(P_n)$ and $T(P_n)$

In this section, we compute d_2-coloring number of central, middle, and total graphs of a path P_n on n vertices.

Theorem 4 *For a path P_n with $n \geq 4$ vertices, $\chi_{d_2}[C(P_n)] = 4$.*

Proof Let $V(P_n) = \{v_1, v_2, \ldots, v_n\}$. Let u_i be the vertex subdividing the edge $v_i v_{i+1}$ $(1 \leq i \leq n)$ of P_n. Then $V[C(P_n)] = V(P_n) \cup \{u_1, u_2, \ldots, u_n\}$. The vertices of $C(P_n)$ are d_2-colored as in Figs. 4, 5 and 6.

Assign the color c_1 to the vertices in the set $V_1 = \{v_i : i \equiv 1 \pmod 2\}$ and assign the color c_2 to each vertex in the set $V_2 = \{v_i : i \equiv 0 \pmod 2\}$. It is clear that V_1 and V_2 form a partition of $V(P_n)$. Let $U_1 = \{u_i : i \equiv 1 \pmod 2\}$. Then $d(u_i, v_1) = d(u_i, v_2) = 2$ for all $u_i \in U_1$. Moreover, $d(u_i, u_j) \geq 3$ for all $u_i, u_j \in U_1$. Therefore, another color c_3 can be assigned to all the vertices of U_1. Similarly, a color c_4

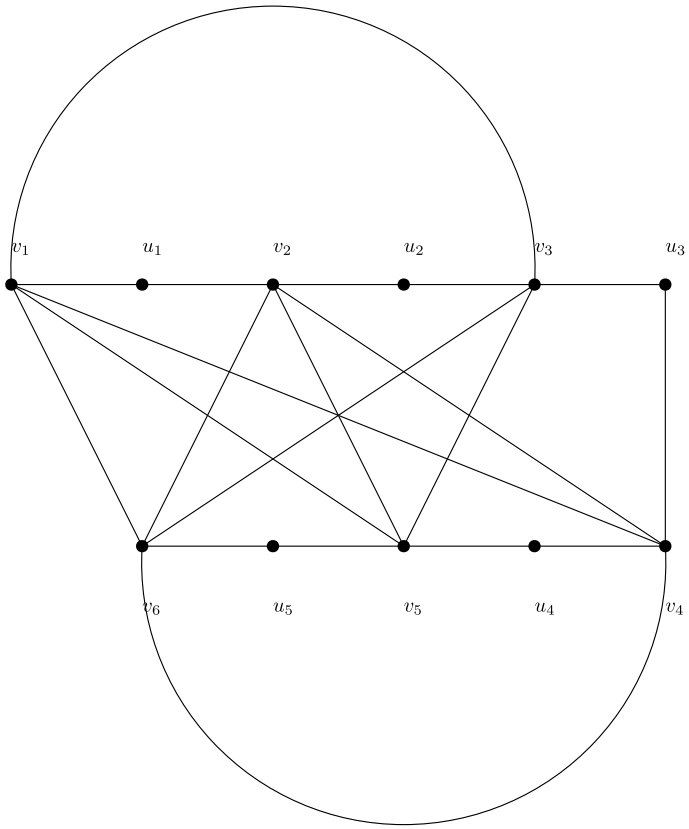

Fig. 4 Central graph $C(P_6)$ of a path P_6

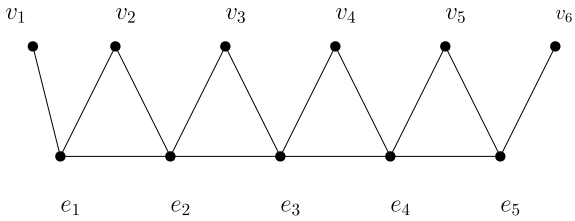

Fig. 5 Middle graph $M(P_6)$ of a path P_6

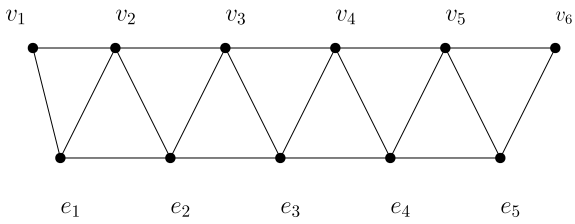

Fig. 6 Total graph $T(P_6)$ of a path P_6

is assigned to every vertex of the set $U_2 = \{u_i : i \equiv 0 \pmod 2\}$. Thus, we have $\chi_{d_2}[C(P_n)] = 4$. □

Theorem 5 *For a path P_n with n vertices* $\chi_{d_2}[M(P_n)] = \begin{cases} 2, & when\ n = 2, 3 \\ 3, & when\ n \geq 4 \end{cases}$.

Proof Let $V(P_n) = \{v_1, v_2, \ldots, v_n\}$ and $E(P_n) = \{e_1, e_2, \ldots, e_n\}$. Then by definition of middle graph, $V[M(P_n)] = V(P_n) \cup E(P_n)$. In order to d_2-color the vertices of $M(P_n)$, we partition the vertex sets $V(P_n)$ and $E(P_n)$ as follows:
$V_1 = \{v_i : i \equiv 1 \pmod 3\}$
$V_2 = \{v_i : i \equiv 2 \pmod 3\}$
$V_3 = \{v_i : i \equiv 0 \pmod 3\}$
$E_1 = \{e_i : i \equiv 1 \pmod 3\}$
$E_2 = \{e_i : i \equiv 2 \pmod 3\}$
$E_3 = \{e_i : i \equiv 0 \pmod 3\}$.

One can observe that $d(x, y) \neq 2$ for all $x, y \in V_j \cup E_j$, where $j = 1, 2, 3$. Therefore, each vertex in $V_j \cup E_j$ can be assigned the color c_j; $j = 1, 2, 3$. Hence, $\chi_{d_2}[M(P_n)] \geq 3$. Also $d(v_i, v_{i+1}) = 2$ for $1 \leq i \leq n-1$ in $M(P_n)$. Assign the color c_1 to every vertex of $V_1 \cup E_1$. Since every vertex in V_1 is a distance of two from a vertex in E_2, the vertices in $V_2 \cup E_2$ are assigned the color c_2. Similarly, the vertices in $V_3 \cup E_3$ are assigned the color c_3 since every vertex in V_2 is of distance two from a vertex in E_3 and so $\chi_{d_2}[M(P_n)] \leq 3$. Hence, $\chi_{d_2}[M(P_n)] = 3$. □

Theorem 6 *For a path P_n with n vertices,* $\chi_{d_2}[T(P_n)] = \begin{cases} 1, & if\ n = 2 \\ 2, & if\ n = 3 \\ 3, & if\ n \geq 4 \end{cases}$.

Proof The proof of this result is similar to Theorem 5. □

2.3 d_2-Coloring of $C[C_n]$, $M[C_n]$ and $T[C_n]$

The following results are about the d_2-coloring number of central, middle, and total graphs of a cycle C_n of length n.

Theorem 7 *For a cycle C_n with n vertices,* $\chi_{d_2}[C(C_n)] = \begin{cases} 3, & when\ n = 3 \\ 4, & when\ n\ is\ even \\ 5, & when\ n\ is\ odd \end{cases}$.

Proof Let $V(C_n) = \{v_1, v_2, \ldots, v_n\}$. Let $U_1 = \{u_1, u_2, \ldots, u_n\}$ be the set of vertices subdividing the edges $v_i v_{i+1}$ $(1 \leq i \leq n-1)$, respectively. Then clearly $V[C(C_n)] = V(C_n) \cup U_1$.
One can easily observe that $\chi_{d_2}[C(C_3)] = 3$.
Case 1: Let n be an even integer.
We partition the vertex sets $V(C_n)$ and U_1 as follows:
$V_1 = \{v_i : i \equiv 1 \pmod 2\}$
$V_2 = \{v_i : i \equiv 0 \pmod 2\}$
$U_2 = \{u_i : i \equiv 1 \pmod 2\}$
$U_3 = \{u_i : i \equiv 0 \pmod 2\}$.
Since a vertex in V_i $(i = 1, 2)$ is of distance two from any vertex of $V_j (i \neq j)$ and $U_k (k = 2, 3)$ we require 4 different colors. Therefore, we have $\chi_{d_2}[C(C_n)] = 4$.
Case 2: Let n be an odd integer.
The vertex sets $V(C_n)$ and U_1 are partitioned as follows:
$V_1 = \{v_i : i \equiv 1 \pmod 2 \text{ and } i \neq n\}$
$V_2 = \{v_i : i \equiv 0 \pmod 2\}$
$V_3 = \{v_n\}$
$U_2 = \{u_i : i \equiv 1 \pmod 2 \text{ and } i \neq n\}$
$U_3 = \{u_i : i \equiv 0 \pmod 2\}$
$U_4 = \{u_n\}$.
Assign color c_1 to every vertex of V_1, c_2 to every vertex of V_2, c_3 to each vertex of U_2 and c_4 to every vertex of U_3. As $d(u_n, v_n) \neq 2$, they can be assigned the same color, say $c \notin \{c_1, c_2, c_3, c_4\}$ since there exist vertices $v_j \in V_1$, $v_k \in V_2$, $u_l \in U_2$, $u_m \in U_3$ such that $d(v_n, v_j) = d(v_n, v_k) = d(u_n, u_l) = d(u_n, u_m) = 2$ for some integers j, k, l, and m. Therefore, $\chi_{d_2}[C(C_n)] = 5$ (Fig. 7). □

Theorem 8 *For a cycle C_n with n vertices,* $\chi_{d_2}[M(C_n)] = \begin{cases} 3, & when\ n \equiv 0\ (mod\ 3) \\ 4, & otherwise \end{cases}$.

Proof Let $V(C_n) = \{v_1, v_2, \ldots, v_n\}$ and $E(C_n) = \{e_1, e_2, \ldots, e_n\}$.
It is clear that $V[M(C_n)] = V(C_n) \cup E(C_n)$. We partition $V(C_n)$ as follows:
$V_1 = \{v_i : i \equiv 1 \pmod 3\}$
$V_2 = \{v_i : i \equiv 2 \pmod 3\}$
$V_3 = \{v_i : i \equiv 0 \pmod 3\}$.
Similarly, $E(C_n)$ can be partitioned as

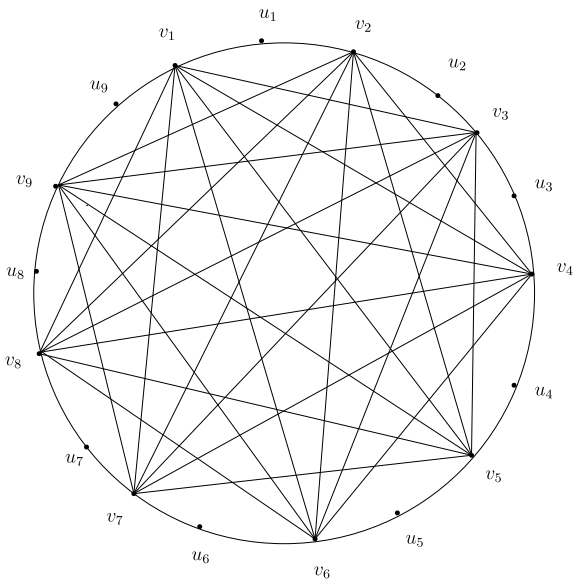

Fig. 7 Central graph $C(C_9)$ of a cycle C_9

$E_1 = \{e_i : i \equiv 1 \pmod 3\}$
$E_2 = \{e_i : i \equiv 2 \pmod 3\}$
$E_3 = \{e_i : i \equiv 0 \pmod 3\}$.

(i) If $n \equiv 0 \pmod 3$, then every vertex of $V_j \cup E_j$ is assigned with color c_j where $j = 1, 2, 3$. Therefore, $\chi_{d_2}[M(C_n)] = 3$.
(ii) If $n \equiv 1 \pmod 3$, then assign the color c_4 to the vertices v_n and e_n. For $1 \leq i < n$ and $j = 1, 2, 3$, assign the color c_j to each vertex in the set $V_j \cup E_j$. Therefore, we have $\chi_{d_2}[M(C_n)] = 4$.
(iii) If $n \equiv 2 \pmod 3$, then assign the color c_4 to the vertices e_{n-1} and e_n. For $1 \leq i < n$ and $j = 1, 2, 3$, we assign the color c_j to every vertex of $V_j \cup E_j$. Thus, we have $\chi_{d_2}[M(C_n)] = 4$ (Fig. 8). □

Theorem 9 *For a cycle C_n with n vertices,* $\chi_{d_2}[T(C_n)] = \begin{cases} 3, & n \equiv 0, 1 \ (mod\ 3) \\ 4, & n \equiv 2 \ (mod\ 3) \end{cases}$.

Proof Let $V(C_n) = \{v_1, v_2, \ldots, v_n\}$ and $E(C_n) = \{e_1, e_2, \ldots, e_n\}$. Then by the definition of total graph $V[T(C_n)] = V(C_n) \cup E(C_n)$. The vertex sets $V(C_n)$ and $E(C_n)$ are partitioned as given in Theorem 8.

(i) If $n \equiv 0 \pmod 3$, then every vertex in $V_j \cup E_j$ is assigned with the color c_j $(j = 1, 2, 3)$. Therefore, $\chi_{d_2}[T(C_n)] = 3$.
(ii) If $n \equiv 1 \pmod 3$, then assign color c_2 to v_{n-1} and c_3 to the vertices v_n, e_{n-1} and e_n. For $1 \leq i < n$ and $j = 1, 2, 3$, each vertex of $V_j \cup E_j$ is assigned the color c_j. Thus, we have $\chi_{d_2}[T(C_n)] = 3$.

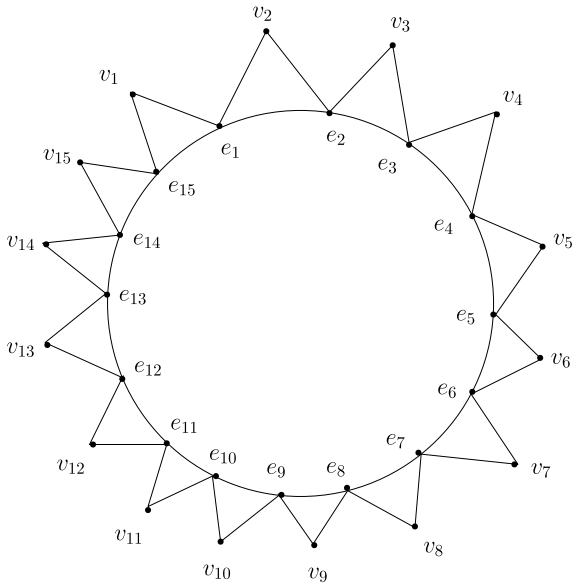

Fig. 8 Middle graph $M(C_{15})$ of a cycle C_{15}

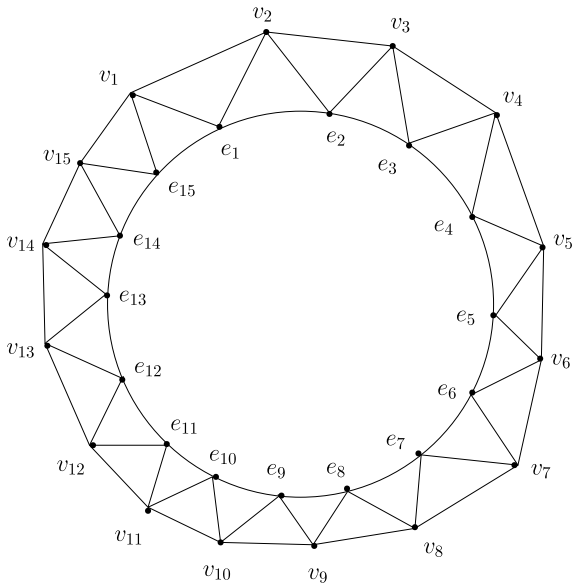

Fig. 9 Total graph $T(C_{15})$ of a cycle C_{15}

(iii) If $n \equiv 2 \pmod 3$, then assign the color c_3 to v_{n-1} and c_4 to the vertices v_n, e_{n-1} and e_n. For $1 \leq i < n$ and $j = 1, 2, 3$, every vertex in $V_j \cup E_j$ is assigned the color c_j. Hence, $\chi_{d_2}[T(C_n)] = 4$ (Fig. 9). □

2.4 Characterization of Cactus Graphs and Block Graphs with $\chi_{d_2}(G) = \chi(G)$

Finally, in this section, we characterize the family of cacti and block graphs for which d_2-coloring number equals the chromatic number.

Definition 4 An edge $e = uv$ of a cactus graph G is cycle-free if e is not in any cycle of G.

Theorem 10 *Let G be a cactus graph. Then $\chi_{d_2}(G) = \chi(G)$ if and only if one of the following holds:*

(a) G is a path
(b) $G = C_{4r}$
(c) every vertex $u \in V(G)$ is either incident with at most one cycle of length ≥ 4 such that $G - N[u]$ has at most two components or incident with some C_3 s and cycle-free edges such that $G - N[u]$ has at most three components.

Proof Assume that $\chi_{d_2}(G) = \chi(G)$.
It is easy to see that for any cactus graph G, $\chi(G) = 2$ or 3.
Case 1: $\chi(G) = 2$
Since $\chi(G) = 2$, G is a bipartite graph. If G is acyclic, then G is a tree.
We claim that $\deg(v) = 1$ or 2 for every vertex $v \in V(G)$.
Assume there is a vertex v in $V(G)$where $\deg(v) = r \geq 3$.Let $N(v) = \{v_1, v_2, \ldots, v_r\}$. Since $d(v_i, v_j) = 2$ for $i \neq j$, any d_2-coloring of G requires at least r colors. As a result, $\chi_{d2}(G) \geq r > 2$, which is a contradiction. Thus, G is a path.
If G is a bipartite graph with at least one cycle C, then we claim it is just a cycle C_n.

Suppose there exists a vertex v in C such that $\deg(v) \geq 3$. Then $\chi_{d_2}(G) \geq \deg(v) \geq 3$, a contradiction to our assumption that $\chi_{d_2}(G) = \chi(G) = 2$. Therefore, $\deg(v) = 2$ for all $v \in V(G)$. Hence, $G \cong C_n$.
Next we claim that $G \cong C_{4r}$.
Let $n = 4r + s$; $0 < s \leq 3$ and $V(C_n) = \{v_1, v_2, \ldots, v_n\}$.
At least two colors say, c_1 and c_2 are required to color the 4-vertex sets $\{v_1, v_2, v_3, v_4\}$, $\{v_5, v_6, v_7, v_8\}, \ldots, \{v_{4r-3}, v_{4r-2}, v_{4r-1}, v_{4r}\}$ in any d_2-coloring of G. If $s = 3$, then v_{4r-2} cannot be assigned the color c_1 or c_2. So we require one more color c_3 to color the vertex v_{4r-2}. Similarly, if $s = 1$, the vertex v_{4r-1} cannot be assigned the colors c_1 or c_2 and if $s = 2$, v_{4r-2} cannot be assigned the c_1 or c_2. Therefore, $G = C_{4r}$.
Case 2: $\chi(G) = 3$
Suppose condition (c) does not hold.
Then there exists a vertex $u \in V(G)$ such that u is in at least one cycle of length ≥ 4 and $G - N[u]$ has at least two components.
Case 2.1: Let u be a cut-vertex of two cycles C_r and C_s where $r, s > 3$.
Because $|N(u)| = 4$ and any two vertices in $N(u)$ are at distance two, any d_2-coloring of G requires four colors, resulting in $\chi_{d2}(G) \geq 4 \neq \chi(G)$, a contradiction. As a result, u is in at most one cycle of length ≥ 4.
Case 2.2: Let u be a cut-vertex of a cycle C_r and s cycle-free edges where $r > 3$ and

$s \geq 2$.
If $r = 4$, one can easily see that the vertex u is incident with at most one cycle-free edge. For otherwise we require $|N(u)|$ distinct colors to d_2-color the vertices of $N(u)$ and hence $\chi_{d_2}(G) \geq |N(u)| > \chi(G)$. So, assume that $r > 4$. Since $|N(u)| = s + 2$ and any two vertices in $N(u)$ are at distance two, we require at least $s + 2$ colors in any d_2-coloring of G. Hence, $\chi_{d_2}(G) \geq s + 2 \geq 4$, a contradiction. This claims the first part of condition (c).
Now, suppose the second part of condition (c) fails.
Let u be a vertex incident with r number of C_3s and s cycle-free edges, where $r, s \geq 2$. Let $F = \{uv_1, uv_2, \ldots, uv_s\}$ be the set of cycle-free edges incident with u. Since r cycles are glued at u, we require r distinct colors in any d_2-coloring of G. Furthermore, any two vertices in the set $F' = \{v_1, v_2, \ldots, v_s\}$ are at distance two and every vertex in F' is of distance two from a vertex $v \in N(u) - F'$, at least s colors are required to color these vertices in any d_2-coloring of G. Therefore, $\chi_{d_2}(G) \geq r + s > 4$, a contradiction.
The converse is obvious. □

Theorem 11 *Let G be a block graph. Then $\chi_{d_2}(G) = \chi(G)$ if and only if there exists at least one cut-vertex v in G such that $\kappa(G - v) = \omega(G)$ where $\kappa(G - v)$ is the number of connected components in $G - v$.*

Proof Let us assume that $\chi_{d_2}(G) = \chi(G)$.
Suppose to the contrary $\kappa(G - v) \neq \omega(G)$ for every cut-vertex $v \in V(G)$. Then we have $\kappa(G - v) < \omega(G)$. This implies $\chi_{d_2}(G) \leq \kappa(G - v) < \omega(G)$, a contradiction.
The converse is obvious. □

Acknowledgements The authors wish to thank the organizers of the conference FMAACM-2021 and the Department of Science and Technology, Government of India for the financial support to the Department of Mathematics, SASTRA Deemed to be University under FIST Programme -Grant No.: SR/FST/MSI-107/2015(c).

References

1. Balakrishnan, R., Ranganathan, K.: A Textbook of Graph Theory, 2nd edn. Universitext, Springer (2012)
2. Benmedjdoub, B., Bouchemakh, I., Sopena, E.: 2-distance colorings of integer distance graphs. Discuss. Math. Graph Theory **39**, 589–603 (2019)
3. Hu, Y., Wang, W.: 2-distance vertex-distinguishing total coloring of graphs. Discrete Math. Algor. Appl. **10**(22), 1850018 (2018)
4. Kramer, F., Kramer, H.: A survey on the distance-coloring of graphs. Discrete Math. **308**, 422–426 (2008)
5. Niranjan, P.K., Srinivasa Rao, K.: The k-distance chromatic number of trees and cycles. AKCE Int. J. Graphs Combin. **16**, 230–235 (2019)
6. Selvakumar, K., Nithya, S.: d_2 coloring of a graph. J. Math. Comput. Sci. **3**(2), 102–111 (2011)
7. Venkatakrishnan, Y.B., Swaminathan, V.: Color class domination number of middle graph and central graph of $K_{1,n}$, C_n, P_n. Adv. Model. Optim. **12**(2), 233–237 (2010)

8. Vernold, V.J., Venkatachalam, M., Akbar, A.M.M.: A note on achromatic coloring of star graph families. Filomat **23**(3), 251–255 (2009)
9. Wei, D., Xu, B.: 2-distance coloring of planar graphs with girth 5. J. Combin. Optim. **34**, 1302–1322 (2017)
10. Yegnanarayanan, V., Parthiban, A.: Vertex coloring of certain distance graphs. Int. J. Pure Appl. Math. **86**(4), 669–688 (2013)

Improved Solution to a Decision-Making Problem Involving TraIFNs Data with TOPSIS Method

P. Vishnukumar, Geetha Sivaraman, and M. Edwin Antony Raj

Abstract The aim of this paper proposes an improved accuracy function (AF) on the collection of trapezoidal intuitionistic fuzzy numbers (TraIFNs) and makes comparisons with existing functions. A trapezoidal intuitionistic fuzzy TOPSIS method based on the proposed AF is applied to rank the alternatives, a trapezoidal intuitionistic fuzzy index matrix based on the proposed accuracy function is applied to rank the alternatives, and the most suitable one(s) can be chosen in the decision-making process.

Keywords Intuitionistic fuzzy values · Trapezoidal intuitionistic fuzzy numbers · Improved accuracy function · TOPSIS method · Trapezoidal intuitionistic fuzzy index matrix · Multi-criteria decision-making

1 Introduction

Intuitionistic fuzzy sets and interval-valued intuitionistic fuzzy sets were established by Atanassov [1], and Atanassov and Gargov [4] play a significant role in control theory, decision analysis and information systems, etc. The class of interval-valued intuitionistic fuzzy numbers (IVIFNs) is a vital subclass of the set of intuitionistic fuzzy numbers (IFNs). It is generally used in decision analysis, information systems and pattern recognition. It is very simple to handle speculative and uncertain information successfully, because the membership and non-membership degrees are indicated only as ranges of values rather than exact value. Trapezoidal intuitionistic fuzzy numbers (TrIFNs) [13] are further generalization of IVFNs which contributes a better modelling of problems with incomplete information.

P. Vishnukumar (✉) · G. Sivaraman
Department of Mathematics, St. Joseph's College (Autonomous), Tiruchirappalli, Tamil Nadu, India

M. Edwin Antony Raj
Department of Mathematics, K. Ramakrishnan College of Engineering, Tiruchirappalli, Tamil Nadu, India

© The Author(s), under exclusive license to Springer Nature Singapore Pte Ltd. 2022

S. R. Kannan et al. (eds.), *Fuzzy Mathematical Analysis and Advances in Computational Mathematics*, Studies in Fuzziness and Soft Computing 419,
https://doi.org/10.1007/978-981-19-0471-4_9

Many researchers have proposed different ranking methods on TrIFNs, but no one could cover the entire class of TrIFNs, and also almost all the methods have a disadvantage that they ranked two different TrIFNs as the same at some point of time. Lakshmana et al. [8] have discussed another type of TraIFNs as generalization of intuitionistic fuzzy values and IVIFNs which is different from the TrIFN introduced by Nehi and Maleki [13]. For clarity, we call the new type of trapezoidal intuitionistic fuzzy numbers by TraIFNs of Lakshmana et al. [8] and the other by conventional TrIFNs.

The concept of index matrix (IM) was introduced by Atanasov in 1987 [2]. Further, (0, 1)—IM was extended to intuitionistic fuzzy index matrix (IFIM) by Atanasov in 2010 [3]. Atanssov et al. introduced an inter-criteria multi-criteria decision-making based on IFIM in [6]. There are 18 aggregation multi-criteria IFIM operators introduced in [5], and Sivaraman et al. [15] introduced the concept of IFIM to trapezoidal intuitionistic fuzzy index matrix (TraIFIM) in the year of 2020.

The rest of this paper is organized as follows. Necessary basic definitions are briefly introduced in Sect. 2. Section 3 proposes an AF on TraIFNs and makes comparisons with existing functions. Section 4 introduces a ranking by improved AF for TraIFN. Section 5 develops a TOPSIS method based on the improved accuracy function to solve trapezoidal intuitionistic fuzzy MCDM problems. Section 5.1 introduced illustrative example based on the above section. In Sect. 6, a TraIFI matrix is analysed, and an algorithmic procedure is given to apply the proposed accuracy function in MCDM based on multi-criteria TraIFIM. In Sect. 6.1, illustrative examples are introduced to show the advantages of the proposed method. In Sect. 7, the paper has consummated.

2 Preliminaries

Definition 2.1. [13, 16] Let $V_k = \left([\mu_a,\ \mu_b,\ \mu_c,\ \mu_d],\ \left[\nu_e,\ \nu_f\ ,\nu_g\ ,\nu_h\right]\right)$ (where $\nu_e \geq \mu_a$, $\nu_f \leq \mu_b \leq \mu_c \leq \nu_g$ and $\nu_h \leq \mu_d$) be a TrIFN. Then the degree of acceptance and degree of rejection functions are defined as follows:

$$\mu_{v_k}(x) = \begin{cases} \frac{x-\mu_a}{\mu_b-\mu_a} & \mu_a \leq x \leq \mu_b \\ 1 & \mu_b \leq x \leq \mu_c \\ \frac{x-\mu_d}{\mu_c-\mu_d} & \mu_c \leq x \leq \mu_d \\ 0 & \text{otherwise} \end{cases};$$

$$\nu_{v_k}(x) = \begin{cases} \frac{x-\nu_e}{\nu_e-\nu_f} & \nu_e \leq x \leq \nu_f \\ 1 & \nu_f \leq x \leq \nu_g \\ \frac{x-\nu_h}{\nu_h-\nu_g} & \nu_g \leq x \leq \nu_h \\ 0 & \text{otherwise} \end{cases}$$

The graphical representation of TrIFN is shown in Fig. 1

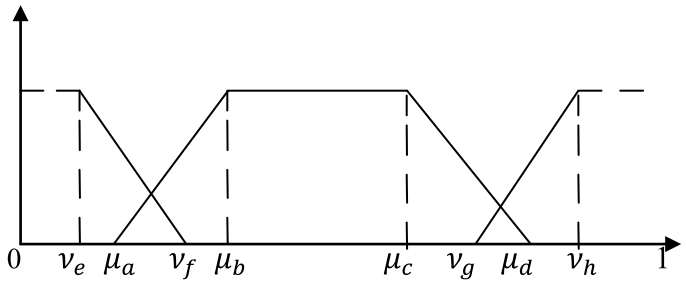

Fig. 1 Conventional type TrIFN

If $\mu_b = \mu_c$ and $\nu_f = \nu_g$ in V_k, then V_k becomes a triangular intuitionistic fuzzy number (TIFN). If $\mu_a = \nu_e$, $\mu_b = \nu_f$, $\mu_c = \nu_g$ and $\mu_d = \nu_h$ in V_k, then V_k becomes a trapezoidal fuzzy number (TrFN). We note that this type of TrIFNs generalizes interval-valued fuzzy numbers (IVFNs). We call this TrIFNs as conventional TrIFNs. Lakshmana et al. [8] have studied another type of TraIFNs which is different from conventional type, and it seems to be the real generalization of real valued and IVIFNs. For clarity, we call this trapezoidal intuitionistic fuzzy number by trapezoidal intuitionistic fuzzy number of new type and is denoted by TraIFN.

Definition 2.2. [8] Let $V_k = \left([\mu_a, \mu_b, \mu_c, \mu_d], \left[\nu_e, \nu_f, \nu_g, \nu_h\right]\right)$ (where $\nu_e \geq \mu_c$, a $\nu_f \geq \mu_d$ (or) and $\nu_g \leq \mu_a$, $\nu_h \leq \mu_b$) be a TraIFN. Then the degree of acceptance and degree of rejection functions are defined as follows:

$$\mu_{v_k}(x) = \begin{cases} \frac{x-\mu_a}{\mu_b-\mu_a} & \mu_a \leq x \leq \mu_b \\ 1 & \mu_b \leq x \leq \mu_c \\ \frac{x-\mu_d}{\mu_c-\mu_d} & \mu_c \leq x \leq \mu_d \\ 0 & \text{otherwise} \end{cases}$$

$$\nu_{v_k}(x) = \begin{cases} \frac{x-\nu_e}{\nu_f-\nu_e} & \nu_e \leq x \leq \nu_f \\ 1 & \nu_f \leq x \leq \nu_g \\ \frac{x-\nu_h}{\nu_g-\nu_h} & \nu_g \leq x \leq \nu_h \\ 0 & \text{otherwise} \end{cases}$$

The graphical representation of TraIFN is shown in Fig. 2

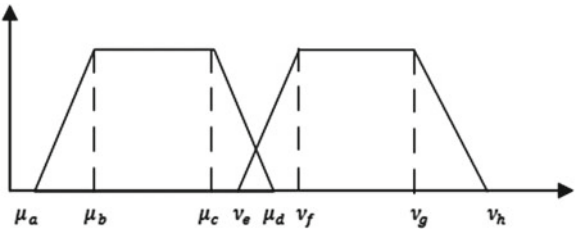

Fig. 2 Lakshmana et al. type TraIFN

Definition 2.3. [8] The α cut of TraIFN is defined as follows:

$$\alpha_{V_k} = \{[\mu_a + \alpha(\mu_b - \mu_a), \mu_d + \alpha(\mu_c - \mu_d)], \\ \left[\nu_e + \alpha\left(\nu_f - \nu_e\right), \nu_h + \alpha\left(\nu_g - \nu_h\right)\right]\}.$$

Remark 2.4. Throughout this paper denotes the TraIFN with $\nu_e \geq \mu_c$ and $\nu_f \geq \mu_d$. The similar results for the TraIFN V_k with $\nu_g \leq \mu_a$ and $\nu_h \leq \mu_b$ can be proved analogously, and hence, they are left to the readers.

Definition 2.5. [17] The score function S of an IVIFN $V_k = ([\mu_a, \mu_b], [\nu_c, \nu_d])$ is given as $(V_k) = (\mu_a + \mu_b - \nu_c - \nu_d)/2$, where $S(V_k) \in [-1, 1]$.

Definition 2.6. [17] The accuracy function H of an IVIFN $V_k = ([\mu_a, \mu_b], [\nu_c, \nu_d])$ is given as $(V_k) = (\mu_a + \mu_b + \nu_c + \nu_d)/2$, where $H(V_k) \in [0, 1]$.

Definition 2.7. [18] The novel accuracy function M of an IVIFN $V_k = ([\mu_a, \mu_b], [\nu_c, \nu_d])$ is given as $H(V_k) = \mu_a + \mu_b - 1 + (\nu_c + \nu_d)/2$, where $M(V_k) \in [-1, 1]$.

Definition 2.8. [14] An improved accuracy function K of an IVIFN $V_k = ([\mu_a, \mu_b], [\nu_c, \nu_d])$ is given as $K(V_k) = K(V_k) = \mu_a + \mu_d(1 - \mu_a - \nu_e) + \mu_d + \mu_a(1 - \mu_d - \nu_h)/2$, where $K(V_k) \in [0, 1]$.

Definition 2.9. [9] Two TraIFNs $V_{k_1} = \left(\left[\mu_{a_1}, \mu_{b_1}, \mu_{c_1}, \mu_{d_1}\right], \left[\nu_{e_1}, \nu_{f_1}, \nu_{g_1}, \nu_{h_1}\right]\right)$, $V_{k_2} = \left(\left[\mu_{a_2}, \mu_{b_2}, \mu_{c_2}, \mu_{d_2}\right], \left[\nu_{e_2}, \nu_{f_2}, \nu_{g_2}, \nu_{h_2}\right]\right)$ are said to compare $\left[\mu_{a_1} \leq \mu_{a_2}, \mu_{b_1} \leq \mu_{b_2}, \mu_{c_1} \leq \mu_{c_2}, \mu_{d_1} \leq \mu_{d_2}\right]$ and $\left[\nu_{a_1} \geq \nu_{a_2}, \nu_{b_1} \geq \nu_{b_2}, \nu_{c_1} \geq \nu_{c_2}, \nu_{d_1} \geq \nu_{d_2},\right]$.

Remark 2.10. If any one of the inequalities is strict $<$, then $V_{k_1} < V_{k_2}$.

Sivaraman et al. introduced [15] (ave, ave)-column aggregation for a given multi-criteria TraIFIM (V_k TraIFIM).

Definition 2.11. [15] Let $H_0 \notin G$ be a fixed index. The (ave, ave)-column aggregation for a given multi-criteria TraIFIM (V_k TraIFIM).

$$\sigma_{\max}(V_k TraIFIM, H_0)$$

$$= \begin{array}{c|c} & H_0 \\ \hline G_1 & 1/n \sum_{j=1}^{n} ([\mu_a, \mu_b, \mu_c, \mu_d])_{k_1 l_j}, \sum_{j=1}^{n} \left([\nu_e, \nu_f, \nu_g, \nu_h]\right)_{k_1 l_j}, \\ & \vdots \\ G_i & 1/n \sum_{j=1}^{n} ([\mu_a, \mu_b, \mu_c, \mu_d])_{k_i l_j}, \sum_{j=1}^{n} \left([\nu_e, \nu_f, \nu_g, \nu_h]\right)_{k_i l_j}, \\ & \vdots \\ G_m & 1/n \sum_{j=1}^{n} ([\mu_a, \mu_b, \mu_c, \mu_d])_{k_m l_j}, \sum_{j=1}^{n} \left([\nu_e, \nu_f, \nu_g, \nu_h]\right)_{k_m l_j}, \end{array}$$

3 Ranking of TraIFN by Accuracy Functions

In some case, the membership and non-membership values in the information may be intervals rather than exact numbers. Further that interval may be generalized to TraIFN form. So in order to solve decision problem when the given information is of TraIFN, the AF H defined on IVIFNs [17] is extended to the TraIFNs in this section.

Using the definition of $H_{NT}(V_k)$ for $\alpha \in [0,\ 1]$, we get

$$\begin{aligned} H_{NT}(V_k) &= \frac{1}{2} \int_0^1 [\mu_a + \alpha(\mu_b - \mu_a) + \mu_d + \alpha(\mu_c - \mu_d) \\ &\quad + \nu_e + \alpha\left(\nu_f - \nu_e\right) + \nu_h + \alpha\left(\nu_g - \nu_h\right)] \mathrm{d}\alpha \end{aligned}$$

$$= \frac{1}{2}\left[\mu_a + (\mu_b - \mu_a)\left[\frac{\alpha^2}{2}\right]_0^1 + \mu_d + (\mu_c - \mu_d)\right)\left[\frac{\alpha^2}{2}\right]_0^1 + \nu_e$$
$$+ \left(\nu_f - \nu_e\right)\left[\frac{\alpha^2}{2}\right]_0^1$$
$$+ \nu_h + \left(\nu_g - \nu_h\right)\left[\frac{\alpha^2}{2}\right]_0^1$$
$$= \frac{1}{2}\left[\mu_a + \left[\frac{\mu_b - \mu_a}{2}\right] + \mu_d + \left[\frac{\mu_c - \mu_d}{2}\right]\right.$$
$$\left. + \nu_e + \left[\frac{\nu_f - \nu_e}{2}\right] + \nu_h + \left[\frac{\nu_g - \nu_h}{2}\right]\right]$$

$$H_{\mathrm{NT}}(V_k) = \left(\mu_a + \mu_b + \mu_c + \mu_d + \nu_e + \nu_f + \nu_g + \nu_h\right)/4$$

Definition 3.12. Let $V_k = \left([\mu_a, \mu_b, \mu_c, \mu_d],\ \left[\nu_e, \nu_f, \nu_g, \nu_h\right]\right)$ be a TraIFN. The accuracy function H_{NT} is defined.

$$H_{NT}(V_k) = \left(\mu_a + \mu_b + \mu_c + \mu_d + \nu_e + \nu_f + \nu_g + \nu_h\right)/4$$

Proposition 3.13. For a fuzzy subset (FS) $V_k = \mu_a = ([\mu_a, \mu_a, \mu_a, \mu_a], [1 - \mu_a, 1 - \mu_a, 1 - \mu_a, 1 - \mu_a])$, the improved AF is $H_{NT}(V_k) = 1$.

For an interval-valued fuzzy subset (IVFS) $V_k = [\mu_a, \mu_b] = ([\mu_a, \mu_a, \mu_b, \mu_b], [1 - \mu_b, 1 - \mu_b, 1 - \mu_a, 1 - \mu_a])$, the improved AF is $H_{NT}(V_k) = 1$.

For an interval-valued intuitionistic fuzzy subset (IVIFS) $V_k = ([\mu_a, \mu_b], [\nu_c, \nu_d]) = ([\mu_a, \mu_a, \mu_b, \mu_b], [\nu_c, \nu_c, \nu_d, \nu_d])$, the improved AF is $H_{NT}(V_k) = (\mu_a + \mu_b + \nu_c + \nu_d)/2 = H(V_k)$.

In particular, if $V_k = ([1,\ 1,\ 1,\ 1],\ [0,\ 0,\ 0,\ 0])$, $H_{NT}(V_k) = 1$.

If $V_k = ([0,\ 0,\ 0,\ 0],\ [1,\ 1,\ 1,\ 1])$, $H_{NT}(V_k) = 1$.

The accuracy function M defined on IVIFNs [18] is extended to the TraIFNs: Let $V_k = \left([\mu_a, \mu_b, \mu_c, \mu_d],\ \left[\nu_e, \nu_f, \nu_g, \nu_h\right]\right)$ be a TraIFN.

$$M_{NT}(V_k) = \int_0^1 [\mu_a + \alpha(\mu_b - \mu_a) + \mu_d + \alpha(\mu_c - \mu_d)]\mathrm{d}\alpha + \int_0^1 \mathrm{d}\alpha$$
$$+ \frac{1}{2}\int_0^1 \left[\nu_e + \alpha\left(\nu_f - \nu_e\right) + \nu_h + \alpha\left(\nu_g - \nu_h\right)\right]\mathrm{d}\alpha$$

$$= \left[\mu_a + (\mu_b - \mu_a)\left[\frac{\alpha^2}{2}\right]_0^1 + \mu_d + (\mu_c - \mu_d)\right)\left[\frac{\alpha^2}{2}\right]_0^1 - \left[\frac{\alpha^2}{2}\right]_0^1$$
$$+ \frac{1}{2}\left[\nu_e + \left(\nu_f - \nu_e\right)\left[\frac{\alpha^2}{2}\right]_0^1 + \nu_h + \left(\nu_g - \nu_h\right)\left[\frac{\alpha^2}{2}\right]_0^1\right]$$
$$= \mu_a + \left[\frac{\mu_b - \mu_a}{2}\right] + \mu_d + \left[\frac{\mu_c - \mu_d}{2}\right] - 1 + \nu_e/2 + \left[\frac{\nu_f - \nu_e}{4}\right]$$
$$+ \nu_h/2 + \left[\frac{\nu_g - \nu_h}{4}\right]$$

$$M_{NT}(V_k) = \frac{\mu_a + \mu_b + \mu_c + \mu_d}{2} - 1 + \frac{\nu_e + \nu_f + \nu_g + \nu_h}{4}$$

Definition 3.14. Let $V_k = \left([\mu_a, \mu_b, \mu_c, \mu_d],\ \left[\nu_e, \nu_f, \nu_g, \nu_h\right]\right)$ be a TraIFN. The accuracy function $\mathrm{H_{NT}}$ is defined.

$$M_{NT}(V_k) = \frac{\mu_a + \mu_b + \mu_c + \mu_d}{2} - 1 + \left(\nu_e + \nu_f + \nu_g + \nu_h\right)/4.$$

Proposition 3.15. For a fuzzy subset (FS) $V_k = \mu_a = ([\mu_a, \mu_a, \mu_a, \mu_a], [1 - \mu_a, 1 - \mu_a, 1 - \mu_a, 1 - \mu_a])$, the improved AF is $M_{NT}(V_k) = \mu_a$.

For an interval-valued fuzzy subset (IVFS) $V_k = [\mu_a, \mu_b] = ([\mu_a, \mu_a, \mu_b, \mu_b],\ [1 - \mu_b, 1 - \mu_b, 1 - \mu_a, 1 - \mu_a])$, the improved AF is $M_{NT}(V_k) = (\mu_a + \mu_b)/2$.

For an interval-valued intuitionistic fuzzy subset (IVIFS) $V_k = ([\mu_a, \mu_b],\ [\nu_c, \nu_d]) = ([\mu_a, \mu_a, \mu_b, \mu_b],\ [\nu_c, \nu_c, \nu_d, \nu_d])$, the improved AF is $M_{NT}(V_k) = (\mu_a + \mu_b + \nu_c + \nu_d)/2 = H(V_k)$.

In particular, if $V_k = ([1, 1, 1, 1],\ [0, 0, 0, 0])$, $M_{NT}(V_k) = 1$.

If $V_k = ([0, 0, 0, 0],\ [1, 1, 1, 1])$, $M_{NT}(V_k) = 0$.

Definition 3.16. Let V_{k_1} and V_{k_2} be two TraIFNs. If $H_{NT}\left(V_{k_1}\right) < H_{NT}\left(V_{k_2}\right)$, then $V_{k_1} < V_{k_2}$.

Example 3.17. Let $V_{k_1} = ([0.1, 0.15, 0.2, 0.25], [0.3, 0.35, 0.4, 0.5])$ and $V_{k_2} = ([0.2, 0.25, 0.3, 0.35],\ [0.4, 0.5, 0.6, 0.65])$ be two TraIFNs for two alternatives. Then $H_{NT}\left(V_{k_1}\right) = 0.5625,\ H_{NT}\left(V_{k_2}\right) = 0.8125$.

Example 3.18. Let $V_{k_1} = ([0.1, 0.2, 0.25, 0.3], [0.35, 0.4, 0.43, 0.45])$ and $V_{k_2} = ([0.2, 0.25, 0.3, 0.31],\ [0.34, 0.35, 0.36, 0.37])$ be two TraIFNs for two alternatives. Then $H_{NT}\left(V_{k_1}\right) = 0.62 = H_{NT}\left(V_{k_2}\right)$, which is illogical.

Example 3.19. But in the above example, $M_{NT}\left(V_{k_1}\right) = -0.1675$, $M_{NT}\left(V_{k_2}\right) = -0.115$, which supports our expectation.

4 Ranking by Improved Accuracy Function for TraIFN

In both the above two Definition 3.12 and Definition 3.14, we have noticed that the novel accuracy function and the accuracy function are inversely proportional to the hesitation. In order to overcome this illogical concept, the new improved accuracy function is defined as follows.

The accuracy function K defined on IVIFNs is extended to the TraIFNs:

Let $V_k = \left([\mu_a, \mu_b, \mu_c, \mu_d],\ [\nu_e, \nu_f, \nu_g, \nu_h]\right)$ be a TraIFN.

$$
\begin{aligned}
M_{NT}(V_k) = \int_0^1 & [\mu_a + \alpha(\mu_b - \mu_a) + \mu_d + \alpha(\mu_c - \mu_d) \\
& [\mu_d + \alpha(\mu_c - \mu_d)][1 - (\mu_a + \alpha(\mu_b - \mu_a)] \\
& + \left(\nu_e + \alpha\left(\nu_f - \nu_e\right)\right) + [\mu_a + \alpha(\mu_b - \mu_a)][1 - (\mu_d + \alpha(\mu_c - \mu_d)] \\
& + \nu_h + \alpha\left(\nu_g - \nu_h\right)]\mathrm{d}\alpha. \\
= \frac{1}{2}\Bigg[& [\mu_a + (\mu_b - \mu_a)\left[\frac{\alpha^2}{2}\right]_0^1 + \mu_d + (\mu_c - \mu_d))\left[\frac{\alpha^2}{2}\right]_0^1 \\
& - \mu_d + (\mu_c - \mu_d))\left[\frac{\alpha^2}{2}\right]_0^1 \\
& \left([\alpha]_0^1 - [\mu_a + (\mu_b - \mu_a)\left[\frac{\alpha^2}{2}\right]_0^1 - \nu_e + \left(\nu_f - \nu_e\right)\left[\frac{\alpha^2}{2}\right]_0^1\right) \\
& + [\mu_a + (\mu_b - \mu_a)\left[\frac{\alpha^2}{2}\right]_0^1\left([\alpha]_0^1 - [\mu_d + (\mu_c - \mu_d)\left[\frac{\alpha^2}{2}\right]_0^1\right. \\
& \left. -\nu_h + \left(\nu_g - \nu_h\right)\left[\frac{\alpha^2}{2}\right]_0^1\right)\Bigg] \\
= \frac{1}{2}\Bigg(& \mu_a + \left[\frac{\mu_b - \mu_a}{2}\right] + \mu_d + \left[\frac{\mu_c - \mu_d}{2}\right] + \mu_d + \left[\frac{\mu_c - \mu_d}{2}\right] \\
& \left(1 - \left(\mu_a + \left[\frac{\mu_b - \mu_a}{2}\right]\right) - \left(\nu_e + \left[\frac{\nu_f - \nu_e}{2}\right]\right)\right) \\
& + \mu_a + \left[\frac{\mu_b - \mu_a}{2}\right]\left(1 - \left(\mu_d + \left[\frac{\mu_c - \mu_d}{2}\right]\right) - \left(\nu_h + \left[\frac{\nu_g - \nu_h}{2}\right]\right)\right)\Bigg)
\end{aligned}
$$

$$
\begin{aligned}
K_{NT}(V_k) = & \frac{\mu_a + \mu_b + \mu_c + \mu_d}{2} - \frac{(\mu_a\mu_d + \mu_b\mu_c)}{3} \\
& - \frac{\left(\mu_c\nu_f + \nu_e\mu_d + \mu_b\nu_g + \mu_a\nu_h + \mu_a\mu_c + \mu_b\mu_d\right)}{6} \\
& - \frac{\left(\mu_d\nu_f + \mu_c\nu_e + \mu_b\nu_h + \mu_a\nu_g\right)}{12}
\end{aligned}
$$

Hence, we introduce the following definition.

Definition 4.20. Let $V_k = \left([\mu_a, \mu_b, \mu_c, \mu_d], \left[\nu_e, \nu_f, \nu_g, \nu_h\right]\right)$ be a TraIFN. The accuracy function H_{NT} is defined.

$$K_{NT}(V_k) = \frac{\mu_a + \mu_b + \mu_c + \mu_d}{2} - \frac{(\mu_a\mu_d + \mu_b\mu_c)}{3} - \frac{\left(\mu_c\nu_f + \nu_e\mu_d + \mu_b\nu_g + \mu_a\nu_h + \mu_a\mu_c + \mu_b\mu_d\right)}{6} - \frac{\left(\mu_d\nu_f + \mu_c\nu_e + \mu_b\nu_h + \mu_a\nu_g\right)}{12}$$

Note If we put $\mu_a = \mu_b$, $\mu_c = \mu_d$ and $\nu_e = \nu_f$, $\nu_g = \nu_h$, we can define the improved AF for an IVIFN [7].

$$K(V_k) = \frac{\mu_a + \mu_d(1 - \mu_a - \nu_e) + \mu_d + \mu_a(1 - \mu_d - \nu_h)}{2}$$

Example 4.21. Let V_{k_1} = ([0.1, 0.2, 0.25, 0.3], [0.35, 0.4, 0.43, 0.45]) and V_{k_2} = ([0.05, 0.21, 0.27, 0.32], [0.33, 0.41, 0.44, 0.45]) be two TraIFN for two alternatives.

By applying Definition 3.12, we obtain $H_{NT}\left(V_{k_1}\right) = 0.62 = H_{NT}\left(V_{k_2}\right)$.
By applying Definition 3.14, $M_{NT}\left(V_{k_1}\right) = -0.1675 = M_{NT}\left(V_{k_1}\right)$.

Remark 4.22. By applying Definition 4.20 to Example 4.21, we obtain $K_{NT}\left(V_{k_1}\right) = 0.2998$ and $K_{NT}\left(V_{k_2}\right) = 0.3041$. Thus, the alternative V_{k_2} is more suitable than the alternative V_{k_1}. But the existing functions do not rank properly, and so we do not recognize which alternative is better. Therefore, we say that our proposed function for TraIFN is more practical and more sensible than the others.

Proposition 4.23. For any trapezoidal intuitionistic fuzzy subset (TraIFSs), $V_k = \left([\mu_a, \mu_b, \mu_c, \mu_d], \left[\nu_e, \nu_f, \nu_g, \nu_h\right]\right)$. The improved AF $K_{NT}(V_k) \in [0, 1]$.

Proposition 4.24. For a fuzzy subset (FS) $V_k = \mu_a = ([\mu_a, \mu_a, \mu_a, \mu_a], [1 - \mu_a, 1 - \mu_a, 1 - \mu_a, 1 - \mu_a])$, the improved AF is $K_{NT}(V_k) = \mu_a$.

In particular, if $V_k = ([1, 1, 1, 1], [0, 0, 0, 0])$, $K_{NT}(V_k) = 1$.
If $V_k = ([0, 0, 0, 0], [1, 1, 1, 1])$, $K_{NT}(V_k) = 0$.

Theorem 1. Let $V_k = \left([\mu_a, \mu_b, \mu_c, \mu_d], \left[\nu_e, \nu_f, \nu_g, \nu_h\right]\right)$ be a TraIFN. Then $K_{NT}(V_k) + K_{NT}\left((V_k)^c\right) \leq 1$.

Now we define a ranking principle on TraIFN using above accuracy function.

Definition 4.25. Let V_{k_1} and V_{k_2} be two TraIFNs. If $K_{NT}\left(V_{k_1}\right) < K_{NT}\left(V_{k_2}\right)$, then $V_{k_1} < V_{k_2}$.

4.1 Significance of the Proposed Method

In this subsection, the proposed definition of ranking is applied through numerical example to show the validity and significance of the proposed method.

Comparison between our proposed AF with a complete of incomplete trapezoidal information [10]

Let $K_{NT}(V_{k_1}) = [(0.3, 0.3, 0.4, 0.4), (0.6, 0.6, 0.6, 0.6)]$, $K_{NT}(V_{k_2}) = [(0.256608238, 0.256608238, 0.256608438, 0.42783361, 0.42783361), (0.506608438, 0.506608438, 0.67783361, 0.67783361)]$ be two TraIFNs. $L(V_{k_1}) = -0.04 = L(V_{k_2})$, $LG(V_{k_1}) = 0.46 = LG(V_{k_2})$, $P_1(V_{k_1}) = -0.8 = P_1(V_{k_2}) \Rightarrow V_{k_1} = V_{k_2}$, $P_2(V_{k_1}) = 0.02$, $P_2(V_{k_2}) = -0.08$. It is noted that the evaluations of the TraIFN are equal when $L(V_k)$, $LG(V_k)$, $P_1(V_k)$ and $P_2(V_k)$ are used. It is found that $P_2(V_{k_1}) \neq P_2(V_{k_2})$ only in P_2 and hence $V_{k_1} \leq V_{k_2}$ which is much laborious. But we can apply the proposed method $V_{k_1} = 0.3700$ and $V_{k_2} = 0.3793 \Rightarrow V_{k_1} < V_{k_2}$.

Comparison between our proposed AF with ranking of incomplete trapezoidal information [11]

Let $K_{NT}(V_{k_1}) = [(0.3, 0.3, 0.4, 0.4), (0.6, 0.6, 0.6, 0.6)]$, $K_{NT}(V_{k_2}) = [(0.256608238, 0.256608238, 0.256608438, 0.42783361, 0.42783361), (0.506608438, 0.506608438, 0.67783361, 0.67783361)]$ be two TraIFNs. $L(V_{k_1}) = -0.04 = L(V_{k_2})$, $LG(V_{k_1}) = 0.46 = LG(V_{k_2}) \Rightarrow V_{k_1} = V_{k_2}$, $P(V_{k_1}) = 0.16$, $P(V_{k_2}) = 0.21$. It is noted that the evaluations of the TraIFN are equal when $L(V_k)$, $LG(V_k)$ are used. It is found that $P(V_{k_1}) \neq P(V_{k_2})$ only in $P(V_k)$, and hence, $V_{k_1} \leq V_{k_2}$ which is much laborious. But we can apply the proposed method $V_{k_1} = 0.3700$ and $V_{k_2} = 0.3793 \Rightarrow V_{k_1} < V_{k_2}$.

5 TOPSIS Method Based on the Improved AF for TraIFN

In this section, by using TOPSIS method, we shall solve fuzzy MCDM problems in which data gathered by decision-makers is expressed as TraIF decision matrix, where every entry is given by TraIF value, and the data about standard weights is known. In order to ascertain the relative closeness coefficients, we apply the improved accuracy function to compute the positive ideal solution and negative ideal solution.

In a MCDM problem, if there exist a set of alternatives $V_k = \{V_{k_1}, V_{k_2}, \ldots V_{k_m}\}$. Every alternative is measured on n criteria, which are indicated by $T = \{T_1, T_2, \ldots, T_n\}$. The evaluation of an alternative V_{k_i} with respect to a criterion T_j can be represented by an TraIFN $Z_{ij} = \left(\left[a_{ij}, b_{ij}, c_{ij}, d_{ij}\right], \left[e_{ij}, f_{ij}, g_{ij}, h_{ij}\right]\right)$ $(i = 1, 2, \ldots, m;\ j = 1, 2, \ldots, n)$ which denotes the membership and non-membership degree of the alternative $V_{k_i} \in V_k$ with respect to the criterion $T_j \in T$. The TraIF decision matrix $D_{m\times n}(\mathrm{Z_{ij}})$ is defined as follows:

$$D_{m\times n}(\mathrm{Z_{ij}}) =$$

$$\begin{bmatrix} ([a_{11},b_{11},c_{11},d_{11}],[e_{11},f_{11},g_{11},h_{11}]) & ([a_{12},b_{12},c_{12},d_{12}],[e_{12},f_{12},g_{12},h_{12}]) & \cdots & ([a_{1n},b_{1n},c_{1n},d_{1n}],[e_{1n},f_{1n},g_{1n},h_{1n}]) \\ ([a_{21},b_{21},c_{21},d_{21}],[e_{21},f_{21},g_{21},h_{21}]) & ([a_{22},b_{22},c_{22},d_{22}],[e_{22},f_{22},g_{22},h_{22}]) & \cdots & ([a_{2n},b_{2n},c_{2n},d_{2n}],[e_{2n},f_{2n},g_{2n},h_{2n}]) \\ \vdots & \vdots & \ddots & \vdots \\ ([a_{m1},b_{m1},c_{m1},d_{m1}],[e_{m1},f_{m1},g_{m1},h_{m1}]) & ([a_{m2},b_{m2},c_{m2},d_{m2}],[e_{m2},f_{m2},g_{m2},h_{m2}]) & \cdots & ([a_{mn},b_{mn},c_{mn},d_{mn}],[e_{mn},f_{mn},g_{mn},h_{mn}]) \end{bmatrix}$$

Now we convert the TrIF decision matrix $D_{m\times n}(Z_{ij})$ into the following accuracy matrix $R_{m\times n}$ $R_{m\times n}\left(K_{NT_{ij}}(Z_{ij})\right)$ using the improved accuracy function K_T

$$R_{m\times n}\left(K_{NT_{ij}}(Z_{ij})\right) = \begin{bmatrix} K_{NT_{11}}(z_{11}) & K_{NT_{12}}(z_{12}) & \cdots & K_{NT_{1n}}(z_{1n}) \\ K_{NT_{21}}(z_{21}) & K_{NT_{22}}(z_{21}) & & K_{NT_{2n}}(z_{2n}) \\ & \vdots & \ddots & \vdots \\ K_{NT_{m1}}(z_{21}) & K_{NT_{m1}}(z_{21}) & \cdots & K_{NT_{mn}}(z_{mn}) \end{bmatrix} \tag{5.1}$$

Let us take the weight of the criterion $T_j (j = 1, 2, \ldots, n)$, is w_j, $w_j \in [0, 1]$ and $\sum_{j=1}^{n} w_j = 1$.

Then the positive and negative ideal solutions of the alternatives are denoted by $V_k^+ = \left\{\left(T_j, [1, 1, 1, 1], [0, 0, 0, 0]\right)/T_j \in T\right\}$, $j = 1, 2, \ldots, n$, and $V_k^- = \left\{\left(C_j, [0, 0, 0, 0], [1, 1, 1, 1]\right)/T_j \in T\right\}$, $j = 1, 2, \ldots, n$, respectively. Thus, the improved accuracy function-based separation measures of every alternative from the negative ideal solution and positive ideal solution, respectively, are obtained from $d_i^-\left(V_k^-, V_{k_i}\right) = \sqrt{\sum_{j=1}^{n}\left[w_j K_{NT_{ij}}(Z_{ij})\right]^2}$ and

$$d_i^+\left(V_k^+, V_{k_i}\right) = \sqrt{\sum_{j=1}^{n}\left[w_j\left(1 - K_{NT_{ij}}(Z_{ij})\right)\right]^2} \tag{5.2}$$

Hence, the relative closeness of an alternative V_{k_i} with respect to the positive ideal solution $V_k^+$is defined as the following general formula:

$$T_i(V_k A_i) = \frac{d_i^-\left(V_k^-, V_{k_i}\right)}{d_i^-\left(V_k^-, V_{k_i}\right) + d_i^+\left(V_k^+, V_{k_i}\right)} \quad (i = 1, 2, \ldots, m) \tag{5.3}$$

is the relative closeness coefficient of V_{k_i} with respect to the positive ideal solution V_k^+ and $0 \le Ti\left(V_{k_i}\right) \le 1$. Then according to the descending order of $T_i(V_{k_i})$, the alternatives can be ranked. Ultimately, the highest value of $T_i(V_{k_i})$ will be the preferable one amongst the alternatives.

5.1 Numerical Examples

In order to show the potency of the improved accuracy function, the following two examples are used as a demonstration.

Example 5.1. A leading company has to select one amongst four candidates for their company for the HR post following these three criteria: (1). C_1 is the academic records. (2). C_2 is his/her IQ and (3). C_3 is the fluency in English. The criterion weight is given by $W = 0.35,\ 0.25,\ 0.40$.

The alternatives $V_{k_i}(i = 1, 2, 3, 4)$ are assessed using the TraIFN by the decision-maker under the above three criteria as listed in the following DM:

$$D_{4\times3}(Z_{ij}) =$$

$$\begin{bmatrix} ([.1,.2,.22,.24],[.25,.3,.35,.4]) & ([.02,.15,.2,.25],[.28,.3,.36,.45]) & ([.15,.2,.25,.28],[.3,.33,.39,.44]) \\ ([.05,.1,.15,.2],[.25,.3,.35,.39]) & ([.3,.35,.38,.4],[.42,.45,.5,.56]) & ([.2,.3,.4,.44],[.5,.52,.54,.55]) \\ ([.3,.4,.45,.5],[.51,.52,.53,.54]) & ([.1,.13,.23,.3],[.34,.36,.4,.45]) & ([.2,.4,.42,.45],[.47,.5,.52,.54]) \\ ([.02,.15,.25,.3],[.32,.33,.42,.45]) & ([.1,.2,.3,.33],[.35,.37,.4,.42]) & ([.3,.34,.4,.45],[.5,.51,.52,.54]) \end{bmatrix}$$

Then we use the proposed approach to select the most enviable one(s). Then the accuracy matrix $R_{4\times3}\left(K_{T_{ij}}\left(x_{ij}\right)\right)$ is obtained by using (5.1)

$$R_{4\times3} \cdot \left(K_{T_{ij}}\left(x_{ij}\right)\right) = \begin{bmatrix} 0.2862 & 0.2421 & 0.3158 \\ 0.1993 & 0.4175 & 0.3902 \\ 0.4433 & 0.2790 & 0.4202 \\ 0.2742 & 0.3307 & 0.4171 \end{bmatrix}$$

We can determine the values of positive and negative ideal solutions by using (5.2) as follows: $d_1^+\left(V_k^+, V_{k_1}\right) = 0.4162, d_2^+\left(V_k^+, V_{k_2}\right) = 0.3990, d_3^+\left(V_k^+, V_{k_3}\right) = 0.3523$, $d_4^+\left(V_k^+, V_{k_4}\right) = 0.3833$

$$d_1^-\left(V_k^-, V_{k_1}\right) = 0.1718, d_2^-\left(V_k^-, V_{k_2}\right) = 0.1997, d_3^-\left(V_k^-, V_{k_3}\right) = 0.2387, d_4^-\left(V_k^-, V_{k_4}\right) = 0.2092$$

We can get the closeness coefficient $C_i\left(V_{k_i}\right)(i = 1, 2, 3, 4)$ by using (5.3): $C_1\left(V_{k_1}\right) = 0.2922, C_2\left(V_{k_2}\right) = 0.3336, C_3\left(V_{k_3}\right) = 0.4039, C_4\left(V_{k_4}\right) = 0.3531$.

Thus, the ranking of the four alternatives is $V_{k_3} > V_{k_4} > V_{k_2} > V_{k_1}$. So clearly V_{k_3} is preferable amongst them.

6 Application of the Proposed Improved AF in MCDM Problem Using IM Algorithm for Multi-Criteria TraIFIM

The algorithmic methodology for the proposed method for the multi-criteria TraIFIM can be condensed as follows:

1. Obtain (ave, ave)-column aggregation for a given multi-criteria TraIFIM (A_{TraIFIM}) which gives the aggregated trapezoidal score for G_i for every $1 \leq i \leq m$.
2. Compute the improved accuracy values $K_{NT}(G_i, H_0)$ $(i = 1, 2, \ldots, m)$ using Definition 4.20.
3. Rank the alternatives G_i $(i = 1, 2, \ldots, m)$ using Definition 4.25.

6.1 Numerical Example

In this section, a numerical illustration of the algorithm for multi-criteria TraIFIM is given.

Example 6.1. A bank needs to choose one amongst four contenders for their manager post, as indicated by the accompanying three criteria: H_1 is the entrance test; (2). H_2 is the personal interview test; (3). H_3 is the communication skill; the alternatives G_i $(i = 1, 2, 3, 4)$ are assessed using the TraIFN by the decision-making under the above three criteria as listed in DM Table 1.

1. By applying the step 1 of the above algorithm, we obtain (ave, ave)-column aggregation for the given multi-criteria TraIFIM (A_{TraIFIM}) with a fixed index $\text{H}_0 \notin \text{G}$ as follows:

$\sigma_{\max}(\text{A}_{\text{TraIFIM}}\ ,\ \text{H}_0)$

	H_0
G_1	$\langle((0.1567, 0.2100, 0.2467, 0.2733\ ), (0.3100, 0.3767, 0.4233, 0.5000)\rangle$
$= G_2$	$\langle((0.1133, 0.1800, 0.2367, 0.2967), (0.3400, 0.4000, 0.4400,\ 0.4867)\rangle$
G_3	$\langle((0.1967, 0.2567, 0.2800,\ 0.3400), (0.3833, 0.4533, 0.5133,\ 0.5833)\rangle$
G_4	$\langle((0.1567, 0.2033, 0.2767, 0.3367), (0.4167, 0.4767\ 0.5400, 0.6000)\rangle$

2. We obtain $NA_1(G_i, H_0)$, $(i = 1, 2, 3, 4)$ as follows:
   $K_{NT}(G_1, H_0) = 0.3091$, $K_{NT}(G_2, H_0) = 0.2915$, $K_{NT}(G_3, H_0) = 0.3401$, $K_{NT}(G_4, H_0) = 0.3122$.
3. Therefore, we get $G_2 < G_1 < G_4 < G_3$. Hence, G_3 is the most suitable object from the given A_{TraIFIM}.

Table 1 A_{TralFIM}

	H_1	H_2	H_3
G_1	$(0.1, 0.13, 0.15, 0.17), (0.2, 0.25, 0.3, 0.35)_{G1,H1}$	$(0.15, 0.25, 0.27, 0.3), (0.32, 0.42, 0.45, 0.55)_{G1,H2}$	$(0.22, 0.25, 0.32, 0.35), (0.41, 0.46, 0.52, 0.6)_{G1,H3}$
G_2	$(0.01, 0.05, 0.15, 0.22), (0.25, 0.32, 0.35, 0.4)_{G2,H1}$	$(0.11, 0.16, 0.21, 0.25), (0.32, 0.35, 0.42, 0.45)_{G2,H2}$	$(0.22, 0.33, 0.35, 0.42), (0.45, 0.53, 0.55, 0.61)_{G2,H3}$
G_3	$(0.17, 0.22, 0.25, 0.32), (0.35, 0.42, 0.45, 0.55)_{G3,H1}$	$(0.14, 0.23, 0.25, 0.3), (0.34, 0.42, 0.53, 0.6)_{G3,H2}$	$(0.28, 0.32, 0.34, 0.4), (0.46, 0.52, 0.56, 0.6)_{G3,H3}$
G_4	$(0.1, 0.16, 0.22, 0.25), (0.32, 0.43, 0.54, 0.65)_{G4,H1}$	$(0.14, 0.2, 0.25, 0.36), (0.47, 0.48, 0.52, 0.55)_{G4,H2}$	$(0.23, 0.25, 0.36, 0.4), (0.46, 0.52, 0.56, 0.6)_{G4,H3}$

7 Conclusion and Future Scope

In this paper, we have extended the AF for IVIFNs into improved AF for TraIFNs. Trapezoidal intuitionistic fuzzy TOPSIS method based on the proposed AF is applied to rank the alternatives, and the most suitable one(s) is chosen in the DM process. In the end of this paper, two illustrative examples are given. Later on, we will keep working on the utilization of our proposed method to various areas.

References

1. Atanassov, K.T.: Intuitionistic fuzzy sets. Fuzzy Sets Syst. **20**, 87–96 (1986)
2. Atanassov, K.: Generalized index matrices. C.R. Acad. Bulgare. Sci. **40**(11), 15–18 (1987)
3. Atanassov, K.: On index matrices. Part 2: intuitionistic fuzzy case. Proc. Jang-Jeon Math. Soc. **13**(2), 121–126 (2010)
4. Atanassov, K.T., Gargov, G.: Interval-valued intuitionistic fuzzy sets. Fuzzy Sets Syst. **31**(3), 343–349 (1989)
5. Atanassov, K.: On extended intuitionistic fuzzy index matrices. Notes Intuitionistic Fuzzy Sets **19**(4), 27–41 (2013)
6. Atanassov, K., Mavrov, D., Atanassova, V.: A new approach for multi-criteria decision making, based on index matrices and intuitionistic fuzzy sets. In: Modern Approaches in Fuzzy Sets, Intuitionistic Fuzzy Sets, Generalized Nets and Related Topics Foundations, vol. 11, pp. 1–8. Warsaw (2014)
7. Bai, Z.Y.: An interval-valued intuitionistic fuzzy TOPSIS method based on an improved score function. Sci. World J. 1–7 (2013) (Article ID 879089)
8. Lakshmana Gomathi Nayagam, V., Venkateshwari, G., Sivaraman, G.: Ranking of intuitionistic fuzzy numbers. In: Proceedings of the IEEE International Conference on Fuzzy Systems (IEEE FUZZ 2008), pp. 1971–1974 (2008)
9. Lakshmana Gomathi Nayagam, V., Muralikrishnan, S., Sivaraman, G.: Multi criteria decision making method based on interval valued intuitionistic fuzzy sets. Expert Syst. Appl. **38**(3), 1464–1467 (2011)
10. Lakshmana Gomathi Nayagam, V., Dhanasekaran, S.P., Jeevaraj, S.: A complete ranking of complete trapezoidal information. J. Intell. Fuzzy Syst. **30**, 3209–3225 (2016)
11. Lakshmana Gomathi Nayagam, V., Jeevaraj, S., Sivaraman, G.: Ranking of incomplete trapezoidal information. Soft Comput. **27**, 7125–7140 (2017)
12. Liu, B., Xia luo, M.: Multi-criteria decision-making method based on interval-valued intuitionistic fuzzy sets. Quant. Logic Soft Comput. **510**, 477–486 (2016)
13. Nehi, H.M., Maleki, H.R.: Intuitionistic fuzzy numbers and its applications in fuzzy optimization problem. In: Proceeding of the 9th WSEAS International Conference on Systems, pp. 11–16. July 11–13, 2005. CSCC Multi Conference Vouliagmeni, Athens, Greece (2005)
14. Sahin, R.: Fuzzy multicriteria decision making method based on the improved accuracy function for interval-valued intuitionistic fuzzy sets. Soft Comput. 1–7 (2015)
15. Sivaraman, G., Vishnukumar, P., Edwin Antony Raj, M.: MCDM based on new membership and non-membership accuracy functions on trapezoidal-valued intuitionistic fuzzy numbers. Soft Comput. **24**, 4283–4293 (2020)
16. Wang, J.Q., Zhang, Z.: Multi-criteria decision making method with incomplete certain information based on intuitionistic fuzzy number. Control Decis. **24**, 226–230 (in Chinese)
17. Xu, Z., Chen, J.: Approach to group decision making based on interval valued intuitionistic judgement matrices. Syst. Eng. Theor. Pract. **27**(4), 126–133 (2007)
18. Ye, J.: Multicriteria fuzzy decision-making method based on a novel accuracy function under interval-valued intuitionistic fuzzy environment. Expert Syst. Appl. **36**, 6899–6902 (2009)

A New Distance and Similarity Measure on Soft Parameter Sets and Their Applications to MCDM Problem

S. Vijayabalaji, A. Ramesh, and P. Balaji

Abstract A new distance and similarity measures between two soft parameter-based sets are defined, and some properties are discussed on them. Soft similarity symmetric matrix on parameter-based soft set is also defined, and some related properties are studied. Finally, a MCDM problem based on soft parameter sets is also provided.

Keywords Soft parameter distance · Soft parameter similarity · Soft symmetric matrix · Polymer electrolyte fuel cell

1 Introduction

Soft set theory was introduced by Molodtsov [13] in 1999 as a contemporary mathematical strategy for dealing with vagueness and uncertainty. Soft set includes the theory of probabilities, and fuzzy sets [29] differ from traditional tools for dealing with uncertainty and are also devoid of the shortcomings of methods for parameterizing such theories [14]. Soft set theory is particularly useful in many domains of science, engineering, economics and medicine because there are no limits on the approximation definitions. Soft set applications can be found in a wide range of domains, including texture categorization and business applications [9, 15, 22, 23].

Some researchers have developed soft set extensions in fuzzy setting [7, 16], intuitionistic fuzzy setting [4, 8, 11], interval-valued fuzzy setting [28], rough setting

S. Vijayabalaji (✉)
Department of Mathematics, University College of Engineering Panruti (A Constituent College of Anna University Chennai), Panruti, Tamil Nadu 607106, India

A. Ramesh
Department of Mathematics, C. Abdul Hakeem College of Engineering and Technology, Melvisharam, Tamil Nadu 632509, India

P. Balaji
Department of Mathematics, MEASI Academy of Architecture, Chennai, Tamil Nadu 600014, India

© The Author(s), under exclusive license to Springer Nature Singapore Pte Ltd. 2022

S. R. Kannan et al. (eds.), *Fuzzy Mathematical Analysis and Advances in Computational Mathematics*, Studies in Fuzziness and Soft Computing 419,
https://doi.org/10.1007/978-981-19-0471-4_10

[30, 31], linguistic setting [19, 21, 32] and belief function setting [18, 20]. Some scholars have focused on the algebraic of soft set [1, 3, 5].

Multi-criteria decision making (MCDM) is a well-known technique for resolving a variety of organizational decision-making challenges in which a final choice is made based on the opinions of individual members. Overly similar viewpoints enhance the probability of making an unacceptably bad conclusion. Making an acceptable decision is already a time-consuming and costly procedure in practice; however, tweaking a wrong decision would be even more costly. In order to avoid this danger, measuring the similarity measure is a significant issue in enhancing decision assistance for critical choice situations.

In information retrieval, the measure of similarity is a crucial notion. It is commonly used to see if a document answers a question or to compare two documents' similarity. In many scientific domains, distance and similarity steps, such as decision making, pattern recognition and machine learning, are very important [24–26]. In general, a metric of similarity can be derived from a distance measure. Euclidean metric, absolute value metric and the Chebyshev metric are all commonly used metrics. Chakraborty and Chakraborty [2] identified a similarity metric whose value is a fuzzy set and used a clustering algorithm to solve a group decision-making problem, noting that the majority of existing similarity metrics eventually generate a crisp numeric value that cannot adequately depict the fuzziness in real-world situations. In soft set theory, distance and similarity metrics were widely used in numerous disciplines [6, 10, 12, 17, 27].

As a result, in this research, we focus on investigating soft set parameter distance and similarity measures and then applying them to multi-criteria decision making in the soft set setting sense.

The rest of this work is structured in the following manner. Section 2 delves into the fundamentals of soft set and soft set parameters. Section 3 defines the definitions of parameter-based distance and similarity measures on soft sets, as well as other properties. In Sect. 4, we define the soft similarity symmetric matrix with an appropriate illustration on a parameter-based soft set. In Sect. 5, we use the distance and similarity measurements to solve the multi-criteria decision-making problem using the soft similarity symmetric matrix. Example of material quality assessment for metallic bipolar polymer electrolyte fuel cell (PEFC) plates used in electric automobiles is also described. Section 6 highlights some of the findings.

2 Preliminaries

In this paper, let K be a $K = \{k_1, k_2, \ldots, k_n\}$ a finite set of objectives (universe) and $T = \{l_1, l_2, \ldots, l_m\}$ be the set of parameters, and $P(k)$ the power set of K and $|L|$ represents the cardinality of a set L.

Definition 1 A soft set on K is a pair $S = (F, L)$, where

1. L is a subset of T;

Table 1 Soft set $S = (F, L)$

	t_1	t_3	t_5	t_7	t_8
k_1	0	1	1	1	1
k_2	1	1	1	0	1
k_3	1	0	1	1	0
k_4	0	1	0	1	1
k_5	0	0	0	0	0
k_6	1	1	1	0	1

2. $F : L \to P(k), \forall l \in L \subseteq T$, $F(l)$ denotes the subset of k corresponding with parameter l. We also use $F(k, l) = 1(F(k, l) = 0)$ to represent that k is (not) an element of $F(l)$.

Definition 2 A parameter-based soft set on T is a pair $P = (F, K)$, where $F : K \to P(l)$, $F(k)$ denotes the subset of l corresponding with object k.

Example 1 Suppose that let $K = \{k_1, k_2, k_3, k_4, k_5, k_6\}$ be the universe set and let $T = \{t_1, t_2, t_3, t_4, t_5, t_6, t_7, t_8\}$ be the set of parameters. Let $L = \{t_1, t_3, t_5, t_7, t_8\} \subset T$. $S = (F, L)$ denote the soft set, and its tabular form is given below.

$$S = (F, L) = \{(t_1, \{k_2, k_3, k_6\}), (t_3, \{k_1, k_2, k_4, k_6\}), (t_5, \{k_1, k_2, k_3, k_6\}),$$
$$(t_7, \{k_1, k_3, k_4\}), (t_8, \{k_1, k_2, k_4, k_6\})\}$$

The above soft set $S = (F, L)$ can be written in the table form as given in Table 1.

The parameter-based soft set can be written as

$$P = (F, K) = \{(k_1, \{t_3, t_5, t_7, t_8\}), (k_2, \{t_1, t_3, t_5, t_8\}), (k_3, \{t_1, t_5, t_7\}),$$
$$(k_4, \{t_3, t_7, t_8\}), (k_5, \phi), (k_6, \{t_1, t_3, t_5, t_8\})\}$$

Definition 3 Let $S = (F, L)$ be a soft set over K. For all $k \in K$, define the support set of parameters for l as the set $\{l \in L | F(k, l) = 1\}$, denoted by supp$(k)$.

Definition 4 Let $S = (F, L)$ be a soft set over K. The function $\sigma_s : K \to N$ defined by $\sigma_s(k) = |\text{supp}(k)| = \sum_{l \in L} F(k, l)$ is called the choice value of S.

3 Parameter-Based Distance and Similarity Measures on Soft Set

In this section, the concept of parameter-based distance and similarity measure on soft set are defined.

Definition 5 For parameter-based soft set $P = (F, K)$ over L, $\forall k_i, k_j \in K$, the distance between $F(k_i)$ and $F(k_j)$ is defined as

$$D(F(k_i), F(k_j)) = \frac{|F(k_i) - \{F(k_i) \cap F(k_j)\}| + |F(k_j) - \{F(k_i) \cap F(k_j)\}|}{|F(k_i) \cup F(k_j)|} \quad (1)$$

Definition 6 Let $F(k_i)$ and $F(k_j)$ be two parameter soft sets over $P = (F, K)$, then the distance between $F(k_i)$ and $F(k_j)$ is defined as $D(F(k_i), F(k_j))$ and satisfies the following conditions.

1. $0 \leq D(F(k_i), F(k_j)) \leq 1$;
2. $D(F(k_i), F(k_j)) = 0$ iff $F(k_i) = F(k_j)$;
3. $D(F(k_i), F(k_j)) = D(F(k_j), F(k_i))$.

Example 2 Let us consider five alternative $K = \{k_1, k_2, k_3, k_4, k_5\}$ of materials for material selection of a product operated in a high-temperature environment. The parameters (attributes) $L = \{l_1, l_2, l_3, l_4\}$ considered are as follows: l_1 =tensile strength (TS), l_2 = yield strength (YS), l_3 = density (D) and l_4 = corrosion resistance (CR). The parameter-based soft set can be written as

$$P = (F, K) = \{(k_1, \{l_1, l_2, l_4\}), (k_2, \{l_2, l_3, l_4\}), (k_3, \{l_1, l_2, l_3, l_4\}),$$
$$(k_4, \{l_1, l_3, l_4\}), (k_5, \{l_1, l_2, l_3\})\}.$$

Then $F(k_1) = \{l_1, l_2, l_4\}$; $F(k_2) = \{l_2, l_3, l_4\}$; $F(k_3) = \{l_1, l_2, l_3, l_4\}$;
$F(k_4) = \{l_1, l_3, l_4\}$; $F(k_5) = \{l_1, l_2, l_3\}$.
The distance between $F(k_1)$ and $F(k_3)$ is

$$D(F(k_1), F(k_3)) = \frac{|F(k_1) - \{F(k_1) \cap F(k_3)\}| + |F(k_3) - \{F(k_1) \cap F(k_3)\}|}{|F(k_1) \cup F(k_3)|}$$
$$= \frac{|\{l_1, l_2, l_4\} - \{\{l_1, l_2, l_4\} \cap \{l_1, l_2, l_3, l_4\}\}| + |\{l_1, l_2, l_3, l_4\} - \{\{l_1, l_2, l_4\} \cap \{l_1, l_2, l_3, l_4\}\}|}{\{l_1, l_2, l_4\} \cup \{l_1, l_2, l_3, l_4\}}$$
$$= \frac{|\{l_1, l_2, l_4\} - \{l_1, l_2, l_4\}| + |\{l_1, l_2, l_3, l_4\} - \{l_1, l_2, l_4\}|}{|\{l_1, l_2, l_3, l_4\}|}$$
$$= \frac{0 + 1}{4} = \frac{1}{4} = 0.25.$$

Similarly, we can find the other distances.

Definition 7 Let $F(k_i)$ and $F(k_j)$ be two parameter soft sets over $P = (F, K)$, then the similarity between $F(k_i)$ and $F(k_j)$ is defined as $S_{\text{im}}(F(k_i), F(k_j))$ and satisfies the following conditions.

1. $0 \leq S_{\text{im}}(F(k_i), F(k_j)) \leq 1$;
2. $S_{\text{im}}(F(k_i), F(k_j)) = 0$ iff $F(k_i) = F(k_j)$;
3. $S_{\text{im}}(F(k_i), F(k_j)) = S_{\text{im}}(F(k_j), F(k_i))$.

Property 1 *If $D(F(k_i), F(k_j))$ is the distance measure between $F(k_i)$ and $F(k_j)$ over $P = (F, K)$, then $S_{im}(F(k_i), F(k_j)) = 1 - D(F(k_i), F(k_j))$ is the similarity between $F(k_i)$ and $F(k_j)$ over $P = (F, K)$.*

Property 2 *If $S_{im}(F(k_i), F(k_j))$ is the similarity between $F(k_i)$ and $F(k_j)$ over $P = (F, K)$, then $D(F(k_i), F(k_j)) = 1 - S_{im}(F(k_i), F(k_j))$ is the distance between $F(k_i)$ and $F(k_j)$ over $P = (F, K)$.*

Property 3 *Let $F(k_1)$, $F(k_2)$ and $F(k_3)$ be three parameter soft sets over $P = (F, K)$, if $F(k_1) \subseteq F(k_2) \subseteq F(k_3)$, then*

1. $D(F(k_1), F(k_2)) \leq D(F(k_1), F(k_3))$;
2. $D(F(k_2), F(k_3)) \leq D(F(k_1), F(k_3))$.

Theorem 1 *Let $F(k_1)$, $F(k_2)$ and $F(k_3)$ be three parameter soft sets over $P = (F, K)$, if $F(k_1) \subseteq F(k_2) \subseteq F(k_3)$, then*

$$(F(k_1), F(k_3)) \leq D(F(k_1), F(k_2)) + D(F(k_2), F(k_3)).$$

Proof Since $F(k_1) \subseteq F(k_2)$ and $F(k_2) \subseteq F(k_3)$, by the definition of distance measure, $D(F(k_1), F(k_2)) \leq 1$, $D(F(k_2), F(k_3)) \leq 1$ and $D(F(k_1), F(k_3)) \leq 1$. Therefore, $D(F(k_1), F(k_3)) \leq D(F(k_1), F(k_2)) + D(F(k_2), F(k_3))$.

4 Soft Similarity Symmetric Matrix on Parameter-Based Soft Set

Definition 8 Let $P = (F, K)$ be a parameter-based soft set. The soft similarity symmetric matrix on parameter-based soft set is defined as

$$\mathrm{SM}_{\mathrm{ps}} = [S_{\mathrm{im}}(F(k_i), F(k_j))]_{(\mathrm{nn})} \text{ and } \mathrm{SM}_{\mathrm{ps}} = 1, \text{ iff} i = j.$$

Example 3 Let $K = \{k_1, k_2, k_3, k_4, k_5, k_6\}$ be the universe set and $L = \{l_1, l_2, l_3, l_4, l_5, l_6, l_7, l_8\}$ be the set of parameters. The parameter-based soft set can be written as

$$F(k_1) = \{l_2, l_3, l_4, l_7, l_8\};\ F(k_2) = \{l_3, l_4, l_5, l_6, l_7, l_8\};\ F(k_3) = \{l_4, l_5, l_6\};$$
$$F(k_4) = \{l_2, l_4, l_7\};\ F(k_5) = \{l_2, l_4, l_7\};\ F(k_6) = \{l_1, l_3, l_4, l_5, l_7\}.$$

The distance between $F(k_1)$ and $F(k_2)$ is

$$D(F(k_1), F(k_2)) = \frac{|\{l_2\}| + |\{l_5, l_6\}|}{|\{l_2, l_3, l_4, l_5, l_6, l_7, l_8\}|} = \frac{3}{7}$$

$$\text{and } S_{\mathrm{im}}(F(k_1), F(k_2)) = 1 - D(F(k_1), F(k_2)) = 1 - \frac{3}{7} = \frac{4}{7}.$$

Similarly, we can find all the similarity values.

The soft similarity symmetric matrix on parameter-based soft set is

$$\mathrm{SM}_{\mathrm{ps}} = \begin{bmatrix} 1 & \frac{4}{7} & \frac{1}{7} & \frac{3}{5} & \frac{3}{5} & \frac{3}{7} \\ \frac{4}{7} & 1 & \frac{1}{2} & \frac{2}{7} & \frac{2}{7} & \frac{4}{7} \\ \frac{1}{7} & \frac{1}{2} & 1 & \frac{1}{5} & \frac{1}{5} & \frac{1}{3} \\ \frac{3}{5} & \frac{2}{7} & \frac{1}{5} & 1 & 1 & \frac{1}{3} \\ \frac{3}{5} & \frac{2}{7} & \frac{1}{5} & 1 & 1 & \frac{1}{3} \\ \frac{3}{7} & \frac{4}{7} & \frac{1}{3} & \frac{1}{3} & \frac{1}{3} & 1 \end{bmatrix}$$

5 Multi-criteria Decision-Making Problem on Soft Similarity Symmetric Matrix

Multi-criteria decision making is becoming increasingly significant in practical decision-making problems, since it is impossible for a single decision maker to analyze all the pertinent parts of the study. In group decision making, the decision makers communicate their thoughts regarding possibilities to settle at an unanimous agreement. In real group decision-making problem, each decision maker expresses his/her judgment of a criterion or an alternative. Let $M = \{m_1, m_2, \ldots, m_i\}$ be a universe set and $Q = \{q_1, q_2, \ldots, q_j\}$ be the set of parameters. Suppose a set of decision makers $D = \{d_1, d_2, \ldots, d_t\}$ evaluating a criterion or an alternative with each decision maker d_t providing his/her evaluation $m_i \in M$ of such a criterion or alternative based on the parameter $q_j \in Q$. In this case, the parameter q_j of alternative m_i is represented by parameters-based soft set $P = (F, M)$. In the next section, we use distance and similarity measurements to analyze a multi-criteria decision-making problem using a soft similarity symmetric matrix and to determine the ranking of each alternative.

5.1 Multi-criteria Decision-Making Algorithm

Step 1: Construct the parameter-based soft set $P = (F, M)$.
Step 2: Find the distance and similarity measures on the alternatives.
Step 3: Construct the soft similarity symmetric matrix.
Step 4: Find $Z_i = \frac{|F(m_i)|}{|Q|}$, $i = 1, 2, 3, \ldots, n$, where $|.|$ denotes the cardinality of a set.
Step 5: Find $\Delta_i = \dfrac{\sqrt[n]{\prod_{l=1, l\neq i}^{n} \frac{(S_{\mathrm{im}}(F(m_i), F(m_l)))}{Z_i + Z_l}}}{\sum_{i=1}^{n} \left(\sqrt[n]{\prod_{l=1, l\neq i}^{n} \frac{(S_{\mathrm{im}}(F(m_i), F(m_l)))}{Z_i + Z_l}} \right)}$.
Step 6: Rank the alternatives.
Step 7: Conclusion.

5.2 Illustrative Example

Consider the material selection of metallic bipolar plates for polymer electrolyte fuel cell (PEFC) used in electric vehicles. The following characteristics (parameters) are required for bipolar plates: (i) high electrical conductivity and thermal compatibility with other components, (ii) high corrosion resistance, (iii) high mechanical strength, (iv) low gas permeation, (v) low mass and volume for fuel cell stack, (vi) easy manufacture in low cost/high volume by automation and (vii) low material cost. We choose six alternative materials in this problem such as $M = \{m_1,\ m_2,\ m_3,\ m_4,\ m_5,\ m_6\}$, and parameters given above can be taken as $Q = \{q_1,\ q_2,\ q_3,\ q_4,\ q_5,\ q_6,\ q_7\}$.

Step 1: The parameter-based soft set can be written as $F\ (m_1) = \{q_1,\ q_2,\ q_3,\ q_4,\ q_7\}$; $F\ (m_2) = \{q_1,\ q_3,\ q_4,\ q_5,\ q_6,\ q_7\}$; $F\ (m_3) = \{q_4,\ q_5,\ q_6\}$; $F\ (m_4) = \{q_2,\ q_4,\ q_7\}$; $F\ (m_5) = \{q_2,\ q_4,\ q_7\}$; $F\ (m_6) = \{q_1,\ q_3,\ q_4,\ q_5,\ q_7\}$.

Step 2: The distance between $F\ (m_1)$ and $F\ (m_2)$ is

$$D\left(F\ (m_1),\ F\ (m_2)\right) = \frac{|\{q_2\}| + |\{q_5,\ q_6\}|}{|\{q_1,\ q_2,\ q_3,\ q_4,\ q_5,\ q_6,\ q_7\}|} = \frac{3}{7}$$

$$\text{and } S_{\text{im}}\left(F\ (m_1),\ F\ (m_2)\right) = 1 - D\left(F\ (m_1),\ F\ (m_2)\right) = 1 - \frac{3}{7} = \frac{4}{7}.$$

Step 3: The soft similarity symmetric matrix on parameter-based soft set is

$$\text{SM}_{\text{ps}} = \begin{bmatrix} 1 & \frac{4}{7} & \frac{1}{7} & \frac{3}{5} & \frac{3}{5} & \frac{3}{7} \\ \frac{4}{7} & 1 & \frac{1}{2} & \frac{2}{7} & \frac{2}{7} & \frac{4}{7} \\ \frac{1}{7} & \frac{1}{2} & 1 & \frac{1}{5} & \frac{1}{5} & \frac{1}{3} \\ \frac{3}{5} & \frac{2}{7} & \frac{1}{5} & 1 & 1 & \frac{1}{3} \\ \frac{3}{5} & \frac{2}{7} & \frac{1}{5} & 1 & 1 & \frac{1}{3} \\ \frac{3}{7} & \frac{4}{7} & \frac{1}{3} & \frac{1}{3} & \frac{1}{3} & 1 \end{bmatrix}$$

Step 4: To find Z_i

$$Z_1 = \frac{|F\ (m_1)|}{|Q|} = \frac{5}{7};\ Z_2 = \frac{|F\ (m_2)|}{|Q|} = \frac{6}{7};\ Z_3 = \frac{|F\ (m_3)|}{|Q|} = \frac{3}{7};$$
$$Z_4 = \frac{|F\ (m_4)|}{|Q|} = \frac{3}{7};\ Z_5 = \frac{|F\ (m_5)|}{|Q|} = \frac{3}{7};\ Z_6 = \frac{|F\ (m_6)|}{|Q|} = \frac{5}{7}.$$

Step 5: To find $\Delta_i = \dfrac{\sqrt[n]{\prod_{\substack{l=1 \\ l\neq i}}^{n} \frac{S_{\text{im}}(F(m_i),\ F(m_l))}{Z_i+Z_l}}}{\sum_{i=1}^{n}\left(\sqrt[n]{\prod_{\substack{l=1 \\ l\neq i}}^{n} \frac{S_{\text{im}}(F(m_i),\ F(m_l))}{Z_i+Z_l}}\right)} = \frac{\beta_i}{\sum_{i=1}^{n}\beta_i},\ i = 1, 2, 3, \ldots,\ n.$

$$\beta_1 = \sqrt[n]{\prod_{\substack{l=1 \\ l\neq i}}^{n} \frac{S_{\text{im}}\left(F\left(m_1\right),\ F\left(m_l\right)\right)}{Z_1 + Z_l}}$$

$$= \sqrt[6]{\frac{S_{\text{im}}\left(F\left(m_1\right),\ F\left(m_2\right)\right)}{Z_1 + Z_2} \times \frac{S_{\text{im}}\left(F\left(m_1\right),\ F\left(m_2\right)\right)}{Z_1 + Z_3} \times \cdots \times \frac{S_{\text{im}}\left(F\left(m_1\right),\ F\left(m_6\right)\right)}{Z_1 + Z_6}}$$

$$\beta_1 = \sqrt[6]{\frac{4}{11} \times \frac{1}{8} \times \frac{21}{40} \times \frac{21}{40} \times \frac{14}{30}} = 0.4245.$$

Similarly, we can find $\beta_2 = 0.3933$; $\beta_3 = 0.3029$; $\beta_4 = 0.4903$; $\beta_5 = 0.4903$; $\beta_6 = 0.4903$.

$$\Delta_1 = \frac{\sqrt[n]{\prod_{\substack{l=1 \\ l\neq i}}^{n} \frac{S_{\text{im}}(F(m_1),\ F(m_l))}{Z_1+Z_l}}}{\sum_{i=1}^{n}\left(\sqrt[n]{\prod_{\substack{l=1 \\ l\neq i}}^{n} \frac{S_{\text{im}}(F(m_1),\ F(m_l))}{Z_i+Z_l}}\right)} = \frac{\beta_1}{\beta_1+\beta_2+\beta_3+\beta_4+\beta_5+\beta_6}$$

$$= \frac{0.4245}{0.4245 + 0.3933 + 0.3029 + 0.4903 + 0.4903 + 0.4903} = 0.1638$$

Similarly, we can find $\Delta_2 = 0.1518$; $\Delta_3 = 0.1169$; $\Delta_4 = 0.1892$; $\Delta_5 = 0.1896$; $\Delta_6 = 0.1891$.

Step 6: Rank of the alternatives is $\Delta_5 \succ \Delta_4 \succ \Delta_6 \succ \Delta_1 \succ \Delta_2 \succ \Delta_3$.

Step 7: The best material is m_5.

6 Conclusion

In this paper, we establish a new distance measure based on two soft sets with two parameters and investigate some of their features. We proposed the parameter-based similarity measure of soft sets and the soft similarity symmetric matrix using parameter-based distance measure. We have used soft similarity symmetric matrix to handle multi-criteria scenario and tackled a material selection problem using this.

References

1. Aktas, H., Cagman, N.: Soft sets and soft groups. Inf. Sci. **177**, 2726–2735 (2007)
2. Chakraborty, C., Chakraborty, D.: A fuzzy clustering methodology for linguistic opinions in group decision making. Appl. Soft Comput. **7**(3), 858–869 (2010)
3. Chen, D., Tsang, E.C.C., Yeung, D.S., Wang, X.: The parameterization reduction of soft sets and its applications. Comput. Math. Appl. **49**, 757–763 (2005)
4. Das, S., Kar, S.: Group decision making in medical system: an intuitionistic fuzzy soft set approach. Appl. Soft Comput. **24**, 196–211 (2014)
5. Irfan Ali, M., Feng, F., Liu, X., Won Keun, M., Shabir, M.: On some new operations in soft set theory. Comput. Math. Appl. **57**, 1547–1553 (2009)
6. Kharal, A.: Distance and similarity measures for soft sets. New Math. Nat. Comput. **6**(3), 321–334 (2010)
7. Maji, P.K., Biswas, R., Roy, A.R.: Fuzzy soft sets. J. Fuzzy Math. **9**(3), 589–602 (2001)
8. Maji, P.K., Biswas, R., Roy, A.R.: Intuitionistic fuzzy soft set. J. Fuzzy Math. **9**(3), 677–692 (2001)
9. Maji, P.K., Biswas, R., Roy, A.R.: An application of soft sets in a decision making problem. Comput. Math. Appl. **44**, 1077–1083 (2002)
10. Majumdar, P., Samanta, S.K.: Similarity measure of soft sets. New Math. Nat. Comput. **4**(1), 1–12 (2008)
11. Mao, J., Yao, D., Wang, C.: Group decision making methods based on intuitionistic fuzzy soft matrices. Appl. Math. Model. **37**, 6425–6436 (2013)
12. Min, W.K.: Similarity in soft set theory. Appl. Math. Lett. **25**, 310–314 (2012)
13. Molodtsov, D.: Soft set theory-first results. Comput. Math. Appl. **37**, 19–31 (1999)
14. Molodtsov, D.: The Theory of Soft Sets. URSS Publishers, Moscow (2004)
15. Mushrif, M.M., Sengupta, S., Ray, A.K.: Texture classification using a novel soft set theory based classification algorithm. Lect. Notes Comput. Sci. **3851**, 246–254 (2006)
16. Roy, A.R., Maji, P.K.: A fuzzy soft set theoretic approach to decision making problems. J. Comput. Appl. Math. **203**(2), 412–418 (2007)
17. Sulaiman, N.H., Mohamad, D.: A Jaccard-based similarity measure for soft sets. In: 2012 IEEE Symposium on Humanities, Science and Engineering Research, pp. 659–663
18. Tang, H.X.: A novel fuzzy soft set approach in decision making based on grey relational analysis and Dempster-Shafer theory of evidence. Appl. Soft Comput. **31**, 317–325 (2015)
19. Tao, Z., Chen, H., Song, X., Zhou, L., Liu, J.: Uncertain linguistic fuzzy soft sets and their applications in group decision making. Appl. Soft Comput. **34**, 587–605 (2015)
20. Vijayabalaji, S., Ramesh, A.: Belief interval-valued soft set. Expert Syst. Appl. **119**, 262–271 (2019)
21. Vijayabalaji, S., Ramesh, A.: Uncertain multiplicative linguistic soft sets and their application to group decision making. J. Intell. Fuzzy Syst. **35**, 3883–3893 (2018)
22. Xiao, Z., Gong, K., Zou, Y.: A combined forecasting approach based on fuzzy soft sets. J. Comput. Appl. Math. **228**, 326–333 (2009)

23. Xiao, Z., Li, Y., Zhong, B., Yang, X.: Research on synthetically evaluating method for business competitive capacity based on soft set. Stat. Res. 52–54 (2003)
24. Xu, Z.S., Chen, J.: Ordered weighted distance measure. J. Syst. Sci. Syst. Eng. **17**, 4320–445 (2008)
25. Xu, Z.S., Chen, J.: An overview of distance and similarity measures of intuitionistic fuzzy sets. Int. J. Uncertainty Fuzz. Knowl. Based Syst. **16**, 529–555 (2008)
26. Xu, Z.S., Xia, M.M.: Distance and similarity measures for hesitant fuzzy sets. Inform. Sci. **181**, 2128–2138 (2011)
27. Yang, W.: New similarity measures for soft sets and their application. Fuzzy Inf. Eng. **1**, 19–25 (2013)
28. Yang, X., Lin, T.Y., Yang, J., Li, Y., Yu, D.: Combination of interval-valued fuzzy set and soft set. Comput. Math. Appl. **58**, 521–527 (2009)
29. Zadeh, L.A.: Fuzzy sets. Inf. Control **8**, 338–353 (1965)
30. Zhan, J.M., Liu, Q., Herawan, T.: A novel soft rough set: soft rough hemirings and corresponding multi-criteria group decision making. Appl. Soft Comput. **54**, 393–402 (2017)
31. Zhan, J.M., Ali, M.I., Mehmood, N.: On a novel uncertain soft set model: Z-soft fuzzy rough set model and corresponding decision making methods. Appl. Soft Comput. **56**, 446–457 (2017)
32. Zhang, Z., Zhang, S.: A novel approach to multi attribute group decision making based on trapezoidal interval type-2 fuzzy soft sets. Appl. Math. Model. **37**, 4948–4971 (2013)

Automated Accurate Sleep Stage Classification System Using Machine Learning Techniques with EEG Signals

Santosh Kumar Satapathy and D. Loganathan

Abstract Sleep is a fundamental requirement of human life. It is one of the vital roles in human life to maintain the proper mental health, physical health, and quality of life. In this proposed research work, we conduct an automated sleep stage classification to properly investigate irregularities during sleep based on a single channel of electroencephalography signal (sleep EEG) using machine learning approaches. The significant advantage of this proposed research work over the standard polysomnography method is (1) it measures the sleep irregularities during sleep by considering three different medical condition subjects of different gender with different age groups. (2) One more important objective of this proposed sleep study is that here we obtain different session recordings to investigate sleep abnormality patterns, which can help to find better diagnosis toward the treatment of sleep-related disorder. (3) In the present work, we have obtained two different time-framework epochs from individual subjects to check which window size is more effective toward identification on sleep irregularities. The present research work based on two-state sleep stage classification problems based on a single channel of EEG signal was performed in a different step-wise manner such as the acquisition of data from participated subjects, preprocessing, feature extraction, feature selection, and classification. We obtained the polysomnographic data from the ISRUC-sleep data repository to measure the proposed framework's performances, where the sleep stages are visually labeled. The obtained results demonstrated that the proposed methodologies achieve high classification accuracy, which supports sleep experts for accurately measuring the irregularities that occurred during sleep and helps the clinicians evaluate the presence and criticality of sleep-related disorders.

Keywords Electroencephalography · Sleep staging · Machine learning

S. K. Satapathy (✉) · D. Loganathan
Pondicherry Engineering College, Puducherry, India
e-mail: santosh.satapathy@pec.edu

© The Author(s), under exclusive license to Springer Nature Singapore Pte Ltd. 2022

S. R. Kannan et al. (eds.), *Fuzzy Mathematical Analysis and Advances in Computational Mathematics*, Studies in Fuzziness and Soft Computing 419,
https://doi.org/10.1007/978-981-19-0471-4_11

1 Introduction

Each human needs to have a night of proper sleep during the night, and it is an essential requirement for the human being, and good sleep quality plays a direct role in our day-to-day life. Sometimes, its impact is reflected in our physiological activities, such as the quality of learning ability, physical activity, mental ability, and performance of the overall activities [1]. This problem is seen across the world with all age groups of people, and this is a global challenge in the health care sector because it has been found from the different research that poor quality of sleep is the significant responsibility of creating critical diseases such as bruxism [2], insomnia [3], narcolepsy [4], obstructive sleep apnea [5], and rapid eye movement behavioral disorder [6]. Currently, there are two essential sleep standards followed during sleep staging analysis. According to both standards, the whole sleep stages are divided into three basic categories: (1) wakefulness (W), (2) non-rapid eye movement (NREM), and (3) rapid eye movement (REM). First sleep handbook edited by the Rechtschaffen and Kales (R&K) in the year 1968 [7] and another recognized sleep recommendation proposed by the American Academy of Sleep Medicine (AASM) in the year 2008 [8]. The sleep cycle is generally repeated at regular intervals between NREM and REM stages, and each duration of the sleep cycle is around 90–110 min [9, 10].

EEG recordings, its hectic situation for sleep experts to monitoring within the 30 s framework and fix the labeling of sleep stages. It is not very easy to part for sleep experts to monitor the recorded EEG signals manually. It raises so many errors because during lengthy 7–8 h. Nowadays, automated sleep stage classification is obtained to analyze the sleep-related disorder and real-time diagnosis to overcome the manual approach. The most crucial step is designing sleep stage classification [11–13]. This approach consumed more time and required more human resources for hours of sleep recordings.

2 Related Work

In most literature, the steps mentioned above were implemented to discriminate the EEG signals between two-six sleep state classifications. Obayya and Abou-Chadi [14] compute sleep stage scoring based on a single input channel to identify sleep disorders and selected subjects for this experiment work limited between 35 and 50. Here, authors have obtained wavelet concept techniques for feature extraction and classified the selected features using the fuzzy algorithm. The classification model provided 85% accuracy. Güneş et al. [15] used K-means clustering and feature weighting techniques to design an ASSC system. Welch spectral transform was considered for feature extraction, and those selected features were forwarded to the decision tree (DT) and obtained with an overall accuracy of 83%. Aboalayon et al. [16] used EEG signal and obtained Butterworth bandpass filters and used SVM classifiers and reported 90% classification accuracy. Hassan and Subasi [17] proposed a

scheme using bootstrap aggregating for classification. He considered patient details from two resources, sleep-EDF and DREAMS, and their accuracy was 92.43% for the two-state sleep stages classification. Diykh et al. [18] introduced the concept of structural graph similarity. The experimental work was completed based on EEG signals and selected as an SVM classifier for classifying sleep stages. The obtained classification accuracy was achieved as 95.93%. Gunnarsdottir et al. have designed an automated sleep stage scoring system with overnight PSG data. The authors extracted both time and frequency domain properties from PSG signals and considered healthy subjects with no prior sleep diseases. The extracted properties were classified through DT classifiers. The overall accuracy for test set data was reported as 80.70% [19]. Sriraam et al. used a multichannel EEG signal from ten healthy subjects. In this study, the author has proposed the automated sleep stage scoring between wake and stage 1 of sleep. This research work extracts spectral entropy features from input channels to distinguish the irregularities among the sleep states. The extracted features were processed through a multilayer perceptron feedforward neural network, and the overall accuracy with 20 hidden units was reported as 92.9%. Subsequently, for 40, 60, 80, and 100 hidden units in MLP, it was reported as 94.6, 97.2, 98.8, and 99.2, respectively [20]. Memar and Faradji considered 25 suspected sleep subjects and 20 healthy subjects for experimental purposes. Here, a total of 13 features are extracted from each eight (alpha, theta, sigma, beta1, beta2, gamma1, and gamma2) sub-band epochs. The extracted features were validated through the Kruskal–Wallis test and applied random forest classifier, and achieved an overall accuracy of 95.31% [21]. Da Silveira et al. used discrete wavelet transform (DWT) for signal segmentation. Skewness, kurtosis, and variance features extracted from respective input channels. The extracted features were applied to a random forest classifier, and overall accuracy was reported as 90% [22]. Pernkopf and O'Leary [23] used polysomnography data features to identify sleep abnormalities from three different medical conditions of subjects and used an SVM classifier for two-state classifications between Wake versus NREM stage and another one in between Wake versus REM stage. The proposed study achieved an overall classification accuracy between Wake-NREM and Wake-REM stage as 85.6% and 97.5%, respectively. Braun et al. introduced the hybrid model for identifying the irregularities that occurred in different stages of sleep during the night, and extracted features were forwarded into random forest classifiers. It has been reported that overall classification accuracy has reached 85.95% [24].

3 Experimental Data

All related recorded data were collected from a comprehensive sleep repository named as ISRUC-Sleep [25]. As per our proposed research objective, the first subject used for experimental work from subgroup-I of ISRUC-sleep repository. In this section, total of 100 subjects recording details were collected. Out of those 100 subjects, the data from male subjects (55) and female subjects (45) between the

Table 1 Detailed information of each subject sleep dataset records used in this study

Database used-ISRUC-sleep						
Subject number/subgroup (I/II/III)	*W*	*N*1	*N*2	*N*3	*R*	Total epochs
Subject-16 subgroup-I/one session	128	125	280	120	97	750
Subject-23 subgroup-I/one session	212	99	270	65	104	750
Subject-3 subgroup-II/one session	68	126	271	175	110	750
Subject-3 subgroup-II/two session	76	127	236	168	143	750
Subject-4 subgroup-II/one session	72	163	329	76	110	750
Subject-4 subgroup-II/two session	111	257	209	79	94	750
Subject-2 subgroup-III/one session	89	120	274	149	118	750
Subject-5 subgroup-III/one session	67	65	287	251	80	750

ages of 20–85 (mean age ± standard deviation, 51 ± 16 years). The second category of a subject taken for our proposed experimental work from subgroup-II of the ISRUC-sleep database. These sections contained recordings of 8 subjects with suspicious sleep apnea symptoms. Among eight subjects, 6 of them as male category and 2 of them as a female category. Here per subject, two session recordings were collected with different dates. The subjects for this section were 26–79 (mean age ± standard deviation, 46.87 ± 18.7 years). The third set of recordings was obtained for proposed research work from subgroup-III of ISRUC-sleep data resource. This section contained ten subjects, nine from the male sex and one from the female sex. All subjects are in healthy condition. Only one session of recordings was extracted from individual subjects. The ages of these subjects for this section in between 30 and 58 (mean age ± standard deviation, 40 ± 10 years).

Table 1 shows the detailed information of sleep records of enrolled subjects in this experimental study. The sleep behavior of the subjects obtained in this study for window length 30 s and 15 s is presented in Figs. 1 and 2, respectively.

4 Methodology

Figure 3 describes the current research study on identifying sleep disorders. In this work, we have obtained subjects with different medical conditions. Here, we also considered different session recordings of subjects during computation of sleep stage scoring. All the steps mentioned in the block diagram are followed during the polysomnography test, and each step description is mentioned.

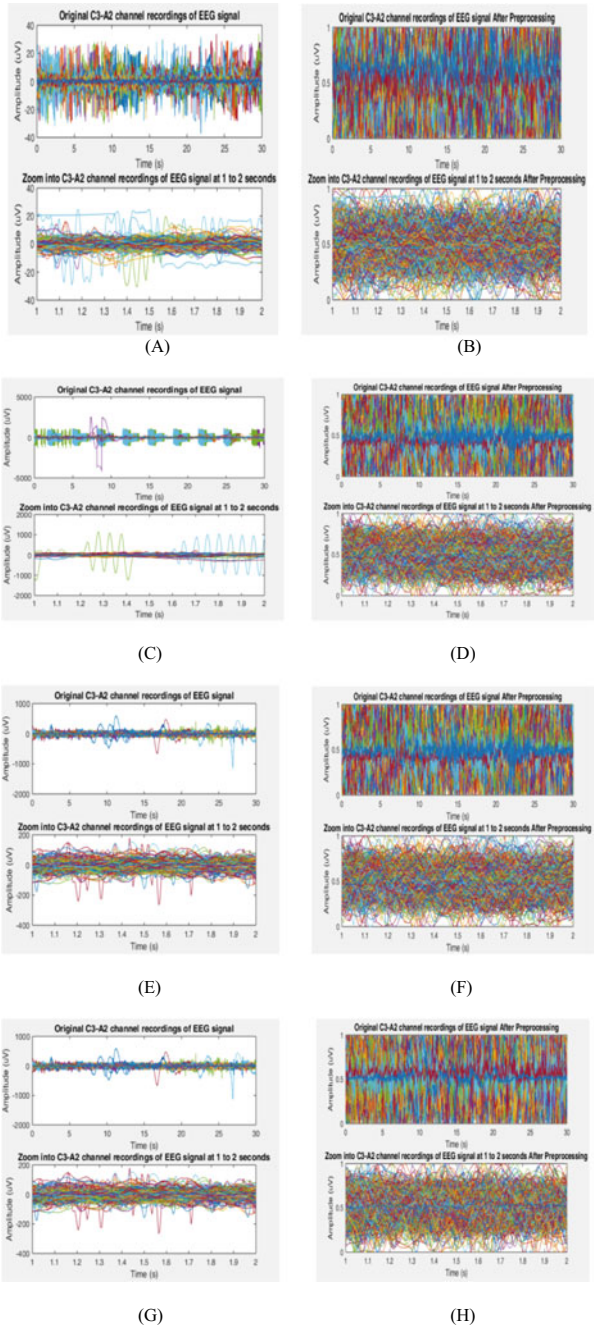
Original C3-A2 channel recordings of EEG signal
Zoom into C3-A2 channel recordings of EEG signal at 1 to 2 seconds
Original C3-A2 channel recordings of EEG signal After Preprocessing
Zoom into C3-A2 channel recordings of EEG signal at 1 to 2 seconds After Preprocessing
Amplitude (uV)
Time (s)
(A)
(B)
(C)
(D)
(E)
(F)
(G)
(H)

Fig. 1 30 s original and filtered signal information of C3-A2 channel of EEG. **A**, **B** for subject-16, **C**, **D** for subject-23, **E**, **F** for subject-03 (session-1 recording), **G**, **H** for subject-03 (session-2 recording), **I**, **J** for subject-04 (session-1), **K**, **L** for subject-04 (session-2), **M**, **N** for subject-02, **O**, **P** for subject-05

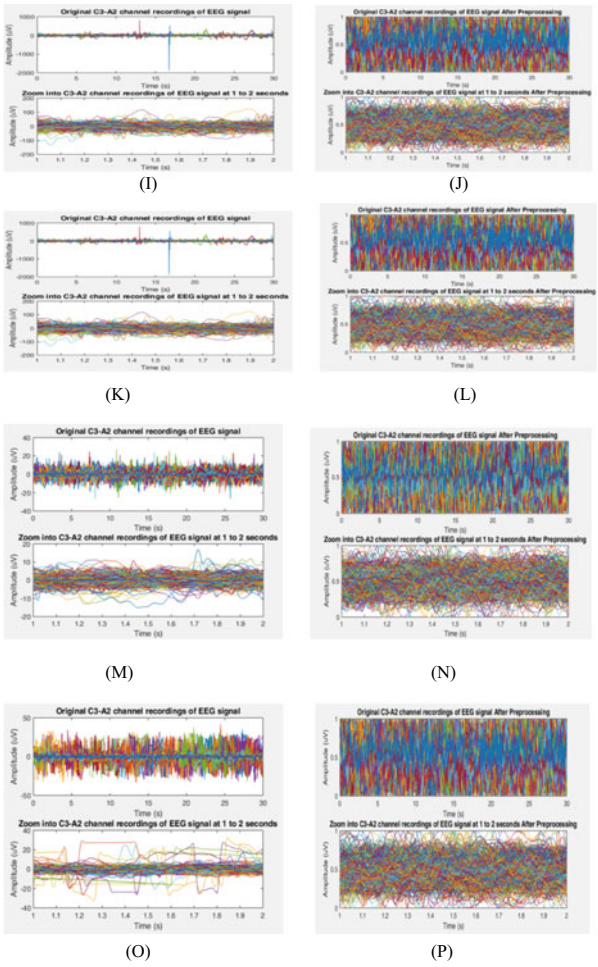
Original C3-A2 channel recordings of EEG signal
Zoom into C3-A2 channel recordings of EEG signal at 1 to 2 seconds
Original C3-A2 channel recordings of EEG signal After Preprocessing
Zoom into C3-A2 channel recordings of EEG signal at 1 to 2 seconds After Preprocessing
Amplitude (uV)
Time (s)
(I)
(J)
(K)
(L)
(M)
(N)
(O)
(P)

Fig. 1 (continued)

4.1 Feature Extraction

As we know, the sleep staging with mapping of single-channel EEG signals is treated as a typical classification task with extracted feature vectors. The selection of inputs for the classifier is the most valuable for identifying sleep pattern abnormality. Even if obtained highly effective classification model performed inferior performance, if inputs are not appropriately selected. It can be found that the different classifiers performed different results for the same set of features; it indicates matching both may found results. On the other hand, sometimes, we have given some features that favor the classification process. The extracted features are briefly described in Table 2.

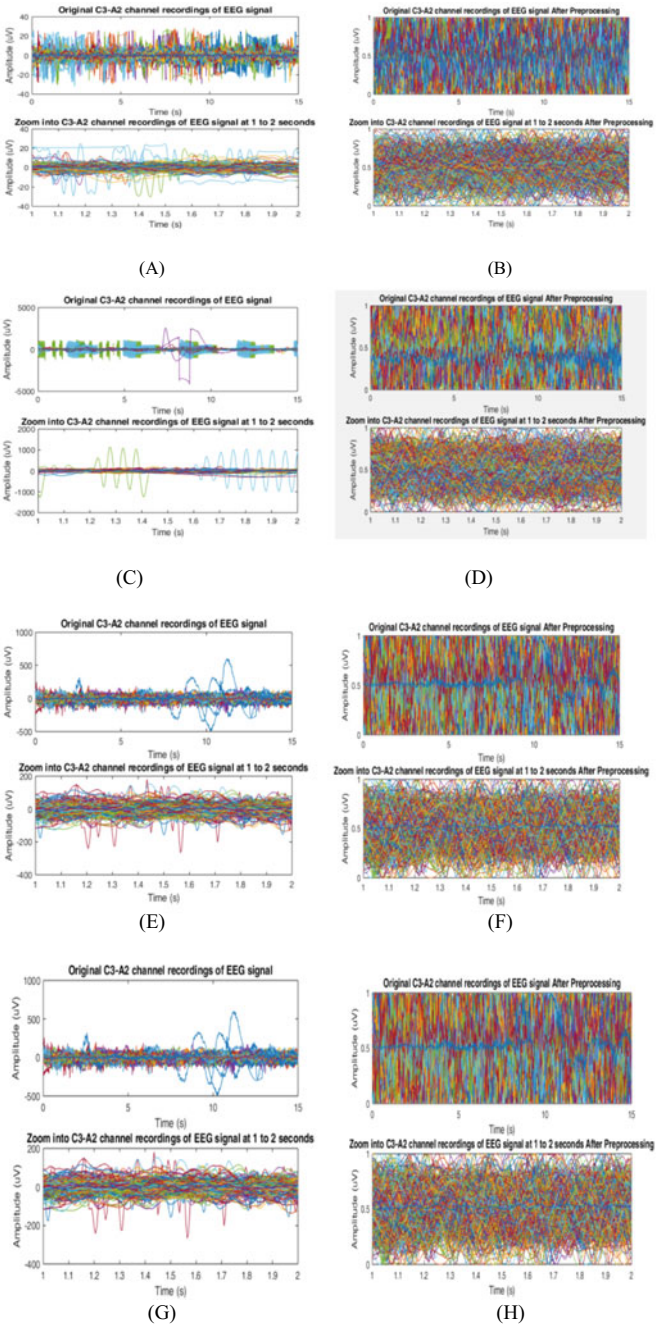
Original C3-A2 channel recordings of EEG signal
Zoom into C3-A2 channel recordings of EEG signal at 1 to 2 seconds
Original C3-A2 channel recordings of EEG signal After Preprocessing
Zoom into C3-A2 channel recordings of EEG signal at 1 to 2 seconds After Preprocessing
Amplitude (uV)
Time (s)
(A)
(B)
(C)
(D)
(E)
(F)
(G)
(H)

Fig. 2 15 s epoch of C3-A2 channel original and filtered signal information. Subject-16 (**A**, **B**), subject-23 (**C**, **D**), subject-03 (session-1 recording) (**E**, **F**), subject-03 (session-2 recording) (**G**, **H**), subject-04 (session-1) (**I**, **J**), subject-04 (session-2) (**K**, **L**), subject-02 (**M**, **N**), subject-05 (**O**, **P**)

Fig. 2 (continued)

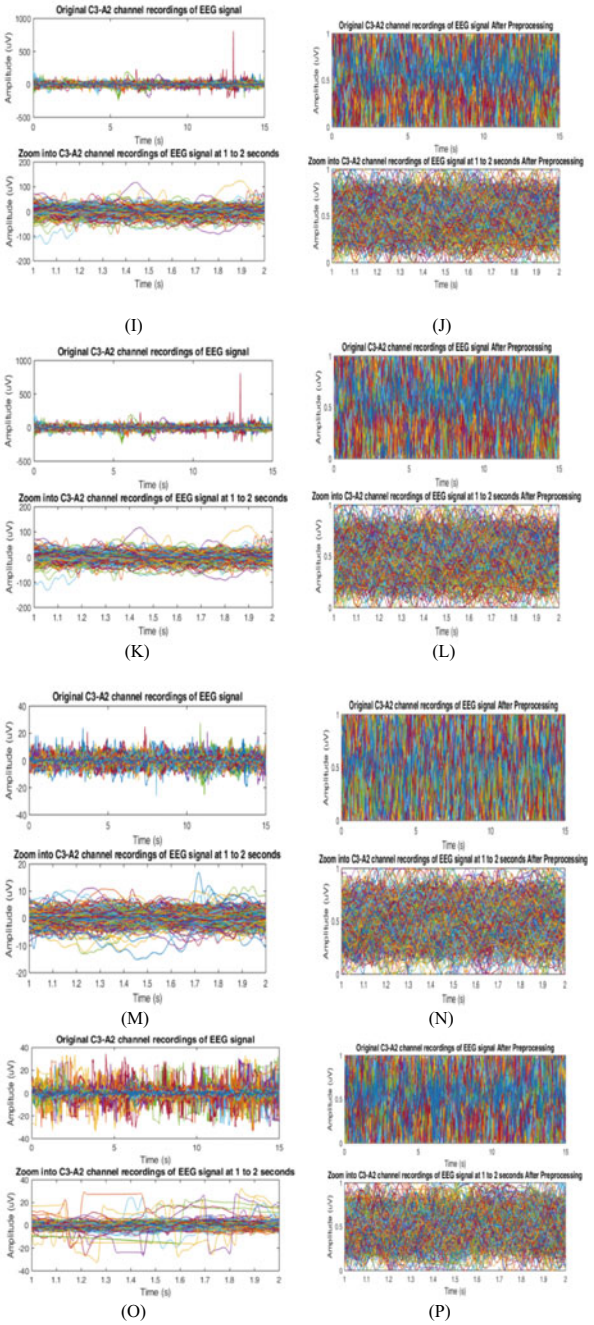
Original C3-A2 channel recordings of EEG signal
Original C3-A2 channel recordings of EEG signal After Preprocessing
Zoom into C3-A2 channel recordings of EEG signal at 1 to 2 seconds
Zoom into C3-A2 channel recordings of EEG signal at 1 to 2 seconds After Preprocessing
Amplitude (uV)
Time (s)
(I)
(J)
(K)
(L)
(M)
(N)
(O)
(P)

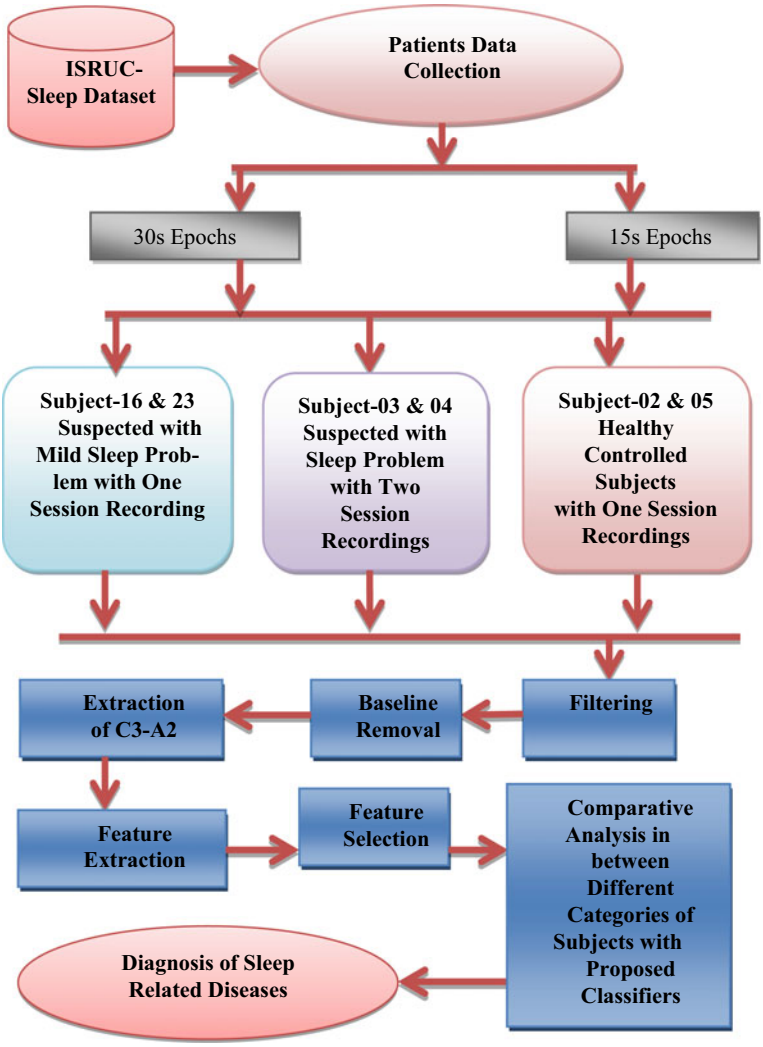
ISRUC-Sleep Dataset
Patients Data Collection
30s Epochs
15s Epochs
Subject-16 & 23 Suspected with Mild Sleep Problem with One Session Recording
Subject-03 & 04 Suspected with Sleep Problem with Two Session Recordings
Subject-02 & 05 Healthy Controlled Subjects with One Session Recordings
Extraction of C3-A2
Baseline Removal
Filtering
Feature Extraction
Feature Selection
Comparative Analysis in between Different Categories of Subjects with Proposed Classifiers
Diagnosis of Sleep Related Diseases

Fig. 3 Proposed AASC work model

To identify the suitable features from the extracted feature vector, we applied the suitable feature screening techniques online streaming feature selection (OSFS) techniques [26]. Finally, the selected features for each subject with a duration of 30 and 15 s epochs are described in Table 3.

Table 2 Explanation of the extracted features for this proposed study

Extracted feature set	Feature No.	Extracted feature set	Feature No.
Extracted time domain features			
Mean	1	Minimum	3
Maximum	2	Standard deviation	4
Median	5	Variance	6
Zero crossing rate	7	75 percentile	8
Signal skewness	9	Signal kurtosis	10
Signal activity	11	Signal mobility	12
Signal complexity	13		
Extracted frequency domain features			
Relative spectral power in delta, theta, beta, and alpha bands	14, 15, 16, 17	Power ratios δ/β, δ/θ, θ/α, θ/β, α/β, α/δ, $(\theta + \alpha)/(\alpha + \beta)$	18, 19, 20, 21, 22, 23, 24
Band power in δ, θ, α, β bands	25, 26, 27, 28		

5 Experimental Results and Discussion

To evaluate the performance of the proposed research work, a series of practical steps were considered, such as preprocessing, feature extraction, feature selection, and classification using the different categories of medical conditions of subjects with their different session recordings described in Sect. 4. As described before, the brain behavior was recorded from enrolled subjects through single-channel C3-A2 of EEG signal [28–36]. Next, we filtered out the muscle artifacts and removed noisy portions from recorded signals through the Butterworth bandpass filter. In the next phase, experiments were conducted to extract the features from both time and frequency domains. As a whole, 28 features were extracted from recorded signals of the subjects, and the exact details are mentioned in Table 2. The size of the feature vectors for all enrolled subjects for both 30 and 15 s epoch length is 28 × 750. The matrix dimension for the feature vector is *feature number* × *epoch number*. The next task is the selection of the most efficient features from among the feature vector. To work out this selection experiment, we have applied OSFS feature selection techniques.

The matrix representation for feature selection vectors is *selected feature number* × *epoch number*. As a whole, we have obtained 16 feature selection vector from 8 subjects through different epoch length time window as 30 and 15 s, these matrixes are 16 × 750, 17 × 750, 15 × 750, 15 × 750, 16 × 750, 15 × 750, 15 × 750, and 15 × 750 for subject-16, subject-23, subject-03 (session-1 recording), subject-03 (session-2 recording), subject-04 (session-1 recording), subject-04 (session-2 recording), subject-02, and subject-05, respectively, for input length of epoch is 30 s. Similarly, for the same subjects with 15 s length of epoch, the size of the

Table 3 Final feature selection list

Participants name/gender	Best feature combination (30 s epochs)	Best feature combination (15 s epochs)
Subject-16 MALE	$F1_{16}$, $F2_{16}$, $F3_{16}$, $F4_{16}$, $F5_{16}$, $F7_{16}$, $F9_{16}$, $F10_{16}$, $F11_{16}$, $F13_{16}$, $F14_{16}$, $F15_{16}$, $F22_{16}$, $F25_{16}$, $F27_{16}$, $F31_{16}$ (16 features)	$F1_{15s16}$, $F2_{15s16}$, $F3_{15s16}$, $F4_{15s16}$, $F5_{15s16}$, $F7_{15s16}$, $F9_{15s16}$, $F11_{15s16}$, $F15_{15s16}$, $F19_{15s16}$, $F20_{15s16}$, $F27_{15s16}$, $F35_{15s16}$ (13 features)
Subject-23 FEMALE	$F1_{23}$, $F2_{23}$, $F3_{23}$, $F4_{23}$, $F5_{23}$, $F7_{23}$, $F11_{23}$, $F12_{23}$, $F15_{23}$, $F16_{23}$, $F17_{23}$, $F20_{23}$, $F24_{23}$, $F26_{23}$, $F31_{23}$, $F33_{23}$, $F37_{23}$ (17 features)	$F1_{15S23}$, $F2_{15S23}$, $F3_{15S23}$, $F4_{15S23}$, $F5_{15S23}$, $F6_{15S23}$, $F7_{15S23}$, $F14_{15S23}$, $F15_{15S23}$, $F20_{15S23}$, $F21_{15S23}$, $F25_{15S23}$, $F28_{15S23}$ (13 features)
Subject-03 MALE (session-1) recording	$F1_{03S1}$, $F2_{03S1}$, $F3_{03S1}$, $F4_{03S1}$, $F5_{03S1}$, $F7_{03S1}$, $F8_{03S1}$, $F9_{03S1}$, $F11_{03S1}$, $F12_{03S1}$, $F13_{03S1}$, $F14_{03S1}$, $F21_{03S1}$, $F22_{03S1}$, $F25_{03S1}$ (15 features)	$F1_{15S03S1}$, $F3_{15S03S1}$, $F4_{15S03S1}$, $F5_{15S03S1}$, $F9_{15S03S1}$, $F11_{15S03S1}$, $F14_{15S03S1}$, $F17_{15S03S1}$, $F22_{15S03S1}$, $F23_{15S03S1}$, $F28_{15S03S1}$ (11 features)
Subject-03 MALE (session-2) recording	$F1_{03S2}$, $F2_{03S2}$, $F3_{03S2}$, $F4_{03S2}$, $F5_{03S2}$, $F7_{03S2}$, $F8_{03S2}$, $F9_{03S2}$, $F11_{03S2}$, $F12_{03S2}$, $F13_{03S2}$, $F14_{03S2}$, $F21_{03S2}$, $F22_{03S2}$, $F25_{03S2}$ (15 features)	$F1_{15S03S2}$, $F2_{15S03S2}$, $F3_{15S03S2}$, $F4_{15S03S2}$, $F5_{15S03S2}$, $F6_{15S03S2}$, $F8_{15S03S2}$, $F11_{15S03S2}$, $F20_{15S03S2}$, $F26_{15S03S2}$, $F27_{15S03S2}$, $F28_{15S03S2}$ (12 features)
Subject-04 FEMALE Session-1 recording	$F1_{04S1}$, $F2_{04S1}$, $F3_{04S1}$, $F4_{04S1}$, $F5_{04S1}$, $F7_{04S1}$, $F8_{04S1}$, $F9_{04S1}$, $F10_{04S1}$, $F11_{04S1}$, $F15_{04S1}$, $F16_{04S1}$, $F18_{04S1}$, $F27_{04S1}$, $F29_{04S1}$, $F37_{04S1}$ (16 features)	$F1_{15s04S1}$, $F2_{15s04S1}$, $F3_{15s04S1}$, $F4_{15s04S1}$, $F5_{15s04S1}$, $F7_{15s04S1}$, $F8_{15s04S1}$, $F11_{15s04S1}$, $F13_{15s04S1}$, $F15_{15s04S1}$, $F16_{15s04S1}$, $F20_{15s04S1}$, $F27_{15s04S1}$ (13 features)
Subject-04 FEMALE Session-2 recording	$F1_{04S2}$, $F2_{04S2}$, $F3_{04S2}$, $F4_{04S2}$, $F5_{04S2}$, $F7_{04S2}$, $F8_{04S2}$, $F9_{04S2}$, $F11_{04S2}$, $F12_{04S2}$, $F13_{04S2}$, $F14_{04S2}$, $F21_{04S2}$, $F22_{04S2}$, $F25_{04S2}$ (15 features)	$F1_{15s04S2}$, $F2_{15s04S2}$, $F3_{15s04S2}$, $F4_{15s04S2}$, $F5_{15s04S2}$, $F6_{15s04S2}$, $F8_{15s04S2}$, $F9_{15s04S2}$, $F11_{15s04S2}$, $F13_{15s04S2}$, $F15_{15s04S2}$, $F16_{15s04S2}$, $F20_{15s04S2}$, $F27_{15s04S2}$ (14 features)
Subject-02 MALE Recording	$F1_{02}$, $F2_{02}$, $F3_{02}$, $F4_{02}$, $F5_{02}$, $F7_{02}$, $F8_{02}$, $F9_{02}$, $F11_{02}$, $F12_{02}$, $F13_{02}$, $F14_{02}$, $F21_{02}$, $F22_{02}$, $F25_{02}$ (15 features)	$F1_{15S02}$, $F2_{15S02}$, $F3_{15S02}$, $F4_{15S02}$, $F5_{15S02}$, $F6_{15S02}$, $F7_{15S02}$, $F8_{15S02}$, $F9_{15S02}$, $F11_{15S02}$, $F12_{15S02}$, $F14_{15S02}$, $F15_{15S02}$, $F16_{15S02}$ (14 features)
Subject-05 FEMALE Recording	$F1_{05}$, $F2_{05}$, $F3_{05}$, $F4_{05}$, $F5_{05}$, $F7_{05}$, $F8_{05}$, $F9_{05}$, $F11_{05}$, $F12_{05}$, $F13_{05}$, $F14_{05}$, $F21_{05}$, $F22_{05}$, $F25_{05}$ (15 features)	$F1_{15S05}$, $F2_{15S05}$, $F3_{15S05}$, $F9_{15S05}$, $F12_{15S05}$, $F26_{15S05}$, $F28_{15S05}$, $F37_{15S05}$ (8 features)

matrixes is 13 × 750, 13 × 750, 11 × 750, 12 × 750, 13 × 750, 14 × 750, 14 × 750, and 8 × 750. The classification results achieved using the tenfold cross validation strategy. The whole experiment was conducted, considering the subject with suspected sleep disorder with one-time session recordings, two-time session recordings from a subject with a symptom of sleep disorder, and finally, the healthy subject with one session recording. In this proposed study, we have evaluated the classification accuracy for all three mentioned cases. Besides, we also conducted a comparative analysis with all these enrolled subjects and their session recordings. Finally, experimental comparison results are presented according to the single channel of EEG signals and two sleep classes (wake vs. sleep). Analysis of the comparative results from conducted experiments and obtained results is presented below.

5.1 Classification Accuracy of Category-I Subject ISRUC-Sleep Database

In this experimental part, we have obtained two subjects who have been affected by some sleep-related disorders, and here from subject one session recorded by sleep experts to diagnose the irregularities that happened during sleep hours. It has been observed that the SVM depicts an overall classification accuracy of 95.6 and 91.20% achieved through DT classifiers for subject-16. For subject-23, the same classifiers SVM and DT reached overall accuracy of 91.46% and 87.73%, respectively, for epoch length 30 s. Similarly, the accuracy achieved for epoch window length 15 s through SVM and DT is 96% and 89.87%, 98.60%, and 97.73% for subject-16 and subject-23, respectively. Table 4 presents the confusion matrix for two-state sleep stage classification problems for both the subject-16 and 23, with the time length of the epoch in the 30 s, and Table 5 shows the confusion matrix for 15 s epoch length.

Table 4 Confusion matrix obtained for subject-16 and subject-23 subgroup-I/session-1 recording (30 s epochs length)

Subject-16(ISRUC-Sleep) Subgroup I/Session1_Recording			
C3-A2		Wake	Sleep
SVM	Wake	133	30
	Sleep	3	584
C3-A2		Wake	Sleep
DT	Wake	134	29
	Sleep	37	550

Subject-23(ISRUC-Sleep) Subgroup I/Session1_Recording			
C3-A2		Wake	Sleep
SVM	Wake	174	38
	Sleep	512	26
C3-A2		Wake	Sleep
DT	Wake	167	45
	Sleep	29	509

Table 5 Confusion matrix obtained for subject-16 and subject-23 subgroup-I/session-1 recording (15 s epochs length)

Subject-16(ISRUC-Sleep)/15s Subgroup I/Session1_Recording			
C3A2		Wake	Sleep
SVM	Wake	173	22
	Sleep	8	547

Subject-23(ISRUC-Sleep)/15s Subgroup I/Session1_Recording			
C3A2		Wake	Sleep
SVM	Wake	229	6
	Sleep	5	510

C3A2		Wake	Sleep
DT	Wake	161	34
	Sleep	42	513

C3A2		Wake	Sleep
DT	Wake	225	10
	Sleep	7	508

The overall performance value of the proposed category-I subject ISRUC-sleep database is measured through the evaluation parameters that are recall, specificity, precision, and $F1$-score, and it reported for subject-16 as 99.49%, 81.60%, 95.11%, and 97.25% through SVM, 93.70%, 82.21%, 94.99%, and 94.34% through DT, respectively; similarly, the same parameters reached for subject-23 through SVM and DT are 95.17%, 82.08%, 93.09% and 94.12%, 91.45%, 78.30%, and 91.45%. With same subjects with 15 s epoch duration, the results achieved for subject-16 are 98.56%, 88.72%, 96.13%, and 97.33% and 92.43%, 82.56%, 93.78%, and 93.10% through SVM and DT classifier, respectively. The results reported for subject-23 for both classifiers as 97.45%, 88.72%, 97.86% and 97.65%, 98.64%, 95.74%, 98.07%, and 98.53%. Figures 4 and 5 display performance statistics for 30 and 15 s epoch length for subject-16 and subject-23.

5.2 Classification Accuracy of Category-II Subject ISRUC-Sleep Database

In the ISRUC-sleep subgroup-II dataset experiment, the proposed sleep stage classification model was based only on a single channel with two different session recordings from two different genders enrolled subjects with suspected sleep-related disorder symptoms. Tables 6 and 7 represent the confusion matrix for both session recordings of subject-03 with the duration of epoch 30 and 15 s.

From each subject, here, we have acquired two different session recordings. It has been observed that subject-03 with session-1 recording SVM classification model depicts an overall accuracy of 91.06% and 84.26% for DT, respectively. Similarly, it has been found that the classification results of subject-03 with session-2 recordings through SVM and DT were reported as 89.46% and 84.2. The accuracy achieved from

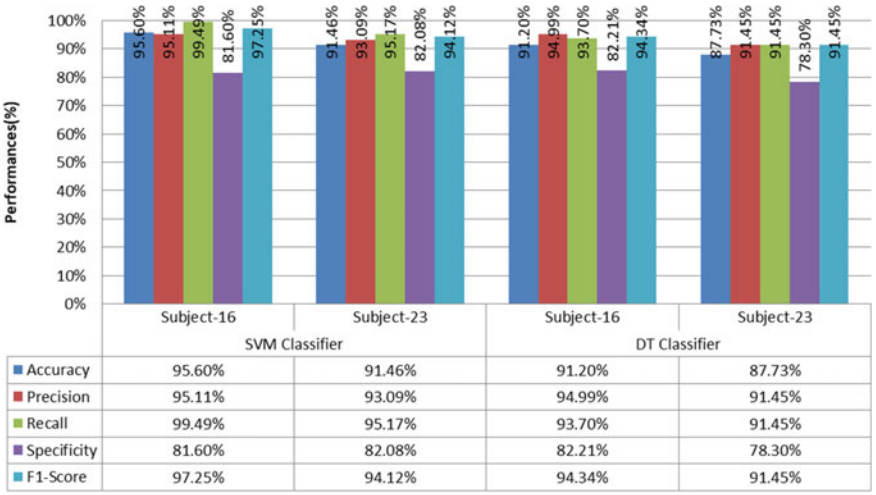

	SVM Classifier		DT Classifier	
	Subject-16	Subject-23	Subject-16	Subject-23
Accuracy	95.60%	91.46%	91.20%	87.73%
Precision	95.11%	93.09%	94.99%	91.45%
Recall	99.49%	95.17%	93.70%	91.45%
Specificity	81.60%	82.08%	82.21%	78.30%
F1-Score	97.25%	94.12%	94.34%	91.45%

Fig. 4 Performance statistics for the two-state sleep classification model with 30 s epoch duration

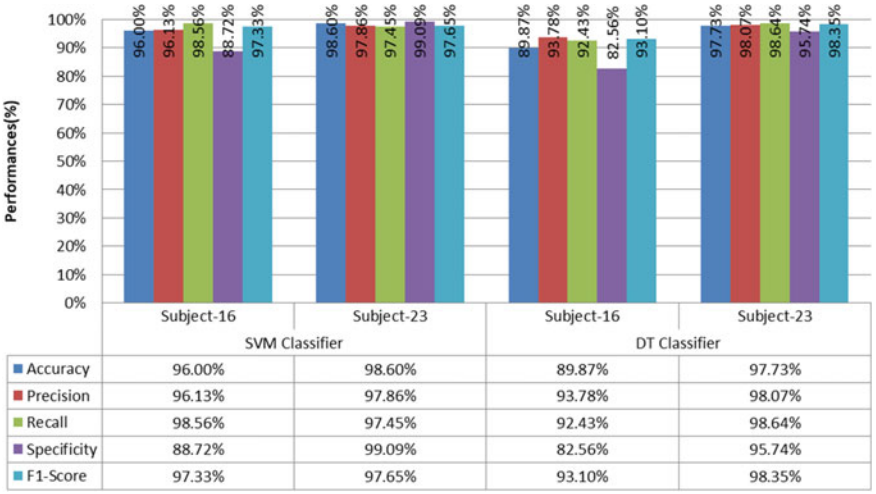

	SVM Classifier		DT Classifier	
	Subject-16	Subject-23	Subject-16	Subject-23
Accuracy	96.00%	98.60%	89.87%	97.73%
Precision	96.13%	97.86%	93.78%	98.07%
Recall	98.56%	97.45%	92.43%	98.64%
Specificity	88.72%	99.09%	82.56%	95.74%
F1-Score	97.33%	97.65%	93.10%	98.35%

Fig. 5 Performance statistics for the two-state sleep classification model with 15 s epoch duration

the same classifiers for 15 s length is 97.46% and 88.26% for session-1 recording and 94% and 80.5% for session-2 recording. The overall performance of recall, specificity, precision, and $F1$-score reported with the session-1 recording of ISRUC-sleep subgroup-II database of subject-03 through SVM as 97.07%, 29.85%, 93.38%, and 95.19%; similarly, for DT classifier, the performances reached 93.70%, 82.21%, 94.99%, and 94.34%. Similarly the performances with session-2 recordings, it is reported as 98.49%, 22.47%, 90.42%, and 94.28% through SVM, 91.45%, 78.30%,

Table 6 Confusion matrix obtained for subject-03 subgroup-II/session-1 and 2 recording for 30 s epoch length

30s Epoch Length

Subject-03(ISRUC-Sleep) Subgroup I/Session1_Recording

C3-A2		Wake	Sleep
SVM	Wake	20	47
	Sleep	20	663

C3-A2		Wake	Sleep
DT	Wake	12	63
	Sleep	55	620

30s Epoch Length

Subject-03(ISRUC-Sleep) Subgroup I/Session2_Recording

C3-A2		Wake	Sleep
SVM	Wake	20	69
	Sleep	10	651

C3-A2		Wake	Sleep
DT	Wake	18	63
	Sleep	40	629

Table 7 Confusion matrix obtained for subject-03 subgroup-II/session-1 and 2 recording for 15 s epoch length

15s Epoch Length

Subject-03(ISRUC-Sleep) Subgroup I/Session1_Recording

C3-A2		Wake	Sleep
SVM	Wake	214	10
	Sleep	9	517

C3-A2		Wake	Sleep
DT	Wake	154	70
	Sleep	18	508

15s Epoch Length

Subject-03(ISRUC-Sleep) Subgroup I/Session2_Recording

C3-A2		Wake	Sleep
SVM	Wake	398	17
	Sleep	28	307

C3-A2		Wake	Sleep
DT	Wake	307	108
	Sleep	38	297

91.45%, and 91.45% through DT. The performance resulted with 15 s length of epoch through SVM and DT are 98.29%, 95.54%, 98.10% and 98.20%, 96.58%, 68.75%, 87.89%, and 92.03% for session-1 recording; similarly for session-2, the performance recorded as 91.64%, 95.90%, 94.75% and 93.17%, 88.66%, 73.98%, 73.33%, and 80.27%. The performance graph results for subject-03 for both session recordings and epoch length are displayed in Figs. 6 and 7.

Confusion matrix representation of the subject-04 for both session recordings with epoch duration of the 30 and 15 s is illustrated in Tables 8 and 9. The performance graph results for subject-04 for both session recordings and epoch length are displayed in Figs. 8 and 9. The overall classification accuracy performances of subject-04 reached with 30 s length of session-1 recording through SVM and DT are

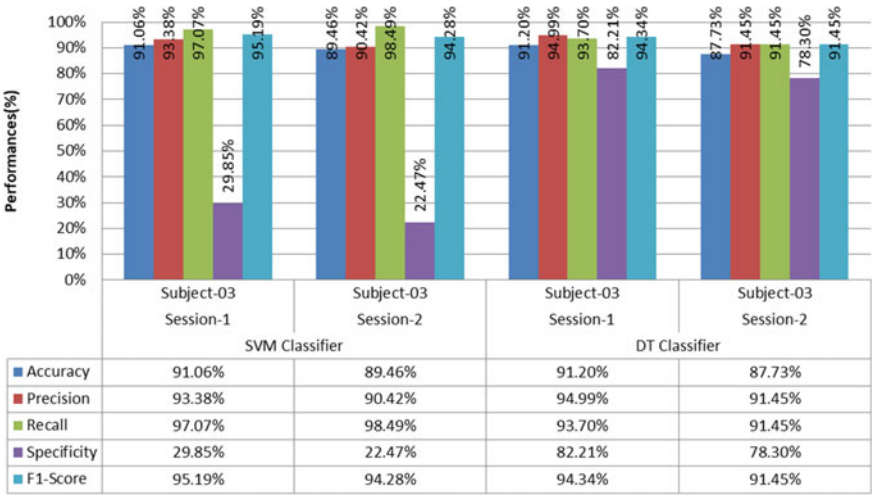

	SVM Classifier		DT Classifier	
	Subject-03 Session-1	Subject-03 Session-2	Subject-03 Session-1	Subject-03 Session-2
Accuracy	91.06%	89.46%	91.20%	87.73%
Precision	93.38%	90.42%	94.99%	91.45%
Recall	97.07%	98.49%	93.70%	91.45%
Specificity	29.85%	22.47%	82.21%	78.30%
F1-Score	95.19%	94.28%	94.34%	91.45%

Fig. 6 Performance measures using SVM and DT classification techniques for the two-state sleep classification model with two session recordings for subject-03 (30 s epochs length)

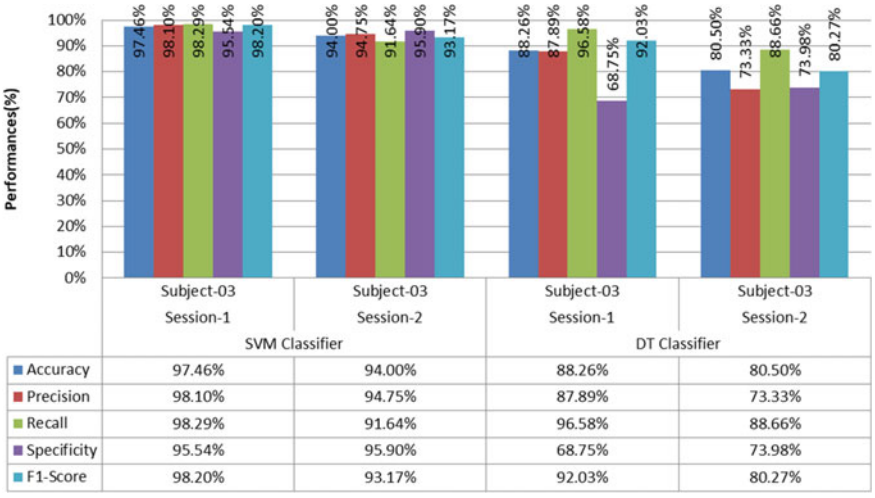

	SVM Classifier		DT Classifier	
	Subject-03 Session-1	Subject-03 Session-2	Subject-03 Session-1	Subject-03 Session-2
Accuracy	97.46%	94.00%	88.26%	80.50%
Precision	98.10%	94.75%	87.89%	73.33%
Recall	98.29%	91.64%	96.58%	88.66%
Specificity	95.54%	95.90%	68.75%	73.98%
F1-Score	98.20%	93.17%	92.03%	80.27%

Fig. 7 Performance measures using SVM and DT classification techniques for the two-state sleep classification model, subgroup-II with two session recordings for subject-03 (30 s epochs length)

99.46% and 97.46%, respectively; similarly for session-2 recording, the classification accuracy reported as 97.73% and 93.86% through SVM and DT, respectively. For 15 s length of epoch, the reported accuracy achieved as 97.3% and 94.8%; similarly, for session-2 recording, it is reported as 98.13% and 95.73%. Similarly, for subject-04, the performances of evaluation matrices results through SVM and DT are 99.69%, 98.20%, 99.69% and 99.69%, 98.44%, 91.89%, 98.59%, and 98.51% for

Table 8 Confusion matrix obtained for subject-04 subgroup-II/session-1 and 2 recording for 30 s epoch length

30s Epoch Length

Subject-04(ISRUC-Sleep) Subgroup I/Session1_Recording

C3-A2		Wake	Sleep
SVM	Wake	109	2
	Sleep	2	637

C3-A2		Wake	Sleep
DT	Wake	102	9
	Sleep	10	629

30s Epoch Length

Subject-04(ISRUC-Sleep) Subgroup I/Session2_Recording

C3-A2		Wake	Sleep
SVM	Wake	150	12
	Sleep	5	583

C3-A2		Wake	Sleep
DT	Wake	141	21
	Sleep	25	563

Table 9 Confusion matrix obtained for subject-04 subgroup-II/session-1 and 2 recording for 15 s epoch length

15s Epoch Length

Subject-04(ISRUC-Sleep) Subgroup I/Session1_Recording

C3-A2		Wake	Sleep
SVM	Wake	147	15
	Sleep	5	583

C3-A2		Wake	Sleep
DT	Wake	137	25
	Sleep	14	574

15s Epoch Length

Subject-04(ISRUC-Sleep) Subgroup I/Session2_Recording

C3-A2		Wake	Sleep
SVM	Wake	156	11
	Sleep	3	580

C3-A2		Wake	Sleep
DT	Wake	144	23
	Sleep	9	574

session-1, respectively; similarly, for session-2 recordings, the performances through same classification techniques are 99.15%, 92.59%, 97.98% and 98.56%, 95.75%, 87.04%, 96.40%, and 96.08%, respectively. The performance achieved through 15 s time framework from both SVM and DT classifier is 99.15%, 90.74%, 97.49% and 98.31%, 97.62%, 84.57%, 95.83%, and 96.71% for session-1 recording, in the same manner for session-2 recording, the reported result as 99.49%, 93.41%, 98.14% and 98.81%, 98.46%, 86.23%, 96.15%, and 97.29% for session-2 recording, respectively.

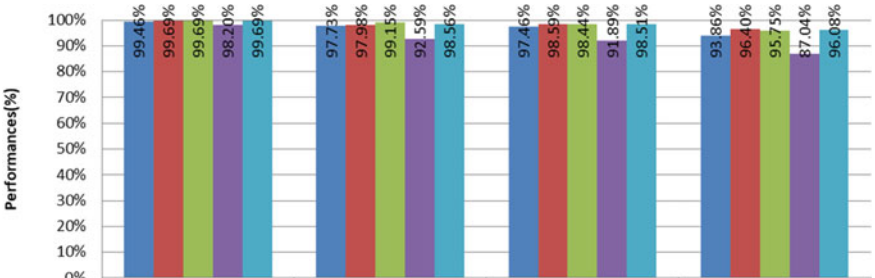

	SVM Classifier		DT Classifier	
	Subject-04 Session-1	Subject-04 Session-2	Subject-04 Session-1	Subject-04 Session-2
Accuracy	99.46%	97.73%	97.46%	93.86%
Precision	99.69%	97.98%	98.59%	96.40%
Recall	99.69%	99.15%	98.44%	95.75%
Specificity	98.20%	92.59%	91.89%	87.04%
F1-Score	99.69%	98.56%	98.51%	96.08%

Fig. 8 Performance measures using SVM and DT classification techniques for the two-state sleep classification model with 30 s length of an epoch, subgroup-II with two session recordings for subject-04

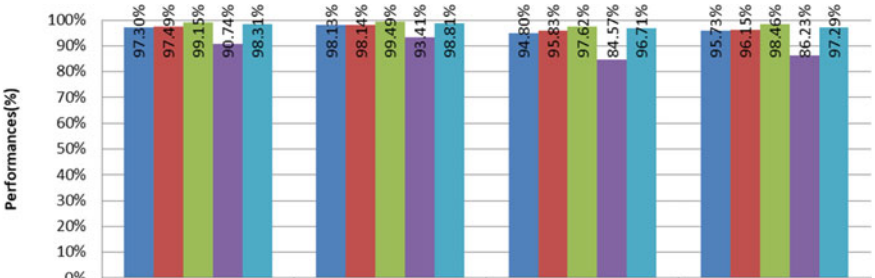

	SVM Classifier		DT Classifier	
	Subject-04 Session-1	Subject-04 Session-2	Subject-04 Session-1	Subject-04 Session-2
Accuracy	97.30%	98.13%	94.80%	95.73%
Precision	97.49%	98.14%	95.83%	96.15%
Recall	99.15%	99.49%	97.62%	98.46%
Specificity	90.74%	93.41%	84.57%	86.23%
F1-Score	98.31%	98.81%	96.71%	97.29%

Fig. 9 Performance measures using SVM and DT classification techniques for the two-state sleep classification model with 15 s epoch window, subgroup-II with two session recordings for subject-04

Table 10 Confusion matrix obtained for subject-2 and subject-5 subgroup-III/session-1 recording for 30 s length of the epoch

Subject-02(ISRUC-Sleep) Subgroup I/Session1_Recording			
C3-A2		Wake	Sleep
SVM	Wake	20	69
	Sleep	25	636

Subject-05(ISRUC-Sleep) Subgroup I/Session1_Recording			
C3-A2		Wake	Sleep
SVM	Wake	235	3
	Sleep	2	510

C3-A2		Wake	Sleep
DT	Wake	3	86
	Sleep	11	650

C3-A2		Wake	Sleep
DT	Wake	212	26
	Sleep	43	469

5.3 *Classification Accuracy of Category-III Subject ISRUC-Sleep Database*

The final experiment for the sleep EEG study is done by obtaining recorded signals from healthy subjects who have no prior sleep-related medication. One session recording was considered for monitoring the sleep abnormality. It has been observed that the overall accuracy for subject-02 achieved with the input of 30 s length of epoch a through SVM and DT is 87.46 and 87.06%. Similarly, for subject-05, the classification accuracy achieved 99.33 and 90.80%. In order to 15 s length of input epoch, the accuracy results are 98% and 98.13% for subject-02, 98.26% and 92.5% for subject-05. The confusion matrix for subject-02 and subject-05 is illustrated in Table 10 for the 30 s and Table 11 for 15 s. The overall performance value of recall, specificity, precision, and $F1$-score reported for subject-02 through SVM and DT is 96.22%, 22.47%, 90.21% and 93.12%, 98.34%, 3.37%, 88.32%, and 93.06%. Similarly, for subject-5, the performance of the metrics is 99.61%, 98.74%, 99.42% and 99.51%, 91.60%, 89.08%, 94.75%, and 93.15% through SVM and DT, respectively. The graph results for the same achieved results are shown in Figs. 10 and 11 concerning the 30 s and 15 s epoch length, respectively.

5.4 *Summary of Comparative Analysis Results of ISRUC-Sleep (I/II/III) Data*

In this study, three different medical condition-oriented subjects were used for two-class sleep stage classification. From ISRUC-sleep-I data, subject-16 reached the highest classification accuracy of 95.60% through the SVM classifier. It has

Table 11 Confusion matrix obtained for subject-2 and subject-5 subgroup-III/session-1 recording for 15 s length of the epoch

Subject-02(ISRUC-Sleep) Subgroup I/Session1_Recording			
C3-A2		Wake	Sleep
SVM	Wake	116	14
	Sleep	1	619

Subject-05(ISRUC-Sleep) Subgroup I/Session1_Recording			
C3-A2		Wake	Sleep
SVM	Wake	184	10
	Sleep	3	553

C3-A2		Wake	Sleep
DT	Wake	122	8
	Sleep	6	614

C3-A2		Wake	Sleep
DT	Wake	171	23
	Sleep	33	523

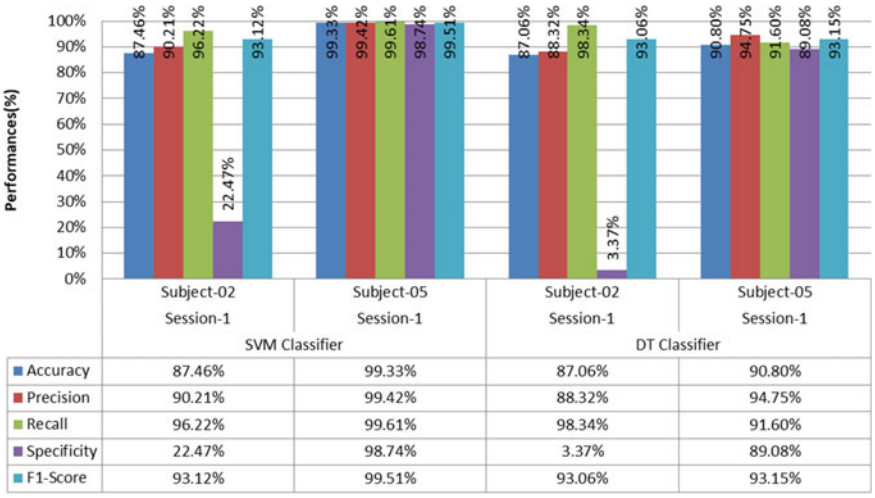

Fig. 10 Performance measures of 30 s length epoch using SVM and DT classification techniques for the two-state sleep classification model, subgroup-III with two session recordings for subject-02 and subject-05

been noticed that the highest overall accuracy rate was achieved with ISRUC-sleep subgroup-II data. The highest classification for the two-state sleep classification problem for subject-04 with one session recording as 99.46%, similarly from ISRUC-sleep subgroup-III, the highest accuracy achieved for subject-05 as 99.33% for the input of 30 s epoch length. Similarly, for the 15 s length of the epoch, the highest accuracy achieved from ISRUC-sleep subgroup-I/II/III as 98.60%, 98.13%, and 98.26% through the SVM classifier, respectively.

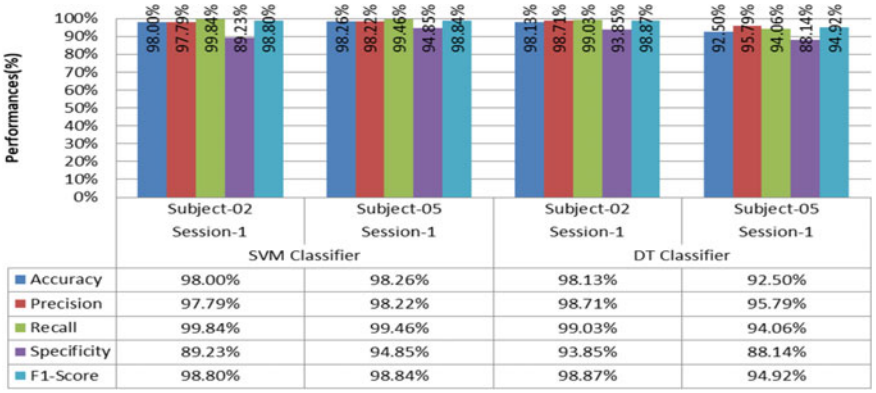

Fig. 11 Performance measures of 15 s length epoch using SVM and DT classification techniques for the two-state sleep classification model, subgroup-III with one session recordings for subject-02 and subject-05

Figures 12 and 13 present the overall accuracy achieved for all categories of subjects irrespective of their signal recordings from the subjects for epoch length of 30 s and 15 s, respectively. Here, we have compared with other similar contributions to measure the proposed research work effectiveness toward identifying sleep disorders. Table 12 compares the performances based on single-channel EEG acquisition among the proposed research work results with five reported works mentioned in Sect. 3.

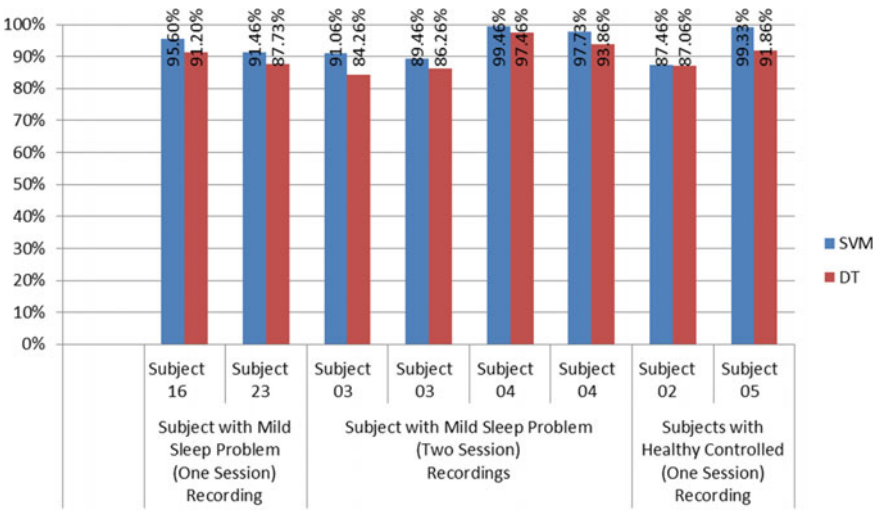

Fig. 12 Overall accuracy performances in the two-class sleep stage classification problem with ISRUC-sleep subgroup-I/II/III dataset for 30 s epoch length

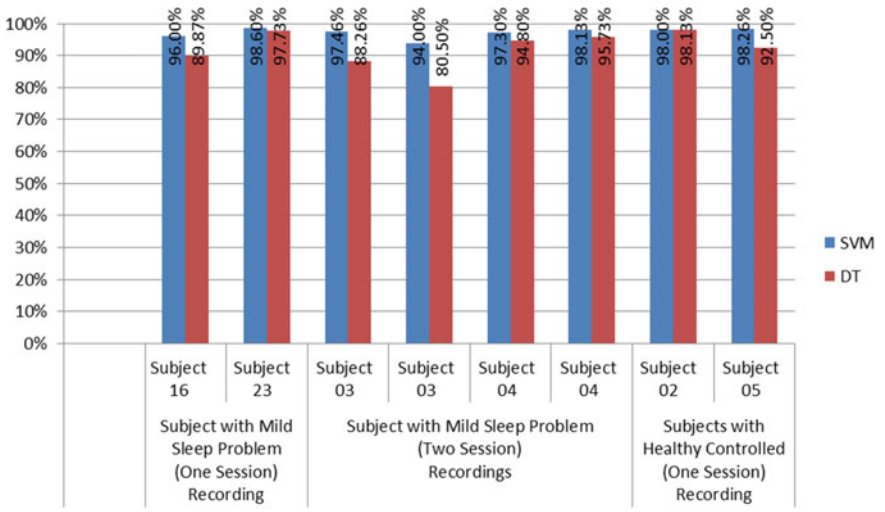

Fig. 13 Overall accuracy performances in the two-class sleep stage classification problem with ISRUC-sleep subgroup-I/II/III dataset for 15 s epoch length

Table 12 Comparison of performances of the proposed work with previously published works

Author	Year	Signal type	Method	Feature number	Accuracy (%)
Ref. [27]	2018	Single-channel EEG signal	FFT + random forest classifier	Eight statistical features	97.1
Ref. [17]	2017	Single-channel EEG signal	Tunable-Q wavelet transform (TQWT) + bootstrap aggregating	Four statistical features	92.43
Ref. [18]	2016	Single-channel EEG signal	Structural graph similarity K-means (SGSKM) + SVM classifier	Twelve statistical features	95.93
Ref. [16]	2014	Single-channel EEG signal	Frequency sub-bands features extraction + SVM classifier	Three features (time and frequency domain)	92.5
Proposed work	2020	Single-channel EEG signal	Sleep EEG study + SVM and DT classifier	Thirteen (time domain) and fifteen (frequency domain)	99.46 97.46

6 Conclusion

The present proposed research work application showed the most effectiveness in the sleep stage scoring by using a single channel of EEG signal. This proposed sleep EEG study would provide an effective mechanism for handling different health conditions of the subjects with high accuracy of sleep abnormality identification from sleep recordings. The main objective of this application is to analyze the irregularities that occurred during sleep hours from various session recordings. Additionally, this application also successfully deals with the specially aged category of subjects with various disease conditions. The central part of this research work is to find the proper solutions based on irregularity's accuracy during sleep. Another important significance of this proposed sleep EEG study is that, according to our best knowledge, this proposed research work considered different session recordings from the participated subjects in these experimental processes.

The general sleep stage classification problem is that annotations of sleep stages are another essential source of information. This experimental research study provides new directions on scoring sleep stages to identify sleep abnormality by extracting different features from both domains, such as frequency and time. The significant changes are shown between the two different session recordings of sleep stages from two different days. These things support the discovery of new concepts of investigation on sleep irregularities during sleep. It may get more advantage for predicting the proper diagnosis plan for treating the disorder.

The proposed scheme automated sleep stage classification based on a single channel of EEG signal benefits from including different session recordings and obtained different health condition subjects. It has been observed from the experimental results that the proposed sleep analysis indicated an excellent agreement between automated sleep staging and the gold standard.

The present research work has certain disadvantages that the (1) data used for the experimental purpose from ISRUC-sleep repository for statistical evaluation were relatively small, (2) only we have included single channel of EEG signal was used for classification, (3) we have not considered the subjects who were effects of diseases, such as narcolepsy and insomnia.

We will focus on including the multiple PSG signal such as EMG, ECG, and other EEG signal channels in our future implementation. Further, we will also consider more clinical sleep data, mainly including the different sleep problem patients, to measure the performance of the proposed research work for higher accuracy.

References

1. Aboalayon, K.A.I., Faezipour, M., Almuhammadi, W.S., et al.: Sleep stage classification using EEG signal analysis: a comprehensive survey and new investigation. Entropy **18**, 272 (2016)

2. Heyat, M.B.B., Akhtar, F., Azad, S.: Comparative analysis of original wave & filtered wave of EEG signal used in the detection of bruxism medical sleep syndrome. Int. J. Trend Sci. Res. Dev. **1**(1), 7–9 (2016)
3. Heyat, M.B.B., Akhtar, S.F., Azad, S.: Power spectral density are used in the investigation of insomnia neurological disorder. In: Proceedings of Pre Congress Symposium, Organized Indian Academy of Social Sciences (ISSA), King George's Medical University, State Takmeelut-Tib College Hospital, Lucknow, Uttar Pradesh, pp. 45–50 (2016)
4. Rahman, F., Heyat, S.: An overview of narcolepsy. IARJSET **3**, 85–87 (2016)
5. Kim, T., Kim, J., Lee, K.: Detection of sleep disordered breathing severity using acoustic biomarker and machine learning techniques. BioMed. Eng. OnLine **17**, 16 (2018)
6. Siddiqui, M., Srivastava, G., Saeed, S.: Diagnosis of insomnia sleep disorder using short time frequency analysis of PSD approach applied on EEG signal using channel ROC-LOC. Sleep Sci. **9**(3), 186–191 (2016)
7. Rechtschaffen, A.: A manual for standardized terminology techniques and scoring system for sleep stages in human subjects. Brain Inf. Serv. (1968)
8. Iber, C.: The AASM manual for the scoring of sleep and associated events: rules, terminology and technical specifications. Am. Acad. Sleep Med. (2007)
9. Carskadon, M.A., Dement, W.C.: Normal human sleep: an overview. In: Kryger, M., Roth, T., Dement, W.C. (eds) Principles and Practice of Sleep Medicine, 6th edn, pp. 15–24. Elsevier, Amsterdam, The Netherlands (2017). [Online]. Available: https://doi.org/10.1016/B978-0-323-24288-2.00002-7
10. Acharya, R.U., Faust, O., Kannathal, N., Chua, T., Laxminarayan, S.: Nonlinear analysis of EEG signals at various sleep stages. Comput. Methods Programs Biomed. **80**(1), 37–45 (2005)
11. Holland, J.V., Dement, W.C., Raynal, D.M.: Polysomnography: a response to a need for improved communication. Presented at the 14th Annual Meeting Association for the Psychophysiological Study of Sleep (1974)
12. Acharya, U.R., et al.: Nonlinear dynamics measures for automated EEG-based sleep stage detection. Eur. Neurol. **74**(5–6), 268–287 (2015)
13. Spriggs, W.H.: Essentials of Polysomnography. World Headquarter Jones & Bartlett Publishers, Sudbury, MA (2014)
14. Obayya, M., Abou-Chadi, F.: Automatic classification of sleep stages using EEG records based on fuzzy c-means (FCM) algorithm. In: 2014 31st National on Radio Science Conference (NRSC), pp. 265–272 (2014)
15. Güneş, Polat, K., Yosunkaya, Ş.: Efficient sleep stage recognition system based on EEG signal using k-means clustering based feature weighting. Expert Syst. Appl. **37**, 7922–7928 (2010)
16. Aboalayon, K., Ocbagabir, H.T., Faezipour, M.: Efficient sleep stage classification based on EEG signals. In: 2014 IEEE Long Island Systems, Applications and Technology Conference (LISAT), pp. 1–6 (2014)
17. Hassan, A.R., Subasi, A.: A decision support system for automated identification of sleep stages from single-channel EEG signals. Knowl.-Based Syst. **128**, 115–124 (2017)
18. Diykh, M., Li, Y., Wen, P.: EEG sleep stages classification based on time domain features and structural graph similarity. IEEE Trans. Neural Syst. Rehabil. Eng. **24**(11), 1159–1168 (2016). https://doi.org/10.1109/tnsre.2016.2552539
19. Gunnarsdottir, K.M., Gamaldo, C.E., Salas, R.M.E., Ewen, J.B., Allen, R.P., Sarma, S.V.: A novel sleep stage scoring system: combining expert-based rules with a decision tree classifier. In: 2018 40th Annual International Conference of the IEEE Engineering in Medicine and Biology Society (EMBC) (2018). https://doi.org/10.1109/embc.2018.8513039
20. Sriraam, N., Padma Shri, T.K., Maheshwari, U.: Recognition of wake-sleep stage 1 multi-channel EEG patterns using spectral entropy features for drowsiness detection. Australas. Phys. Eng. Sci. Med. **39**(3), 797–806 (2016). https://doi.org/10.1007/s13246-016-0472-8
21. Memar, P., Faradji, F.: A novel multi-class EEG-based sleep stage classification system. IEEE Trans. Neural Syst. Rehabil. Eng. **26**(1), 84–95 (2018). https://doi.org/10.1109/tnsre.2017.2776149

22. Da Silveira, T.L.T., Kozakevicius, A.J., Rodrigues, C.R.: Single-channel EEG sleep stage classification based on a streamlined set of statistical features in wavelet domain. Med. Biol. Eng. Comput. **55**(2), 343–352 (2016). https://doi.org/10.1007/s11517-016-1519-4
23. Pernkopf, F., O'Leary, P.: Feature selection for classification using genetic algorithms with a novel encoding. In: Skarbek, W. (eds.) Computer Analysis of Images and Patterns. CAIP 2001. Lecture Notes in Computer Science, vol. 2124. Springer, Berlin, Heidelberg (2001)
24. Braun, E.T., Kozakevicius, A.D.J., Da Silveira, T.L.T., Rodrigues, C.R., Baratto, G.: Sleep stages classification using spectral based statistical moments as features. Rev. Inf. Teór. Apl. **25**(1), 11 (2018)
25. Khalighi, S., Sousa, T., Santos, J.M., Nunes, U.: ISRUC-sleep: a comprehensive public dataset for sleep researchers. Comput. Methods Programs Biomed. **124**, 180–192 (2016)
26. Ocak, H.: A medical decision support system based on support vector machines and the genetic algorithm for the evaluation of fetal wellbeing. J. Med. Syst. **37**(2), 1–9 (2013)
27. Hanaoka, M., Kobayashi, M., Yamazaki, H.: Automated sleep stage scoring by decision tree learning. In: Proceedings of the 23rd Annual EMBS International Conference, Istanbul, Turkey, 25–28 Oct 2001
28. Chung, M.-H., Kuo, T.B., Hsu, N., Chu, H., Chou, K.-R., Yang, C.C.: Sleep and autonomic nervous system changes? Enhanced cardiac sympathetic modulations during sleep in permanent night shift nurses. Scand. J. Work Environ. Health 180–187 (2009)
29. Cortes, C., Vapnik, V.: Support vector networks. Mach. Learn. **20**(3), 273–297 (1995). Kavzoglu, T., Colkesen, I.: Classification of satellite images using decision trees: Kocaeli case. Electron. J. Map Technol. **2**(1), 36–45 (2010)
30. İlhan, H.O., Bilgin, G.: Sleep stage classification via ensemble and conventional machine learning methods using single channel EEG signals. Int. J. Intell. Syst. Appl. Eng. **5**(4), 174–184 (2017)
31. Bajaj, V., Pachori, R.B.: Automatic classification of sleep stages based on the time-frequency image of EEG signals. Comput. Methods Programs Biomed. **112**(3), 320–328 (2013)
32. Hsu, Y.-L., Yang, Y.-T., Wang, J.-S., Hsu, C.-Y.: Automatic sleep stage recurrent neural classifier using energy features of EEG signals. Neurocomputing **104**, 105–114 (2013)
33. Zibrandtsen, I., Kidmose, P., Otto, M., Ibsen, J., Kjaer, T.W.: Case comparison of sleep features from ear-EEG and scalp-EEG. Sleep Sci. **9**(2), 69–72 (2016)
34. Berry, R.B., Brooks, R., Gamaldo, C.E., Hardsim, S.M., Lloyd, R.M., Marcus, C.L., Vaughn, B.V.: The AASM Manual for the Scoring of Sleep and Associated Events: Rules, Terminology and Technical Specifications, Version 2.1. American Academy of Sleep Medicine, Darien (2014)
35. Sim, J., Wright, C.C.: The kappa statistic in reliability studies: use, interpretation, and sample size requirements. Phys. Ther. **85**(3), 257–268 (2005)
36. Liang, S.-F., Kuo, C.-E., Hu, Y.-H., Cheng, Y.-S.: A rule-based automatic sleep staging method. J. Neurosci. Methods **205**(1), 169–176 (2012)

On Comparative Study of Clustering Using Finite Mixture of Non-Gaussian Distributions

R. Deepana and C. Kiruthika

Abstract Finite mixture models are broadly used in model-based clustering approaches for heterogeneous data. Model-based clustering techniques attempt to optimize the fit between the given data and some mathematical model. This paper compares finite mixtures of non-normal distributions such as lognormal, geometric skew normal, skew Laplace, skew-*t*, and skew normal for model-based clustering approaches. The model selection criteria and parameter estimation for the finite mixture of the non-normal distribution are also discussed. The comparative study was carried out based on the new initialization technique for obtaining the initial component parameters in the EM algorithm. This comparative study is illustrated using real datasets.

Keywords Model-based clustering · Finite mixture models · Skewed distributions · EM algorithm · Model selection

1 Introduction

The main aim in cluster analysis is to find meaningful groups from the datasets. The "model-based" methods of clustering are based on finite mixture models. Model-based clustering is a popular technique for cluster analysis. Finite mixture models use a convex combination of probability density to model data that arises from two or more groups. In particular, Gaussian finite mixture models provide a framework for model-based clustering for heterogeneous data. The density of a G component finite mixture models is given by,

$$f(x) = \sum_{k=1}^{G} \pi_k f_k(x)$$

R. Deepana (✉)
Department of Mathematics, Hindustan University, Chennai 603103, India

C. Kiruthika
Department of Statistics, Pondicherry University, Puducherry 605014, India

© The Author(s), under exclusive license to Springer Nature Singapore Pte Ltd. 2022

S. R. Kannan et al. (eds.), *Fuzzy Mathematical Analysis and Advances in Computational Mathematics*, Studies in Fuzziness and Soft Computing 419,
https://doi.org/10.1007/978-981-19-0471-4_12

where $\pi_k > 0$ such that $\sum_{k=1}^{G} \pi_k = 1$ is the mixing proportions, and $f_k(x)$ is the kth component parametric finite mixture density, for $k = 1, 2, \ldots, G$. Each component density $f_k(x)$ is generally assumed to follow the same statistical distribution.

Finite mixture models of Gaussian and non-Gaussian distributions are widely used for model-based clustering approaches. The use of clustering applications in finite mixture models is explained in detail in the text books of Everitt and Hand [12], Titterington et al. [34], McLachlan and Basford [24], Lindsay [22], McLachlan and Peel [26], Fruhwirth-Schnatter [15], and Mengersen et al. [30]. Also, many review articles on clustering using finite mixture models are available, which include Banfield and Raftery [3], Melnykov and Maitra [29], Stahl and Sallis [33], McNicholas [28], Grun [16], and McLachlan et al. [27].

In recent times, there have been many contributions in the area of model-based clustering using finite mixtures of non-Gaussian distributions. In particular, finite mixtures of skew-*t* and skew normal distributions are used to capture the kurtosis and skewness in heterogeneous datasets directly without any transformation. Azzalini [2] proposed the skew normal distribution and also explained in detail the applications of this distribution. It is an alternative to normal distribution. The skew normal density function is dependent upon the additional shape parameter. It also includes Gaussian density as a special case. Davenport et al. [6] have compared two approaches to the estimation of component densities in univariate normal finite mixture distributions. McLachlan and Peel [25] considered the fitting of finite mixture models using an EM algorithm when the data are grouped and truncated. Lin et al. [20] introduced a robust finite mixture model based on the univariate skew-*t* distributions to deal with both heavy tails and skewness. They compared skew-*t* mixture models with other mixture models such as normal and t distributions. Lin et al. [21] have proposed the finite mixture model using the univariate skew normal distribution. The component of skew normal and skew-*t* mixture models is used to capture skewness and extreme outliers present in the datasets. Liu et al. [23] have proposed the use of a two-component finite mixture lognormal model to approximate lognormal sum distributions. Basso et al. [4] studied a class of finite mixture models where the component densities are scaled mixtures of the univariate skew normal distribution. Wengrzik [35] has proposed parameter estimation for finite mixture models in grouped data. They compared their work to other finite mixture models such as gamma, Weibull, and lognormal distributions. Sattayatham and Talangtam [32] have shown that the actual motor insurance claim can be fitted by a finite mixture model with a lognormal distribution. Deepana and Kiruthika [9, 10] have studied the possibility of using finite mixtures of lognormal and geometric skew normal distributions in clustering applications.

A skewed distribution plays a central role in clustering techniques when data follows asymmetric behavior and outliers. This paper provides a concise overview of model-based clustering using finite mixtures of lognormal, geometric skew normal, skew Laplace, skew normal, and skew-*t* distributions. Parameter estimation is carried out using an EM algorithm. Also, the EM algorithm is often sensitive to the choice of the initial values. An initialization technique for obtaining the initial component parameters in the EM algorithm is proposed in this paper, which is based on the

weighted k-means clustering algorithm [8]. For model selection, the Bayesian information criterion (BIC) and Akaike information criterion (AIC) criteria are used. The clustering performance is evaluated by the adjusted Rand index (ARI) and the misclassification rate (MR). An illustration is given based on the performance of finite mixtures of these distributions in clustering using a real dataset.

The remainder of this paper is organized as follows. In Sect. 2, the proposed initialization method for determining the initial values for the model parameters in the EM algorithm is presented. The model-based clustering using finite mixtures of lognormal, geometric skew normal, skew Laplace, skew normal, and skew-*t* distributions is discussed in Sect. 3. Section 4 presents numerical results and comparisons of the finite mixture models of lognormal, geometric skew normal, skew Laplace, skew normal, and skew-*t* to clustering. Finally, some concluding remarks are given in Sect. 5.

2 Initialization Method—Weighted K-means Algorithm (WKM)

The expectation–maximization (EM) algorithm is a tool for maximum likelihood estimation in model-based clustering using finite mixture models. The main pitfalls of the EM algorithm are good initial values, slow convergence, and stopping criteria. The issue of initialization techniques has been addressed by various researchers for model-based clustering methods. The standard technique for tackling the issue of initialization in the EM algorithm is the multiple restart approach (MREM). In MREM, each run is started with different random initial values [26]. The extension of the MREM method is emEM. The emEM initialization technique is proposed by Biernacki and Lourme [5]. The concept of emEM is to use the EM algorithm with several random initial values of the component parameters. Karlis and Xekalaki [17] have proposed a simulation study comparing several initialization techniques for finite mixture models in the univariate case. Another random initialization technique is called Rnd-spherical. The Rnd-spherical initialization method is to choose a mixing proportion equal to $1/G$. The component means are chosen randomly, and the variance is taken to be the proposed initialization technique for the EM algorithm is based on the weighted k-means algorithm discussed in Deepana [8].

Input: Dataset X and the number of groups G.

Output: Cluster indicator $z_1, z_2, \ldots, z_k$.

1. Determine the range of the dataset X.
2. Sort the data in ascending order based on the range.
3. Divide the sorted data into G groups.
4. Obtain the mean of the G groups. Take these mean as the initial mean for obtaining the weighted Euclidean distance measures.

5. Use Euclidean distance measure to calculate the distance between each sample x_i and cluster center C_k. The samples are assigned to the cluster at a minimum distance from the cluster center. The weights are obtained by minimizing the below equation using Lagrange's multiplier method.

$$M = \sum_{i=1}^{n} \sum_{k=1}^{G} (W_{ik})^{\alpha} D_{ik}$$

$$\text{Subject to} \sum_{k=1}^{G} W_{ik} = 1; \quad i = 1, 2, \ldots n$$

$$W_{ik} \geq 0$$

6. Calculate the weights for each sample using the equation

$$W_{ik} = 1 / \sum_{t=1}^{G} \left[\frac{D_{ik}}{D_{tk}} \right]^{1/\alpha - 1}; \; t = 1, 2, \ldots, G$$

where D_{ik} is the distance between ith sample and kth cluster centroid, and W_{ik} is the weight of the ith sample assigned to kth cluster. D_{tk} is the distance between tth sample in kth cluster centroid. W_{ik} can be expressed as $1/\alpha - 1$th root of reciprocal of sum of ratio of D_{tk} and D_{ik}. α is the parameter of weights. The main use of α is to decrease the noise points from a dataset given by clustering results. The α values affect the clustering results. If α value is too large, then it leads to poor performance, (or) it creates more noise points in the clustering results. If $\alpha = 1$, then it is equivalent to the clustering results of k-means clustering without weights. In general, it is suggested to take values of α between 2.001 and 2.09.

7. Repeat for ($k = 1, 2, \ldots, G$).
8. Assign the each observation to the closest mean.
9. Calculate the new mean values based on the assignments.
10. Repeat the same procedures until same means are obtained
11. end for

After the convergence is reached, find $\pi_k^{(0)}$, $\mu_k^{(0)}$, and $\sigma_k^{2^{(0)}}$ based on the cluster indicator $z_1, z_2, \ldots, z_k$. The above algorithm is used to obtain the initial values of component parameters in the EM algorithm. The initial values are to initiate the iterative procedures in the EM algorithm which is used in numerical experiments. The following section discusses the finite mixture models of some non-Gaussian distributions for cluster analysis.

3 Model-Based Clustering Using Non-Gaussian Distributions

In this section, model-based clustering using finite mixture models lognormal, geometric skew normal, skew Laplace, skew normal and skew-t distributions, and the EM algorithm are discussed.

3.1 Model-Based Clustering Using Lognormal Mixture Models

Let the dataset $\{X_1, X_2, \ldots, X_n\}$ be a random sample of size n from the lognormal mixture model and the finite mixture of lognormal density is given by

$$f(x;\theta_k) = \sum_{k=1}^{G} \pi_k \frac{1}{x\sqrt{2\pi}\sigma_k} \exp\left\{-1/2\sigma_k^2[\ln x - \mu_k]^2\right\};$$
$$x > 0, -\infty < \mu_k < \infty, \sigma_k > 0 \tag{1}$$

where $\pi_k > 0$ denotes mixing proportion with $\sum_{k=1}^{G} \pi_k = 1$, and $f(x;\theta_k)$ denotes the density of lognormal with corresponding parameters $\theta_k = \left\{\mu_k, \sigma_k^2\right\}$. Estimation of the model parameters of the lognormal mixture models is carried out by applying EM [11] algorithm.

E-step

The expectation of $l(\Theta; X, Z)$ over Z/X based on current parameter choice $\Theta^{(s)}$ is $Q(\Theta, \Theta^{(s)})$

$$\begin{aligned} Q(\Theta, \Theta^{(s)}) &= E_{Z/X}\left[l(\Theta; X, Z); \Theta^{(s)}\right] \\ &= \sum_{i=1}^{n}\sum_{k=1}^{G} \hat{\tau}_{ik} \log \pi_k + n/2 \log(2\pi) + \frac{1}{2}\sum_{i=1}^{n}\sum_{k=1}^{G} \hat{\tau}_{ik} \log\left(\sigma_k^2\right) \\ &\quad + \sum_{k=1}^{G}\sum_{i=1}^{n} \hat{\tau}_{ik} \log(x_i) - \sum_{k=1}^{G}\sum_{i=1}^{n} \hat{\tau}_{ik}\left(\frac{(\ln(x_i) - \mu_k)^2}{2\sigma_k^2}\right) \end{aligned} \tag{2}$$

where $\hat{\tau}_{ik}$ is the probability of observation i belonging group k based on the current parameter choice $\Theta^{(s)}$ and can be calculated by

$$\hat{\tau}_{ik} = \frac{\pi_k^{(s)} f_k\left(x_i; \mu_k^{(s)}, k^{(s)}\right)}{\sum_{k=1}^{G} \pi_k^{(s)} f_k\left(x_i; \mu_k^{(s)}, \sigma_k^{2(s)}\right)} \tag{3}$$

M-step

Find the estimated $\hat{\Theta}$, which maximizes $Q(\Theta, \Theta^{(s)})$ for fixed $\Theta^{(s)}$. Using Lagrange's multiplier $Q(\Theta, \Theta^{(s)})$ with subject to the equation, $\sum_{k=1}^{G} \pi_k = 1$. Maximize the equation

$$\psi = Q(\Theta, \Theta^{(s)}) + \lambda\left(1 - \sum_{k=1}^{G} \pi_k\right)$$

Maximize the function ψ and $Q(\Theta, \Theta^{(s)})$ with respect to π_k, μ_k, and σ_k^2 equating them 0.

$$\hat{\pi}_k = \frac{\sum_{i=1}^{n} \hat{\tau}_{ik}}{n}; \quad k = 1, 2, \ldots, G \tag{4}$$

$$\hat{\mu}_k = \frac{\sum_{i=1}^{n} \hat{\tau}_{ik} \ln(x_i)}{\sum_{i=1}^{n} \hat{\tau}_{ik}}; \quad k = 1, 2, \ldots, G \tag{5}$$

$$\hat{\sigma}_k^2 = \frac{\sum_{i=1}^{n} \hat{\tau}_{ik} \left(\ln(x_i) - \hat{\mu}_j\right)^2}{\sum_{i=1}^{n} \hat{\tau}_{ik}}; \quad k = 1, 2, \ldots, G \tag{6}$$

3.2 Model-Based Clustering Using Geometric Skew Normal Mixture Models

The concept of geometric skew normal (GSN) distribution is proposed by Kundu [19]. A random variable X follows a GSN distribution with parameters (μ, σ, p). The joint probability density function is given by

$$f(x; \mu, \sigma, p) = \frac{1}{\sigma\sqrt{2\pi n}} e^{-\frac{1}{2n\sigma^2}(x - n\mu)^2} p(1-p)^{n-1}; \\ 0 < p < 1, -\infty < x < \infty, \sigma > 0 \tag{7}$$

Note that if $p = 1$, the density of X reduces to the normal probability density function.

Finite mixture of GSN distributions is given by

$$f(x; \pi, \theta) = \sum_{k=1}^{G} \pi_k \frac{1}{\sigma_k\sqrt{2\pi n}} e^{-\frac{1}{2n\sigma_k^2}(x - n\mu_k)^2} p_k(1-p_k)^{n-1}; \quad 0 < p < 1 \tag{8}$$

Parameter estimation is carried out using EM algorithm. The estimated parameters are calculated in Deepana and Kiruthika [10] are used in this paper.

3.3 Model-Based Clustering Using Skew Laplace Mixture Models

Consider n independent random variables taken from a mixture of skew Laplace distribution. The density of G component finite mixture skew Laplace model is given by

$$f(x;\Theta) = \sum_{k=1}^{G} \pi_k \frac{1}{2\tau_k\sigma_k} \exp\left\{-\tau_k \frac{|x-\mu_k|}{\sigma_k} + \rho_k \frac{(x-\mu_k)}{\sigma_k^2}\right\} \tag{9}$$

Kheirolah et al. [18] have derived the observed information matrix for obtaining the asymptotic standard error of parameter estimates. They have also discussed the estimation of parameters in finite mixtures of skew Laplace distributions. In this paper, skew Laplace (SL) finite mixture modeling presented by Kheirolah et al. [18] is considered for model-based clustering. The initial value for the component parameters of skew Laplace finite mixtures is obtained by using Sect. 2.

3.4 Model-Based Clustering Using Skew Normal Mixture Models

The study of skew normal (SN) was first discussed by Azzalini [2]. A random variable X is said to be SN distribution, with location at μ, scale at σ, and shape parameter α. The SN distribution is denoted by $X \sim \mathrm{SN}(\mu, \delta^2, \alpha)$, and its probability density function is given by

$$f(x;\mu,\sigma,\alpha) = \frac{2}{\sigma}\varphi\left(\frac{x-\mu}{\sigma}\right)\Phi\left(\alpha\frac{x-\mu}{\sigma}\right); \quad x \in R;\ \sigma > 0;\ \mu,\alpha \in R \tag{10}$$

where φ and Φ denote the standard normal density and its distribution function, respectively. If $\mu = 0$ and $\sigma = 1$, it follows standard SN density, denoted by SN(α). The kth component density of SN mixture model is given by

$$f_k(x;\theta_k) = \sum_{k=1}^{G} \pi_k \frac{2}{\sigma_k}\varphi\left(\frac{x-\mu_k}{\sigma_k}\right)\Phi\left(\alpha_k\frac{x-\mu_k}{\sigma_k}\right) \tag{11}$$

where π_k represents the kth mixing proportions. The $f_k(x;\theta_k)$ denotes the component density of SN distribution, and θ is the parameter which is given by $\theta_k = \{\pi_1, \pi_2, \ldots, \pi_k, \mu_1, \mu_2, \ldots, \mu_k, \sigma_1, \sigma_2, \ldots, \sigma_k, \alpha_1, \alpha_2 \ldots, \alpha_k\}$. The maximum likelihood estimates of the parameters of Eq. (7) can be obtained by using EM algorithm. The estimated parameters is given by

$$\hat{\mu}_k = \frac{\sum_{i=1}^{n} \hat{\tau}_{ik} n\left(1 + \alpha_k^2 a_0\right)}{\sum_{i=1}^{n} \hat{\tau}_{ik} \sigma_k^2} \tag{12}$$

where $a_g = E\left[\left(\frac{x-\mu_k}{\sigma_k}\right)^g \left\{\frac{\alpha_k \varphi\left(\frac{x-\mu_k}{\sigma_k}\right)}{\alpha_k \Phi\left(\alpha_k \frac{x-\mu_k}{\sigma_k}\right)}\right\}\right];\ g = 0, 1, 2$

$$\hat{\sigma}_k^2 = \frac{\sum_{i=1}^{n} \hat{\tau}_{ik} n\left(1 + \alpha_k^2 a_2\right)}{\sum_{i=1}^{n} \hat{\tau}_{ik} \hat{\mu}_k^2} \tag{13}$$

$$\hat{\alpha}_k = \frac{\sum_{i=1}^{n} \hat{\tau}_{ik} n a_0}{\sum_{i=1}^{n} \hat{\tau}_{ik}} \tag{14}$$

3.5 *Model-Based Clustering Using Skew-*t *Mixture Models*

A random variable X is said to follow the Skew-t (ST) distribution $\mathrm{ST}\left(\mu, \sigma^2, \alpha, \nu\right)$ with location parameter $\mu \in R$, scale parameter $\sigma^2 \in (0, \infty)$, skewness parameter $\alpha \in R$ and degrees of freedom $\nu \in (0, \infty)$ if the following representation:

$$f(x; \mu, \sigma, \alpha, \nu) = \mu + \sigma \frac{Z}{\sqrt{\tau}},\ Z \sim \mathrm{SN}(\alpha),\ \tau \sim \sqrt{}(\nu/2, \nu/2) \tag{15}$$

Consider a kth component mixture model in which a set of random sample $X_1, X_2, \ldots, X_n$ arise from a mixture of ST distribution, given by

$$f_k(x; \theta_k) = \sum_{k=1}^{G} \pi_k f(x; \mu_k, \sigma_k, \alpha_k, \nu_k) \tag{16}$$

The $f_k(x; \theta_k)$ represents the component density of ST distribution, and θ is the parameter which is given by $\theta_k = \{\pi_1, \pi_2, \ldots, \pi_k, \mu_1, \mu_2, \ldots, \mu_k, \sigma_1, \sigma_2, \ldots, \sigma_k, \alpha_1, \alpha_2 \ldots, \alpha_k, \nu_1, \ldots, \nu_k\}$. Parameter estimation is carried out using an EM algorithm. In this paper, ST finite mixture modeling presented by Lin et al. [20] is considered for model-based clustering. The estimated parameters are obtained by Lin et al. [20] and are used in this paper.

The BIC is a long-established tool for model selection. Dasgupta and Raftery [7] proposed the use of BIC for model selection in the finite mixture for clustering technique. Many researchers considered BIC criteria for model selection in the clustering technique. We consider both AIC as well as BIC criteria herein. The BIC and AIC formula is given by

$$\mathrm{BIC} = 2l - m \log(n) \text{ and } \mathrm{AIC} = 2l - 2m$$

where l is the maximized observed data log likelihood; m is the number of parameters in the model, and n is the number of observations. The model with the largest BIC is selected. BIC has been a useful tool for selecting the model among finite mixture models [1, 14].

EM—Algorithm

Input: Dataset X and the number of components G.

1. **Initialization**: The initial values are obtained using the algorithm (WKM), random method and k-means (KM) clustering techniques.
2. **While** $\varepsilon > 0$;
3. **E-step**: To obtain the expected responsibilities $(\hat{\tau}_{ik}^{(s)})$ on each and every observation.
4. **M-step**: Update the parameters $\hat{\Theta}^{(s)}$.
5. Compute the log likelihood $(l_k^{(s)})$ and compare $l_{k+1}^{(s)}$ and $l_k^{(s)}$. If $\left\| l_{k+1}^{(s)} - l_k^{(s)} \right\| < \varepsilon$. STOP;
6. Compute model selection criteria based on BIC, AIC, ARI, and misclassification rate.
7. end for

Output: $\hat{\Theta}^{(s)}$, $\hat{\tau}_{ik}^{(s)}$, $l_k^{(s)}$, BIC, AIC, ARI, and MR.

Using the above EM algorithm, the component parameters using finite mixtures of skewed distributions for clustering are obtained.

4 Numerical Experiments

In this section, the clustering performance of the lognormal, geometric skew normal, skew Laplace, skew normal, and skew-t mixture models is assessed by its implementation on real datasets. The clustering performance of these mixture models is assessed in terms of BIC, AIC, ARI, and misclassification rate (MR). All numerical computations have been calculated through a program developed in R software. In this section, clustering results have been presented based on finite mixtures of skewed distributions.

4.1 Banknote Dataset

The Swiss banknote dataset is considered for model-based clustering using skewed mixture models. The Swiss banknote dataset consists of 200 observations (100 genuine and 100 counterfeit). The Swiss banknote dataset is available from the MixGHD package in R. The variable considered for this experiment is diagonal measurement. Descriptive statistics are presented for the Swiss banknote dataset in

Table 1 Descriptive statistics of banknote dataset

MIN	Q1	Median	Mean	Q3	MAX
137.8	139.5	140.4	140.5	141.5	142.4

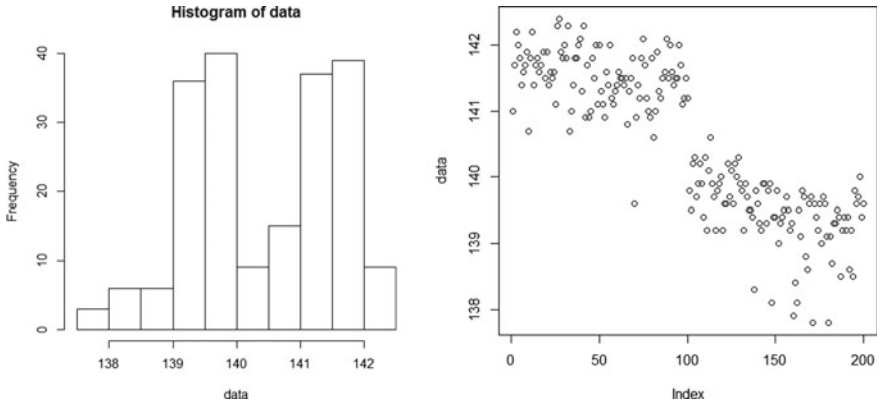

Fig. 1 Histogram and scatter plot for banknote dataset

Table 1. The banknote dataset is positively skewed. Figure 1a, b shows the scatter plot and histogram of the banknote dataset.

The banknote dataset shows an asymmetric pattern (Fig. 1a, b); hence, a two-component mixture model is fitted to the dataset. Three initialization techniques, namely random, k-means clustering, and weighted k-means clustering, are used for the EM algorithm. The initial values for the model parameters of the finite mixtures of the skewed distributions are obtained using these three initialization methods.

The known classification of the banknote dataset by status has two groups, and each group contains 100 observations. We ran the skewed mixture models with three initialization techniques. The summary of the clustering results is given in Table 2. For model comparison, BIC and AIC criteria are computed. Also, Table 2 shows the values of the misclassification rate, ARI, BIC, AIC, and log likelihood corresponding to the fitted two-component skewed mixture models. The solution with the largest BIC and AIC model is chosen for the five skewed finite mixtures, namely log normal, geometric skew normal, skew Laplace, skew normal, and skew-*t*. The same initial values and stopping criteria are applied for five skewed mixture models. The clustering performance of the skewed mixture models with three initialization techniques is compared with each other. A better clustering result is marked in Table 2.

It is observed that generally, LN mixture models achieved the lowest misclassification rate (0.02) and highest ARI (0.971), indicating close match to the true clustering for weighted k-means initialization technique. The GSN, SN, SL, and ST mixture models also gave reasonable clustering results, achieving moderate misclassification rates and ARI values compared to the LN mixture models. The LN mixture models fit well for banknote datasets, which is indicated by high BIC (565.26) and AIC

Table 2 Clustering performance of five skewed mixture models on the banknote dataset

Initialization techniques	Mixture models	BIC	AIC	MR	ARI	Log likelihood
Random	**LN**	**563.51**	**547.0184**	**0.075**	**0.931**	**−268.5092**
	GSN	546.25	538.53	0.14	0.8512	−245.54
	SL	539.49	535.95	0.12	0.8693	−249.52
	SN	559.62	540.26	0.11	0.918	−251.41
	ST	560.93	543.08	0.13	0.927	−253.52
KM	LN	562.18	544.43	0.07	0.909	−270.39
	GSN	547.26	528.51	0.10	0.928	−252.39
	SL	538.39	539.25	0.09	0.941	−249.36
	SN	558.15	539.01	0.095	0.933	−251.41
	ST	**563.38**	**549.76**	**0.065**	**0.963**	**−269.24**
WKM	**LN**	**565.26**	**548.21**	**0.02**	**0.971**	**−270.39**
	GSN	549.27	531.56	0.08	0.902	−252.39
	SL	541.35	541.37	0.07	0.928	−249.36
	SN	560.52	541.63	0.09	0.951	−251.41
	ST	561.27	544.15	0.10	0.967	−253.52

(548.21) values. The ST mixture model gives better results than the k-means-based initialization method. Table 3 presents the classified and misclassified samples for five skewed mixture models based on the three initialization techniques.

The number of misclassified bank notes is four with the weighted k-means initialization method for lognormal mixture models. Interestingly, for random initialization techniques, five notes are all true notes in genuine that have been misclassified as cluster 1, and ten notes are misclassified as cluster 2. The fitted and classification plot for LN mixture models is shown in Fig. 2. Figure 3 shows the classification results of GSN, SL, ST, and SN mixture models with different colors and symbols indicating different clusters.

4.2 Diabetes Dataset

The diabetes dataset is considered for this study. This dataset was first introduced by Reaven and Miller [31]. Later, it was analyzed by Fraley and Raftery [13], and this dataset is available in the Mclust package in R. The diabetes dataset consists of three measurements and 145 observations with three classes, such as chemical (36), overt (33), and normal (76). The steady-state plasma glucose (SSPG) variable is considered for this study because it shows asymmetric behavior. Descriptive statistics are provided in Table 4.

Table 3 Classification table for skewed mixture models using three initialization techniques

Actual group	Clusters		Actual group	Clusters		Actual group	Clusters	
	Cluster 1	Cluster 2		Cluster 1	Cluster 2		Cluster 1	Cluster 2
LN (Random)			LN (KM)			LN (WKM)		
1	95	5	1	93	7	1	100	0
2	10	90	2	7	93	2	4	96
GSN (Random)			GSN (KM)			GSN (WKM)		
1	84	16	1	89	11	1	92	8
2	12	88	2	9	91	2	8	92
SL (Random)			SL (KM)			SL (WKM)		
1	93	7	1	95	5	1	91	9
2	17	83	2	13	87	2	5	95
SN (Random)			SN (KM)			SN (WKM)		
1	91	9	1	92	8	1	92	8
2	13	87	2	11	89	2	10	90
ST (Random)			ST (KM)			ST (WKM)		
1	89	11	1	95	5	1	91	9
2	15	85	2	8	92	2	11	89

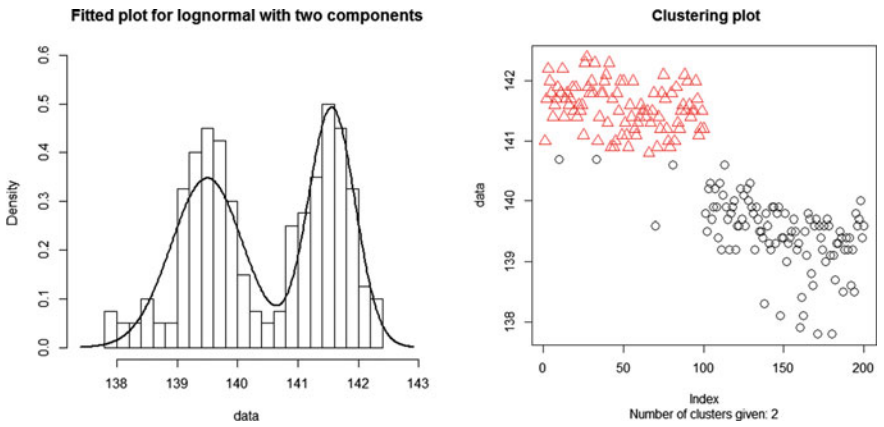

Fig. 2 Fitted plot and cluster plot of lognormal mixture models for banknote data

Figure 4 shows the scatter plot and histogram of the diabetes dataset. The histogram shows the data are positively skewed. The model-based clustering results using a finite mixture of skewed distributions for the diabetes dataset are summarized in Table 5. The AIC, BIC, ARI, MR, and log-likelihood values for five skewed distributions are presented in Table 5. Better results are marked in Table 5.

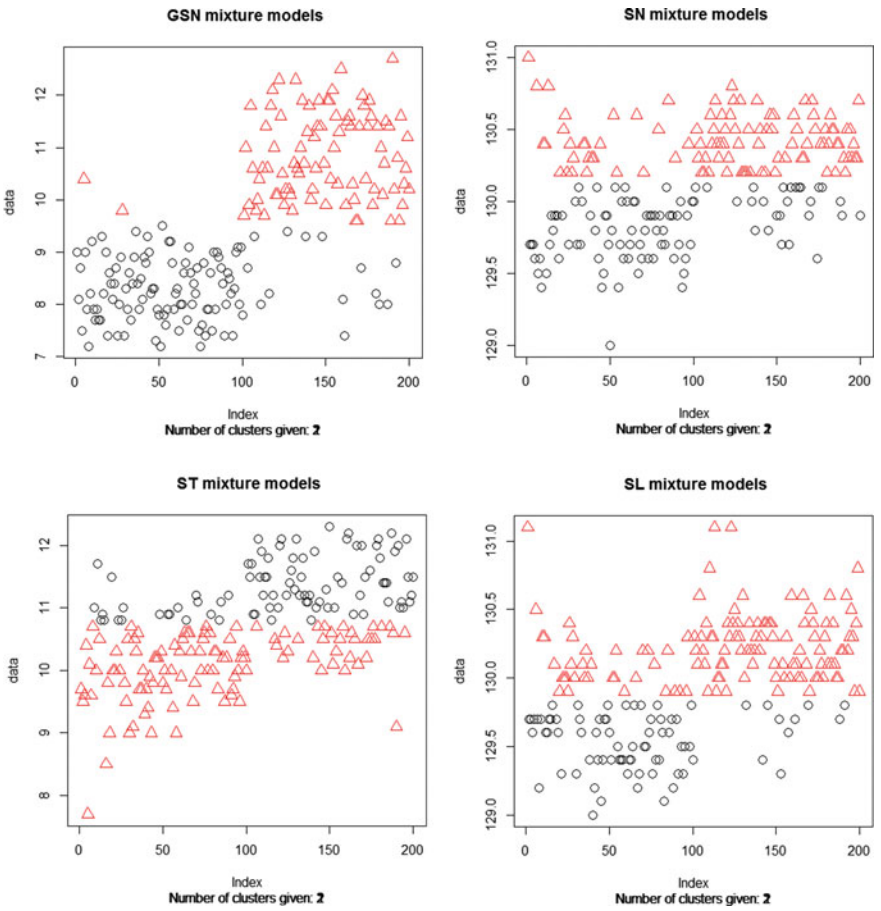

Fig. 3 Cluster plots for GSN, SN, ST, and SL mixture models using WKM initialization techniques

Table 4 Descriptive statistics of diabetes dataset

MIN	Q1	Median	Mean	Q3	MAX
10	118	156	186.1	221	748

For the diabetes dataset, among three initialization techniques, the weighted initialization technique produces better classification results for skewed mixture models. Overall, among the five mixture models using three initialization techniques, ST mixture models give better clustering results because they give the highest ARI and lowest misclassification rate. According to BIC and AIC values, the ST mixture models are fitted for the diabetes dataset.

From Table 6, it is observed that 11 samples are misclassified into other groups for skew-*t* mixture models based on the weighted k-means initialization technique.

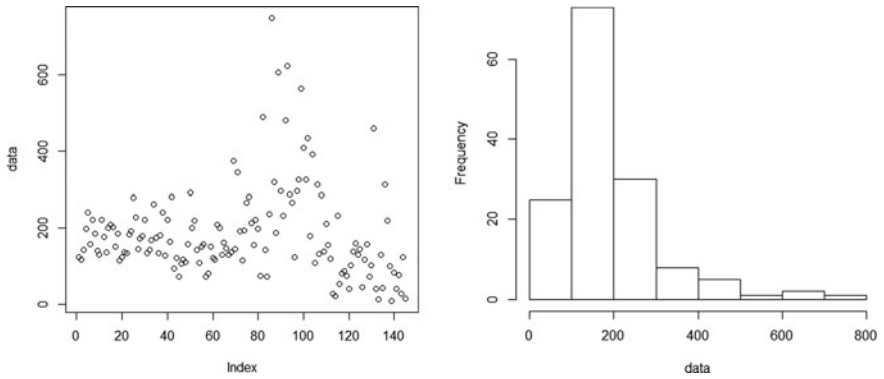

Fig. 4 Scatter plot and histogram for diabetes dataset with three components

Table 5 Clustering results for diabetes dataset using three initialization techniques

Initialization techniques	Mixture models	BIC	AIC	MR	ARI	Log likelihood
Random	LN	575.37	543.29	0.15	0.702	−280.03
	GSN	551.25	549.83	0.19	0.834	−276.36
	SL	450.26	419.29	0.27	0.723	−199.109
	SN	572.15	542.87	0.17	0.683	−279.26
	ST	**596.02**	**584.26**	**0.08**	**0.794**	**−285.69**
KM	LN	576.29	546.59	0.14	0.725	−281.13
	GSN	553.18	551.47	0.15	0.851	−280.95
	SL	452.37	423.13	0.28	0.796	−227.26
	SN	572.99	542.09	0.13	0.673	−279.18
	ST	**597.58**	**585.93**	**0.08**	**0.853**	**−288.35**
WKM	LN	577.42	548.32	0.13	0.748	−284.48
	GSN	556.39	553.54	0.12	0.894	−287.26
	SL	458.36	426.49	0.25	0.806	−218.48
	SN	574.29	543.19	0.16	0.697	−281.53
	ST	**599.16**	**589.37**	**0.07**	**0.893**	**−290.14**

For skew-*t* mixture models, 12 samples are misclassified into other groups based on the random and k-means initialization techniques. Figure 5 shows the clustering plot and fitted plot for skew-*t* mixture models with three components. The density plot in Fig. 5 shows three distinct peaks, and it shows that they are equally distributed. The clusters are represented using three different characters (o, +, and D). Figure 6 displays the clustering plot for GSN, SN, LN, and SL mixture models, with different colors indicating different clusters.

Table 6 Classification table for skewed mixture models

Actual group	Clusters			Actual group	Clusters		
	Cluster1	Cluster2	Cluster3		Cluster1	Cluster2	Cluster3
ST (Random)				ST (WKM)			
1	35	0	1	Chemical	36	0	0
2	1	29	3	Overt	1	28	4
3	2	5	69	Normal	2	4	70
LN (Random)				LN (WKM)			
Chemical	33	1	2	Chemical	35	1	0
Overt	3	27	3	Overt	1	28	4
Normal	3	10	63	Normal	2	11	63
GSN (Random)				GSN (WKM)			
Chemical	31	1	4	Chemical	36	0	0
Overt	5	22	6	Overt	1	28	4
Normal	6	9	61	Normal	0	13	63
SL (Random)				SL (WKM)			
Chemical	25	6	5	Chemical	28	4	4
Overt	7	18	8	Overt	7	20	6
Normal	4	10	62	Normal	8	8	60
SN (Random)				SN (WKM)			
Chemical	30	2	4	Chemical	35	1	0
Overt	4	26	3	Overt	0	29	4
Normal	3	10	63	Normal	2	9	65
LN (KM)				GSN (KM)			
Chemical	34	1	1	Chemical	35	1	0
Overt	4	25	4	Overt	2	26	5
Normal	2	9	65	Normal	1	14	61
SL (KM)				SN (KM)			
Chemical	26	5	5	Chemical	34	1	1
Overt	8	18	7	Overt	2	28	3
Normal	9	8	59	Normal	3	10	63
ST (KM)							
Chemical	35	1	0				
Overt	2	28	3				
Normal	3	3	70				

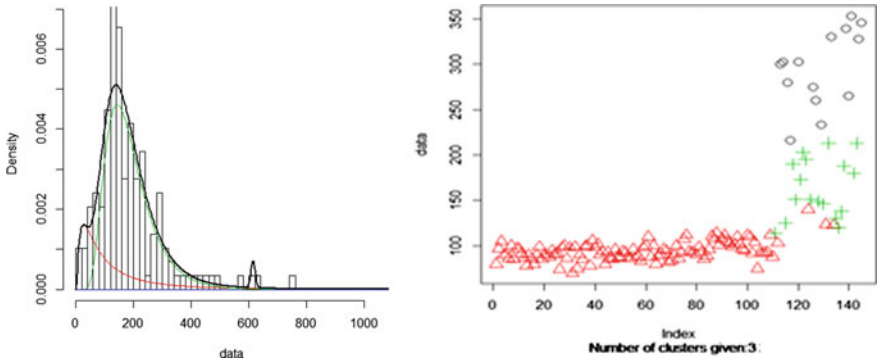

Fig. 5 Fitted and cluster plot of diabetes dataset for ST mixture models

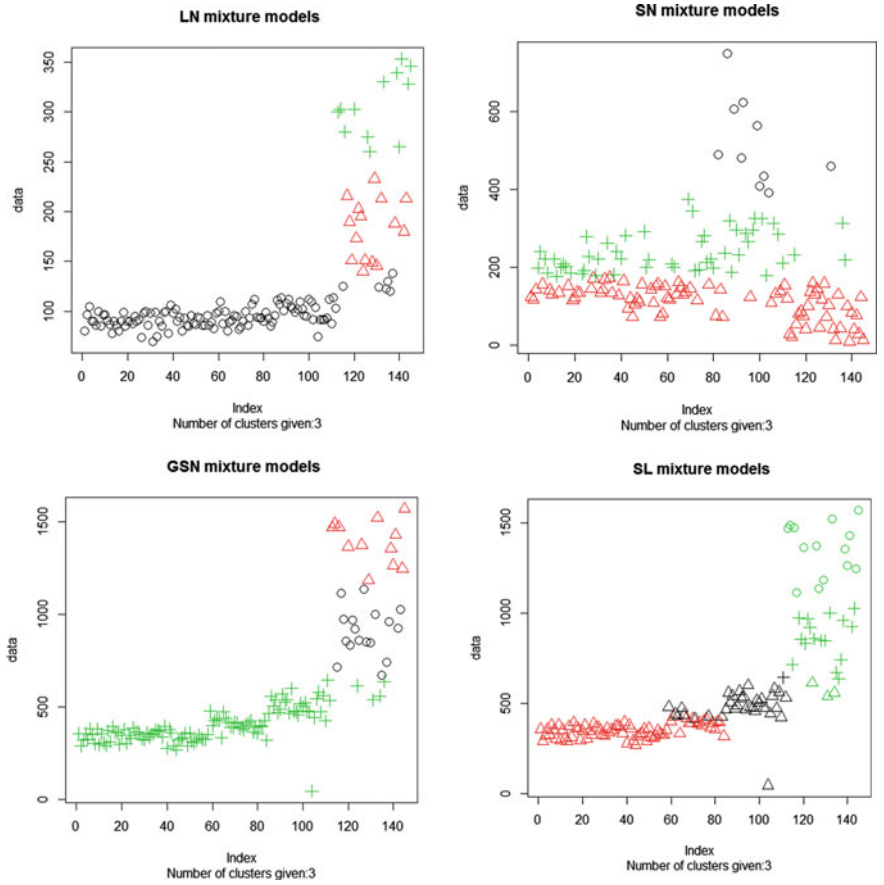

Fig. 6 Cluster plots for GSN, SN, LN, and SL mixture models using weighted k-means initialization techniques

5 Conclusion

In this paper, we have discussed some of the more popular skewed distributions in finite mixture models for clustering. The clustering results are compared to those obtained via skewed mixture models based on three initialization techniques. In both the banknote and diabetes illustrations, the model-based clustering using skewed mixture models gave better clustering results with respect to the true labels. Among five skewed mixture models, it has been observed that from the real datasets, the weighted k-means initialization technique produces better clustering results for non-normal mixture models.

References

1. Andrews, J.L., McNicholas, P.D.: Extending mixtures of multivariate t-factor analyzers. Stat. Comput. **21**(3), 361–373 (2011)
2. Azzalini, A.: A class of distributions which includes the normal ones. Scand. J. Stat. (Theory Appl.) **12**(2), 171–178 (1985)
3. Banfield, J.D., Raftery, A.E.: Model-based Gaussian and non-Gaussian clustering. Biometrics **49**(3), 803–821 (1993)
4. Basso, R.M., Lachos, V.H., Cabral, C.R.B., Ghosh, P.: Robust mixture modeling based on scale mixtures of skew-normal distributions. Comput. Stat. Data Anal. **54**(12), 2926–2941 (2010)
5. Biernacki, C., Lourme, A.: Stable and visualizable Gaussian parsimonious clustering models. Stat. Comput. **24**(6), 953–969 (2014)
6. Davenport, J.W., Bezdek, J.C., Hathaway, R.J.: Parameter estimation for finite mixture distributions. Comput. Math. Appl. **15**(10), 819–828 (1988)
7. Dasgupta, A., Raftery, A.E.: Detecting features in spatial point processes with clutter via model-based clustering. J. Am. Stat. Assoc. **93**(441), 294–302 (1998)
8. Deepana, R.: On sample weighted clustering algorithm using Euclidean and Mahalanobis distances. Int. J. Stat. Syst. **12**(3), 421–430 (2017)
9. Deepana, R., Kiruthika, C.: Model based clustering using finite mixture models of lognormal distribution. Res. Rev. J. Stat. **7**(3), 58–67 (2018)
10. Deepana, R., Kiruthika, C.: Clustering using finite geometric skew normal mixture models. Int. J. Sci. Res. Math. Stat. Sci. **6**(3), 136–143 (2019)
11. Dempster, A.P., Laird, N.M., Rubin, D.B.: Maximum likelihood for incomplete data via the EM algorithm. J. R. Stat. Soc. Ser. B (Methodol.) **39**(1), 1–38 (1977)
12. Everitt, B.S., Hand, D.J.: Finite Mixture Distributions, Monographs on Applied Probability and Statistics. Chapman and Hall, London (1981)
13. Fraley, C., Raftery, A.E.: How many clusters? Which clustering methods? Answers via model-based cluster analysis. Comput. J. **41**(8), 578–588 (1998)
14. Fraley, C., Raftery, A.E.: Model-based clustering, discriminant analysis, and density estimation. J. Am. Stat. Assoc. **97**(458), 611–631 (2002)
15. Fruhwirth-Schnatter, S.: Finite Mixture and Markov Switching Models. In: Springer Series in Statistics. Springer, New York (2006)
16. Grun, B.: Model based clustering. J. Stat. Methodol. 1–38 (2018)
17. Karlis, D., Xekalaki, E.: Choosing initial values for the EM algorithm for finite mixtures. Comput. Stat. Data Anal. **41**(3–4), 577–590 (2003)
18. Kheirolah, O., Mozafari, M., Naderi, M.: Skew Laplace finite mixture modeling. J. Iran. Stat. Soc. **16**(2), 97–110 (2017)

19. Kundu, D.: Geometric skew normal distribution. Sankhya Indian J. Stat. B **76**(2), 167–189 (2014)
20. Lin, T.I., Lee, J.C., Hsieh, W.J.: Robust mixture modeling using the skew t distribution. Stat. Comput. **17**(2), 81–92 (2007)
21. Lin, T.I., Lee, J.C., Yen, S.Y.: Finite mixture modelling using the skew normal distribution. Stat. Sin. **17**(3), 909–927 (2007)
22. Lindsay, B.G.: Mixture models: theory, geometry, and applications. In: NSF-CBMS Regional Conference Series in probability and Statistics, vol. 5. Institute of Mathematical Statistics and the American Statistical Association, Alexandria, VA (1995)
23. Liu, Z., Almhana, J., Wang, F., McGorman, R.: Mixture lognormal approximations to lognormal sum distributions. IEEE Commun. Lett. **11**(9), 711–713 (2007)
24. McLachlan, G.J., Basford, K.E.: Mixture Models: Inference and Applications, Statistics: Textbooks and Monographs. Marcel Dekker, New York (1988)
25. McLachlan, G.J., Peel, D.: Robust cluster analysis via mixtures of multivariate-t distributions. In: Lecture Notes in Computer Science, vol. 1451, pp. 658–666. Springer-Verlag, Berlin (1998)
26. McLachlan, G.J,. Peel, D.: Finite Mixture Models. In: Wiley Series in Probability and Statistics. Wiley, New York (2000)
27. McLachlan, G.J., Lee, X.L., Rathnayake, I.S.: Finite mixture models. Annu. Rev. Stat. Appl. **6**(1), 355–378 (2019)
28. McNicholas, P.D.: Model-based clustering. J. Classif. **33**(3), 331–373 (2016)
29. Melnykov, V., Maitra, R.: Finite mixture models and model based clustering. Stat. Surv. **4**, 80–116 (2010)
30. Mengersen, K.L., Robert, C.P., Titterington, D.M.: Mixtures: Estimation and Applications. In: Wiley Series in Probability and Statistics. Wiley, New York (2011)
31. Reaven, G.M., Miller, R.G.: An attempt to define the nature of chemical diabetes using a multidimensional analysis. Diabetologia **16**, 17–24 (1979)
32. Sattayatham, P., Talangtam, T.: Fitting of finite mixture distributions to motor insurance claims. J. Math. Stat. **8**(1), 49–56 (2012)
33. Stahl, D., Sallis, H.: Model-based cluster analysis. WIREs Comput. Stat. **4**(4), 341–358 (2012)
34. Titterington, D., Smith, A., Makov, U.: Statistical Analysis of Finite Mixture Distributions. In: Wiley Series in Probability and Mathematical Statistics, Applied Probability and Statistics. Wiley, New York (1985)
35. Wengrzik, J.: Parameter estimation for mixture models given grouped data. Dissertation, University of Bremen, Bremen (2012)

$M/G/1$ Retrial Queueing System with Working Vacation and Starting Failure

P. Rajadurai, R. Madhumidha, M. Sundararaman, and D. Narasimhan

Abstract A single server retrial queueing model with multiple working vacations and starting failure is discussed in this paper. The server goes for multiple working vacations when orbit becomes empty at any service completion instant. We obtain the steady-state probability generating function (PGF) for this model's system size and orbit size, mean orbit size, and mean system size by using the supplementary variable technique. Necessary system performance measures and some exceptional cases are discussed.

Keywords Retrial queue · Working vacation · Starting failure

1 Introduction

The topic of retrial queues and working vacation in queueing theory has been an exciting research topic in the last two decades from Artalejo and Corral [1] and Chandrasekaran et al. [2]. Such queueing systems play essential roles in analyzing many telephone switching systems, telecommunication networks, and computer systems. In the working vacation period, the server serves customers at a lower service rate. This queueing model like network service, web service, etc. Some of the authors [3–6] have recently analyzed a single server retrial queue with working vacations. In this paper, we have generalized the concept of working vacations in the presence of starting failure breakdowns.

P. Rajadurai (✉) · R. Madhumidha · M. Sundararaman · D. Narasimhan
Department of Mathematics, Srinivasa Ramanujan Centre, SASTRA Deemed University, Kumbakonam, Tamil Nadu 612001, India
e-mail: narasimhan@src.sastra.edu

© The Author(s), under exclusive license to Springer Nature Singapore Pte Ltd. 2022

S. R. Kannan et al. (eds.), *Fuzzy Mathematical Analysis and Advances in Computational Mathematics*, Studies in Fuzziness and Soft Computing 419,
https://doi.org/10.1007/978-981-19-0471-4_13

2 Description of the Model

We investigate an $M/G/1$ retrial queueing system with working vacation and starting failure. The description of the basic assumption of the model is as follows:

(i) **Arrival process**: The customers arrive into the system according to a Poisson process of rate λ. There are two types of customers arriving into the system. They are ordinary and priority customers.
(ii) **The retrial process**: If an arriving customer finds the server free, they get service immediately. Otherwise, the customer finds the server busy, then they join the pool of waiting customers called orbit in accordance with FCFS discipline. Inter-retrial times have an arbitrary distribution $R(t)$ with corresponding Laplace–Stieltjes transform (LST) $R^*(v)$.
(iii) **The regular service process**: A single server in the normal busy period provides regular service and no option for re-service. Service time has a general distribution $S_b(t)$ with corresponding LST $S_b^*(v)$.
(iv) **The working vacation process**: The server begins a working vacation each time when the orbit becomes empty. During this period, the server gives lower speed service. If there are customers in orbit at the lower speed service completion instant, the server will stop the vacation and return to the normal busy period. When vacation ends, the server switches to the normal working level if customers are in orbit. The vacation time follows exponential distribution $S_v(t)$ with corresponding LST $S_v^*(t)$.
(v) **The repair process**: When the server fails, it will be sent to repair immediately. After completion of the repair, the server will treat as well as new. The repair time of the server is assumed to be arbitrarily distributed with distribution function $G(t)$ having LST $G^*(v)$.

3 Steady-State Analysis of the System

For an $M/G/1$ retrial queueing with working vacation and starting failure, we develop the steady-state difference-differential equations based on the supplementary variable technique (SVT).

The following processes are retrial, regular service, working vacation service, and repair, considered a general distribution. The distribution functions are $R(x)$, $S_b(x)$, $S_v(x)$ and $G(x)$ Laplace–Stieltjes transforms for the above process, $R^*(\theta)$, $S_b^*(\theta)$, $S_v^*(\theta)$ and $G^*(\theta)$ and the elapsed time at t for the above process, $R^0(t)$, $S_b^0(t)$ $S_v^0(t)$ and $G^0(t)$. The conditional completion rates are $r(x)\mathrm{d}x = \frac{\mathrm{d}R(x)}{1-R(x)}$, $\mu_b(x)\mathrm{d}x = \frac{\mathrm{d}S_b(x)}{1-S_b(x)}$, $\mu_v(x)\mathrm{d}x = \frac{\mathrm{d}S_v(x)}{1-S_v(x)}$, $\eta(x)\mathrm{d}x = \frac{\mathrm{d}G(x)}{1-G(x)}$.

Assume that $R(0) = 0$, $R(\infty) = 1$,$S_b(0) = 0$, $S_b(\infty) = 1$, $S_v(0) = 0$, $S_v(\infty) = 1$ $G(0) = 0$, $G(\infty) = 1$ are continuous at $x = 0$.

Further, the random variables for the bivariate Markov process $(C(t), N(t), t \geq 0)$ are presented, where $N(t)$ is the number of customers in the orbit at time t and $C(t)$ denotes the server state (0, 1, 2, 3, 4). The server states depend on whether the server state is idle, free, busy on regular service, working vacation periods, and repair.

The state probabilities are defined as follows:
$P_0(t) = P\{C(t) = 0, N(t) = 0\}$ and for $t \geq 0, x \geq 0, n \geq 1$,
$P_n(x,t)\mathrm{d}x = P\{C(t) = 1, N(t) = n, x \leq R^0(t) < x + \mathrm{d}x\}$,
$Q_n(x,t)\mathrm{d}x = P\{C(t) = 2, N(t) = n, x \leq S_{\mathrm{b}}^0(t) < x + \mathrm{d}x\}$,
$R_n(x,t)\mathrm{d}x = P\{C(t) = 3, N(t) = n, x \leq S_{\mathrm{v}}^0(t) < x + \mathrm{d}x\}$,
$S_n(x,t)\mathrm{d}x = P\{C(t) = 4, N(t) = n, x \leq G^0(t) < x + \mathrm{d}x\}$.

Then the limiting probabilities are $P_0(x) = \lim_{t\to\infty} P_0(t)$,
$P_n(x) = \lim_{t\to\infty} P_n(x,t)$, $Q_n(x) = \lim_{t\to\infty} Q_n(x,t)$,
$R_n(x) = \lim_{t\to\infty} R_n(x,t)$, $S_n(x) = \lim_{t\to\infty} S_n(x,t)$.

3.1 The Steady-State Equations

Using the method of SVT, we obtain the following system of equations.

$$(\lambda+\theta)P_0 = \theta P_0 + \int_0^\infty Q_0(x)\mu_{\mathrm{b}}(x)\mathrm{d}x + \int_0^\infty R_0(x)\mu_{\mathrm{v}}(x)\mathrm{d}x + \int_0^\infty S_1(x)\eta(x)\mathrm{d}x \tag{1}$$

$$\frac{\mathrm{d}P_n(x)}{\mathrm{d}x} + (\lambda + r(x))P_n(x) = 0, n \geq 1 \tag{2}$$

$$\frac{\mathrm{d}Q_n(x)}{\mathrm{d}x} + (\lambda + \mu_{\mathrm{b}}(x))Q_n(x) = \lambda Q_{n-1}(x), n \geq 1. \tag{3}$$

$$\frac{\mathrm{d}R_n(x)}{\mathrm{d}x} + (\lambda + \mu_{\mathrm{v}}(x) + \theta)R_n(x) = \lambda R_{n-1}(x), n \geq 1. \tag{4}$$

$$\frac{\mathrm{d}S_n(x)}{\mathrm{d}x} + (\lambda + \eta(x))S_n(x) = \lambda S_{n-1}(x), n > 1. \tag{5}$$

The steady-state boundary conditions at $x = 0$ are

$$P_n(0) = \int_0^\infty Q_n(x)\mu_{\mathrm{b}}(x)\mathrm{d}x + \int_0^\infty R_n(x)\mu_{\mathrm{v}}(x)\mathrm{d}x + \int_0^\infty S_n(x)\eta(x)\mathrm{d}x, n \geq 1 \tag{6}$$

$$Q_n(0) = \alpha \int_0^\infty \lambda P_n(x)\mathrm{d}x + \alpha \int_0^\infty P_{n+1}(x)r(x) + \int_0^\infty \theta R_n(x)\mathrm{d}x, n \geq 1 \quad (7)$$

$$R_0(0) = \lambda P_0, n \geq 0 \quad (8)$$

$$R_n(0) = 0 \quad (9)$$

$$S_n(0) = \bar{\alpha} \int_0^\infty \lambda P_{n-1}(x)\mathrm{d}x + \bar{\alpha} \int_0^\infty r(x) P_n(x)\mathrm{d}x \quad (10)$$

The normalization condition is

$$P_0 + \sum_{n=1}^{\infty} P_n(x)\mathrm{d}x + \sum^{\infty} \left(\int_0^\infty Q_n(x)\mathrm{d}x + \int_0^\infty R_n(x)\mathrm{d}x + \int_0^\infty S_n(x)\mathrm{d}x \right) = 1 \quad (11)$$

3.2 The Steady-State Solutions

To analyze the developed queueing model, we make use of the SVT and PGF methods.

We define the generating functions for $|z| < 1$ as follows: $P(x, z) = \sum_{n=1}^{\infty} P_n(x)z^n$; $Q(x, z) = \sum_{n=0}^{\infty} Q_n(x)z^n$; $R(x, z) = \sum_{n=0}^{\infty} R_n(x)z^n$; $S(x, z) = \sum_{n=0}^{\infty} S_n(x)z^n$.

Multiplying the steady-state equations and boundary condition (1) to (10) by z^n and summing over n, $(n = 0, 1, 2, \ldots)$ and make some manipulation, finally, we get the limiting probability generating functions $P(x, z)$, $Q(x, z)$, $R(x, z)$, and $S(x, z)$.

Next we are interested in investigating the marginal orbit size distributions due to system state of the server in following results.

3.3 Results

Under the stability condition $\rho < R^*(\lambda)$, the PGF of the number of customers in the orbit when the server is idle, busy, working vacation, and under repair are given by

$$P(z) = \int_0^\infty P(x, z)\mathrm{d}x \quad (12)$$

$$P(z) = \frac{z(1 - R^*(\lambda))P_0[\alpha v(z)S_{\mathrm{b}}^*(\lambda - \lambda z) + \alpha S_{\mathrm{v}}^*(\lambda - \lambda z) + \bar{\alpha}G^*(\lambda - \lambda z) - 1]}{z - R(z)(\alpha S_{\mathrm{b}}^*(\lambda - \lambda z) + \bar{\alpha} z G^*(\lambda - \lambda z))}$$

$$Q(z) = \int_0^\infty Q(x, z)\mathrm{d}x \tag{13}$$

$$Q(z) = \frac{\alpha P_0(1 - S_b^*(\lambda - \lambda z))[R(z)(\alpha S_v^*(\lambda - \lambda z) + \bar{G}^*(\lambda - \lambda z)(1 - zv(z)) - 1) + zv(z)]}{(1 - z)[z - R(z)(\alpha S_b^*(\lambda - \lambda z) + \bar{\alpha} G^*(\lambda - \lambda z))]}$$

$$R(z) = \int_0^\infty R(x, z)\mathrm{d}x = \alpha\lambda P_0 \frac{v(z)}{\theta} \tag{14}$$

$$S(z) = \int_0^\infty S(x, z)\mathrm{d}x \tag{15}$$

$$S(z) = \frac{z\bar{\alpha} P_0[\Gamma(z)](1 - G^*(\lambda - \lambda z))}{(1 - z)[z - R(z)(\alpha S_b^*(\lambda - \lambda z) + \bar{\alpha} z G^*(\lambda - \lambda z))]}$$

where

$$R(z) = R^*(\lambda) + z(1 - R^*(\lambda))$$

$$\Gamma(z) = R(z)(\alpha(S_v^*(\lambda - \lambda z) + S_b^*(\lambda - \lambda z)(v(z) - 1)) + (1 - z)\bar{\alpha} G^*(\lambda - \lambda z) - 1) + z$$

$$v(z) = \frac{1 - S_v^*(\theta + \lambda - \lambda z)}{\theta + \lambda - \lambda z}$$

Applying the normalizing condition, $P_0 + P(1) + Q(1) + R(1) + S(1) = 1$ and using the equations by setting $z = 1$ in (12) to (15), we get the idle probability P_0.

Corollary 1 *If the system satisfies the stability condition, $\rho < R^*(\lambda)$.*
The PGF of the number of customers in the system

$$K(z) = P_0 + P(z) + zQ(z) + zR(z) + S(z) \tag{16}$$

The PGF of the number of customers in the orbit

$$H(z) = P_0 + P(z) + Q(z) + R(z) + S(z). \tag{17}$$

4 Performance Measures

By setting $z = 1$ and applying L-Hospital's rule whenever necessary, then we get the following results:

(i) Let P be the steady-state probability that the server is idle during the retrial time

$$P(1) = \left[\alpha\lambda(1 - s_{\mathrm{v}}^{*}(\theta))\left(E(S_{\mathrm{b}}) + \frac{1}{\theta}\right) + \bar{\alpha}\lambda E(G)\right]\frac{P_0(1 - R^{*}(\lambda))}{\eta}$$

(ii) The probability that the server is busy serving a customer is given by

$$Q(1) = \frac{\alpha\lambda E(S_{\mathrm{b}})p_0}{\eta}[\bar{\alpha}S_{\mathrm{v}}^{*}(\theta)\lambda E(G)] + S_{\mathrm{v}}^{*'}(\theta)(\theta - \bar{\alpha}\lambda) + ((1 - S_{\mathrm{v}}^{*}(\theta))\left[\alpha\left(1 - \frac{\lambda}{\theta}\right) - (1 + R^{*}(\lambda))\right]$$

(iii) The probability that the server is on working vacation is given by

$$R(1) = \frac{\alpha\lambda P_0(1 - S_{\mathrm{v}}^{*}(\theta))}{\theta}$$

(iv) The probability that the server is on repair under starting failure is given by

$$S(1) = \left[R^{*}(\lambda) - \left[\bar{\alpha} + \alpha\left(\lambda E(S_{\mathrm{b}})S_{\mathrm{v}}^{*}(\theta) + \frac{\lambda}{\theta}\left(1 - S_{\mathrm{v}}^{*}(\theta)\right)\right)\right]\right]\frac{\bar{\alpha}\lambda P_0 EG}{\eta}$$

where $\eta = R^{*}(\lambda) - (\alpha\lambda E(s_{\mathrm{b}}) + \bar{\alpha}(1 + \lambda E(G)))$.

(v) The expected number of customers in the orbit L_{q} is obtained by differentiating with concerning z and evaluating at $z = 1$,

$$L_{\mathrm{q}} = H'(1) = \lim_{z\to 1}\frac{\mathrm{d}}{\mathrm{d}z}H(z)$$

$$\text{(i.e.),}\ L_{\mathrm{q}} = P_0 + P^{'}(1) + Q^{'}(1) + R^{'}(1) + S^{'}(1)$$

where $P^{'}(1) = \mathrm{Nr1/Dr}$, $Q^{'}(1) = \mathrm{Nr2/Dr}$, $S^{'}(1) = \mathrm{Nr3/Dr}$

$$\begin{aligned}\mathrm{Nr1} = P_0(1-R^*(\lambda))[2(\alpha\lambda(1-S_{\mathrm{v}}^*(\theta))(E(S_{\mathrm{b}})+\frac{1}{\theta}))\\ +\bar{\alpha}\lambda E(G)+\alpha\lambda^2 E(s_{\mathrm{b}}^2)(\frac{(1-S_{\mathrm{v}}^*(\theta))}{\theta})+\alpha 2\lambda E(s_{\mathrm{b}})v^{'}(1)\\ +\alpha\frac{\lambda^2}{\theta^2}(1-S_{\mathrm{v}}^*(\theta))+\bar{\alpha}\lambda^2 E(G^2)]\end{aligned}$$

$$\mathrm{Nr2} = \alpha P_0\left\{-3s_{\mathrm{b}}^{'}A_{\mathrm{b}}^{'}J^{'}-5\alpha^2 E(s_{\mathrm{b}}^2)I\right\}$$

$$\begin{aligned}J^{'} = (1-R^*(\lambda))[\alpha\lambda s_{\mathrm{v}}^{*''}(\theta)-\bar{\alpha}(zv^{''}(1)+2v^{'}(1))-2\alpha\lambda E(G)\\ \left(v^{'}(1)+\left(\frac{(1-S_{\mathrm{v}}^{'}(\theta))}{\theta}\right)\right)+\bar{\alpha}E(G^2(1-v(1))]\end{aligned}$$

$$R^{'}(1) = \alpha\lambda P_0\frac{v^{'}(1)}{\theta}$$

$$\mathrm{Nr3} = \bar{\alpha}P_0\left\{-3\lambda E(G)J^{''}-5(1-R^*(\lambda))J\right\}$$

where

$$\begin{aligned}J^{''} = \alpha\lambda^2 s_{\mathrm{v}}^{''}(\theta)+\alpha\lambda^2 E(s_{\mathrm{b}}^2)(v(1)-1)+2\alpha v^{'}(1)\lambda E(s_{\mathrm{b}})\\ -2\bar{\alpha}\lambda E(G)-\bar{\alpha}\end{aligned}$$

$$J = \bar{\alpha}\lambda P_0 E(G)[R^*(\lambda)-[\bar{\alpha}+\alpha(\lambda E(S_{\mathrm{b}})S_{\mathrm{v}}^*(\theta)+\frac{\lambda}{\theta}(1-S_{\mathrm{v}}^*(\theta)))]]$$

$$\begin{aligned}\mathrm{Dr} = -[2(1-R^*(\lambda)\,(\alpha\lambda E(s_{\mathrm{b}})+\bar{\alpha}(1+\lambda E(G)))\\ +\alpha\lambda^2 E(s_{\mathrm{b}}^2)+2\bar{\alpha}\lambda E(G)+\bar{\alpha}\lambda^2 E(G^2)]\end{aligned}$$

$$v^{'}(1) = \frac{\lambda}{\theta}\left[1-s_{\mathrm{v}}^*(\theta)+\theta s_{\mathrm{v}}^{*'}(\theta)\right]$$

(vi) The mean number of customers in the system L_{s} under steady-state condition is obtained by differentiating concerning z and evaluating at $z = 1$,

$$L_{\mathrm{s}} = K'(1) = \lim_{z\to 1}\frac{\mathrm{d}}{\mathrm{d}z}K(z) = L_{\mathrm{q}}+\rho$$

(vii) The average time a customer spends in the system (W_s) is $W_s = \frac{L_s}{\lambda}$.

(viii) The average time a customer spends in the queue (W_q) is $W_q = \frac{L_q}{\lambda}$.

5 Special Cases

(i) **No working vacation and no starting failure**

In this case, the model is reduced to an $M/G/1$ retrial queueing system when $\theta = \alpha = 0$.

(ii) **No retrial, no working vacation, and no starting failure**

By substituting $a = \theta = \alpha = 0$, this model reduced to $M/G/1$ queue with general retrial queues.

6 Conclusion

We have studied an $M/G/1$ retrial queueing system with working vacation and starting failure in this work. Applying the PGF approach and the supplementary variable technique, the probability generating functions for the numbers of customers in the system and its orbit when it is free, regular busy, on lower speed service, and on repair under starting failure are derived. Various system performance measures and some important exceptional cases are discussed. Further, the explicit expressions for the average queue length of orbit and system are also obtained.

References

1. Artalejo, J.R., Corral: Retrial Queueing Systems. Springer, Berlin, Germany (2008)
2. Chandrasekaran, V.M., Indhira, K., Saravanarajan, M.C., Rajadurai, P.: A survey on working vacation queueing models. Int. J. Pure Appl. Math. **106**(6), 33–41 (2016)
3. Wu, D., Takagi, H.: M/G/1 retrial queue with multiple working vacations. Perform. Eval. **63**, 654–681 (2006)
4. Rajadurai, P.: A study on M/G/1 preemptive priority retrial queue with Bernoulli working vacations and vacation interruption. Int. J. Process Manag. Benchmark. **9**(2), 193–215 (2019)
5. Krishnakumar, K., Vijayakumar, A., Madheswari, S.P.: The M/G/1 retrial queue with feedback and starting failures. Appl. Math. Model. **26**(11), 1057–1075 (2002)
6. Arivudainambi, D., Godhandaraman, P., Rajadurai, P.: Performance analysis of single server retrial queue with working vacation. OPSEARCH **51**(3), 434–462 (2014)

Analysis of $MAP/PH_1, PH_2/2$ Queue with Working Breakdown, Starting Failure, and Bernoulli Vacation

G. Ayyappan and R. Gowthami

Abstract In this article, we examine a classical queueing model with heterogeneous servers. Customers reach the system by following the Markovian arrival process (MAP). The service times of both the servers are assumed to be phase-type (PH) distributed. The vacation policies considered, respectively, for server-1 and server-2 are Bernoulli schedule multiple vacations and single vacation. Even after failure, server-1 can provide service to the current customer at a reduced rate in our model. We have also assumed that server-2 may face loss at the beginning of the service commencement. The assumptions for both servers have greater importance in the context of the working environment. We have studied our model by using the matrix-analytic method. We have performed the active period analysis and also derived the distribution function for the waiting time. To the end, some graphical exemplifications are provided for clear insight into our model. We have validated our model by comparing its particular case with the existing articles in the literature.

Keywords PH distribution · MAP · Vacation · Working breakdown · Starting failure

G. Ayyappan · R. Gowthami (✉)
Department of Mathematics, Pondicherry Engineering College, Puducherry, India

© The Author(s), under exclusive license to Springer Nature Singapore Pte Ltd. 2022

S. R. Kannan et al. (eds.), *Fuzzy Mathematical Analysis and Advances in Computational Mathematics*, Studies in Fuzziness and Soft Computing 419,
https://doi.org/10.1007/978-981-19-0471-4_14

1 Introduction

Nowadays, most of the recruitments in both government and private sectors are on a contract basis. Each newly appointed server is supposed to work under a well-trained/experienced server for a certain period to get enhanced knowledge in that field. We have considered one such trained server with a newly appointed server. Both the servers can perform all the tasks assigned to them but at different service rates. The trained server may undergo other works (vacation) after completing each job, whereas the newly appointed server can go for vacation provided there is no job to perform. The freshly appointed server that has just come from vacation may feel difficulty beginning the career (starting failure). So he is supposed to learn the procedure to do it (repair process), and at the end, the server will begin to perform the task. On the other hand, the trained server which faces difficulty in the midst of conducting a job will manage to complete it but at a slower rate (working breakdown), and at the end of which the trained server will rectify himself so that he will not commit it again (repair process). By considering all these everyday situations in government/private sectors, we have framed our system.

After our literature review, we conclude that one or few parameters have been studied, but not in the context of the working environment. The basis for MAP, which helps study correlated/uncorrelated arrivals, has come from the versatile Markovian point process (VMPP) that has been introduced by Neuts [13]. Later on, Lucantoni et al. [12] have contributed to coining two new notions, namely MAP and BMAP, for easy understanding of VMPP. A crystal clear understanding of MAP and PH distribution, respectively, can be gained by referring to the works of Chakravarthy [2] and Latouche and Ramaswami [10].

Chakravarthy and Alfa [4] have discussed the multi-server finite capacity model with MAP arrival and group services. They have proved that if the inter-arrival times are of phase type, so does the invariant distribution of the sojourn time and has derived the well-organized algorithmic procedures for finding the consistent densities of the size of the waiting line. A multi-server model with MAP arrival, exponential service, and resequencing buffer of infinite size has been investigated by Chakravarthy et al. [5]. They have proved the matrix geometric nature of their invariant probability vector and the phase-type nature of the sojourn time.

Keilson and Servi [8] have introduced a new policy for the server to take a vacation. According to this policy, the server decides to take a break at each service completion or not with complementary probabilities. A single server system with PH service, vacation, and MAP arrival has been discussed by Chakravarthy [3]. He has done the steady-state analysis and has computed the adequate service time by employing the matrix-analytic method. He has also compared his model with the already available works in the literature.

The concept of working breakdown is that after facing the failure, the server may either go to the repair process immediately with probability p or go after completing the current service with probability $1 - p$. It was introduced by Kalidass and Kasturi [7]. Liou [11] has investigated a Markovian queue with the working breakdown

and impatient customers. He has employed the matrix-analytic method for finding stability conditions and invariant probabilities, derived the mean sojourn time, and constructed two different objective models for the cost analysis. The decision-makers can utilize his work to improve their decision-making quality.

The idea of starting failure in a retrial queue with batch arrival and general service time has been incorporated by Wang and Zhou [14]. Ayyappan and Udayageetha [1] have examined a priority model where the server is supposed to experience the starting failure. They have also incorporated other parameters like vacation and feedback into their model and made a detailed analysis by finding various invariant distribution functions for server state and orbit size.

The uniqueness of our model is that we have studied various situations faced by two different servers, namely a trained and a junior at a time. We have considered the MAP for arrivals, and it is best suited for studying both correlated and uncorrelated arrivals. Then, we have used PH distribution for the service time, which is best for studying the working environment which provides service in phases. We have utilized one of the best methods for carrying out our model's invariant analysis, namely the matrix-analytic method. The articles in the literature have individually discussed some issues in the working environment but not how we have modeled. Our model fits very well for analyzing the most common problems in all kinds of working environments and could provide suggestions for improving the system's efficiency.

The overall objectives of our work are summarized below:

- To convert some of the everyday situations which are supposed to be faced by trained and newly appointed servers in a working environment into mathematical form.
- To obtain the condition that is needed by the system to remain balanced.
- To analyze the active period of the system.
- To compute the average time that the customers are supposed to spend to get the service.
- To perform the numerical computations for providing some suggestions to the system for enhancing the utility of the servers.

Our manuscript is structured in the following manner: Sect. 2 briefly contains the narration of our model. The generator matrix of our system is furnished in Sect. 3. Section 4 includes the analysis of our model in the steady state. The study of the active period of our system has been done in Sect. 5. Section 6 is devoted to enlisting some system measures. Section 7 compares the particular case for our model with the existing articles in the literature. In Sect. 8, the analysis of waiting time has been carried out for our system. Finally, in Sect. 9, numerical analysis of our system has been provided.

2 Model Description

Consider a classical queueing model with two heterogeneous servers in which arrival follows MAP with parameter matrices (D_0, D_1), each of which is of dimension n. The incoming customers form a single waiting line, and they get the service on FCFS discipline. The service times of both servers follow PH distribution with representation (α, T) of order m_1 and (β, S) of order m_2. At the end of providing service, server-1 can either go on a vacation with probability p_1 or start to serve the subsequent customer with probability q_1. At the end of the break, server-1 starts to serve the customer, if any. If not, it continues the vacation. During the busy period, server-1 may face failure

Server-1 begins new service to the current customer at that instant but at a slower rate. The service times of server-1 during the breakdown period also follow PH distribution with representation $(\alpha, \theta T)$, where $(0 < \theta < 1)$. At the end of providing service at a slower rate, server-1 will be sent to the repair process. After being repaired, server-1 starts its service to the customer, if any. If not, server-1 goes on vacation.

Similarly, at the service completion, server-2 can go on vacation provided the queue size is zero. If not, server-2 has to serve the subsequent customer. Server-2 may experience a breakdown during its advent from vacation with probability p_2 or begin service to the customer with probability q_2. If server-2 experiences a breakdown, then it will be sent to the repair process. After being repaired, server-2 will start providing service to the customer, if any, in the system. Otherwise, server-2 goes on vacation. The vacation times of both the servers are, respectively, exponentially distributed with parameters η_1 and η_2. The breakdown times of server-1 follow the exponential distribution with parameter σ_1. The repair times of both the servers are, respectively, exponentially distributed with parameters δ_1 and δ_2 (Fig. 1).

3 The Generator Matrix

Notations

- $N(t)$: Number of units in the system at epoch t
- I_n: An $n \times n$ identity matrix
- $\mathbf{0}$: The zero matrix of the needed dimension
- e_r: A $r \times 1$ vector with all its entries as 1
- $e = e_{6n}$
- $e_1 = e_{4n+6m_1n+2m_2n}$
- $e_2 = e_{4n+4m_1n+2m_2n+2m_1m_2n}$
- $e(1)$: A $(6n \times 1)$ vector in which the first n components are one and the rest of the elements are zero
- $e(i+1)$: A $(6n \times 1)$ vector with $(in+1)$ to $(i+1)n$ elements to be one and the other elements are zero, where $i = 1, 2, 3, 4, 5$

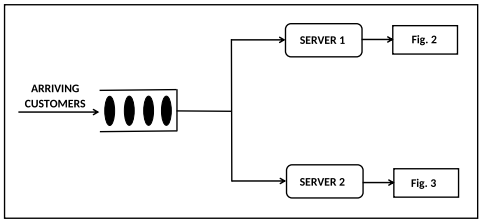

(a) Fig 1

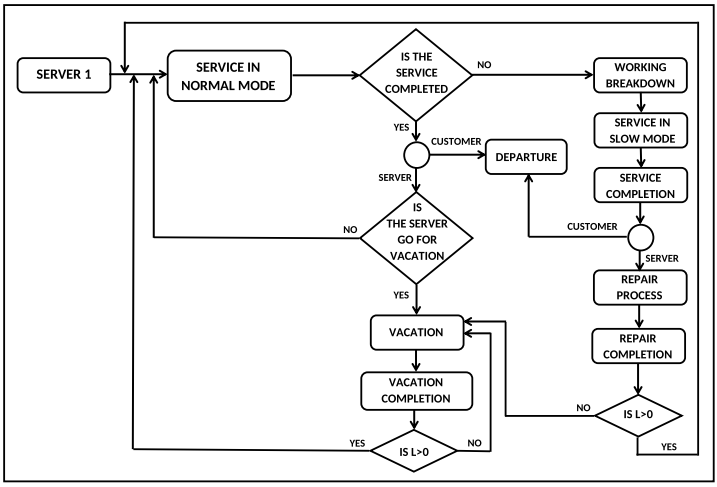

(b) Fig 2

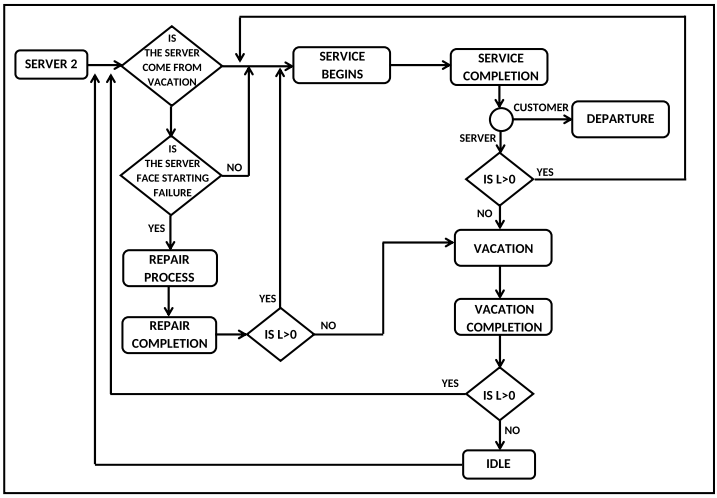

(c) Fig 3

Fig. 1 Pictorial representation

- $e_1(1)$: A $((4n + 6m_1n + 2m_2n) \times 1)$ vector in which initial n components are one and the rest of the elements are zero
- $e_1(i + 1)$: A $((4n + 6m_1n + 2m_2n) \times 1)$ vector with $in + 1$ to $(i + 1)n$ elements to be one and the other elements are zero, where $i = 1, 2, 3$
- $e_1(i + 4)$: A $((4n + 6m_1n + 2m_2n) \times 1)$ vector with $4n + (i - 1)m_1n + 1$ to $4n + im_1n$ elements to be one and the other elements are zero, where $i = 1, 2, 3, 4, 5, 6$
- $e_1(i + 10)$: A $((4n + 6m_1n + 2m_2n) \times 1)$ vector with $4n + 6m_1n + (i - 1)m_2n + 1$ to $4n + 6m_1n + im_2n$ elements to be one and the other elements are zero, where $i = 1, 2$
- $e_2(1)$: A $((4n + 4m_1n + 2m_2n + 2m_1m_2n) \times 1)$ vector in which initial n components are one and the rest of the elements are zero
- $e_2(i + 1)$: A $((4n + 4m_1n + 2m_2n + 2m_1m_2n) \times 1)$ vector with $(in + 1)$ to $(i + 1)n$ elements to be one and the other elements are zero, where $i = 1, 2, 3$
- $e_2(i + 4)$: A $((4n + 4m_1n + 2m_2n + 2m_1m_2n) \times 1)$ vector with $4n + (i - 1)m_1n + 1$ to $4n + im_1n$ elements to be one and the other elements are zero, where $i = 1, 2, 3, 4$
- $e_2(i + 8)$: A $((4n + 4m_1n + 2m_2n + 2m_1m_2n) \times 1)$ vector with $4n + 4m_1n + (i - 1)m_2n + 1$ to $4n + 4m_1n + im_2n$ elements to be one and the other elements to be zero, where $i = 1, 2$
- $e_2(i + 10)$: A $((4n + 4m_1n + 2m_2n + 2m_1m_2n) \times 1)$ vector with $4n + 4m_1n + 2m_2n + (i - 1)m_1m_2n + 1$ to $4n + 4m_1n + 2m_2n + im_1m_2n$ elements to be one and the other elements are zero, where $i = 1, 2$
- $\otimes$: Kronecker multiplication
- $\oplus$: Kronecker addition
- $Y_1(t)$—Status of server-1 at epoch t,
  where

$$Y_1(t) = \begin{cases} 0, & \text{if server-1 is on vacation} \\ 1, & \text{if server-1 is busy in normal mode} \\ 2, & \text{if server-1 is busy during the breakdown} \\ 3, & \text{if server-1 is in the repair process} \end{cases}$$

- $Y_2(t)$—Status of server-2 at epoch t,
  where

$$Y_2(t) = \begin{cases} 0, & \text{if server-2 is on vacation} \\ 1, & \text{if server-2 is idle} \\ 2, & \text{if server-2 is busy} \\ 3, & \text{if server-2 is in the repair process} \end{cases}$$

- $S_1(t)$: Service phase of server-1 at epoch t
- $S_2(t)$: Service phase of server-2 at epoch t
- $M(t)$: Arrival phase of the customers at epoch t

- λ: Fundamental arrival rate and is given by $\lambda = \pi D_1 \mathbf{e}$ in which π is the stationary probability vector of the matrix $D = D_0 + D_1$
- γ_1: The rate at which server-1 offers service and $\gamma_1 = [\alpha(-T)^{-1}\mathbf{e}]^{-1}$
- γ_2: The rate at which server-2 offers service and $\gamma_2 = [\beta(-S)^{-1}\mathbf{e}]^{-1}$.

It is clear that $\{(N(t), Y_1(t), Y_2(t), S_1(t), S_2(t), M(t)) : t \geq 0\}$ is a continuous-time Markov chain (CTMC), and its state space is given by

$$\Omega = l(0) \cup l(1) \cup l(i),$$

where

$$l(0) = \{(0, j_1, j_2, l) : j_1, j_2 = 0, 1, 3; 1 \leq l \leq n\}$$

$$\begin{aligned} l(1) &= \{(1, 0, 0, l) : 1 \leq l \leq n\} \cup \{(1, 0, 2, k_2, l) : 1 \leq k_2 \leq m_2; 1 \leq l \leq n\} \\ &\cup \{(1, j_1, j_2, k_1, l) : j_1 = 1, 2; j_2 = 0, 1, 3; 1 \leq k_1 \leq m_1; 1 \leq l \leq n\} \\ &\cup \{(1, 3, 2, k_2, l) : 1 \leq k_2 \leq m_2; 1 \leq l \leq n\} \cup \{(1, 3, 3, l) : 1 \leq l \leq n\} \\ &\cup \{(1, 0, 3, l) : 1 \leq l \leq n\} \cup \{(1, 3, 0, l) : 1 \leq l \leq n\} \end{aligned}$$

For $i \geq 2$,

$$\begin{aligned} l(i) &= \{(i, 0, 0, l) : 1 \leq l \leq n\} \cup \{(i, 0, 2, k_2, l) : 1 \leq k_2 \leq m_2; 1 \leq l \leq n\} \\ &\cup \{(i, 0, 3, l) : 1 \leq l \leq n\} \cup \{(i, 1, 0, k_1, l) : 1 \leq k_1 m_1; 1 \leq l \leq n\} \\ &\cup \{(i, 1, 2, k_1, k_2, l) : 1 \leq k_1 \leq m_1; 1 \leq k_2 \leq m_2; 1 \leq l \leq n\} \\ &\cup \{(i, 1, 3, k_1, l) : 1 \leq k_1 \leq m_1; 1 \leq l \leq n\} \cup \{(i, 2, 0, k_1, l) : 1 \leq k_1 \leq m_1; 1 \leq l \leq n\} \\ &\cup \{(i, 2, 2, k_1, k_2, l) : 1 \leq k_1 \leq m_1; \leq k_2 \leq m_2; 1 \leq l \leq n\} \\ &\cup \{(i, 2, 3, k_1, l) : 1 \leq k_1 \leq m_1; 1 \leq l \leq n\} \cup \{(i, 3, 0, l) : 1 \leq l \leq n\} \\ &\cup \{(i, 3, 2, k_2, l) : 1 \leq k_2 \leq m_2; 1 \leq l \leq n\} \cup \{(i, 3, 3, l); 1 \leq l \leq n\} \end{aligned}$$

The generator matrix of our model is given by

$$Q = \begin{bmatrix} B_{00} & B_{01} & \mathbf{0} & \mathbf{0} & \mathbf{0} & \mathbf{0} & \mathbf{0} & \mathbf{0} & \cdots \\ B_{10} & B_{11} & B_{12} & \mathbf{0} & \mathbf{0} & \mathbf{0} & \mathbf{0} & \mathbf{0} & \cdots \\ \mathbf{0} & B_{21} & A_1 & A_0 & \mathbf{0} & \mathbf{0} & \mathbf{0} & \mathbf{0} & \cdots \\ \mathbf{0} & \mathbf{0} & A_2 & A_1 & A_0 & \mathbf{0} & \mathbf{0} & \mathbf{0} & \cdots \\ \mathbf{0} & \mathbf{0} & \mathbf{0} & A_2 & A_1 & A_0 & \mathbf{0} & \mathbf{0} & \cdots \\ \cdots & \cdots & \cdots & \ddots & \ddots & \ddots & \cdots & \cdots & \cdots \end{bmatrix}$$

where

$$B_{00} = \begin{bmatrix} B_{11}^{00} & \mathbf{0} \\ B_{21}^{00} & B_{22}^{00} \end{bmatrix}, B_{01} = \begin{bmatrix} B_{11}^{01} & \mathbf{0}\,\mathbf{0} & \mathbf{0} \\ \mathbf{0} & \mathbf{0}\,\mathbf{0} & B_{24}^{01} \end{bmatrix},$$

$$B_{11}^{00} = \begin{bmatrix} D_0 - \eta_2 I_n & \eta_2 I_n & \mathbf{0} \\ \mathbf{0} & D_0 & \mathbf{0} \\ \delta_2 I_n & \mathbf{0} & D_0 - \delta_2 I_n \end{bmatrix}, B_{21}^{00} = \begin{bmatrix} \delta_1 I_n & \mathbf{0} & \mathbf{0} \\ \mathbf{0} & \delta_1 I_n & \mathbf{0} \\ \mathbf{0} & \mathbf{0} & \delta_1 I_n \end{bmatrix},$$

$$B_{22}^{00} = \begin{bmatrix} D_0 - (\eta_2 + \delta_1) I_n & \eta_2 I_n & \mathbf{0} \\ \mathbf{0} & D_0 - \delta_1 I_n & \mathbf{0} \\ \delta_2 I_n & \mathbf{0} & D_0 - (\delta_1 + \delta_2) I_n \end{bmatrix},$$

$$B_{11}^{01} = \begin{bmatrix} D_1 & \mathbf{0} & \mathbf{0} \\ \mathbf{0} & \beta \otimes q_2 D_1 & p_2 D_1 \\ \mathbf{0} & \mathbf{0} & D_1 \end{bmatrix}, B_{24}^{01} = \begin{bmatrix} D_1 & \mathbf{0} & \mathbf{0} \\ \mathbf{0} & \beta \otimes q_2 D_1 & p_2 D_1 \\ \mathbf{0} & \mathbf{0} & D_1 \end{bmatrix},$$

$$B_{10} = \begin{bmatrix} B_{11}^{10} & \mathbf{0} \\ B_{21}^{10} & \mathbf{0} \\ \mathbf{0} & B_{32}^{10} \\ \mathbf{0} & B_{42}^{10} \end{bmatrix}, B_{11} = \begin{bmatrix} B_{11}^{11} & B_{12}^{11} & \mathbf{0} & \mathbf{0} \\ \mathbf{0} & B_{22}^{11} & B_{23}^{11} & \mathbf{0} \\ \mathbf{0} & \mathbf{0} & B_{33}^{11} & \mathbf{0} \\ B_{41}^{11} & B_{42}^{11} & \mathbf{0} & B_{44}^{11} \end{bmatrix},$$

$$B_{11}^{10} = \begin{bmatrix} \mathbf{0} & \mathbf{0}\ \mathbf{0} \\ S^0 \otimes I_n & \mathbf{0}\ \mathbf{0} \\ \mathbf{0} & \mathbf{0}\ \mathbf{0} \end{bmatrix}, B_{21}^{10} = \begin{bmatrix} T^0 \otimes I_n & \mathbf{0} & \mathbf{0} \\ \mathbf{0} & T^0 \otimes I_n & \mathbf{0} \\ \mathbf{0} & \mathbf{0} & T^0 \otimes I_n \end{bmatrix},$$

$$B_{32}^{10} = \begin{bmatrix} \theta T^0 \otimes I_n & \mathbf{0} & \mathbf{0} \\ \mathbf{0} & \theta T^0 \otimes I_n & \mathbf{0} \\ \mathbf{0} & \mathbf{0} & \theta T^0 \otimes I_n \end{bmatrix}, B_{42}^{10} = \begin{bmatrix} \mathbf{0} & \mathbf{0}\ \mathbf{0} \\ S^0 \otimes I_n & \mathbf{0}\ \mathbf{0} \\ \mathbf{0} & \mathbf{0}\ \mathbf{0} \end{bmatrix},$$

$$B_{11}^{11} = \begin{bmatrix} D_0 - (\eta_1 + \eta_2) I_n & \beta \otimes q_2 \eta_2 I_n & p_2 \eta_2 I_n \\ \mathbf{0} & S \oplus D_0 & \mathbf{0} \\ \mathbf{0} & \beta \otimes \delta_2 I_n & D_0 - (\eta_1 + \delta_2) I_n \end{bmatrix},$$

$$B_{12}^{11} = \begin{bmatrix} \alpha \otimes \eta_1 I_n & \mathbf{0} & \mathbf{0} \\ \mathbf{0} & \mathbf{0} & \mathbf{0} \\ \mathbf{0} & \mathbf{0} & \alpha \otimes \eta_1 I_n \end{bmatrix},$$

$$B_{22}^{11} = \begin{bmatrix} T \oplus (D_0 - (\sigma_1 + \eta_2) I_n) & \eta_2 I_{m_1 n} & \mathbf{0} \\ \mathbf{0} & T \oplus (D_0 - \sigma_1 I_n) & \mathbf{0} \\ \delta_2 I_{m_1 n} & \mathbf{0} & T \oplus (D_0 - (\sigma_1 + \delta_2) I_n) \end{bmatrix},$$

$$B_{23}^{11} = \begin{bmatrix} \alpha \otimes e_{m_1} \otimes \sigma_1 I_n & \mathbf{0} & \mathbf{0} \\ \mathbf{0} & \alpha \otimes e_{m_1} \otimes \sigma_1 I_n & \mathbf{0} \\ \mathbf{0} & \mathbf{0} & \alpha \otimes e_{m_1} \otimes \sigma_1 I_n \end{bmatrix},$$

$$B_{33}^{11} = \begin{bmatrix} \theta T \oplus (D_0 - \eta_2 I_n) & \eta_2 I_{m_1 n} & \mathbf{0} \\ \mathbf{0} & \theta T \oplus D_0 & \mathbf{0} \\ \delta_2 I_{m_1 n} & \mathbf{0} & \theta T \oplus (D_0 - \delta_2 I_n) \end{bmatrix}, B_{41}^{11} = \begin{bmatrix} \mathbf{0} & \mathbf{0} & \mathbf{0} \\ \mathbf{0} & \delta_1 I_{m_2 n} & \mathbf{0} \\ \mathbf{0} & \mathbf{0} & \mathbf{0} \end{bmatrix},$$

$$B_{42}^{11} = \begin{bmatrix} \alpha \otimes \delta_1 I_n & \mathbf{0} & \mathbf{0} \\ \mathbf{0} & \mathbf{0} & \mathbf{0} \\ \mathbf{0} & \mathbf{0} & \alpha \otimes \delta_1 I_n \end{bmatrix},$$

$$B_{44}^{11} = \begin{bmatrix} D_0 - (\delta_1 + \eta_2) I_n & \beta \otimes q_2 \eta_2 I_n & p_2 \eta_2 I_n \\ \mathbf{0} & S \oplus (D_0 - \delta_1 I_n) & \mathbf{0} \\ \mathbf{0} & \beta \otimes \delta_2 I_n & D_0 - (\delta_1 + \delta_2) I_n \end{bmatrix},$$

$$B_{12} = \begin{bmatrix} B_{11}^{12} & \mathbf{0} & \mathbf{0} & \mathbf{0} \\ \mathbf{0} & B_{22}^{12} & \mathbf{0} & \mathbf{0} \\ \mathbf{0} & \mathbf{0} & B_{33}^{12} & \mathbf{0} \\ \mathbf{0} & \mathbf{0} & \mathbf{0} & B_{44}^{12} \end{bmatrix}, B_{21} = \begin{bmatrix} B_{11}^{21} & \mathbf{0} & \mathbf{0} & \mathbf{0} \\ B_{21}^{21} & B_{22}^{21} & \mathbf{0} & \mathbf{0} \\ \mathbf{0} & \mathbf{0} & B_{33}^{21} & B_{34}^{21} \\ \mathbf{0} & \mathbf{0} & \mathbf{0} & B_{44}^{21} \end{bmatrix},$$

$$B_{11}^{12} = \begin{bmatrix} D_1 & \mathbf{0} & \mathbf{0} \\ \mathbf{0} & I_{m_2} \otimes D_1 & \mathbf{0} \\ \mathbf{0} & \mathbf{0} & D_1 \end{bmatrix}, B_{22}^{12} = \begin{bmatrix} I_{m_1} \otimes D_1 & \mathbf{0} & \mathbf{0} \\ \mathbf{0} & I_{m_1} \otimes q_2\beta \otimes D_1 & I_{m_1} \otimes p_2 D_1 \\ \mathbf{0} & \mathbf{0} & I_{m_1} \otimes D_1 \end{bmatrix},$$

$$B_{33}^{12} = \begin{bmatrix} I_{m_1} \otimes D_1 & \mathbf{0} & \mathbf{0} \\ \mathbf{0} & I_{m_1} \otimes q_2\beta \otimes D_1 & I_{m_1} \otimes p_2 D_1 \\ \mathbf{0} & \mathbf{0} & I_{m_1} \otimes D_1 \end{bmatrix}, B_{44}^{12} = \begin{bmatrix} D_1 & \mathbf{0} & \mathbf{0} \\ \mathbf{0} & I_{m_2} \otimes D_1 & \mathbf{0} \\ \mathbf{0} & \mathbf{0} & D_1 \end{bmatrix},$$

$$B_{11}^{21} = \begin{bmatrix} \mathbf{0} & \mathbf{0} & \mathbf{0} \\ \mathbf{0} & S^0\beta \otimes I_n & \mathbf{0} \\ \mathbf{0} & \mathbf{0} & \mathbf{0} \end{bmatrix}, B_{21}^{21} = \begin{bmatrix} p_1 T^0 \otimes I_n & \mathbf{0} & \mathbf{0} \\ \mathbf{0} & T^0 \otimes I_{m_2 n} & \mathbf{0} \\ \mathbf{0} & \mathbf{0} & p_1 T^0 \otimes I_n \end{bmatrix},$$

$$B_{22}^{21} = \begin{bmatrix} q_1 T^0 \alpha \otimes I_n & \mathbf{0} & \mathbf{0} \\ I_{m_1} \otimes S^0 \otimes I_n & \mathbf{0} & \mathbf{0} \\ \mathbf{0} & \mathbf{0} & q_1 T^0 \alpha \otimes I_n \end{bmatrix}, B_{33}^{21} = \begin{bmatrix} \mathbf{0} & \mathbf{0} & \mathbf{0} \\ I_{m_1} \otimes S^0 \otimes I_n & \mathbf{0} & \mathbf{0} \\ \mathbf{0} & \mathbf{0} & \mathbf{0} \end{bmatrix},$$

$$B_{34}^{21} = \begin{bmatrix} \theta T^0 \otimes I_n & \mathbf{0} & \mathbf{0} \\ \mathbf{0} & \theta T^0 \otimes I_{m_2 n} & \mathbf{0} \\ \mathbf{0} & \mathbf{0} & \theta T^0 \otimes I_n \end{bmatrix}, B_{44}^{21} = \begin{bmatrix} \mathbf{0} & \mathbf{0} & \mathbf{0} \\ \mathbf{0} & S^0\beta \otimes I_n & \mathbf{0} \\ \mathbf{0} & \mathbf{0} & \mathbf{0} \end{bmatrix},$$

$$A_1 = \begin{bmatrix} A_{11}^1 & A_{12}^1 & \mathbf{0} & \mathbf{0} \\ \mathbf{0} & A_{22}^1 & A_{23}^1 & \mathbf{0} \\ \mathbf{0} & \mathbf{0} & A_{33}^1 & \mathbf{0} \\ \mathbf{0} & A_{42}^1 & \mathbf{0} & A_{44}^1 \end{bmatrix}, A_0 = \begin{bmatrix} A_{11}^0 & \mathbf{0} & \mathbf{0} & \mathbf{0} \\ \mathbf{0} & A_{22}^0 & \mathbf{0} & \mathbf{0} \\ \mathbf{0} & \mathbf{0} & A_{33}^0 & \mathbf{0} \\ \mathbf{0} & \mathbf{0} & \mathbf{0} & A_{44}^0 \end{bmatrix},$$

$$A_{11}^1 = \begin{bmatrix} D_0 - (\eta_1 + \eta_2) I_n & \beta \otimes q_2 \eta_2 I_n & p_2 \eta_2 I_n \\ \mathbf{0} & S \oplus (D_0 - \eta_1 I_n) & \mathbf{0} \\ \mathbf{0} & \beta \otimes \delta_2 I_n & D_0 - (\eta_1 + \delta_2) I_n \end{bmatrix},$$

$$A_{12}^1 = \begin{bmatrix} \alpha \otimes \eta_1 I_n & \mathbf{0} & \mathbf{0} \\ \mathbf{0} & \alpha \otimes \eta_1 I_{m_2 n} & \mathbf{0} \\ \mathbf{0} & \mathbf{0} & \alpha \otimes \eta_1 I_n \end{bmatrix},$$

$$A_{22}^1 = \begin{bmatrix} T \oplus (D_0 - (\sigma_1 + \eta_2) I_n) & I_{m_1} \otimes \beta \otimes q_2 \eta_2 I_n & p_2 \eta_2 I_{m_1 n} \\ \mathbf{0} & T \oplus S \oplus (D_0 - \sigma_1 I_n) & \mathbf{0} \\ \mathbf{0} & I_{m_1} \otimes \beta \otimes \delta_2 I_n & T \oplus (D_0 - (\sigma_1 + \delta_2) I_n) \end{bmatrix},$$

$$A_{23}^1 = \begin{bmatrix} \alpha \otimes e_{m_1} \otimes \sigma_1 I_n & \mathbf{0} & \mathbf{0} \\ \mathbf{0} & \alpha \otimes e_{m_1} \otimes \sigma_1 I_{m_2 n} & \mathbf{0} \\ \mathbf{0} & \mathbf{0} & \alpha \otimes e_{m_1} \otimes \sigma_1 I_n \end{bmatrix},$$

$$A_{33}^1 = \begin{bmatrix} \theta T \oplus (D_0 - \eta_2 I_n) & I_{m_1} \otimes \beta \otimes q_2 \eta_2 I_n & p_2 \eta_2 I_{m_1 n} \\ \mathbf{0} & \theta T \oplus S \oplus D_0 & \mathbf{0} \\ \mathbf{0} & I_{m_1} \otimes \beta \otimes \delta_2 I_n & \theta T \oplus (D_0 - \delta_2 I_n) \end{bmatrix},$$

$$A_{42}^1 = \begin{bmatrix} \alpha \otimes \delta_1 I_n & \mathbf{0} & \mathbf{0} \\ \mathbf{0} & \alpha \otimes \delta_1 I_{m_2 n} & \mathbf{0} \\ \mathbf{0} & \mathbf{0} & \alpha \otimes \delta_1 I_n \end{bmatrix},$$

$$A_{44}^1 = \begin{bmatrix} D_0 - (\delta_1 + \eta_2) I_n & \beta \otimes q_2 \eta_2 I_n & p_2 \eta_2 I_n \\ \mathbf{0} & S \oplus (D_0 - \delta_1 I_n) & \mathbf{0} \\ \mathbf{0} & \beta \otimes \delta_2 I_n & D_0 - (\delta_1 + \delta_2) I_n \end{bmatrix},$$

$$A_{11}^0 = \begin{bmatrix} D_1 & \mathbf{0} & \mathbf{0} \\ \mathbf{0} & I_{m_2} \otimes D_1 & \mathbf{0} \\ \mathbf{0} & \mathbf{0} & D_1 \end{bmatrix}, A_{22}^0 = \begin{bmatrix} I_{m_1} \otimes D_1 & \mathbf{0} & \mathbf{0} \\ \mathbf{0} & I_{m_1 m_2} \otimes D_1 & \mathbf{0} \\ \mathbf{0} & \mathbf{0} & I_{m_1} \otimes D_1 \end{bmatrix},$$

$$A_{33}^0 = \begin{bmatrix} I_{m_1} \otimes D_1 & \mathbf{0} & \mathbf{0} \\ \mathbf{0} & I_{m_1 m_2} \otimes D_1 & \mathbf{0} \\ \mathbf{0} & \mathbf{0} & I_{m_1} \otimes D_1 \end{bmatrix}, A_{44}^0 = \begin{bmatrix} D_1 & \mathbf{0} & \mathbf{0} \\ \mathbf{0} & I_{m_2} \otimes D_1 & \mathbf{0} \\ \mathbf{0} & \mathbf{0} & D_1 \end{bmatrix},$$

$$A_2 = \begin{bmatrix} A_{11}^2 & \mathbf{0} & \mathbf{0} & \mathbf{0} \\ A_{21}^2 & A_{22}^2 & \mathbf{0} & \mathbf{0} \\ \mathbf{0} & \mathbf{0} & A_{33}^2 & A_{34}^2 \\ \mathbf{0} & \mathbf{0} & \mathbf{0} & A_{44}^2 \end{bmatrix}, A_{11}^2 = \begin{bmatrix} \mathbf{0} & \mathbf{0} & \mathbf{0} \\ \mathbf{0} & S^0 \beta \otimes I_n & \mathbf{0} \\ \mathbf{0} & \mathbf{0} & \mathbf{0} \end{bmatrix},$$

$$A_{21}^2 = \begin{bmatrix} p_1 T^0 \otimes I_n & \mathbf{0} & \mathbf{0} \\ \mathbf{0} & p_1 T^0 \otimes I_{m_2 n} & \mathbf{0} \\ \mathbf{0} & \mathbf{0} & p_1 T^0 \otimes I_n \end{bmatrix},$$

$$A_{22}^2 = \begin{bmatrix} q_1 T^0 \alpha \otimes I_n & \mathbf{0} & \mathbf{0} \\ \mathbf{0} & (q_1 T^0 \alpha \oplus S^0 \beta) \otimes I_n & \mathbf{0} \\ \mathbf{0} & \mathbf{0} & q_1 T^0 \alpha \otimes I_n \end{bmatrix},$$

$$A_{33}^2 = \begin{bmatrix} \mathbf{0} & \mathbf{0} & \mathbf{0} \\ \mathbf{0} & I_{m_1} \otimes S^0 \beta \otimes I_n & \mathbf{0} \\ \mathbf{0} & \mathbf{0} & \mathbf{0} \end{bmatrix},$$

$$A_{34}^2 = \begin{bmatrix} \theta T^0 \otimes I_n & \mathbf{0} & \mathbf{0} \\ \mathbf{0} & \theta T^0 \otimes I_{m_2 n} & \mathbf{0} \\ \mathbf{0} & \mathbf{0} & \theta T^0 \otimes I_n \end{bmatrix}, A_{44}^2 = \begin{bmatrix} \mathbf{0} & \mathbf{0} & \mathbf{0} \\ \mathbf{0} & S^0 \beta \otimes I_n & \mathbf{0} \\ \mathbf{0} & \mathbf{0} & \mathbf{0} \end{bmatrix}.$$

4 System Analysis

4.1 Stability Condition

If $A = A_0 + A_1 + A_2$, then it is clearly a generator matrix, and hence, we could find its invariant probability vector, denoted by Ψ such that

$$\Psi A = 0, \quad \Psi \mathbf{e} = 1$$

where Ψ is given by $\Psi = (\psi_0, \psi_1, \psi_2, \psi_3, \psi_4, \psi_5, \psi_6, \psi_7, \psi_8, \psi_9, \psi_{10}, \psi_{11})$ and is determined by solving the subsequent equations:

$$\psi_0[D-(\eta_1+\eta_2)I_n]+\psi_3[p_1T^0\otimes I_n]=0,$$
$$\psi_0[\beta\otimes q_2\eta_2 I_n]+\psi_1[(S+S^0\beta)\oplus(D-\eta_1 I_n)]+\psi_2[\beta\otimes\delta_2 I_n]$$
$$+\psi_4[p_1T^0\otimes I_{m_2n}]=0,$$
$$\psi_0[p_2\eta_2 I_n]+\psi_2[D-(\eta_1+\delta_2)I_n]+\psi_5[p_1T^0\otimes I_n]=0,$$
$$\psi_0[\alpha\otimes\eta_1 I_n]+\psi_3[(T+q_1T^0\alpha)\oplus(D-(\sigma_1+\eta_2)I_n]+\psi_9[\alpha\otimes\delta_1 I_n]=0,$$
$$\psi_1[\alpha\otimes\eta_1 I_{m_2n}]+\psi_3[I_{m_1}\otimes\beta\otimes q_2\eta_2 I_n]$$
$$+\psi_4[(T+q_1T^0\alpha)\oplus(S+S^0\beta)\oplus(D-\sigma_1 I_n)]$$
$$+\psi_5[I_{m_1}\otimes\beta\otimes\delta_2 I_n]+\psi_{10}[\alpha\otimes\delta_1 I_{m_2n}]=0,$$
$$\psi_2[\alpha\otimes\eta_1 I_n]+\psi_3[p_2\eta_2 I_{m_1n}]+\psi_5[(T+q_1T^0\alpha)\oplus(D-(\sigma_1+\delta_2)I_n)]$$
$$+\psi_{11}[\alpha\otimes\delta_1 I_n]=0,$$
$$\psi_3[\alpha\otimes e_{m_1}\otimes\sigma_1 I_n]+\psi_6[\theta T\oplus(D-\eta_2 I_n)]=0,$$
$$\psi_4[\alpha\otimes e_{m_1}\otimes\sigma_1 I_{m_2n}]+\psi_6[I_{m_1}\otimes\beta\otimes q_2\eta_2 I_n]+\psi_7[\theta T\oplus(S+S^0\beta)\oplus D]$$
$$+\psi_8[I_{m_1}\otimes\beta\otimes\delta_2 I_n]=0,$$
$$\psi_5[\alpha\otimes e_{m_1}\otimes\sigma_1 I_n]+\psi_6[p_2\eta_2 I_{m_1n}]+\psi_8[\theta T\oplus(D-\delta_2 I_n)]=0,$$
$$\psi_6[\theta T^0\otimes I_n]+\psi_9[D-(\delta_1+\eta_2)I_n]=0,$$
$$\psi_7[\theta T^0\otimes I_{m_2n}]+\psi_9[\beta\otimes q_2\eta_2 I_n]+\psi_{10}[(S+S^0\beta)\oplus(D-\delta_1 I_m)]$$
$$+\psi_{11}[\beta\otimes\delta_2 I_n]=0,$$
$$\psi_8[\theta T^0\otimes I_n]+\psi_9[p_2\eta_2 I_n]+\psi_{11}[D-(\delta_1+\delta_2)I_n]=0,$$

subject to

$$\psi_0 e_n+\psi_1 e_{m_2n}+\psi_2 e_n+\psi_3 e_{m_1n}+\psi_4 e_{m_1m_2n}+\psi_5 e_{m_1n}+\psi_6 e_{m_1n}$$
$$+\psi_7 e_{m_1m_2n}+\psi_8 e_{m_1n}+\psi_9 e_n+\psi_{10}e_{m_2n}+\psi_{11}e_n=1.$$

The necessary and sufficient condition for maintaining the stability is $\Psi A_0\mathbf{e}<\Psi A_2\mathbf{e}$, i.e.,

$$\Big\{(\psi_0+\psi_2+\psi_9+\psi_{11})D_1e_n+(\psi_1+\psi_{10})(e_{m_2}\otimes D_1e_n)$$
$$+(\psi_3+\psi_5+\psi_6+\psi_8)(e_{m_1}\otimes D_1e_n)+(\psi_4+\psi_7)(e_{m_1m_2}\otimes D_1e_n)\Big\}$$
$$<\Big\{(\psi_1+\psi_{10})(S^0\otimes e_n)+(\psi_3+\psi_5)(T^0\otimes e_n)+\psi_4((T^0\oplus S^0)\otimes e_n)$$
$$+(\psi_6+\psi_8)(\theta T^0\otimes e_n)+\psi_7((\theta T^0\oplus S^0)\otimes e_n)\Big\}.$$

4.2 The Invariant Probability Vector

Let the probability vector of Q in the steady state be indicated by $\mathbf{x}$, and its dimension is infinite.

This probability vector is subdivided as follows: $\mathbf{x} = (\mathbf{x}_0, \mathbf{x}_1, \mathbf{x}_2, \ldots)$, where $\mathbf{x}_0$ is of dimension $6n$, $\mathbf{x}_1$ is of dimension $(4n + 6m_1n + 2m_2n)$, and all other $\mathbf{x}_i's$ are of dimension $(4n + 4m_1n + 2m_2n + 2m_1m_2n)$, for $i \geq 2$.
Since $\mathbf{x}$ is a steady probability vector of Q, it will satisfy the following:

$$\mathbf{x}Q = 0 \quad \text{and} \quad \mathbf{x}\mathbf{e} = 1.$$

After the attainment of stability, we can evaluate the invariant probability vector $\mathbf{x}$ by solving the following equations:

$$\mathbf{x}_{i+1} = \mathbf{x}_2 R^{i-1}, \quad i \geq 2$$

where R is the least non-negative solution of the equation

$$R^2 A_2 + RA_1 + A_0 = 0$$

and the vectors $\mathbf{x}_0$, $\mathbf{x}_1$, and $\mathbf{x}_2$ can be computed by solving the succeeding equations:

$$\begin{aligned}
&\mathbf{x}_0 B_{00} + \mathbf{x}_1 B_{10} = 0,\\
&\mathbf{x}_0 B_{01} + \mathbf{x}_1 B_{11} + \mathbf{x}_2 B_{21} = 0,\\
&\mathbf{x}_1 B_{12} + \mathbf{x}_2 [A_1 + RA_2] = 0
\end{aligned}$$

based on the normalizing condition

$$\mathbf{x}_0 e + \mathbf{x}_1 e_1 + \mathbf{x}_2 [I - R]^{-1} e_2 = 1.$$

The rate matrix R can be computed using the "logarithmic reduction algorithm" specified by Latouche and Ramaswami [10].

5 Analysis of Busy Period

The duration between the customer's arrival to the empty system and the system size becomes zero for the first time which is a busy period.

Notations

- $G_{jj'}(k, x)$—The probability that the QBD process gets into the level $i - 1$ by making precisely k changeovers to the left and also by getting into the state (i, j') with the constraint that it started in the state (i, j) at epoch $t = 0$.
- $\tilde{G}_{jj'}(z, s) = \sum_{k=1}^{\infty} z^k \int_0^{\infty} e^{-sx} dG_{jj'}(k, x) : |z| \leq 1, \ \mathrm{Re}(s) \geq 0$
- $\tilde{G}(z, s)$ − The matrix $(\tilde{G}_{jj'}(z, s))$
- $G = (G_{jj'}) = \tilde{G}(1, 0)$—The matrix governs the first passage times without including the boundary state.
- $G_{jj'}^{(0,0)}(k, x)$—The first return time to level 0.

- $\mathbb{E}_{1j}, \mathbb{E}_{2j}$—The mean first passage time and the mean number of services completed in the first passage time between the levels i and $i-1$, respectively, with the condition that the process is in the state (i, j) at the epoch $t = 0$.
- $\mathbb{E}_{\mathbf{1}}, \mathbb{E}_2$—The column vectors with $\mathbb{E}_{1j}$ and $\mathbb{E}_{2j}$ as their entries, respectively.
- $\mathbb{E}_1^{(2,1)}, \mathbb{E}_2^{(2,1)}$—The vectors, respectively, providing the mean first passage time from level 2 to level 1 and the mean number of service completion in that duration.
- $\mathbb{E}_1^{(1,0)}, \mathbb{E}_2^{(1,0)}$—The vectors, respectively, providing the mean first passage time from level 1 to level 0 and the mean number of service completion in that duration.
- $\mathbb{E}_1^{(0,0)}, \mathbb{E}_2^{(0,0)}$—The vectors, respectively, providing the mean first return time to level 0 and the mean number of service completion in that duration.

Clearly, the matrix $\tilde{G}(z, s)$ satisfies the following equation:

$$\text{“}\tilde{G}(z,s) = z[sI - A_1]^{-1}A_2 + [sI - A_1]^{-1}A_0\tilde{G}^2(z,s)\text{”}.$$

After the computation of the rate matrix R, the matrix G may be obtained by using the following:

$$\text{“}G = -[A_1 + RA_2]^{-1}A_2\text{”}.$$

The succeeding equations which are, respectively, obeyed by $\tilde{G}^{(2,1)}(z, s)$, $\tilde{G}^{(1,0)}(z, s)$ and $\tilde{G}^{(0,0)}(z, s)$ are for the boundary states, namely 2, 1, and 0.

$$\text{“}\tilde{G}^{(2,1)}(z,s) = z[sI - A_1]^{-1}B_{21} + [sI - A_1]^{-1}A_0\tilde{G}(z,s)\tilde{G}^{(2,1)}(z,s)\text{”},$$

$$\text{“}\tilde{G}^{(1,0)}(z,s) = z[sI - B_{11}]^{-1}B_{10} + [sI - B_{11}]^{-1}B_{12}\tilde{G}^{(2,1)}(z,s)\tilde{G}^{(1,0)}(z,s)\text{”},$$

and

$$\text{“}\tilde{G}^{(0,0)}(z,s) = [sI - B_{00}]^{-1}B_{01}\tilde{G}^{(1,0)}(z,s)\text{”}.$$

Because of the stochastic nature of the matrices, viz. G, $\tilde{G}^{(2,1)}(1,0)$, $\tilde{G}^{(1,0)}(1,0)$, and $\tilde{G}^{(0,0)}(1,0)$, we may easily compute the successive moments. At $z = 1$ and $s = 0$,

$$\mathbb{E}_{\mathbf{1}} = -\frac{\partial}{\partial s}\{\tilde{G}(z,s)\} = -[A_0(G+I) + A_1]^{-1}e_2,$$

$$\mathbb{E}_{\mathbf{2}} = \frac{\partial}{\partial z}\{\tilde{G}(z,s)\} = -[A_0(G+I) + A_1]^{-1}A_2e_2,$$

$$\mathbb{E}_{\mathbf{1}}{}^{(2,1)} = -\frac{\partial}{\partial s}\{\tilde{G}^{(2,1)}(z,s)\} = -[A_1 + A_0G]^{-1}[e_2 + A_0\mathbb{E}_{\mathbf{1}}],$$

$$\mathbb{E}_{\mathbf{2}}{}^{(2,1)} = \frac{\partial}{\partial z}\{\tilde{G}^{(2,1)}(z,s)\} = -[A_1 + A_0G]^{-1}[A_0\mathbb{E}_{\mathbf{2}} + B_{21}e_2],$$

$$\mathbb{E}_{\mathbf{1}}{}^{(1,0)} = -\frac{\partial}{\partial s}\{\tilde{G}^{(1,0)}(z,s)\} = -[B_{11} + B_{12}\mathbf{G}^{(2,1)}(1,0)]^{-1}[e_1 + B_{12}\mathbb{E}_1^{(2,1)}],$$

$$\mathbb{E}_{\mathbf{2}}{}^{(1,0)} = \frac{\partial}{\partial z}\{\tilde{G}^{(1,0)}(z,s)\} = -[B_{11} + B_{12}\mathbf{G}^{(2,1)}(1,0)]^{-1}[B_{12}\mathbb{E}_2^{(2,1)} + B_{10}e_1],$$

$$\mathbb{E}_{\mathbf{1}}{}^{(0,0)} = -\frac{\partial}{\partial s}\{\tilde{G}^{(0,0)}(z,s)\} = -B_{00}^{-1}[e + B_{01}\mathbb{E}_1^{(1,0)}],$$

$$\mathbb{E}_{\mathbf{2}}{}^{(0,0)} = \frac{\partial}{\partial z}\{\tilde{G}^{(0,0)}(z,s)\} = -B_{00}^{-1}B_{01}\mathbb{E}_2^{(1,0)}.$$

6 System Measures

- The expected system size:
  $E_{\text{system}} = \mathbf{x}_1 e_1 + \mathbf{x}_2[2(I-R)^{-1} + R(I-R)^{-2}]e_2$
- The probability of both the servers are on vacation:
  $P_0 = \mathbf{x}_0 e(1) + \mathbf{x}_1 e_1(1) + \mathbf{x}_2(I-R)^{-1}e_2(1)$
- The probability of server-1 is on vacation:
  $P_{\text{v.}} = \mathbf{x}_0[e(1)+e(2)+e(3)] + \mathbf{x}_1[e_1(1)+e_1(2)+e_1(3)] + \mathbf{x}_2(I-R)^{-1}[e_2(1)+e_2(2)+e_2(3)]$
- The probability of server-2 is on vacation:
  $P_{\text{.v}} = \mathbf{x}_0[e(1)+e(4)] + \mathbf{x}_1[e_1(1)+e_1(4)+e_1(7)+e_1(10)] + \mathbf{x}_2(I-R)^{-1}[e_2(1)+e_2(4)+e_2(7)+e_2(10)]$
- The probability of server-2 is idle:
  $P_{\text{.i}} = \mathbf{x}_0[e(2)+e(5)] + \mathbf{x}_1[e_1(5)+e_1(8)]$
- The probability of server-1 is busy in normal mode:
  $P_{\text{b.}} = \mathbf{x}_1[e_1(4)+e_1(5)+e_1(6)] + \mathbf{x}_2(I-R)^{-1}[e_2(4)+e_2(5)+e_2(6)]$
- The probability of server-1 is busy in working breakdown:
  $P_{\text{wb.}} = \mathbf{x}_1[e_1(7)+e_1(8)+e_1(9)] + \mathbf{x}_2(I-R)^{-1}[e_2(7)+e_2(8)+e_2(9)]$
- The probability of server-2 is busy:
  $P_{\text{.b}} = \mathbf{x}_1[e_1(2)+e_1(11)] + \mathbf{x}_2(I-R)^{-1}[e_2(2)+e_2(5)+e_2(8)+e_2(11)]$
- The probabilities of both the servers are under repair:
  $P_{\text{rr}} = \mathbf{x}_0 e(6) + \mathbf{x}_1 e_1(12) + \mathbf{x}_2(I-R)^{-1}e_2(12).$

7 Particular Case

- Assume that the inter-arrival times are exponentially distributed; both servers' service times are distributed exponentially. They are homogeneous together with no vacation for both the servers, no breakdown for server-1, no starting failure for server-2, and no repair process for both servers. Our model coincides with the classical M/M/c model with c = 2 studied by Gross and Harris [6].
- Suppose there is no breakdown for server-1, no starting failure for server-2, no repair process for both the servers, and no vacation for server-2. In that case, our model coincides with MAP/PH(1), PH(2)/2 model with Bernoulli vacations (without a break for server-2) studied by Kumar et al. [9].

8 Analysis of Waiting Time Distribution

In a Markov chain, the duration until absorption is considered to be the waiting time. Let $\tilde{Q}$ be the transition matrix for this absorbing Markov chain and let the distribution function for the waiting time of the tagged customer be $W(t)$. $t \geq 0$.

Then, the LST for the waiting time distribution is as below:

$$\bar{W}(s) = \mathbf{z}_0(0)\ \phi(0, s) + \mathbf{z}_1(0)\ \phi(1, s) + \omega(s)\ \phi(2, s). \tag{1}$$

and the average waiting time is

$$EW = -\mathbf{z}_0(0)\acute{\phi}(0, 0) - \mathbf{z}_1(0)\acute{\phi}(1, 0) - \acute{\omega}(0)e_{4+4m_1+2m_2+2m_1m_2} - \omega(0)\acute{\phi}(2, 0), \tag{2}$$

where $\mathbf{z}(0) = (\mathbf{z}_0(0), \mathbf{z}_1(0), \mathbf{z}_2(0), \cdots)$ can be interpreted as a conditional probability distribution of the system's state conditioned on the occurrence of the tagged customer arrival.

$$\phi(0, s) = [sI - F_0]^{-1}H_0, \tag{3}$$

$$\phi(1, s) = [sI - F_1]^{-1}F_{10}\phi(0, s) + [sI - F_1]^{-1}H_1, \tag{4}$$

$$\phi(2, s) = [sI - F]^{-1}F_{21}\phi(1, s) + [sI - F]^{-1}H_2. \tag{5}$$

$$\acute{\phi}(0, 0) = (-1)[-F_0]^{-2}H_0, \tag{6}$$

$$\acute{\phi}(1, 0) = (-1)[-F_1]^{-2}F_{10}\phi(0, 0) + [-F_1]^{-1}F_{10}\acute{\phi}(0, 0) - [-F_1]^{-2}H_1, \tag{7}$$

$$\acute{\phi}(2, 0) = (-1)[-F]^{-2}F_{21}\phi(1, 0) + [-F]^{-1}F_{21}\acute{\phi}(1, 0) - [-F]^{-2}H_2. \tag{8}$$

$$\omega(0) = \sum_{i=2}^{\infty} \mathbf{z}_i(0)V^{i-2}, \tag{9}$$

where $V = [-F]^{-1}F_2$.

$$\begin{aligned}(-1)\acute{\omega}(0)e_{4+4m_1+2m_2+2m_1m_2} = \Big\{&\mathbf{x}_2[I - R]^{-1}\Big[I_{4+4m_1+2m_2+2m_1m_2} \otimes \tfrac{D_1e_n}{\lambda}\Big] \\ &+\mathbf{x}_2R[I - R]^{-2} \times \Big[I_{4+4m_1+2m_2+2m_1m_2} \otimes \tfrac{D_1e_n}{\lambda}\Big] \\ &V_2 - \omega(0)\Big\}[I - V + V_2]^{-1}[-F]^{-1}e_{4+4m_1+2m_2+2m_1m_2}.\end{aligned} \tag{10}$$

9 Numerical Analysis

We took the following distinctive MAP representations for the arrival patterns so that their mean is the same, say 1, and Chakravarthy [2] suggests these values.

(A-Erl)-Erlang of Order 2:

$$D_0 = \begin{bmatrix} -2 & 2 \\ 0 & -2 \end{bmatrix}; \quad D_1 = \begin{bmatrix} 0 & 0 \\ 2 & 0 \end{bmatrix}$$

(A-Hyp-Exp)-Hyperexponential:

$$D_0 = \begin{bmatrix} -1.90 & 0 \\ 0 & -0.19 \end{bmatrix}; \quad D_1 = \begin{bmatrix} 1.710 & 0.190 \\ 0.171 & 0.019 \end{bmatrix}$$

The successive PH distributions have been taken for service times suggested by Chakravarthy [2].

(S-Erl)-Erlang of Order 2:

$$\alpha = (1, 0); \quad T = \begin{bmatrix} -2 & 2 \\ 0 & -2 \end{bmatrix}$$

(S-Exp)-Exponential:

$$\alpha = (1); \quad T = \begin{bmatrix} -1 \end{bmatrix}$$

(S-Hyp-Exp)-Hyperexponential:

$$\alpha = (0.8, 0.2); \quad T = \begin{bmatrix} -2.8 & 0 \\ 0 & -0.28 \end{bmatrix}$$

9.1 Example

With the aid of Figs. 2, 3, 4, 5, 6, and 7, we understand that the effect of the vacation rate (η_2) and repair rate (δ_2) of server-2 on the probability of server-2 is busy (P_{b}). Let $\lambda = 4,\ \gamma_1 = \gamma_2 = 9,\ p_1 = 0.4,\ q_1 = 0.6,\ p_2 = 0.2,\ q_2 = 0.8,\ \theta = 0.5,\ \sigma = 1$, and $\eta_1 = \delta_1 = 3$ so that the stability is maintained.

A quick view of Figs. 2, 3, 4, 5, 6, and 7 reveals that P_{b} increases while raising the vacation (η_2) and the repair rates (δ_2) of server-2 for a different combination of service and arrival times. Besides, it goes up high for A-Erl and gradually for A-Hyp-Exp. From the service point of view, the rate of increment is fast for S-Erl and slow for S-Hyp-Exp. An increase in the vacancy rate and the repair rate can help increase the availability of server-2 so that the system can improve the utilization of server-2.

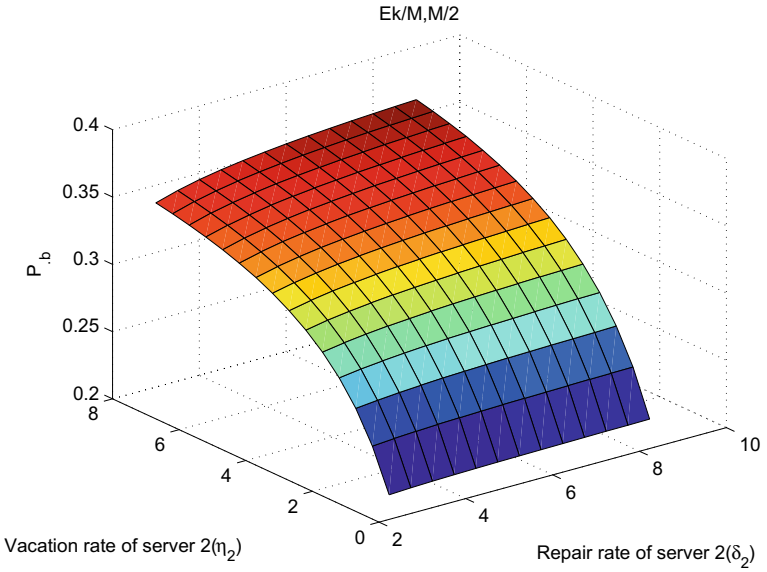

Fig. 2 (Vacation and repair rates—server-2) versus P_{b}

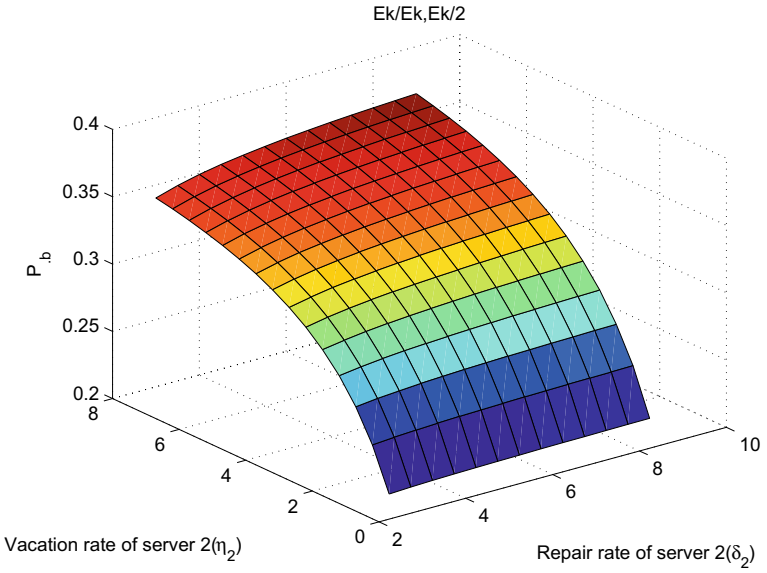

Fig. 3 (Vacation and repair rates—server-2) versus P_{b}

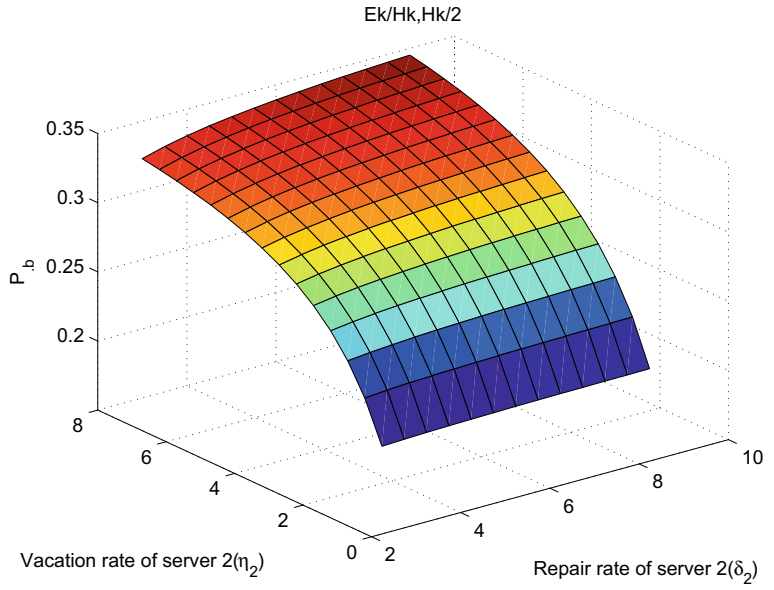

Fig. 4 (Vacation and repair rates—server-2) versus P_{b}

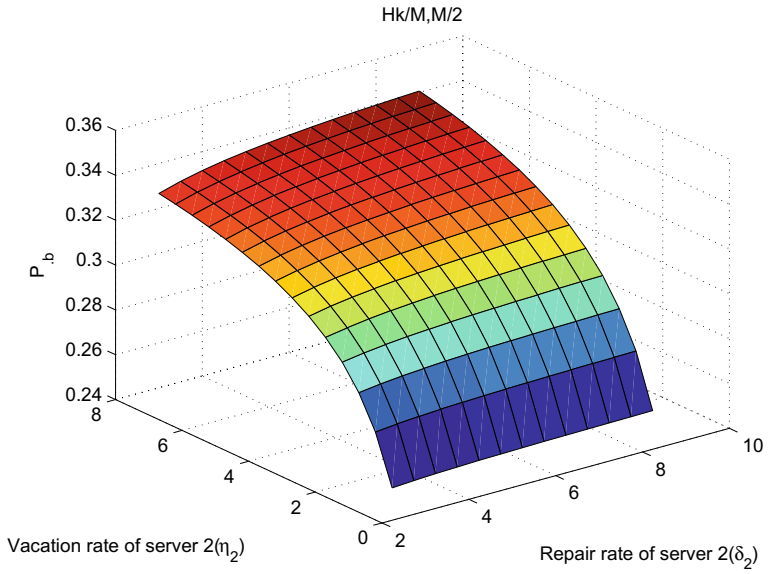

Fig. 5 (Vacation and repair rates—server-2) versus P_{b}

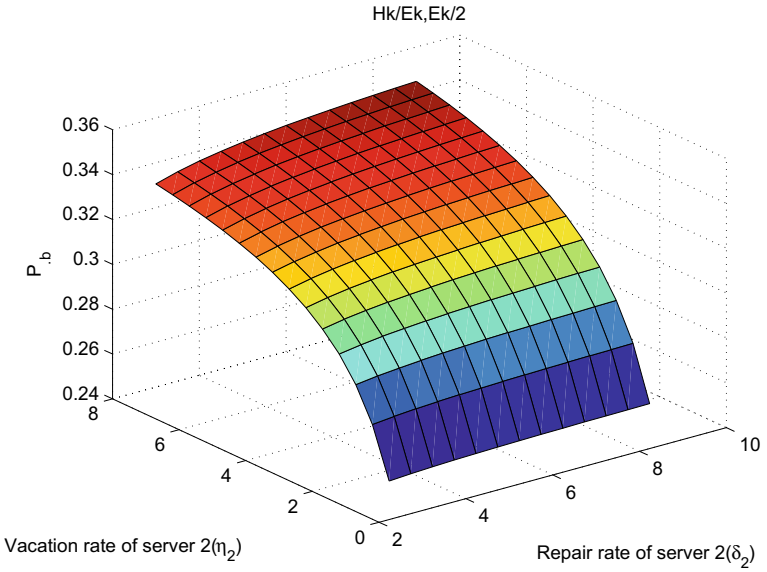

Fig. 6 (Vacation and repair rates—server-2) versus $P_{.b}$

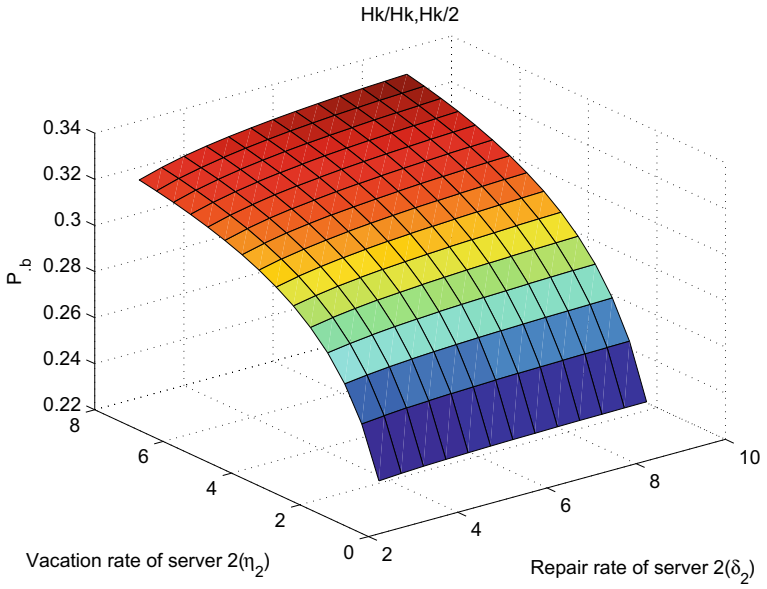

Fig. 7 (Vacation and repair rates—server-2) versus $P_{.b}$

10 Conclusion

We have studied a queueing model with MAP arrival, two servers, PH distributed service time for both the servers along with vacation, working breakdown, and starting failure. We have derived the stability condition and analyzed the active period and the waiting time. By using 3D graphs, we have visualized the impact of different parameters on some system measures. The uniqueness of our effort is that we have attempted to study the basic problems/situations faced by new and trained servers in both government/private sector jobs under study. We have suggested some of the ways for the efficient use of the server. Since we have assumed that only one junior is working under a trained server, it will be suggested to consider multiple juniors working under a trained one.

References

1. Ayyappan, G., Udayageetha, J.: Analysis of preemptive priority retrial queueing system with starting failure, modified Bernoulli vacation with vacation interruption, repair, immediate feedback, and impatient customers. Int. J. Math. Appl. **6**(1-E), 1013–1023 (2018)
2. Chakravarthy, S.R.: Markovian arrival processes. In: Wiley Encyclopedia of Operations Research and Management Science (2011)
3. Chakravarthy, S.R.: Analysis of MAP/PH1, PH2/1 queue with vacations and optional secondary services. Appl. Math. Model. **37**(20–21), 8886–8902 (2013)
4. Chakravarthy, S.R., Alfa, A.S.: A finite capacity queue with Markovian arrivals and two servers with group services. J. Appl. Math. Stoch. Anal. **7**(2), 161–178 (1994)
5. Chakravarthy, S.R., Chukova, S., Dimitrov, B.: Analysis of MAP/m/2/k queueing model with infinite resequencing buffer. Perform. Eval. **31**(3–4), 211–228 (1998)
6. Gross, D., Shortie, J.F., Thompson, J.M., Harris, C.M.: Fundamentals of Queueing Theory. Wiley (2008)
7. Kalidass, K., Kasturi, R.: A queue with working breakdowns. Comput. Ind. Eng. **63**(4), 779–783 (2012)
8. Keilson, J., Servi, L.D.: Oscillating random walk models for GI/G/1 vacation systems with Bernoulli schedules. J. Appl. Probab. **23**(3), 790–802 (1986)
9. Kumar, B.K., Rukmani, R., Thangaraj, V.: Analysis of MAP/PH(1), PH(2)/2 queue with Bernoulli vacations. J. Appl. Math. Stoch. Anal. **2008**, 1–20 (2008)
10. Latouche, G., Ramaswami, V.: Introduction to Matrix Analytic Methods in Stochastic Modeling. Society for Industrial and Applied Mathematics (1999)
11. Liou, C.-D.: Markovian queue optimization analysis with an unreliable server subject to working breakdowns and impatient customers. Int. J. Syst. Sci. **46**(12), 2165–2182 (2013)
12. Lucantoni, D.M., Meier-Hellstern, K.S., Neuts, M.F.: A single-server queue with server vacations and a class of non-renewal arrival processes. Adv. Appl. Probab. **22**(3), 676–705 (1990)
13. Neuts, M.F.: A versatile Markovian point process. J. Appl. Probab. **16**(04), 764–779 (1979)
14. Wang, J., Zhou, P.-F.: A batch arrival retrial queue with starting failures, feedback, and admission control. J. Syst. Sci. Syst. Eng. **19**(3), 306–320 (2010)

Results on Revan and Hyper Revan Indices of Some HEX Derived Networks

D. Narasimhan, R. Vignesh, and Kalyani Desikan

Abstract The theory of chemical reaction networks is a branch of mathematics that aims to mimic real-world behavior. This has received increasing attention of researchers, primarily due to its biological and empirical chemistry applications. Because of the fascinating problems that emerge from the mathematical structures involved, it has aroused interest of pure mathematicians. Topological indices are real numbers related to molecular graphs that help predict the compound characteristics. Many researchers evaluated various topological indices for the HEX-derived networks based on their vertex degrees. This paper is an extended version of such works, and we calculate Revan and hyper-Revan topological indices of HDN1, HDN2, HDN3, THDN3, and RHDN3 and also provide an accurate equation for those graphs.

Keywords Topological indices · Revan degree · HEX derived networks

1 Introduction

Graphs considered in this chapter are simple, with no loops and multiple edges. Let $V(\Gamma)$ and $E(\Gamma)$ be the collection of vertices and edges, respectively, of graph Γ and let d_p indicate the degree of node p in Γ. Let $\Delta(\Gamma)$ and $\delta(\Gamma)$ indicate the highest and lowest degrees of Γ, respectively. Chen et al. [1] introduced the hexagonal mesh network in the year 1990. Imran et al. [2] calculated some degree-based topological

D. Narasimhan (✉)
Department of Mathematics, Srinivasa Ramanujan Centre,
SASTRA Deemed to be University, Kumbakonam, Tamil Nadu, India
e-mail: narasimhan@src.sastra.edu

R. Vignesh · K. Desikan
Division of Mathematics, School of Advanced Sciences, Vellore Institute of Technology,
Chennai, Tamil Nadu, India
e-mail: rvignesh.2018@vitstudent.ac.in

K. Desikan
e-mail: kalyanidesikan@vit.ac.in

© The Author(s), under exclusive license to Springer Nature Singapore Pte Ltd. 2022

S. R. Kannan et al. (eds.), *Fuzzy Mathematical Analysis and Advances in Computational Mathematics*, Studies in Fuzziness and Soft Computing 419,
https://doi.org/10.1007/978-981-19-0471-4_15

indices like general Randić, Zagreb, ABC indices for some HEX derived networks in 2016. Further, Ali et al. [3, 4] computed some degree-based indices in year 2019, and those works led us to work on the Revan and Hyper Revan indices for these networks. Throughout the chapter, we denote the HEX derived networks as Γ_1, Γ_2, Γ_3, $T\Gamma_3$, and $R\Gamma_3$. The Revan vertex degree of p in Γ defined as $r(p) = \Delta(\Gamma) + \delta(\Gamma) - d_p$ [5, 6]. Many works have been done with these indices and HEX derived networks [7–10]. For the HEX derived networks, refer [3, 4].

$$R_1(\Gamma) = \sum_{uv \in E} \left[r_u + r_v\right] \tag{1}$$

$$R_2(\Gamma) = \sum_{uv \in E} \left[r_u * r_v\right] \tag{2}$$

$$R_3(\Gamma) = \sum_{uv \in E} \left[|r_u - r_v|\right] \tag{3}$$

$$HR_1(\Gamma) = \sum_{uv \in E} \left[r_u + r_v\right]^2 \tag{4}$$

$$HR_2(\Gamma) = \sum_{uv \in E} \left[r_u * r_v\right]^2 \tag{5}$$

In this paper, we have computed Revan and Hyper Revan indices for the HEX derived Networks $HDN1$, $HDN2$, $HDN3$, $THDN3$, and $RHDN3$. We use the general notations from the book [11].

Partition of $E(\Gamma_1)$ concerning the degree of end vertices of each edge is given in Table 1.

Table 1 Edge partitions of Γ_1

$E_{(d_u,d_v)}$	Number of edges
$E_{(3,5)}$	12
$E_{(3,7)}$	$18n - 36$
$E_{(3,12)}$	$18n^2 - 54n + 42$
$E_{(5,7)}$	12
$E_{(5,12)}$	6
$E_{(7,7)}$	$6n - 18$
$E_{(7,12)}$	$12n - 24$
$E_{(12,12)}$	$9n^2 - 33n + 30$

We now list the computed Revan values corresponding to the degree d_u of $E(\Gamma_1)$. We have the maximum degree $\Delta(\Gamma_1) = 12$ and the minimum degree $\delta(\Gamma_1) = 3$ (Table 2).

Partition of $E(\Gamma_2)$ concerning the degree of end vertices of each edge is given in Table 3.

We now list the computed Revan values corresponding to the degree d_u of $E(\Gamma_2)$. We have the maximum degree $\Delta(\Gamma_2) = 12$ and the minimum degree $\delta(\Gamma_2) = 5$ (Table 4).

Partition of $E(\Gamma_3)$ concerning the degree of end vertices of each edge is given in Table 5.

Partition of $E(T\Gamma_3)$ concerning each edges degree of end vertices is given in Table 6.

Partition of $E(R\Gamma_3)$ concerning each edges degree of end vertices is given in Table 7.

We now list the computed Revan values corresponding to the degree d_u of $E(\Gamma_3)$. We have

$$\Delta(\Gamma_3) = \Delta(T\Gamma_3) = \Delta(R\Gamma_3) = 18$$

$$\delta(\Gamma_3) = \delta(T\Gamma_3) = \delta(R\Gamma_3) = 4.$$

Table 2 Revan values of Γ_1

d_u	r_u
3	12
5	10
7	8
12	3

Table 3 Edge partitions of Γ_2

$E_{(d_u,d_v)}$	Number of edges
$E_{(5,5)}$	18
$E_{(5,6)}$	$12n - 24$
$E_{(5,7)}$	$12n - 12$
$E_{(5,12)}$	$6n$
$E_{(6,6)}$	$9n^2 - 33n + 30$
$E_{(6,7)}$	$6n - 12$
$E_{(6,12)}$	$18n^2 - 60n + 48$
$E_{(7,7)}$	$6n - 18$
$E_{(7,12)}$	$12n - 24$
$E_{(12,12)}$	$9n^2 - 33n + 30$

Table 4 Revan values of Γ_2

d_u	r_u
5	12
6	11
7	10
12	5

Table 5 Edge partitions of Γ_3

$E_{(d_u,d_v)}$	Number of edges
$E_{(4,4)}$	$18n^2 - 36n + 18$
$E_{(4,7)}$	24
$E_{(4,10)}$	$36n - 72$
$E_{(4,18)}$	$36n^2 - 108n + 84$
$E_{(7,10)}$	12
$E_{(7,18)}$	6
$E_{(10,10)}$	$6n - 18$
$E_{(10,18)}$	$12n - 24$
$E_{(18,18)}$	$9n^2 - 33n + 30$

Table 6 Edge partitions of $T\Gamma_3$

$E_{(d_u,d_v)}$	Number of edges
$E_{(4,4)}$	$3n^2 - 6n + 9$
$E_{(4,10)}$	$18n - 30$
$E_{(4,18)}$	$6n^2 - 30n + 36$
$E_{(10,10)}$	$3n - 6$
$E_{(10,18)}$	$6n - 18$
$E_{(18,18)}$	$\frac{3n^2-21n+36}{2}$

Table 7 Edge partitions of $R\Gamma_3$

$E_{(d_u,d_v)}$	Number of Edges
$E_{(4,4)}$	$6n^2 - 12n + 10$
$E_{(4,7)}$	8
$E_{(4,10)}$	$24n - 44$
$E_{(7,18)}$	2
$E_{(10,10)}$	$4n - 10$
$E_{(10,18)}$	$8n - 20$
$E_{(18,18)}$	$3n^2 - 16n + 21$

Table 8 Revan values of Γ_3, $T\Gamma_3$, $R\Gamma_3$

d_u	r_u
4	18
7	15
10	12
18	4

We now list the computed Revan values corresponding to the degree d_u of Γ_3,$T\Gamma_3$, $R\Gamma_3$. We have the maximum degree $\Delta(\Gamma_3) = 18$ and the minimum degree $\delta(\Gamma_3) = 4$ (Table 8).

2 Results and Discussion on Revan and Hyper Revan Indices of HEX Derived Networks

This section presents a few results based on the Revan and Hyper Revan indices of $HDN1$, $HDN2$, $HDN3$, $THDN3$, and $RHDN3$.

Theorem 1 *Let Γ_1 be the first type HEX derived network. Then*

$$R_1(\Gamma_1) = 324n^2 - 420n + 96.$$

Proof From Tables 1 and 2, we compute the first Revan index of Γ_1 as

$$\begin{aligned} R_1(\Gamma_1) &= |E_{(3,5)}|\big[12+10\big] + |E_{(3,7)}|\big[12+8\big] + |E_{(3,12)}|\big[12+3\big] \\ &\quad + |E_{(5,7)}|\big[10+8\big] + |E_{(5,12)}|\big[10+3\big] + |E_{(7,7)}|\big[8+8\big] \\ &\quad + |E_{(7,12)}|\big[8+3\big] + |E_{(12,12)}|\big[3+3\big] \\ &= 324n^2 - 420n + 96. \end{aligned}$$

Theorem 2 *Let Γ_1 be the first type HEX derived network. Then*

$$R_2(\Gamma_1) = 729n^2 + 159n - 822.$$

Proof From Tables 1 and 2, we compute the second Revan index of Γ_1 as

$$\begin{aligned} R_2(\Gamma_1) &= |E_{(3,5)}|\big[12*10\big] + |E_{(3,7)}|\big[12*8\big] + |E_{(3,12)}|\big[12*3\big] \\ &\quad + |E_{(5,7)}|\big[10*8\big] + |E_{(5,12)}|\big[10*3\big] + |E_{(7,7)}|\big[8*8\big] \\ &\quad + |E_{(7,12)}|\big[8*3\big] + |E_{(12,12)}|\big[3*3\big] \\ &= 729n^2 + 159n - 822. \end{aligned}$$

Theorem 3 *Let Γ_1 be the first type HEX derived network. Then*

$$R_3(\Gamma_1) = 162n^2 - 354n + 204.$$

Proof From Tables 1 and 2, we compute the third Revan index of Γ_1 as

$$\begin{aligned} R_3(\Gamma_1) &= |E_{(3,5)}|[2] + |E_{(3,7)}|[4] + |E_{(3,12)}|[9] + |E_{(5,7)}|[2] \\ &\quad + |E_{(5,12)}|[7] + |E_{(7,7)}|[0] + |E_{(7,12)}|[5] + |E_{(12,12)}|[0] \\ &= 162n^2 - 354n + 204. \end{aligned}$$

Theorem 4 *Let Γ_1 be the first type HEX derived network. Then*

$$HR_1(\Gamma_1) = 4374n^2 - 3150n - 672.$$

Proof From Tables 1 and 2, we compute the first Hyper Revan index of Γ_1 as

$$\begin{aligned} HR_1(\Gamma_1) &= |E_{(3,5)}|[12+10]^2 + |E_{(3,7)}|[12+8]^2 + |E_{(3,12)}|[12+3]^2 \\ &\quad + |E_{(5,7)}|[10+8]^2 + |E_{(5,12)}|[10+3]^2 + |E_{(7,7)}|[8+8]^2 \\ &\quad + |E_{(7,12)}|[8+3]^2 + |E_{(12,12)}|[3+3]^2 \\ &= 4374n^2 - 3150n - 672. \end{aligned}$$

Theorem 5 *Let Γ_1 be the first type HEX derived network. Then*

$$HR_2(\Gamma_1) = 24057n^2 + 124719n - 107466.$$

Proof From Tables 1 and 2, we compute the second Hyper Revan index of Γ_1 as

$$\begin{aligned} HR_2(\Gamma_1) &= |E_{(3,5)}|[12*10]^2 + |E_{(3,7)}|[12*8]^2 + |E_{(3,12)}|[12*3]^2 \\ &\quad + |E_{(5,7)}|[10*8]^2 + |E_{(5,12)}|[10*3]^2 + |E_{(7,7)}|[8*8]^2 \\ &\quad + |E_{(7,12)}|[8*3]^2 + |E_{(12,12)}|[3*3]^2 \\ &= 24057n^2 + 124719n - 107466. \end{aligned}$$

Theorem 6 *Let Γ_2 be the second type HEX derived network. Then*

$$R_1(\Gamma_2) = 576n^2 - 948n + 372.$$

Proof From Tables 3 and 4, we compute the first Revan index of Γ_2 as

$$\begin{aligned} R_1(\Gamma_2) &= |E_{(5,5)}|[12+12] + |E_{(5,6)}|[12+11] + |E_{(5,7)}|[12+10] \\ &\quad + |E_{(5,12)}|[12+5] + |E_{(6,6)}|[11+11] + |E_{(6,7)}|[11+10] \\ &\quad + |E_{(6,12)}|[11+5] + |E_{(7,7)}|[10+10] \\ &\quad + |E_{(7,12)}|[10+5] + |E_{(12,12)}|[5+5] \\ &= 576n^2 - 948n + 372. \end{aligned}$$

Theorem 7 *Let* Γ_2 *be the second type HEX derived network. Then*

$$R_2(\Gamma_2) = 2304n^2 - 2874n + 684.$$

Proof From Tables 3 and 4, we compute the second Revan index of Γ_2 as

$$\begin{aligned} R_2(\Gamma_2) &= |E_{(5,5)}|[12*12] + |E_{(5,6)}|[12*11] + |E_{(5,7)}|[12*10] \\ &\quad + |E_{(5,12)}|[12*5] + |E_{(6,6)}|[11*11] + |E_{(6,7)}|[11*10] \\ &\quad + |E_{(6,12)}|[11*5] + |E_{(7,7)}|[10*10] \\ &\quad + |E_{(7,12)}|[10*5] + |E_{(12,12)}|[5*5] \\ &= 2304n^2 - 2874n + 684. \end{aligned}$$

Theorem 8 *Let* Γ_2 *be the second type HEX derived network. Then*

$$R_3(\Gamma_2) = 108n^2 - 216n + 108.$$

Proof From Tables 3 and 4, we compute the third Revan index of Γ_2 as

$$\begin{aligned} R_3(\Gamma_2) &= |E_{(5,5)}|[0] + |E_{(5,6)}|[1] + |E_{(5,7)}|[2] + |E_{(5,12)}|[7] + |E_{(6,6)}|[0] \\ &\quad + |E_{(6,7)}|[1] + |E_{(6,12)}|[6] + |E_{(7,7)}|[0] + |E_{(7,12)}|[5] + |E_{(12,12)}|[0] \\ &= 108n^2 - 216n + 108. \end{aligned}$$

Theorem 9 *Let* Γ_2 *be the second type HEX derived network. Then*

$$HR_1(\Gamma_2) = 9864n^2 - 12996n + 3780.$$

Proof From Tables 3 and 4, we compute the first Hyper Revan index of Γ_2 as

$$\begin{aligned} HR_1(\Gamma_2) &= |E_{(5,5)}|[12+12]^2 + |E_{(5,6)}|[12+11]^2 + |E_{(5,7)}|[12+10]^2 \\ &\quad + |E_{(5,12)}|[12+5]^2 + |E_{(6,6)}|[11+11]^2 + |E_{(6,7)}|[11+10]^2 \\ &\quad + |E_{(6,12)}|[11+5]^2 + |E_{(7,7)}|[10+10]^2 \\ &\quad + |E_{(7,12)}|[10+5]^2 + |E_{(12,12)}|[5+5]^2 \\ &= 9864n^2 - 12996n + 3780. \end{aligned}$$

Theorem 10 *Let Γ_2 be the second type HEX derived network. Then*

$$HR_2(\Gamma_2) = 191844n^2 - 119190n + 252.$$

Proof From Tables 3 and 4, we compute the first Hyper Revan index of Γ_2 as

$$\begin{aligned} HR_2(\Gamma_2) &= |E_{(5,5)}|\big[12*12\big]^2 + |E_{(5,6)}|\big[12*11\big]^2 + |E_{(5,7)}|\big[12*10\big]^2 \\ &\quad + |E_{(5,12)}|\big[12*5\big]^2 + |E_{(6,6)}|\big[11*11\big]^2 + |E_{(6,7)}|\big[11*10\big]^2 \\ &\quad + |E_{(6,12)}|\big[11*5\big]^2 + |E_{(7,7)}|\big[10*10\big]^2 \\ &\quad + |E_{(7,12)}|\big[10*5\big]^2 + |E_{(12,12)}|\big[5*5\big]^2 \\ &= 191844n^2 - 119190n + 252. \end{aligned}$$

Theorem 11 *Let Γ_3 be the third type HEX derived network. Then*

$$R_1(\Gamma_3) = 1512n^2 - 2520n + 990.$$

Proof From Tables 5 and 8, we compute the first Revan index of Γ_3 as

$$\begin{aligned} R_1(\Gamma_3) &= |E_{(4,4)}|\big[18+18\big] + |E_{(4,7)}|\big[18+15\big] + |E_{(4,10)}|\big[18+12\big] \\ &\quad + |E_{(4,18)}|\big[18+4\big] + |E_{(7,10)}|\big[15+12\big] + |E_{(7,18)}|\big[15+4\big] \\ &\quad + |E_{(10,10)}|\big[12+12\big] + |E_{(10,18)}|\big[4+12\big] + |E_{(18,18)}|\big[4+4\big] \\ &= 1512n^2 - 2520n + 990. \end{aligned}$$

Theorem 12 *Let Γ_3 be the third type HEX derived network. Then*

$$R_2(\Gamma_3) = 8568n^2 - 10752n + 2064.$$

Proof From Tables 5 and 8, we compute the second Revan index of Γ_3 as

$$\begin{aligned} R_2(\Gamma_3) &= |E_{(4,4)}|\big[18*18\big] + |E_{(4,7)}|\big[18*15\big] + |E_{(4,10)}|\big[18*12\big] \\ &\quad + |E_{(4,18)}|\big[18*4\big] + |E_{(7,10)}|\big[15*12\big] + |E_{(7,18)}|\big[15*4\big] \\ &\quad + |E_{(10,10)}|\big[12*12\big] + |E_{(10,18)}|\big[4*12\big] + |E_{(18,18)}|\big[4*4\big] \\ &= 8568n^2 - 10752n + 2064. \end{aligned}$$

Theorem 13 *Let Γ_3 be the third type HEX derived network. Then*

$$R_3(\Gamma_3) = 504n^2 - 1200n + 726.$$

Proof From Tables 5 and 8, we compute the third Revan index of Γ_3 as

$$\begin{aligned} R_3(\Gamma_3) &= |E_{(4,4)}|[0] + |E_{(4,7)}|[3] + |E_{(4,10)}|[6] + |E_{(4,18)}|[14] \\ &\quad + |E_{(7,10)}|[3] + |E_{(7,18)}|[11] + |E_{(10,10)}|[0] \\ &\quad + |E_{(10,18)}|[8] + |E_{(18,18)}|[0] \\ &= 504n^2 - 1200n + 726. \end{aligned}$$

Theorem 14 *Let Γ_3 be the third type HEX derived network. Then*

$$HR_1(\Gamma_3) = 41328n^2 - 62112n + 21642.$$

Proof From Tables 5 and 8, we compute the first Hyper Revan index of Γ_3 as

$$\begin{aligned} HR_1(\Gamma_3) &= |E_{(4,4)}|[18+18]^2 + |E_{(4,7)}|[18+15]^2 + |E_{(4,10)}|[18+12]^2 \\ &\quad + |E_{(4,18)}|[18+4]^2 + |E_{(7,10)}|[15+12]^2 + |E_{(7,18)}|[15+4]^2 \\ &\quad + |E_{(10,10)}|[12+12]^2 + |E_{(10,18)}|[4+12]^2 + |E_{(18,18)}|[4+4]^2 \\ &= 41328n^2 - 62112n + 21642. \end{aligned}$$

Theorem 15 *Let Γ_3 be the third type HEX derived network. Then*

$$HR_2(\Gamma_3) = 2078496n^2 - 2515776n + 704928.$$

Proof From Tables 5 and 8, we compute the second Hyper Revan index of Γ_3 as

$$\begin{aligned} HR_2(\Gamma_3) &= |E_{(4,4)}|[18*18]^2 + |E_{(4,7)}|[18*15]^2 + |E_{(4,10)}|[18*12]^2 \\ &\quad + |E_{(4,18)}|[18*4]^2 + |E_{(7,10)}|[15*12]^2 + |E_{(7,18)}|[15*4]^2 \\ &\quad + |E_{(10,10)}|[12*12]^2 + |E_{(10,18)}|[4*12]^2 + |E_{(18,18)}|[4*4]^2 \\ &= 2078496n^2 - 2515776n + 704928. \end{aligned}$$

Theorem 16 *Let $T\Gamma_3$ be the Triangular third type HEX derived network. Then*

$$R_1(T\Gamma_3) = 252n^2 - 252n - 72.$$

Proof From Tables 6 and 8, we compute the first Revan index of $T\Gamma_3$ as

$$\begin{aligned} R_1(T\Gamma_3) &= |E_{(4,4)}|[18+18] + |E_{(4,10)}|[18+12] + |E_{(4,18)}|[18+4] \\ &\quad + |E_{(10,10)}|[12+12] + |E_{(10,18)}|[4+12] + |E_{(18,18)}|[4+4] \\ &= 252n^2 - 252n - 72. \end{aligned}$$

Theorem 17 *Let $T\Gamma_3$ be the Triangular third type HEX derived network. Then*

$$R_2(T\Gamma_3) = 1428n^2 + 336n - 2412.$$

Proof From Tables 6 and 8, we compute the second Revan index of $T\Gamma_3$ as

$$\begin{aligned} R_2(T\Gamma_3) &= |E_{(4,4)}|\big[18*18\big] + |E_{(4,10)}|\big[18*12\big] + |E_{(4,18)}|\big[18*4\big] \\ &\quad + |E_{(10,10)}|\big[12*12\big] + |E_{(10,18)}|\big[4*12\big] + |E_{(18,18)}|\big[4*4\big] \\ &= 1428n^2 + 336n - 2412. \end{aligned}$$

Theorem 18 *Let $T\Gamma_3$ be the Triangular third type HEX derived network. Then*

$$R_3(T\Gamma_3) = 84n^2 - 264n + 180.$$

Proof From Tables 6 and 8, we compute the third Revan index of $T\Gamma_3$ as

$$\begin{aligned} R_3(T\Gamma_3) &= |E_{(4,4)}|\big[0\big] + |E_{(4,10)}|\big[6\big] + |E_{(4,18)}|\big[14\big] \\ &\quad + |E_{(10,10)}|\big[0\big] + |E_{(10,18)}|\big[8\big] + |E_{(18,18)}|\big[0\big] \\ &= 84n^2 - 264n + 180. \end{aligned}$$

Theorem 19 *Let $T\Gamma_3$ be the Triangular third type HEX derived network. Then*

$$HR_1(T\Gamma_3) = 6888n^2 - 3504n - 4824.$$

Proof From Tables 6 and 8, we compute the first Hyper Revan index of $T\Gamma_3$ as

$$\begin{aligned} HR_1(T\Gamma_3) &= |E_{(4,4)}|\big[18+18\big]^2 + |E_{(4,10)}|\big[18+12\big]^2 + |E_{(4,18)}|\big[18+4\big]^2 \\ &\quad + |E_{(10,10)}|\big[12+12\big]^2 + |E_{(10,18)}|\big[4+12\big]^2 + |E_{(18,18)}|\big[4+4\big]^2 \\ &= 6888n^2 - 3504n - 4824. \end{aligned}$$

Theorem 20 *Let $T\Gamma_3$ be the Triangular third type HEX derived network. Then*

$$HR_2(T\Gamma_3) = 346416n^2 + 127776n - 429552.$$

Proof From Tables 6 and 8, we compute the second Revan index of $T\Gamma_3$ as

$$\begin{aligned} HR_2(T\Gamma_3) &= |E_{(4,4)}|\big[18*18\big]^2 + |E_{(4,10)}|\big[18*12\big]^2 + |E_{(4,18)}|\big[18*4\big]^2 \\ &\quad + |E_{(10,10)}|\big[12*12\big]^2 + |E_{(10,18)}|\big[4*12\big]^2 + |E_{(18,18)}|\big[4*4\big]^2 \\ &= 346416n^2 + 127776n - 429552. \end{aligned}$$

Theorem 21 *Let $R\Gamma_3$ be the Rectangular third type HEX derived network. Then*

$$R_1(R\Gamma_3) = 504n^2 - 672n + 6.$$

Proof From Tables 7 and 8, we compute the first Revan index of $R\Gamma_3$ as

$$\begin{aligned} R_1(R\Gamma_3) &= |E_{(4,4)}|\big[18+18\big] + |E_{(4,7)}|\big[18+15\big] + |E_{(4,10)}|\big[18+12\big] \\ &\quad + |E_{(4,18)}|\big[18+4\big] + |E_{(7,18)}|\big[15+4\big] + |E_{(10,10)}|\big[12+12\big] \\ &\quad + |E_{(10,18)}|\big[12+4\big] + |E_{(18,18)}|\big[4+4\big] \\ &= 504n^2 - 672n + 6. \end{aligned}$$

Theorem 22 *Let $R\Gamma_3$ be the Rectangular third type HEX derived network. Then*

$$R_2(R\Gamma_3) = 2856n^2 - 1456n - 2592.$$

Proof From Tables 7 and 8, we compute the second Revan index of $R\Gamma_3$ as

$$\begin{aligned} R_2(R\Gamma_3) &= |E_{(4,4)}|\big[18*18\big] + |E_{(4,7)}|\big[18*15\big] + |E_{(4,10)}|\big[18*12\big] \\ &\quad + |E_{(4,18)}|\big[18*4\big] + |E_{(7,18)}|\big[15*4\big] + |E_{(10,10)}|\big[12*12\big] \\ &\quad + |E_{(10,18)}|\big[12*4\big] + |E_{(18,18)}|\big[4*4\big] \\ &= 2856n^2 - 1456n - 2592. \end{aligned}$$

Theorem 23 *Let $R\Gamma_3$ be the Rectangular third type HEX derived network. Then*

$$R_3(R\Gamma_3) = 168n^2 - 464n + 294.$$

Proof From Tables 7 and 8, we compute the third Revan index of $R\Gamma_3$ as

$$\begin{aligned} R_3(R\Gamma_3) &= |E_{(4,4)}|\big[0\big] + |E_{(4,7)}|\big[3\big] + |E_{(4,10)}|\big[6\big] + |E_{(4,18)}|\big[14\big] \\ &\quad + |E_{(7,18)}|\big[11\big] + |E_{(10,10)}|\big[0\big] + |E_{(10,18)}|\big[8\big] + |E_{(18,18)}|\big[0\big] \\ &= 168n^2 - 464n + 294. \end{aligned}$$

Theorem 24 *Let $R\Gamma_3$ be the Rectangular third type HEX derived network. Then*

$$HR_1(R\Gamma_3) = 13776n^2 - 13776n - 3510.$$

Proof From Tables 7 and 8, we compute the first Hyper Revan index of $R\Gamma_3$ as

$$\begin{aligned} HR_1(R\Gamma_3) &= |E_{(4,4)}|\big[18+18\big]^2 + |E_{(4,7)}|\big[18+15\big]^2 + |E_{(4,10)}|\big[18+12\big]^2 \\ &\quad + |E_{(4,18)}|\big[18+4\big]^2 + |E_{(7,18)}|\big[15+4\big]^2 + |E_{(10,10)}|\big[12+12\big]^2 \\ &\quad + |E_{(10,18)}|\big[12+4\big]^2 + |E_{(18,18)}|\big[4+4\big]^2 \\ &= 13776n^2 - 13776n - 3510. \end{aligned}$$

Theorem 25 *Let $R\Gamma_3$ be the Rectangular third type HEX derived network. Then*

$$HR_2(R\Gamma_3) = 692832n^2 - 291520n - 411936.$$

Proof From Tables 7 and 8, we compute the second Hyper Revan index of $R\Gamma_3$ as

$$\begin{aligned} HR_2(R\Gamma_3) &= |E_{(4,4)}|\big[18*18\big]^2 + |E_{(4,7)}|\big[18*15\big]^2 + |E_{(4,10)}|\big[18*12\big]^2 \\ &\quad + |E_{(4,18)}|\big[18*4\big]^2 + |E_{(7,18)}|\big[15*4\big]^2 + |E_{(10,10)}|\big[12*12\big]^2 \\ &\quad + |E_{(10,18)}|\big[12*4\big]^2 + |E_{(18,18)}|\big[4*4\big]^2 \\ &= 692832n^2 - 291520n - 411936. \end{aligned}$$

3 Conclusion

In this paper, we calculated the Revan and Hyper Revan indices for the HEX derived networks. These exact results are helpful in both chemical and pharmaceutical sciences. As future work, we are planning to compute further edge-based chemical indices for these HEX derived networks Γ_1, Γ_2, Γ_3, $T\Gamma_3$, and $R\Gamma_3$.

References

1. Chen, M.S., Shin, K.G., Kandlur, D.D.: Addressing, routing, and broadcasting in hexagonal mesh multiprocessors. IEEE Trans. Comput. **39**(1), 10–18 (1990)
2. Imran, M., Baig, A.Q., Ali, H.: On molecular topological properties of hex-derived networks. J. Chemom. **30**(3), 121–129 (2016)
3. Ali, H., Binyamin, M.A., Shafiq, M.K., Gao, W.: On the degree-based topological indices of some derived networks. Mathematics **7**(7), 612 (2019)
4. Ali, H., Sajjad, A., Sajjad, A.: On further results of hex derived networks. Open J. Discrete Appl. Math. **2**(1), 32–40 (2019)
5. Kulli, V.R.: Revan indices of oxide and honeycomb networks. Int. J. Math. Appl. **5**(4-E), 663–667 (2017)
6. Kulli, V.R.: Hyper-Revan indices and their polynomials of silicate networks. Int. J. Curr. Res. Sci. Technol. **4**(3), 17–21 (2018)
7. Raj, F.S., George, A.: On the metric dimension of HDN 3 and PHDN 3. In: 2017 IEEE International Conference on Power, Control, Signals and Instrumentation Engineering (ICPCSI), 21 Sep 2017, pp. 1333–1336. IEEE
8. Ali, H., Binyamin, M.A., Shafiq, M.K.: On topological properties of third type of hex derived networks. arXiv preprint arXiv:1904.10827, 24 Apr 2019
9. Kulli, V.R.: Connectivity Revan indices of chemical structures in drugs. Int. J. Eng. Sci. Res. Technol. **7**(5), 11–16 (2018)
10. Kulli, V.R.: The sum connectivity Revan index of silicate and hexagonal networks. Ann. Pure Appl. Math. **14**(3), 401–406 (2017)
11. West, D.B.: Introduction to Graph Theory. Prentice Hall, Upper Saddle River (2001)

Dufour and Soret Effects on MHD Flow of Cu-Water and Al_2O_3-Water Nanofluid Flow Over a Permeable Rotating Cone

K. Padmaja and B. Rushi Kumar

Abstract In this paper, we investigate numerically the nanofluid flow about a permeable, vertical, rotating cone with Dufour and Soret effects in the presence of thermal radiation, magnetic field, and chemical reaction. The heat and mass transfer of a MHD nanofluid about a porous vertically rotating cone is analyzed. The fluid flow considered is steady, laminar, and incompressible. A uniform suction/injection of the fluid is present on the surface of the cone. The cone is symmetric about the axis of rotation and is rotating with an angular rotating velocity. The governing equations pertinent to the fluid flow and the thermophysical properties of the nanofluid are nonlinear partial differential equations (PDEs). Using similarity transformation variables, these partial differential equations are converted into ordinary differential equations (ODEs). MATLAB's bvp4c solver is used to solve the converted system of ODEs. To achieve a clear understanding on the physical insights of the problem, the two nanofluids—copper in water and alumina in water are analyzed. The graphical representations of tangential, normal, circumferential velocity profiles, temperature profiles, and concentration profiles with respect to various fluid flow parameters are investigated. The Dufour and Soret numbers and the thermal radiation parameter have a significant impact on the rates of heat and mass transfer.

Keywords Bvp4c · Heat transfer · Mass transfer · Nanofluid · Thermal radiation · Vertical cone

Nomenclature

a	Absorption parameter
B_O	Magnetic field strength

K. Padmaja · B. Rushi Kumar (✉)
Department of Mathematics, School of Advanced Sciences, VIT, Vellore, Tamil Nadu 632014, India
e-mail: rushikumar@vit.ac.in

K. Padmaja
e-mail: padmaja.k@vit.ac.in

© The Author(s), under exclusive license to Springer Nature Singapore Pte Ltd. 2022

S. R. Kannan et al. (eds.), *Fuzzy Mathematical Analysis and Advances in Computational Mathematics*, Studies in Fuzziness and Soft Computing 419,
https://doi.org/10.1007/978-981-19-0471-4_16

C_p	Specific heat at constant pressure
C_s	Concentration susceptibility
C	Local concentration of the nanofluid
C_w	Concentration of the nanofluid on the wall
C_∞	Concentration of the nanofluid in the free stream
Da^{-1}	Inversion of Darcy number
D_m	Molecular diffusivity
Df	Dufour number
f_w	Dimensionless suction/injection parameter
g	Acceleration due to gravity
K	Permeability parameter
K_f	Thermal conductivity of the base fluid
K_{nf}	Thermal conductivity of nanofluid
K_s	Thermal conductivity of nanoparticles
K_T	Thermal diffusivity ratio
k_r	Chemical reaction parameter
M	Dimensionless magnetic field parameter
N	Buoyancy parameter
Pr	Prandtl number
Q_0	Heat generation parameter
q_r	Radiative heat flux
Re	Reynolds number
Ri	Richardson number
Rd	Dimensionless radiation parameter
Sr	Soret number
Sc	Schmidt number
T	Local temperature of the nanofluid
T_w	Temperature of the nanofluid on the wall
T_∞	Temperature of the nanofluid in the free stream
β_f	Thermal expansion coefficient of base fluid
β_{nf}	Thermal expansion coefficient of nanofluid
β_s	Thermal expansion coefficient of nanoparticles
δ	Dimensionless heat generation parameter
γ	Dimensionless chemical reaction parameter
ρ_f	Density of base fluid
ρ_s	Density of nanoparticles
ρ_{nf}	Density of nanofluid
$(\rho C_p)_{nf}$	Heat capacitance of nanofluid
μ_f	Dynamic viscosity of base fluid
μ_s	Dynamic viscosity of nanoparticles
μ_{nf}	Dynamic viscosity of nanofluid
ν_f	Kinematic viscosity of base fluid
ν_s	Kinematic viscosity of nanoparticles
ν_{nf}	Kinematic viscosity of nanofluid
σ_{nf}	Electrical conductivity of the fluid

θ	Dimensionless temperature
ϕ	Dimensionless concentration
ϕ_{nf}	Volume fraction of the nanofluid

Subscripts Used

nf	Nanofluid
f	Base fluid
s	Nanoparticles
∞	Condition in free stream
w	Condition on the wall

1 Introduction

In many industries like turbomachine manufacturing, polymer production, food processing, water treatment, chemical and metallurgical industries, the process of heat and mass transfer plays a vital role. Much information about heat and mass transfer in a rotating cone embedded in a porous medium can be studied in the papers by Tien and Tsuji [1], Chamkha and Rashad [2], Kumar and Sivaraj [3], and Reddy et al. [4]. Shah et al. [5] analyzed the effects of Dufour, Soret, and Prandtl number along with suction and radiation parameter on the fluid flow of a viscous fluid over a rotating disk. Afify [6] investigated the Dufour and Soret effects over a porous vertical surface of a MHD, non-Darcy fluid along with the effects of time-dependent viscosity.

Nanofluids are colloidal suspensions of nanoparticles and base fluid introduced by Choi and Eastman [7]. A bigger range of real-life applications of nanofluids has been studied by Wong and De Leon [8]. Nanofluids have gained recent interest because of their wide range of applications in industries such as food processing industries, water treatment industries, and chemical industries. It is a very compatible fluid that can be used to reduce or induce the level of heat transfer. Ravindhranath and Ramamoorty [9] analyzed the synthesis of alumina using an eco-friendly, cost-effective, bio-method, and its potential usage in water treatment. The alumina nanoparticle has a great advantage in many applications because of its significant physical and chemical properties. Farhana et al. [10] analyzed the importance of nanofluids based on thermal conductivity, heat transfer, and cooling efficiency. Dankovich and Smith [11] analyzed the efficient usage of copper nanoparticles in purifying drinking water. The copper nanoparticle is significantly cost-effective and easier in its synthesis.

Reddy and Chamkha [12] investigated the heat and mass transfer along with the influence of heat generation/absorption in two nanofluids Al_2O_3 water and TiO_2 water past a stretching porous sheet. Pandey and Kumar [13] analyzed the flow of a MHD, nanofluid over a wedge in a porous medium along with the effects of viscous dissipation. Mallikarjuna et al. [14] investigated the heat and mass transfer

in a rotating cone along with the chemical reaction, magnetic effects, and impacts of porosity. Reddy et al. [15] analyzed the transfer of heat and mass in two nanofluids—Cu-water and Ag-water in two different volume fractions. Dzulkifli et al. [16] studied the boundary layer flow and heat transfer analysis through a stretching sheet of a nanofluid along with the effects of thermophoresis and Brownian motion parameters.

Janke et al. [17] investigated the heat transfer rates of Cu-water and Al_2O_3-water along with the conducting dust particles to enhance the heat transfer in a cone along with the impacts of non-uniform source/sink. Kumar et al. [18] analyzed the Soret effects of three nanofluids namely, Al_2O_3-water, TiO_2-water, and Ag-water past a vertical plate in a porous medium along with effects of a second-order chemical reaction and thermal radiation. Abbas and Magdy [19] investigated the rotating nanofluids—Cu-water, Al_2O_3-water, TiO_2-water in a moving rotating plate and the rates of heat transfer based on the shapes of the nanoparticles.

Kalavathamma and Lakshmi [20] studied the effects of variable fluid flow parameters on the heat transfer rate and mass transfer rate in a cone embedded in a porous medium saturated with nanofluid. Ahmad et al. [21] have analyzed the heat and mass transfer of a two-dimensional, MHD nanofluid over a rotating cone and plate. The effects of various numbers like Prandtl number, Dufour number, Soret number, and Schmidt number are depicted. It is illustrated that a rotating cone has better heat and mass transfer capacities than that of a rotating plate.

Based on such an in-depth literature review, we analyzed that although there have been studies on the heat and mass transfer through a rotating cone in the past, the study of nano-fluid with the inclusion of heat and mass transfer along with magnetic, thermal radiation effects in a rotating porous cone has not been investigated yet. In this regard, we consider, a rotating porous cone with two nano fluids-copper in water and alumina in water. The nanoparticles copper (Cu) and alumina (Al_2O_3) are considered because of their emerging usage in many food processing, water purification, and chemical industries. The thermodynamical properties of the nanoparticles and base fluid are taken into account to analyze the boundary layer equations. The influence and impacts of various parameters involved in the tangential, normal, and circumferential velocities, temperature, and concentration profiles are presented through graphs.

The rest of the work is organized as follows. In Sect. 2, the mathematical formulation of the governing equations considering the geometry of the problem, Df and Sr effect and magnetic parameter, chemical reactions, and radiation parameters are described. In Sect. 3, the above nonlinear equations are solved by discretizing them using the Runge–Kutta method. Section 4 describes the effects of fluid flow parameters on the velocity measurements, θ, and ϕ profiles, and their results. Finally, Sect. 5 presents our conclusions.

2 Mathematical Modeling

Consider an upward-directed, permeable, rotating cone, and rotating around the x-axis with a rotational velocity Ω along with magnetic field B_0 in the z-axis as

Fig. 1 Flow geometry

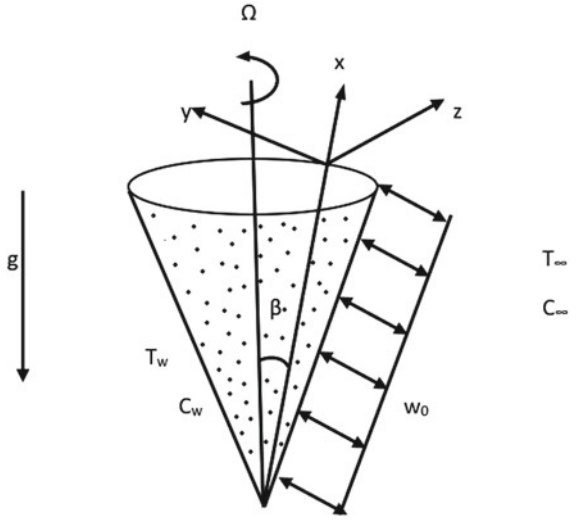

shown in Fig. 1. A steady-state, laminar, incompressible nanofluid flow is considered. A uniform suction/injection of the nanofluid of velocity w_0 is present at the surface of the cone. Within the sights of Soret and Dufour impacts, along with the consideration of mass concentration, the governing fluid flow equations of the boundary layer are analyzed. By incorporating the above assumptions and Boussinesq's approximation into the basic governing equations, we get

$$\frac{\partial u}{\partial x} + \frac{\partial w}{\partial z} + \frac{u}{x} = 0 \tag{1}$$

$$\rho_{\mathrm{nf}}\left(u\frac{\partial u}{\partial x} + w\frac{\partial u}{\partial z} + \frac{u^2}{x}\right) = \mu_{\mathrm{nf}}\left(\frac{\partial^2 u}{\partial z^2}\right) - \sigma_{\mathrm{nf}}B_{\mathrm{o}}^2 u - \frac{\mu_{\mathrm{nf}}}{K}u + (\rho\beta)_{\mathrm{nf}}g(T - T_\infty)\cos\beta + (\rho\beta)_{\mathrm{nf}}g(C - C_\infty)\cos\beta \tag{2}$$

$$\rho_{\mathrm{nf}}\left(u\frac{\partial v}{\partial x} + w\frac{\partial v}{\partial z} + \frac{uv}{x}\right) = \mu_{\mathrm{nf}}\left(\frac{\partial^2 v}{\partial z^2}\right) - \sigma_{\mathrm{nf}}B_{\mathrm{o}}^2 v - \frac{\mu_{\mathrm{nf}}}{K}v \tag{3}$$

$$u\frac{\partial T}{\partial x} + w\frac{\partial T}{\partial z} = \frac{\kappa_{\mathrm{nf}}}{(\rho C_{\mathrm{p}})_{\mathrm{nf}}}\frac{\partial^2 T}{\partial z^2} + \frac{D_{\mathrm{m}}K_{\mathrm{T}}}{C_{\mathrm{s}}C_{\mathrm{p}}}\frac{\partial^2 C}{\partial z^2} + \frac{Q_0(T - T_\infty)}{(\rho C_{\mathrm{p}})_{\mathrm{nf}}} - \frac{1}{(\rho C_{\mathrm{p}})_{\mathrm{nf}}}\frac{\partial q_{\mathrm{r}}}{\partial z} \tag{4}$$

$$u\frac{\partial C}{\partial x} + w\frac{\partial C}{\partial z} = D_{\mathrm{m}}\frac{\partial^2 C}{\partial z^2} + \frac{D_{\mathrm{m}}K_{\mathrm{T}}}{T_{\mathrm{m}}}\frac{\partial^2 T}{\partial z^2} - k_{\mathrm{r}}(C - C_\infty). \tag{5}$$

The resultant boundary conditions are

$$\begin{aligned} &u = 0, v = x\Omega \sin\beta, w = w_0, T = T_w(x), C = C_w(x) \text{ at } z = 0 \\ &u \to 0, v \to 0, T \to T_\infty, C \to C_\infty \text{ at } z \to \infty \end{aligned} \tag{6}$$

Here, u, v, w are the velocities in the x, y, and z directions, respectively. T is the local temperature of the fluid and C is the local concentration of the fluid. ρ_{nf} is the density of the nanofluid, μ_{nf} is the dynamic viscosity of the nanofluid, κ_{nf} is the conductivity of the nanofluid, C_p is the specific heat.

The radiation heat flux [22] is given by

$$\frac{\partial q_r}{\partial z} = -4a\sigma^* \left(T_\infty^4 - T^4\right) \tag{7}$$

T^4 can be expanded using Taylor's series about T_∞ as

$$T^4 = 4T_\infty^3 - 3T_\infty^4 \tag{8}$$

The thermodynamical properties of the nanofluids are

$$\begin{aligned} \mu_{nf} &= \frac{\mu_f}{(1-\phi_{nf})^{2.5}}, \\ \nu_{nf} &= \frac{\mu_{nf}}{\rho_{nf}}, \\ \rho_{nf} &= (1-\phi_{nf})\rho_f + \phi_{nf}\rho_s, \\ (\rho\beta)_{nf} &= (1-\phi_{nf})(\rho\beta)_f + \phi_{nf}(\rho\beta)_s, \\ (\rho C_p)_{nf} &= (1-\phi_{nf})(\rho C_p)_f + \phi_{nf}(\rho C_p)_s \\ K_{nf} &= \frac{(K_s + 2K_f) - 2\phi_{nf}(K_f - K_s)}{(K_s + 2K_f) + 2\phi_{nf}(K_f + K_s)} \end{aligned} \tag{9}$$

The following similarity transformations (10) are derived using Buckingham's π theorem. These transformations help to simplify the governing Eqs. (1–5) along with the boundary condition (6).

$$\eta = \left(\frac{\Omega \sin\beta}{\nu}\right)^{1/2} z, u = -\frac{1}{2}x\Omega \sin\beta f'(\eta), v = x\Omega \sin\beta h(\eta),$$
$$w = (\nu\Omega \sin\alpha)^{1/2} f(\eta), \theta = \frac{T - T_\infty}{T_w - T\infty}, \phi = \frac{C - C_\infty}{C_w - C_\infty},$$
$$T_w - T_\infty = \frac{(T_L - T_\infty)x}{L}, C_w - C_\infty = \frac{(C_L - C_\infty)x}{L}, M = \frac{\sigma_{nf} B_o^2}{\rho_f \Omega \sin\beta},$$
$$\gamma = \frac{k_r}{\Omega \sin\beta}, \mathrm{Gr} = \frac{g\beta_f \cos\alpha (T_w - T_\infty)L^3}{\nu^2}, \mathrm{Da}^{-1} = \frac{\nu_f}{K\Omega \sin\beta},$$
$$\mathrm{Re} = \frac{\Omega L^2 \sin\beta}{\nu_f}, \mathrm{Ri} = \frac{\mathrm{Gr}}{(\mathrm{Re})^2}, \mathrm{Pr} = \frac{(\mu C_p)_f}{K_f},$$
$$\mathrm{Sc} = \frac{\nu}{D_m}, \mathrm{Df} = \frac{D_m K_t}{C_s C_p \nu}\frac{C_w(x) - C_\infty}{T_w(x) - T_\infty}, \mathrm{Sr} = \frac{D_m K_t}{\nu T_m}\frac{T_w(x) - T\infty}{C_w(x) - C_\infty},$$
$$\mathrm{Rd} = \frac{16\nu a * T_\infty^3}{K_f \Omega \sin\alpha}, \delta = \frac{Q_0}{(\rho C_p)_f \Omega \sin\beta}, N = \frac{C_w(x) - C_\infty}{T_w(x) - T_\infty} \tag{10}$$

In the above quantities, L is cone's slant height, T_L denotes cone shallow's temperature, and C_L is cone shallow's concentration;

By substituting (9) and (10) in Eqs. (1–5),

$$f'^2 + f''f = -a_1 f''' + \frac{Mf'}{a_2} - \mathrm{Da}^{-1} a_1 f' + 2\frac{a_3}{a_2}\mathrm{Ri}(\theta + N\phi) \tag{11}$$

$$h'f - f'h = a_1 h'' - \frac{Mh}{a_2} - \mathrm{Da}^{-1} a_1 h \tag{12}$$

$$\theta'' = \frac{1}{a_4}\left[\mathrm{Rd}\theta - \delta\mathrm{Pr}\theta - \mathrm{DfPr}\phi'' + a_5 \mathrm{Pr} f\theta' - \frac{1}{2}\mathrm{Pr}a_5 f'\theta\right] \tag{13}$$

$$\phi'' = \mathrm{Sc} f\phi' - \frac{1}{2}\mathrm{Sc} f'\phi - \mathrm{SrSc}\theta'' + \delta\mathrm{Sc}\phi \tag{14}$$

The associated boundary conditions are

$$\begin{aligned} &f = 0.1, f' = 0, h = 1, \theta = 1, \phi = 1 \text{ at } \eta = 0 \\ &f = 0, h = 0, \theta = 0, \phi = 0 \text{ at } \eta \to \infty \end{aligned} \tag{15}$$

where primes refer the derivatives about η;

$$a_1 = \frac{1}{(1 - \phi_{nf})^{2.5}} \frac{1}{(1 - \phi_{nf}) + \phi_{nf}\left(\frac{\rho_s}{\rho_f}\right)},$$

$$a_2 = (1 - \phi_{\mathrm{nf}}) + \phi_{\mathrm{nf}} \left(\frac{\rho_{\mathrm{s}}}{\rho_{\mathrm{f}}} \right),$$

$$a_3 = (1 - \phi_{\mathrm{nf}}) + \phi_{\mathrm{nf}} \left(\frac{(\rho\beta)_{\mathrm{s}}}{(\rho\beta)_{\mathrm{f}}} \right),$$

$$a_4 = \frac{(K_{\mathrm{s}} + 2K_{\mathrm{f}}) - 2\phi(K_{\mathrm{f}} - K_{\mathrm{s}})}{(K_{\mathrm{s}} + 2K_{\mathrm{f}}) + 2\phi(K_{\mathrm{f}} + K_{\mathrm{s}})},$$

$$a_5 = \left((1 - \phi_{\mathrm{nf}})(\rho C_{\mathrm{p}})_{\mathrm{f}} + \phi_{\mathrm{nf}}(\rho C_{\mathrm{p}})_{\mathrm{s}} \right).$$

3 Method of Solution

Runge–Kutta method alongside shooting technique is implemented to solve Eqs. (10–14) with the related boundary condition (15). To solve this problem with bvp4c package in MATLAB, we provide functions that evaluate the differential equations and the residual in the boundary conditions. We consider

$$f = F(1);\ f' = F(2);\ f'' = F(3);\ h = F(4);\ h' = F(5);\ \theta = F(6);$$
$$\theta' = F(7);\ \phi = F(8);\ \phi' = F(9).$$

The nonlinear differential Eqs. (9–13) are converted into the following first-order differential equations

$$\begin{bmatrix} f' \\ f'' \\ f''' \\ h' \\ h'' \\ \theta' \\ \theta'' \\ \phi' \\ \phi'' \end{bmatrix} = \begin{bmatrix} F(2) \\ F(3) \\ \frac{1}{(a_1)} \left[\frac{\mathrm{MF}(2)}{a_2} - (F(1))^2 - F(1)F(3) + \mathrm{Da}^{-1} F(2) a_1^2 + 2\frac{a_3}{a_2} \mathrm{Ri}(F(6) + \mathrm{NF}(8)) \right] \\ F(5) \\ \frac{1}{(a_1)} \left[\frac{\mathrm{MF}(4)}{a_2} - F(2)F(4) + F(1)F(5) - \mathrm{Da}^{-1} F(4) a_1^2 \right] \\ F(7) \\ \frac{1}{\mathrm{SrScDfPr} - a_4} [F(1) \left[\mathrm{ScDfPrF}(9) - a_5 \mathrm{PrF}(7) \right] - \frac{F(2)}{2} [\mathrm{ScDfPrF}(8) - \mathrm{Pra}_5 F(6) \\ -F(6) [\mathrm{Rd} - \delta \mathrm{Pr}] + \delta \mathrm{ScDfPrF}(8)] \\ F(9) \\ \frac{1}{\mathrm{SrScDfPr} - a_4} [F(1) \left[\mathrm{Sca}_4 F(9) + a_5 \mathrm{PrSrScF}(7) \right] - \frac{F(2)}{2} \left[\mathrm{Pra}_5 \mathrm{SrScF}(6) - \mathrm{Sca}_4 F(8) \right] \\ +F(6) [\mathrm{RdSrSc} - \delta \mathrm{PrSrSc}] - \delta \mathrm{Sca}_4 F(8)] \end{bmatrix}$$

This problem is solved numerically by considering it as an initial value problem and is solved using bvp4c package in MATLAB.

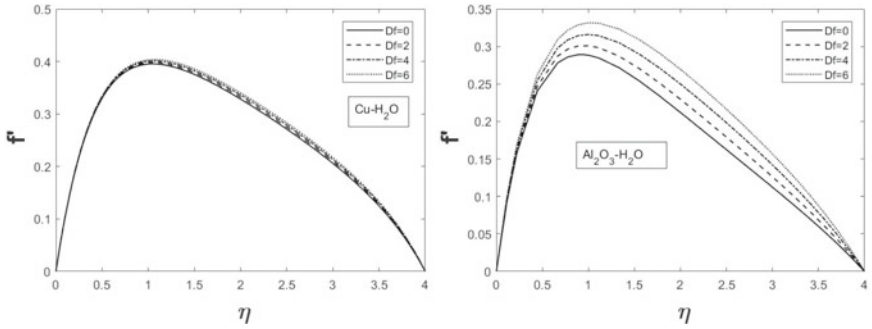

(a) Cu–H_2O (b) Al_2O_3–H_2O

Fig. 2 Tangential velocity profile for distinct values of Df

4 Results and Discussions

The prime objective of this paper is the numerical study of Dufour and Soret effects on the convective flow of a MHD nanofluid past a rotating vertical porous cone. Additionally, the impacts of M, Rd, Da^{-1}, on the velocity of the flow, temperature, and concentration for the two nanofluids—$\mathrm{Cu} - \mathrm{H_2O}$ and $\mathrm{Al_2O_3} - \mathrm{H_2O}$ are presented by graphs in Figs. 2, 3, 4, 5, 6, 7, 8, 9, 10, 11, 12 and 13. The thermodynamical properties of the nanoparticles and the base fluid are taken into account while solving the problem. The thermodynamical properties of both the nanoparticles and the base fluid are given in Table 1.

So as to achieve a clear understanding of the considered problem, we consider the two nanoparticles—copper (Cu) and alumina ($\mathrm{Al_2O_3}$) with the base fluid water ($\mathrm{H_2O}$) with the volume fraction of the formed nanofluid as 0.15. In this paper, we have used these fixed values for the fluid flow parameters $\delta = 0.5$, $\mathrm{Pr} = 6.2$, $\mathrm{Ri} = 1$, $\mathrm{Sc} = 0.78$, $M = 1$, $N = 1$, $\mathrm{Df} = 7$, $\mathrm{Sr} = 0.78$, $\gamma = 0.5$, $\mathrm{Rd} = 1$, $\mathrm{Da}^{-1} = 3$.

The impacts of the Dufour number on the tangential velocity are depicted in Fig. 2. It is observed that the velocity in the tangential direction increases as Df increases. The impacts of the Dufour number on the temperature profile are depicted in Fig. 3. There is a rise in temperature with a rise in Df. This is because the increase in Df increases the rate at which the heat transfer takes place which in turn increases the temperature. The impacts of the Dufour number on the concentration profile are depicted in Fig. 4. As Df relates the concentration gradient and energy flux, an increase in Df increments the concentration gradient which reduces the concentration.

Figure 5 depicts the effect of soret number on temperature profiles. As Soret number is the ratio of temperature difference to concentration, an increase in it increases the temperature. Figure 6 depicts the effect of soret number on concentration profiles. An increase in Sr decreases the concentration. It can be seen from the graphs that there is an increase in temperature curves with an increase in soret number in

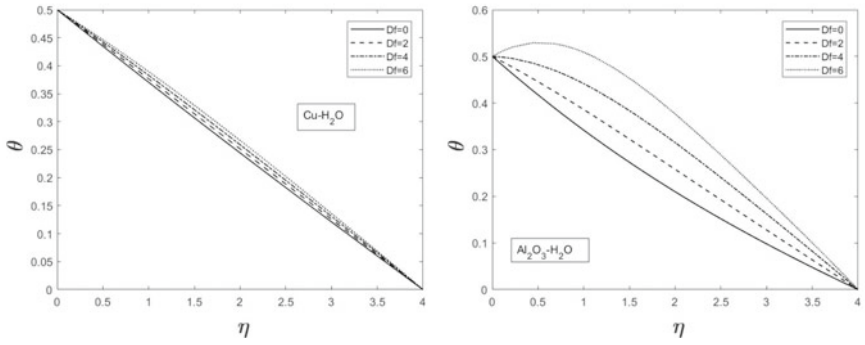

(a) $Cu–H_2O$ (b) $Al_2O_3–H_2O$

Fig. 3 Temperature profile for distinct values of Df

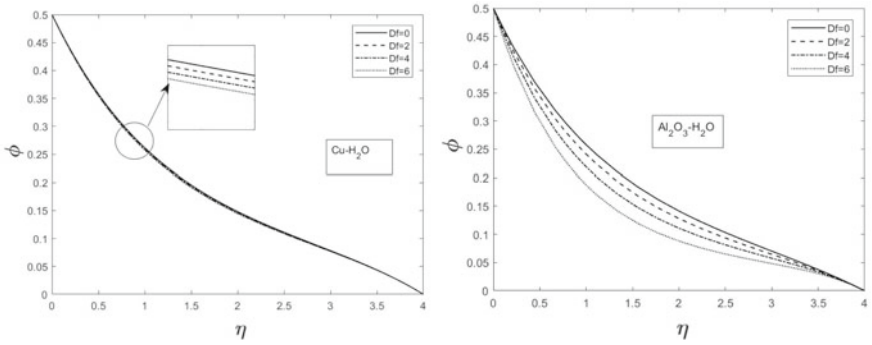

(a) $Cu–H_2O$ (b) $Al_2O_3–H_2O$

Fig. 4 Concentration profile for distinct values of Df

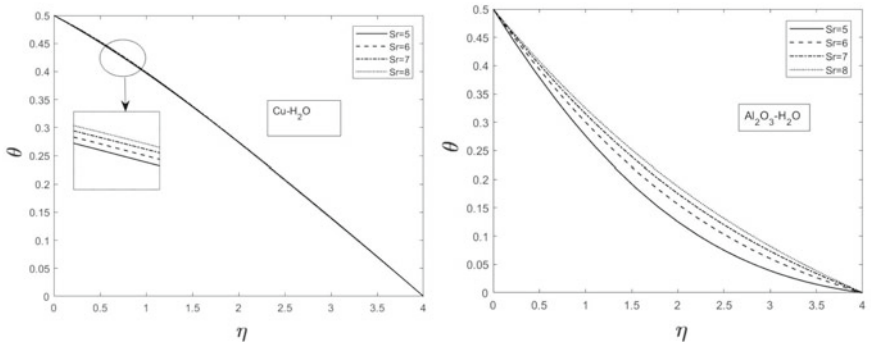

(a) $Cu–H_2O$ (b) $Al_2O_3–H_2O$

Fig. 5 Temperature profile for distinct values of Sr

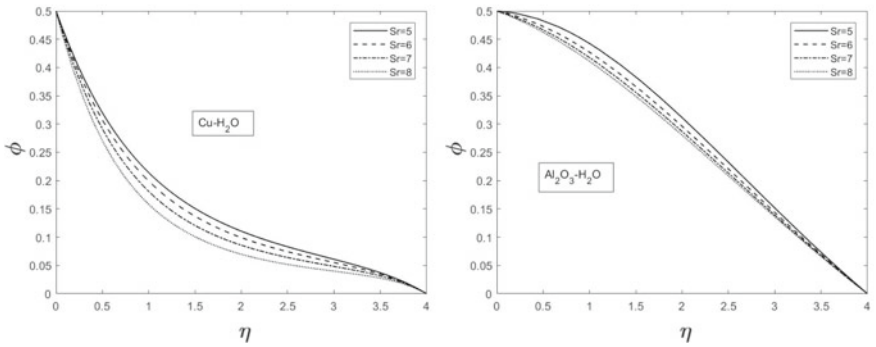

(a) $Cu–H_2O$ (b) $Al_2O_3–H_2O$

Fig. 6 Concentration profile for distinct values of Sr

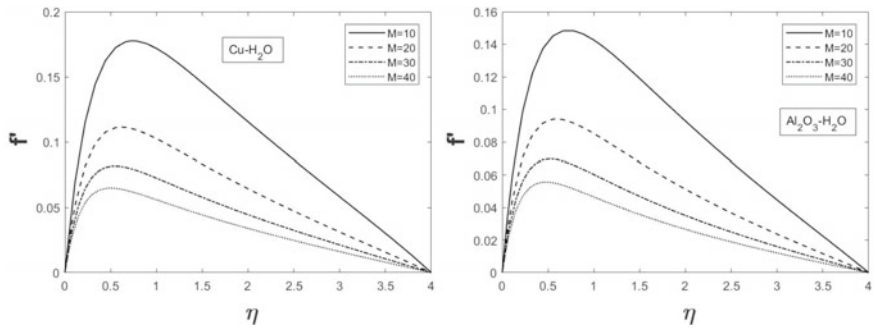

(a) $Cu–H_2O$ (b) $Al_2O_3–H_2O$

Fig. 7 Tangential velocity profile for distinct values of M

both the nanofluids, and with an increase in Soret number, there is a decrease in concentration in both the nanofluids.

The influence of the magnetic parameter on the tangential and circumferential velocity profiles is depicted in Figs. 7 and 8. With an increase in the magnetic parameter, there is a decrease in the velocity profiles. This is because as the magnetic parameter increases, a Lorentz force sets in, which reduces the velocity. Both the nanofluids depict the same trend.

Figure 9 depicts the tangential velocity for various values of the Radiation parameter. With an increase in radiation parameter, there is an increase in the velocity curves. As the thermal radiation parameter increases, the intensity of heat generation increases which in turn breaks the bond between the molecules and rises the velocity. Figure 10 depicts the temperature profile for various values of the Radiation parameter. With an increase in radiation parameter, there is an increase in the temperature curves. As the radiation parameter increases, there is an increase in surface heat flux which leads to an increase in the temperature curves.

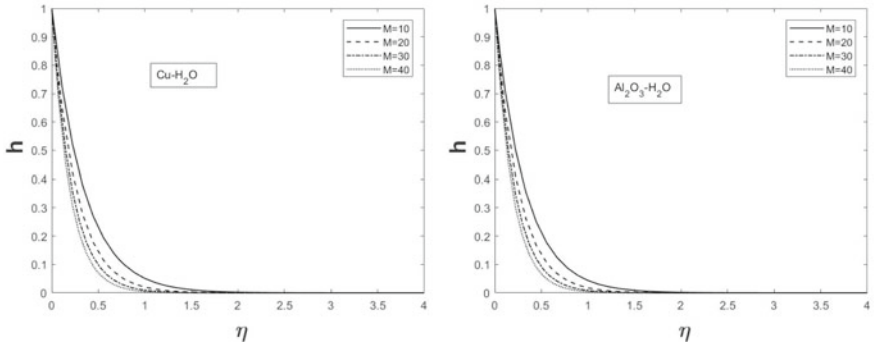

(a) $Cu–H_2O$ (b) $Al_2O_3–H_2O$

Fig. 8 Circumferential velocity profile for distinct values of M

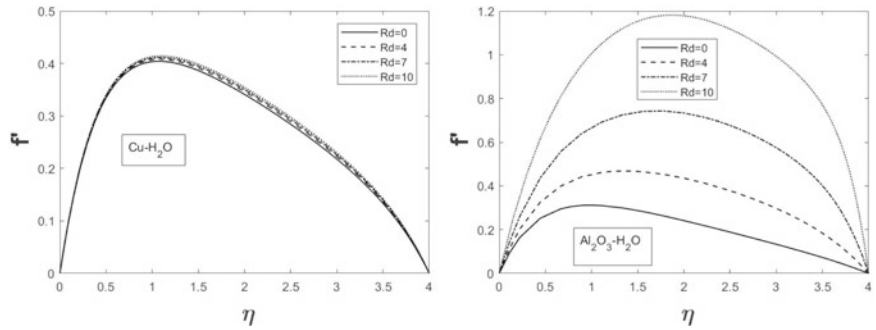

(a) $Cu–H_2O$ (b) $Al_2O_3–H_2O$

Fig. 9 Tangential velocity profile for distinct values of Rd

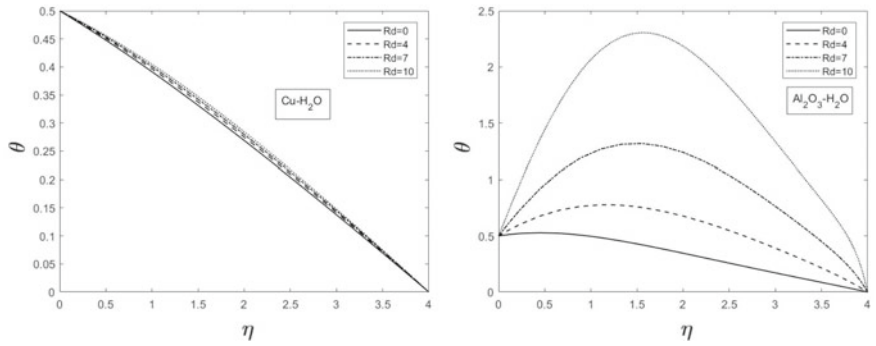

(a) $Cu–H_2O$ (b) $Al_2O_3–H_2O$

Fig. 10 Temperature profile for distinct values of Rd

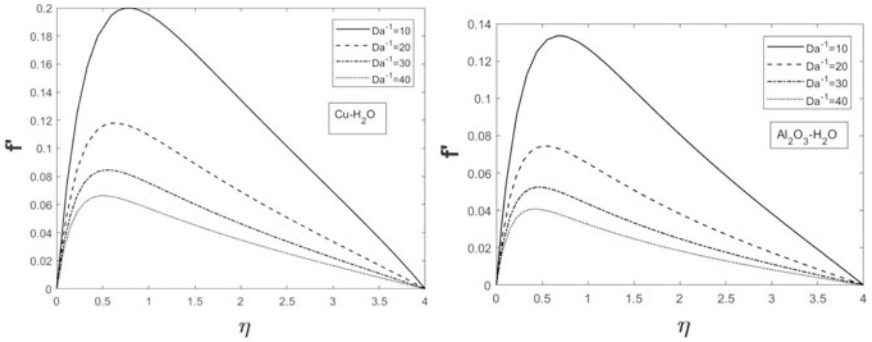

(a) Cu–H_2O (b) Al_2O_3–H_2O

Fig. 11 Tangential velocity profile for distinct values of Da^{-1}

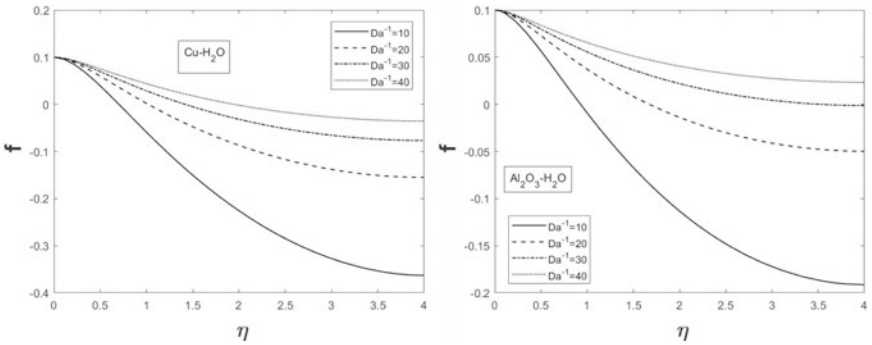

(a) Cu–H_2O (b) Al_2O_3–H_2O

Fig. 12 Normal velocity profile for distinct values of Da^{-1}

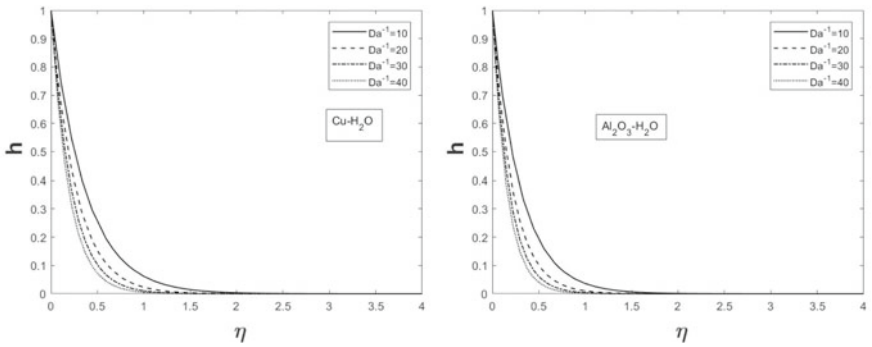

(a) Cu–H_2O (b) Al_2O_3–H_2O

Fig. 13 Circumferential velocity profile for distinct values of Da^{-1}

Table 1 Thermodynamical properties

Thermodynamical properties	Water	Copper	Alumina
C_p (J/(kgK))	4179	385	765
ρ (kg/m^3)	997.1	8933	3970
K (W/mK)	0.613	400	40
$\beta * 10^{-5}$ (K$^-$1)	21	1.67	0.85

The impacts of the inversion of the Darcy number on the tangential velocity profiles are depicted in Fig. 11. As the inversion of the Darcy number increases, there is an increase in the tangential velocity profiles. The impacts of the inversion of the Darcy number on the normal velocity profiles are depicted in Fig. 12. With an increase in the inversion of the Darcy number, there is an increase in the normal velocity profiles. The impacts of the inversion of the Darcy number on the circumferential velocity profiles are depicted in Fig. 13. There is an increase in the circumferential velocity profiles with an increase in the inversion of Darcy number. As the inversion of the Darcy number increases, the permeability parameter decreases. When the permeability decreases, the fluid flow resistance increases which in turn raises the velocity of the flow. This rise in velocity can be observed in Figs. 11, 12 and 13.

5 Conclusion

A detailed investigation is done by analyzing the impacts of the magnetic parameter, radiation parameter, and chemical reaction parameter along with Dufour and Soret effects in two nanofluids over a vertical rotating cone. Based on this present investigation, the following conclusions are derived.

- The heat transfer rate of the nanofluid copper in water is better compared to that of the nanofluid alumina in water because of the high thermal conductivity of copper.
- The mass transfer capacity of the nanofluid alumina in water is comparatively better than the nanofluid copper in water because of the higher specific heat of alumina.
- The greater values of M lower the velocity profiles.
- The increase in Sr and Df increases the temperature profile and decreases the concentration profile.
- With an increase in the Rd, the velocity in the tangential direction and temperature increases.
- With a decrease in the permeability (i.e., increase in the inversion of Darcy number), the tangential, normal, and circumferential velocities increases.

References

1. Tien, C., Tsuji, I.: A theoretical analysis of laminar forced flow and heat transfer about a rotating cone (1965)
2. Chamkha, A., Rashad, A.: Natural convection from a vertical permeable cone in a nanofluid saturated porous media for uniform heat and nanoparticles volume fraction fluxes. Int. J. Numer. Methods Heat Fluid Flow (2012)
3. Kumar, B., Sivaraj, R.: Heat and mass transfer in MHD viscoelastic fluid flow over a vertical cone and flat plate with variable viscosity. Int. J. Heat Mass Transf. **56**(1–2), 370–379 (2013)
4. Reddy, S., Raju, G., Kumar, A.: A numerical investigation on MHD couple heat and mass transfer past a rotating vertical cone embedded in a porous medium. Int. J. Eng. Technol. **7**(4.10), 956–962 (2018)
5. Shah, Z., Kumam, P., Deebani, W.: Radiative MHD Casson nanofluid flow with activation energy and chemical reaction over past nonlinearly stretching surface through entropy generation. Sci. Rep. **10**(1), 1–14 (2020)
6. Afify, A.: Effects of temperature-dependent viscosity with Soret and Dufour numbers on non-Darcy MHD free convective heat and mass transfer past a vertical surface embedded in a porous medium. Transp. Porous Media **66**(3), 391–401 (2007)
7. Choi, S., Eastman, J.: Enhancing thermal conductivity of fluids with nanoparticles. No. ANL/MSD/CP-84938; CONF-951135-29. Argonne National Lab., IL (United States) (1995)
8. Wong, K., De Leon, O.: Applications of nanofluids: current and future. Adv. Mech. Eng. **2**, 519–659 (2010)
9. Ravindhranath, K., Ramamoorty, M.: Nano aluminum oxides as adsorbents in water remediation methods: a review. Rasayan J. Chem. **10**, 716–722 (2017)
10. Farhana, K., Kadirgama, K., Rahman, M., Noor, M., Ramasamy, D., Samykano, M., Najafi, G., Sidik, N., Tarlochan, F.: Significance of alumina in nanofluid technology. J. Therm. Anal. Calorim. **138**(2), 1107–1126 (2019)
11. Dankovich, T., Smith, J.: Incorporation of copper nanoparticles into paper for point-of-use water purification. Water Res. **63**, 245–251 (2014)
12. Reddy, P.S., Chamkha, A.J.: Soret and Dufour effects on MHD convective flow of Al_2O_3-water and TiO-water nanofluids past a stretching sheet in porous media with heat generation/absorption. Adv. Powder Technol. 1207–1218 (2016)
13. Pandey, A., Kumar, M.: Effect of viscous dissipation and suction/injection on MHD nanofluid flow over a wedge with porous medium and slip. Alex. Eng. J. **55**(4), 3115–3123 (2016)
14. Mallikarjuna, B., Rashad, A., Chamkha, A., Raju, S.: Chemical reaction effects on MHD convective heat and mass transfer flow past a rotating vertical cone embedded in a variable porosity regime. Afr. Mat. **27**(3–4), 645–665 (2016)
15. Reddy, S.P., Sreedevi, P., Chamkha, A.J.: MHD boundary layer flow, heat and mass transfer analysis over a rotating disk through porous medium saturated by Cu-water and Ag-water nanofluid with chemical reaction. Powder Technol. **307**, 46–55 (2017)
16. Dzulkifli, N., Bachok, N., Pop, I., Yacob, N., Arifin, N., Rosali, H.: Soret and Dufour effects on unsteady boundary layer flow and heat transfer of nanofluid over a stretching/shrinking sheet: a stability analysis. J. Chem. Eng. Process Technol. **8**(3), 1000336 (2017)
17. Janke, V., Naramgari, S., Vangala, S.: MHD flow of a nanofluid embedded with dust particles due to cone with volume fraction of dust and nano particles. Procedia Eng. **127**, 1026–1033 (2015)
18. Kumar, A., Singh, R., Seth, G., Tripathi, R.: Soret effect on transient magnetohydrodynamic nanofluid flow past a vertical plate through a porous medium with second order chemical reaction and thermal radiation. Int. J. Heat Technol. **36**(4), 1430–1437 (2018)
19. Abbas, W., Magdy, M.: Heat and mass transfer analysis of nanofluid flow based on Cu, Al_2O_3, and TiO_2 over a moving rotating plate and impact of various nanoparticle shapes. Math. Probl. Eng. **2020** (2020)

20. Kalavathamma, B., Lakshmi, C.: Effect of variable properties on heat and mass transfer flow of nanofluid over a vertical cone saturated by porous medium under enhanced boundary conditions. Int. J. Appl. Eng. Res. **13** (2018)
21. Ahmad, S., Ali, K., Saleem, R., Bashir, H.: Thermal analysis of nanofluid flow due to rotating cone/plate—a numerical study. AIP Adv. **10**(7), 075024 (2020)
22. Beg, O., Ghosh, S.: Analytical study of magnetohydrodynamic radiation-convection with surface temperature oscillation and secondary flow effects. Int. J. Appl. Math. Mech. **6**, 1–22 (2010)

Adaptive Feedback Cancelation in Hearing Aids Using Least Squares Delay-Based Fuzzy Interactive Controller

G. Jayanthi and Latha Parthiban

Abstract The acoustic feedback is a persistent and annoying issue in hearing aids (HA), which either limits the maximum gain accessible by the user or degrades the sound quality of the device or both. The feedback cancelers are utilized in general, to produce a replica of the feedback signal (FS), in order to remove the original FS before being delivered to the loudspeaker component; however, a bias due to correlation of input–output signals was introduced into the HA system due to the spectrally colored nature of input signal. A novel approach of introducing a fuzzy interactive controller (FIC) with least squares delay (LSD)-based adaptive algorithm was utilized to minimize the bias, through which the filter coefficients were updated individually under reduced convergence rate. The magnitude of estimated filter coefficients in proportion to the system output was then evaluated by incorporating a rule-decision-table and achieved a steady-state performance in HA. The performance measures of FIC-LSD were compared with various well-known adaptive techniques and the obtained results proved that the proposed algorithm would provide a significant and robust acoustic feedback cancelation in the presence of varying environmental conditions.

Keywords Acoustic feedback · Least squares filter · Fuzzy controller · Hearing aids · Stable gain

1 Introduction

The signal processing unit of HA whenever provides a necessary amplification to the audible sounds, there is also a possibility of enhancing the auditory feedback signal that is generated in the hearing device. In general, the sound signals are traversed

G. Jayanthi (✉)
Department of Electrical and Electronics Engineering, Dr. M.G.R. Educational and Research Institute, Chennai, India

L. Parthiban
Department of Computer Science, Pondicherry University CC, Pondicherry, India

© The Author(s), under exclusive license to Springer Nature Singapore Pte Ltd. 2022

S. R. Kannan et al. (eds.), *Fuzzy Mathematical Analysis and Advances in Computational Mathematics*, Studies in Fuzziness and Soft Computing 419,
https://doi.org/10.1007/978-981-19-0471-4_17

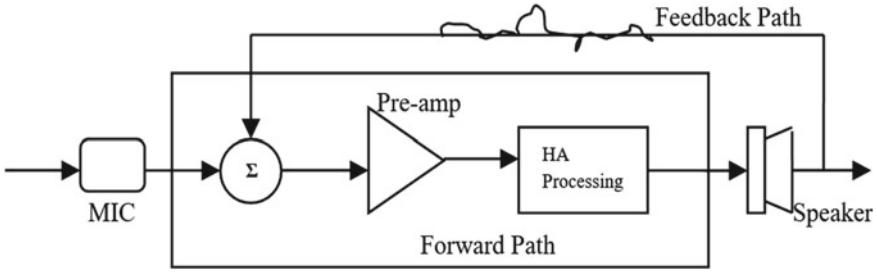

Fig. 1 Block schematic of hearing aid

from the near-end microphone to the far-end loudspeaker in the forward path for amplification (Fig. 1). However, this amplified sounds are picked up by the microphone from the feedback path, which is termed as acoustic feedback signal [8, 11, 13]. Then, this signal along with the original signal would get transmitted to the speaker that might interrupt the conversation.

The acoustic feedback signal (FS) is an attenuated, delayed, and a part of the distorted loudspeaker signal, which is perceived as a whistling or ringing sound in hearing aids [7, 11, 14, 26]. The phenomenon of FS particularly occurs when the amplified sounds from microphone to receiver are higher than the attenuation of the amplified signals from receiver to microphone. To cancel this undesired feedback, a perfect acoustic feedback canceler (AFC) was chosen; thus, the auditory device could provide maximum amplification to the desired signals, which offer a required compensation on the removal of feedback.

2 Literature Survey

In the recent years, several algorithms have been suggested to enhance the efficiency of feedback cancelers, which are limited by long lengths of acoustic feedback paths and non-stationarities in the acoustic environment. However, the major techniques utilized in either of the cancelers were considerably mentioned below.

2.1 High-Frequency Gain Control

The acoustic feedback in the hearing system occurs in high frequency, particularly when the input signal reaches the maximum gain [1, 12]. The signal without feedback would properly deliver in the high-frequency (HF) peak, while the signal with feedback would drastically decrease with a high-frequency cut [11, 18]. Thus, to

achieve a significant reduction in FS, the primary oscillational peaks are progressively reduced in frequency and amplitude, by reducing the gain at the HF regions, which is attempted by gradually diminishing the average gain at high frequencies.

When the gains at greater frequencies are, however, progressively reduced, the fundamental oscillational peaks are significantly decreased in its magnitude and lead to the reduction in the typical fundamental peak of the received signal. Hence, the fitting becomes unable to deliver the required amplification and the technique unfortunately leads to the same problem, the howling effect.

2.2 Phase Cancelation

Pradhan et al. [24] stated that the acoustic feedback typically occurs during the unfortunate combination of HF gain and phase, particularly when the high-frequency gain reaches 0° phase crossing. To stop the audible oscillations at 0° crossing, the FS needs to be perfectly out-of-phase to the microphone signal, during when the two waves subtract and cancel with each other.

However, this condition might never happen with the unknown—undesired feedback signal practically. Hence, diminishing the amplitude of resultant signal at the output in the phenomenon of FS would rarely occur. Therefore, the phase cancelation techniques contradict the key objective of audio reinforcement systems and create a distinctive high-pitched howl [2].

2.3 Notch Filtering

Since FS do not occur at all the high frequencies, it is appropriate to detect the gain at a particular feedback frequency, and at the very same time, not to impact the adjacent frequencies [7]. This can be done with notch filtering, which reduces the gain selectively at a specific frequency that tends to cause feedback [4]. Notch filters are the frequency selective circuits, useful in eliminating the frequency distortions from the audio devices.

When a notch filter was added to the circuit, it selectively reduced the gain at a given frequency that triggers the feedback around the center frequency. The filter also monitored the generation of whistling sounds, and whenever the potential of whistling feedback signal was distinguished, the notch filters were generated to suppress those whistling signals at the feedback frequencies.

In notch filters, the gain appeared to be reduced in the narrow frequency bands around the critical frequencies, during the occurrence of feedback, which was tried to compromise the basic frequency response of the system. Since, the incoming signal would also have the same frequency components in the rejected range, reduction in gain leads to an information loss. This cause a serious impact on sound quality and found to be inappropriate from a sound quality point of view [21, 27].

3 Adaptive Feedback Cancelation

3.1 Adaptive Filtering

Adaptive filters are the class of digital filters, used to remove the unwanted noise in the signal processing circuits, particularly when the signal varies from time to time [15]. The adaptive filtering method is preferred in feedback cancelation, whenever (i) a randomly varying noise is available in the system, whose variations are unknown and/or unable to filter out the noise in real-time using digital filters, and (ii) the feedback frequencies vary in different acoustical environments, and the adjustments to the effective frequencies in each environment are required [22].

The misalignment property of steady-state error for the given period of time was compared for various feedback controlling techniques (Fig. 2), among which the adaptive filtering method provided comparatively a lower misalignment and made this technique more appealing for feedback cancelation in hearing aids.

The adaptive filter $H(z)$ of linear and transverse finite-duration impulse response (FIR) filters was chosen for feedback cancelation. The signal processing of a hearing aid shown in Fig. 3 consists of a forward path $G(z)$ that includes amplification components ADC and DAC. The input to the hearing aid is the desired signal $s(n)$, processed through microphone (MIC), amplified by $G(z)$, and obtained as loudspeaker signal $y(n)$.

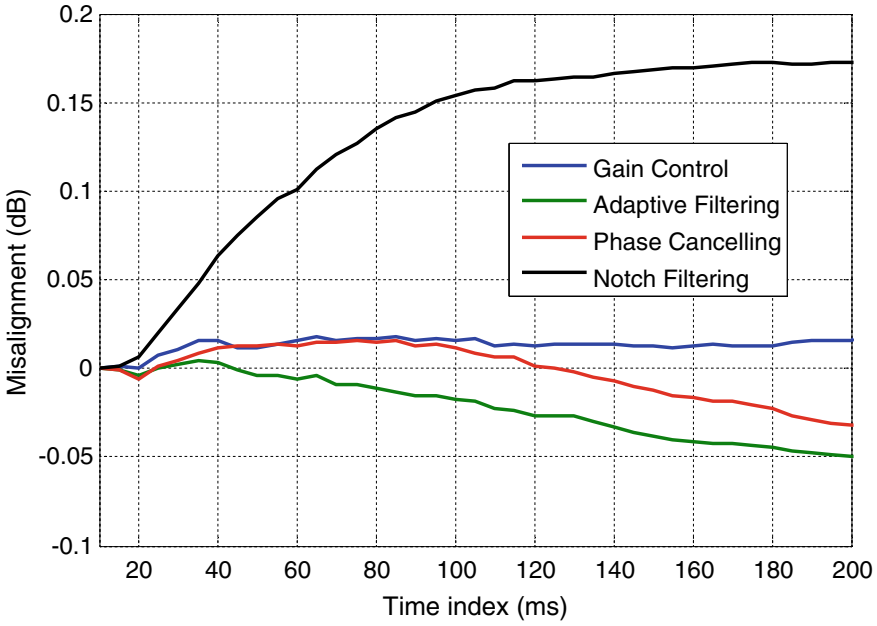

Fig. 2 Misalignment graph for various feedback control

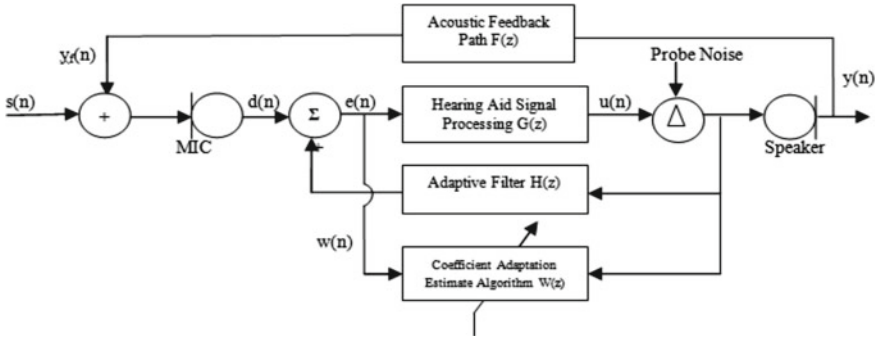

Fig. 3 Block diagram of adaptive feedback canceler

The $y(n)$ is fed back to the microphone, forming a feedback path $F(z)$, and tends to introduce non-linearities into the MIC that heard as a feedback signal $y_f(n)$, which affects the audibility of hearing aid system [10]. To cancel this $y_f(n)$, the adaptive FIR filter $H(z)$ was placed in parallel to $G(z)$, thereby to estimate the $F(z)$.

Although, the feedback path cannot be predicted with certainty, the adaptive algorithms (dealt in Sect. 3.2) in the filtering circuit estimate the transfer function of feedback path, which is then subtracted from the microphone signal, in order to achieve the desired signal [3].

The adaptive estimate algorithm $W(z)$ is implemented in $H(z)$, to generate the filter coefficients $w(n)$. The product of $y(n)$ and $w^T(n)$ provided the equivalent value of $y_f(n)$, which is then subtracted from the desired response $d(n)$, to obtain the error signal $e(n)$.

$$e(n) = d(n) - w^T(n)y(n) \tag{1}$$

In order to achieve, $y(n) = e(n) \approx d(n)$ in Eq. (1), the transfer function between $y(n)$ and $s(n)$ of the closed loop system is obtained using Eq. (2);

$$H(z) = \frac{G(z)}{1 - G(z)F(Z)} \tag{2}$$

Whenever $G(z)$ is much greater than $F(z)$ and $G(z)F(z)$ becomes 1 at a specific frequency, the hearing system is said to be unstable. Also, when $s(n)$ is spectrally colored, the desired signal $s(n)$ and the loudspeaker signal $y(n)$ become correlated and make the feedback signal $y_f(n)$ and $s(n)$ cancel each other; hence, the system is said to be biased. The occurrence of biased convergence leads to an oscillation that would drive the hearing aid at its maximum level and makes it unstable.

3.2 Adaptive Algorithms

Adaptive filter algorithms implemented in the filtering circuits have recursive formulations in the least square error Wiener filter such as the recursive least squares (RLSs), the steepest descent, and the least mean square (LMS) [28, 29]. The primary principle followed in the adaptive algorithms is that the filter coefficients $w(n) = \left[w_0(n), w_1(n), \ldots, w_{L-1}(n)\right]^T$ are adjusted, to minimize the error difference, at each sampling instant. In the initial state $\hat{w}_0(n)$, the adaptive filter started with the periodic updating of filter coefficients, typically on a sample-to-sample analysis.

The difference between the filter output $\hat{w}(n)$ and the signal to be desired $y(n)$ was decreased to obtain the adaptation formula in the general recursive form [28]:

$$\begin{pmatrix}\text{Estimation}\\ \text{of Present}\\ \text{vector}\\ \text{parameter}\end{pmatrix} = \begin{pmatrix}\text{Estimation}\\ \text{of Past}\\ \text{vector}\\ \text{parameter}\end{pmatrix} + \begin{pmatrix}\text{Function}\\ \text{of error}\\ \text{Update}\end{pmatrix} \tag{3}$$

The Wiener filtering technique provides a solution to identify the bias presents in the system and for de-correlating the signals. The cross-correlation among the signals is found to estimate the filter coefficients, which are then computed and copied into feedback algorithm [17]. However, the cross-correlation vector must satisfy zero error, which is generally not the case in practice; hence, the estimation of $F[z]$ is said to be biased.

The least mean square (LMS) adaptive algorithm is stochastic gradient-based algorithms, used for filter coefficient calculation. It utilizes the gradient vector of the filter tap weights to converge on the optimal Wiener solution using the given Eq. (4) as

$$w(n+1) = w(n) + \mu e(n) y(n) \tag{4}$$

Since, the coefficients held fixed even after their updating, the rate of convergence of system remains slow.

The normalized version of the LMS algorithm (NLMS) comes with improved convergence speed, more stability but has increased computational complexity. In order to model $F(z)$, the weight updation in NLMS is obtained as

$$w(n+1) = w(n) + \frac{\mu}{y^T(n)y(n) + \delta} e(n) y(n) \tag{5}$$

where δ is a small positive constant used to avoid zero dividing error. Figure 4 gives out the error response of an acoustic signal under various filtering systems.

The configuration of either LMS or NLMS algorithm is generally provide a trade-off between slow convergence and lesser misalignment versus rapid convergence and high rate of steady-state error [6, 9, 28]. Hence, in order to achieve both

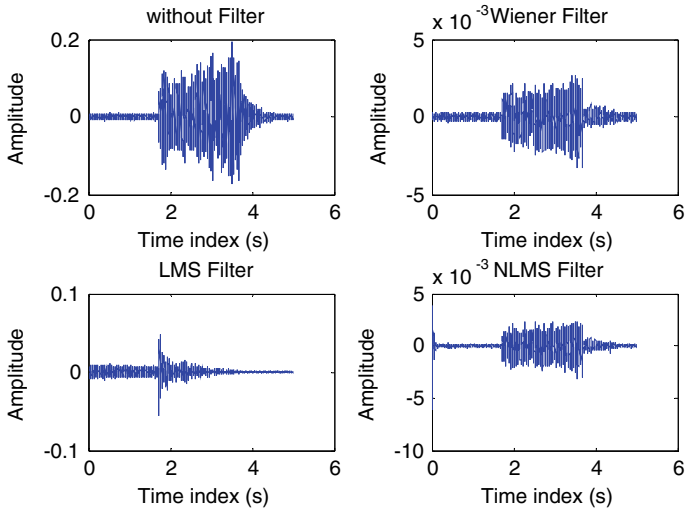

Fig. 4 Error response of an acoustic signal under various filter systems

fast convergence as well as low steady-state misalignment and to reduce the computational burden due to Wiener and NLMS filter algorithms, the proposed least square delay (LSD)-based algorithm was introduced in to the adaptive filter system.

In LSD algorithm, a smart delay was introduced in to the LMS algorithm, for the system objectives required to have faster convergence rate during the processes that are time-varying. However, after performing the de-correlation, the continuous signal was found to be impassive and needed a rigorous deployment in implementation. Hence, an interactive fuzzy controller was introduced in the adaptive filter algorithm, for making intellectual decisions on which the filter coefficients were updated accordingly [19].

Hence, a novel strategy of presenting fuzzy interactive controller (FIC) integrated with LSD algorithm increases the maximum stable gain (MSG) of the hearing system to achieve a required compensation for the feedback effect. Thus, the methodology for the proposed algorithm explained in Sect. 4, outperformed the existing adaptive algorithms in terms of convergence rate and steady-state error, and recommended for complete cancelation of feedback in hearing aids.

4 Methodology

In the proposed method, adaptive feedback cancelation algorithm was performed by injecting a probe signal in the forward path of the hearing system, to provide a good estimate of $F(z)$ in the filter circuit. The white Gaussian pseudo random noise was utilized as probe signal and added in to the receiver unit. Δ is the delay input added

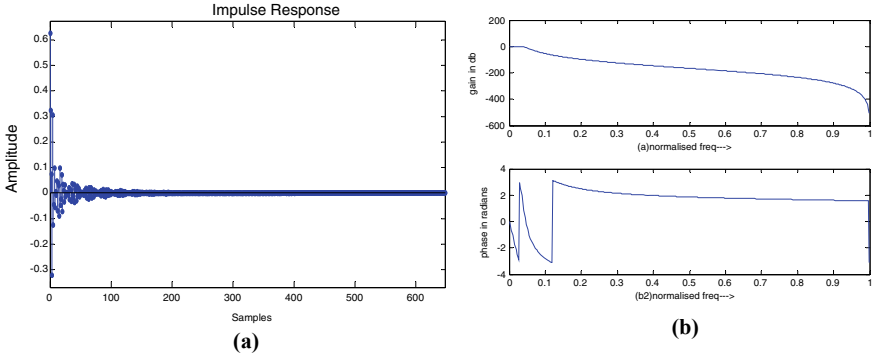

Fig. 5 **a** Impulse response of an actual sinusoid, **b** magnitude and phase response of given sinusoid

to de-correlate the input signal $s(n)$ and the feedback signal $y_f(n)$. The delay Δ was applied before the loudspeaker output, to identify the effective path of $H(z)$, in order to track the convergence-status between $d(n)$ and $u(n)$ [20].

The probe signal followed by a unit delay was developed for the transfer of weights into the filter system. The level of probe noise was controlled gradually with the time delay, reduced the problem of biased convergence in adaptive filters.

In the initial approach of LSD algorithm, the impulse response of the desired signal at a particular instant was presented with respect to its samples, whose magnitude and the phase response were shown in Fig. 5a and b, respectively. The power of the largest sinusoidal component of the desired signal was estimated on updating the filter coefficients. Whenever the sinusoid of microphone signal was said to have more power than the preset threshold, the feedback signal was said to be generated. Hence, the filter coefficients were updated till the sinusoid reached to have lesser power.

4.1 FIC Implementation

A fuzzy interactive controller (FIC) was intervened into the adaptive system, since the FIC could adjust the system input by observing the outputs from the history of the information provided by the filter system; thereby, the convergence rate in LSD system was reduced. The FIC was designed based on the principles of fuzzy logic and the fuzzy sets developed by [30].

The FIC consists of three main processors, namely fuzzifier for fuzzification of input variables, the rule-decision-table (RDT) for fuzzy inference, and a centroid defuzzifier for defuzzification of desired response. In FIC, the input variables obtained from LSD were mapped for fuzzification to manage the linguistic definitions created by RDT under the weighted summation that provided the decisions due to which the filter coefficients of LSD were updated. The adaptation process was frozen,

once a better solution was attained. Thereby, the feedback path was estimated on continuously monitoring the rate of convergence in the hearing system using LSD-FIC algorithm in adaptive filters.

5 Simulation

The estimation of an impulse response is a system identification problem that could be solved using computer simulation method. Various audio signals were captured and evaluated under real-time impulse response for identifying the system performance. The time domain representations of four set of real-time signals: ambulance sound, telephone sound, speech segment of a female voice ("hello how are you")—recorded in a sound-proof room, and babble sound, all acquired under varying environments were shown in Fig. 6.

The audio wave files were loaded into the MATLAB platform, and a set of selected signals were measured for its magnitude with respect to its samples per second. The test files were converted into.wav format and trimmed accurately for 5 s, and the bit-rate was set to 16 bits/sec. The input sinusoidal signal with amplitude of 0.7 which was added with a random noise of amplitude 0.08 with each part of the microphone signal, in order to get the mixed signal that gives the actual value of sinusoid.

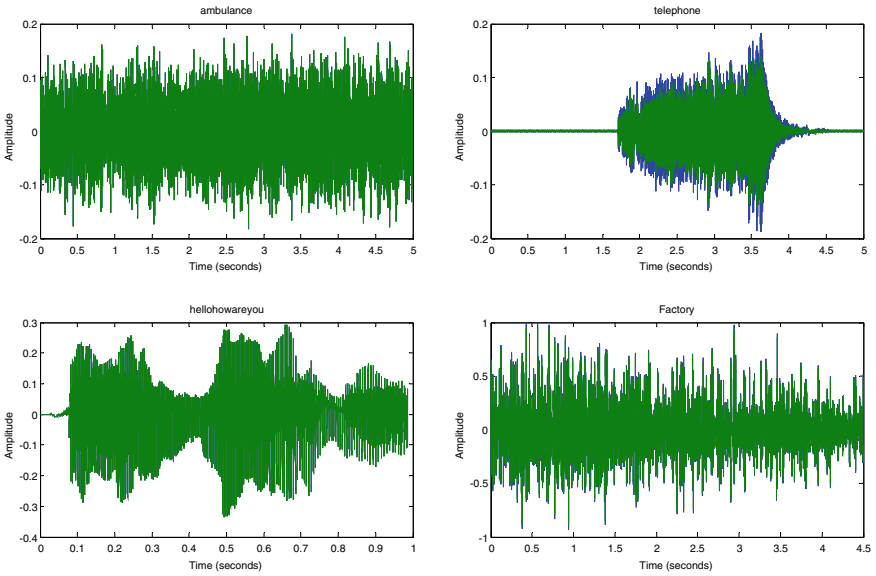

Fig. 6 Time domain response of ambient signals at varying environmental conditions

In FIC, the obtained acoustic input signals were applied to the fuzzifier and the membership functions for fuzzification process were individually attained. The rule-decision-table (RDT) of FIC provided different levels for each input in terms of linguistic variables as subsets, to obtain the control outputs in terms of crisp values [19]. The four levels of RDT signals considered for analysis were "gradual" (ambulance sound), "short" (telephone sound), "quiet" (speech segment), and "continuous" (factory sound); thus, the output control signals were determined from the fuzzy variables.

The membership functions and the frequency response obtained from the values of linguistic subsets, provided the uniform distribution of gain and phase values, among the output variables of the system, represented in Fig. 7a and b.

The algorithmic steps for applying LSD-FIC adaptive filter algorithm using computer simulation method:

- A MATLAB graphical user interface (GUI) created to facilitate the estimation of impulse responses in which two plot areas were available on the left side: the top one is for the impulse response of feedback path (FP) and the bottom one for the frequency response of FP; while the control parameters for measurement are on the right side.
- A pair of audio files (loudspeaker and microphone signals) were loaded into the simulation platform.
- The length of FP, decimation factor, number of taps required for each iteration was set to modify automatically, when one parameter is changed.
- An adaptive FIR transversal filter of sampling frequency 16 kHz with filter order 32 was utilized.

Each impulse response measurement involved playing a white noise under Gaussian distribution, as reference signal through the loudspeaker of the hearing system and measuring the reproduced signal through MIC and all the signals were assumed to be real-valued for simplicity. The signal processing in the forward path of hearing aid $G[z]$ would often implement the sample-to-sample in frame-wise, for the algorithm could be tested with varying environments.

The window width of M sound samples from the microphone input $y(n) = [y_i(n); \quad \text{for } i = 0,\ 1,\ \ldots\ M-1]$ was processed for each time during the traverse of the main loop [23].

The transfer function is modeled as a fixed delay of duration 0.85 ms, for processing the input signal, approximately equals the average group delay of the FP transfer function [5]. Having a constant delay would allow to use a shorter FIR filter that eliminates a larger number of approximations, which in turn reduce the complexity in computations. Figure 8 provided the time domain response of the ambient signals after applying LSD algorithm.

During the onset of oscillation, the characteristics of ambient signal such as the impulse response, the actual and estimated filter weights, and their corresponding magnitude response were obtained and the probe noise signal was injected, whenever the filter coefficients were needed to be adjusted.

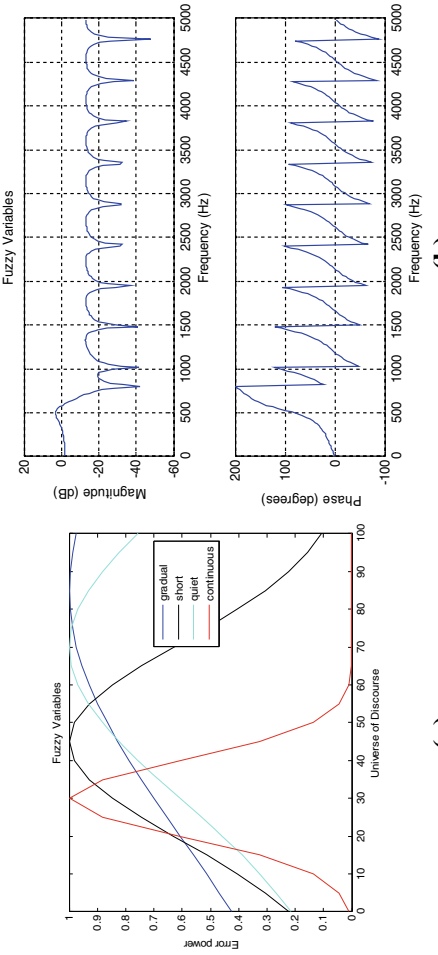

Fig. 7 **a** Membership functions using FIC, **b** frequency response of FIC

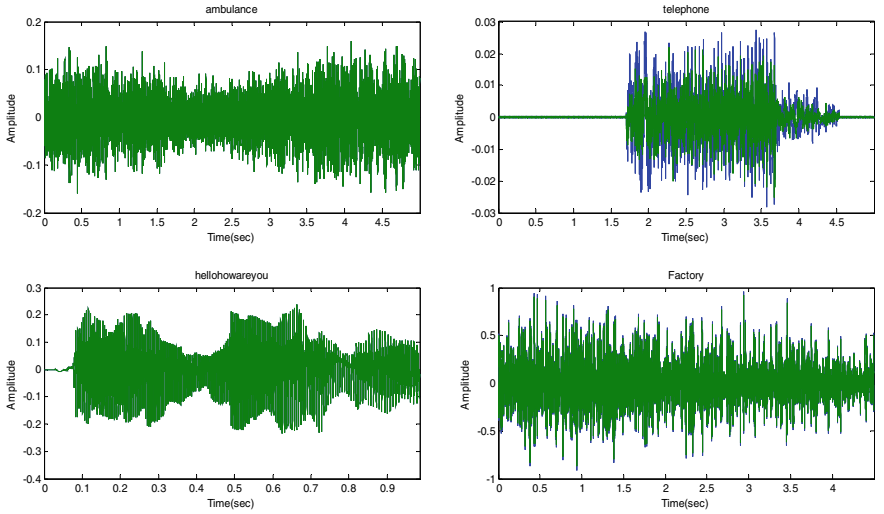

Fig. 8 Time domain response of acoustic signals after applying LSD algorithm

When the magnitude of feedback signals $y_f(n)$ is closer to $s(n)$, the feedback cancelation system immediately reacted to the sinusoid ambient signal. This leads to the re-estimation of feedback path $F(z)$, for the ambient signal to reappear at its proper intensity, for which the estimate $y_f(n)$ was subtracted from $d(n)$; hence, the filter coefficients were computed using the derived LSD-FIC algorithm.

The proposed LSD adaptive algorithm integrated with FIC determined the coefficients $\hat{w}(n)$ from the filter output $w(n)$, which was then deducted from the noise corrupted signal $y(n)$ to produce the required error signal using Eq. (6):

$$e(n) = \hat{w}(n) - y(n) \tag{6}$$

The adaptive algorithm adjusted the coefficients $\hat{w}(n)$, to reduce the error signal as minimum as possible. Once the condition $e(n) = 0$ or $\hat{w}(n) = y_f(n) \approx y(n)$ was reached, the training would be completed with converging the filter output.

Figure 9 showed the plot of frequency spectrum for a sample of the original and filtered signals. An effective measure in frequency domain approximations was derived to illustrate how the algorithm estimated the rate of convergence and the steady-state behavior of the entire cancelation system, without knowing the true feedback paths and the results obtained were able to quickly control the gain frequency response.

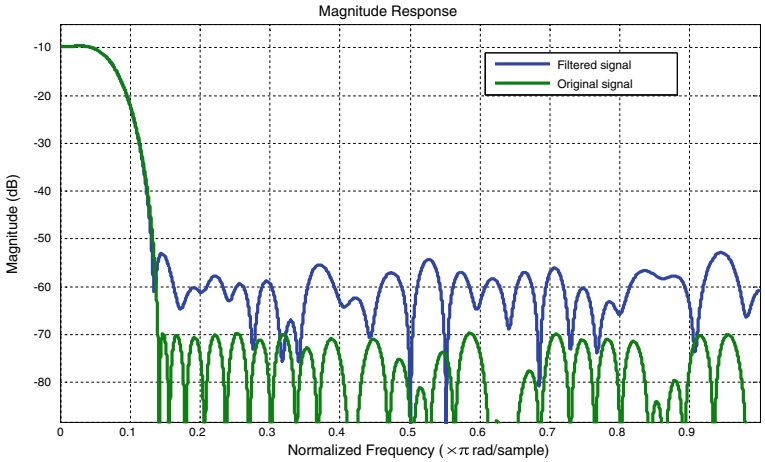

Fig. 9 Measurement of magnitude response of original and filtered signals

Table 1 Convergence rate for various filter algorithms

Type of algorithm	Wiener	LMS	NLMS	LSD-FIC
Convergence rate (%)	26.4	33.8	36.2	36.7

5.1 Measuring Convergence Rate

The number of iterations required to converge the algorithm to reach its mean square steady-state error is defined as rate of convergence [25]. Increase in convergence shows the ability of the filter algorithm to adapt its coefficients from zero to their estimated values at a faster rate.

The rate of convergence measured for the proposed method was compared with the existing methods, and from Table 1, it was proved that the proposed algorithm would offer a faster convergence rate compared to the existing techniques.

In Fig. 10, the convergence rate measured from the proposed LSD-FIC method proved to provide a better convergence for varying filter order.

5.2 Measuring SNR

The stable gain was computed in terms of signal-to-noise (SNR) ratio, in order to find the rate of compensation provided by the algorithm during the elimination of feedback signal [14]. The SNR estimate was obtained by from the estimation of microphone signal $s(n)$, using $e(n)$ as a reference signal.

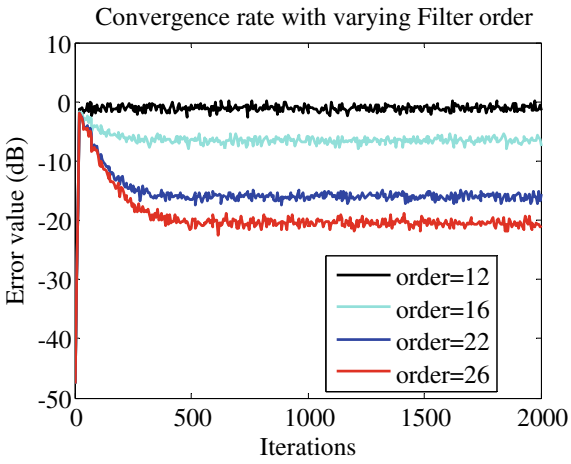

Fig. 10 Convergence rate for AFC under varying filter order

The SNR ratio exemplifies the noise control efficiency of the hearing aid. Higher the SNR, better the noise reduction performance of hearing aid.

$$\mathrm{SNR} = 10\log_{10}\frac{\sum_{n=0}^{N-1} s^2(n)}{\sum_{n=0}^{N-1}\left[\hat{s}(n) - s(n)\right]^2} \tag{7}$$

In Eq. (7), $s^2(n)$ is the power of pure tone applied at MIC and $\hat{s}^2(n)$ is the power of output signal at the receiver. Whenever the obtained SNR value is greater than or equal to T, a small increment, say 0.1 was added gradually. The same procedure was repeated for number of iterations; and when it was found less than T, the previous Δ value was used to estimate the SNR. Table 2 provided the estimated SNR ratio of the proposed method and tabulated with the existing methods, and the SNR value was intended to provide 23 dB for a 12-tap adaptive filter in a sound-proof room for an LMS algorithm [16].

The process was terminated, and the steps were repeated for both before and after filtering of signals to obtain the stable gain of an audio file. The above steps were repeated for multiple audio files, and the resultant SNR values were averaged to obtain the final stable gain estimate.

Table 2 Estimation of SNR ratio of pure tone signals

Pure tone signals	Before filtering of signals			After filtering of signals		
	LMS	NLMS	LSD-FIC	LMS	NLMS	LSD-FIC
Ambulance sound	19.0355	19.7654	19.5243	21.4513	20.7389	21.7896
Telephone sound	20.5528	21.9399	21.8104	21.9875	21.1512	22.8765
Babble sound	17.2441	17.6322	17.6567	22.9998	22.3224	21.9975
In a sound-proof room	21.8732	21.9494	22.0157	24.1924	24.0909	23.1092

Figure 11 shows the frequency response of ambient signals before and after applying FIC integrated LSD adaptive algorithm. Also, the error signal $e(n)$ is shown to approach $x(n)$, which relatively increase the sound quality. The simulations proved that the LSD-FIC algorithm outperformed for the highly time-varying sound signal such as speech and music and the mismatch between $\hat{F}[z]$ and $F[z]$ decreased, by increasing the forward path gain.

Sound files of 1–8 kHz "gradual" level sinusoid were computed, sampled at 16 kHz of order 64 by adding white noise with variance 0.001. When the input frequency range was of 1000–7999 Hz, the system tended to provide a stable gain for N at 64. And it was observed that exactly after 8 kHz, the gain was getting reduced and started providing negative values. Hence, a major variation in their magnitude response in time domain characteristics after applying LSD was obtained, while the continuous signal shown unaffected.

6 Discussion

The amplifier gain was unstable during the presence of feedback, while the receiver output of LSD algorithm was same as that of LMS or Wiener filter; hence, the proposed algorithm suffered from system bias, for the non-stationary signals.

Although, the algorithm was able to track the given input sinusoid of about 1 kHz to 8 kHz for 1000 samples (50 ms), whose SNR value exceeded 50 dB SPL, during which the normal hearing aid processing got disengaged.

The time delay occurred between hearing aid output and input signal would impact the calculation of signal-to-noise (SNR) ratio. Therefore, the shift in time was calculated and synchronized prior to the study.

7 Conclusions

In this paper, the proposed method was intended to obtain the feedback signal estimates, neither by interrupting the normal speech nor by affecting the speech intelligibility of the original signal. The feedback path was estimated and their experimental results were measured over a period of time. The results were compared with the existing filter algorithms, among which the LSD-FIC showed a noticeable improvement in SNR value after an extra iteration carried out. Thus, the proposed method proved that it would provide a significant cancelation of feedback on considerably increasing the stable gain on stationary signals. The results could further be improved through a greater number of iterations, but with a reduced convergence rate.

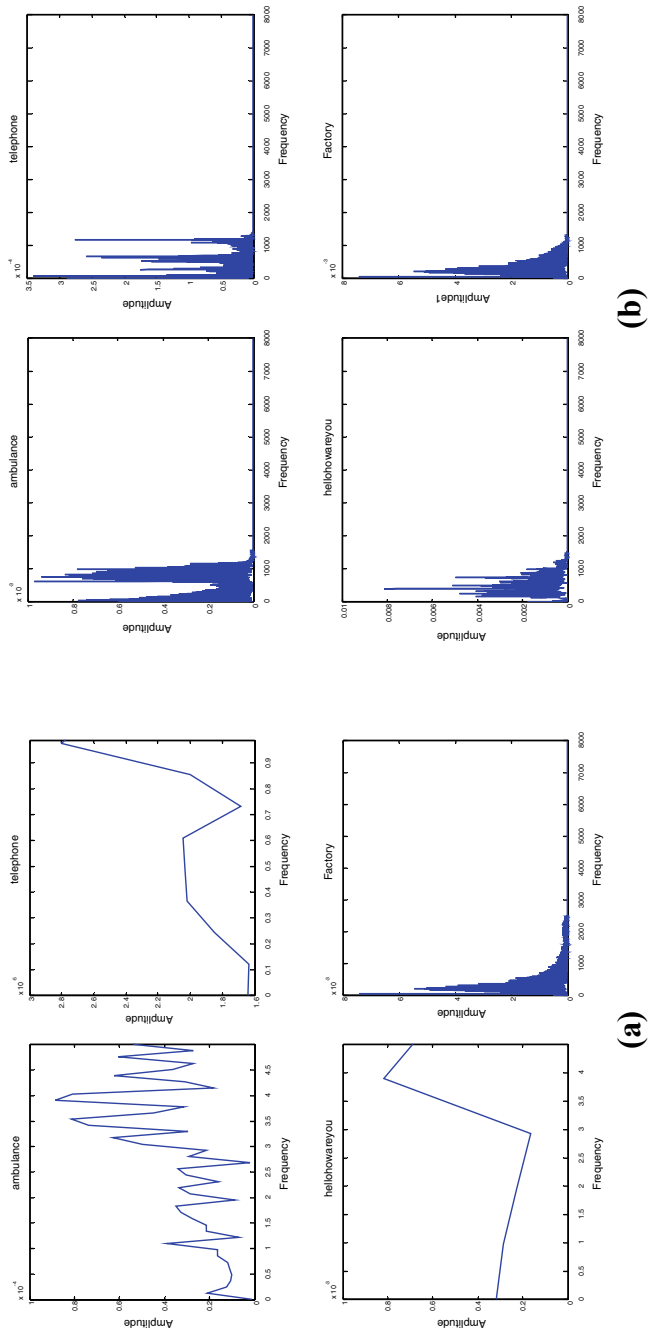

Fig. 11 Frequency response of auditory signals. **a** Before filtering and **b** after filtering of signals

References

1. Agnew, J.: Acoustic feedback and other audible artifacts in hearing aids. Trends Amplif: **1**(2), 45–82 (1996)
2. Akhtar, M.T., Albu, F., Nishihara, A.: Acoustic feedback cancellation in hearing aids using dual adaptive filtering and gain-controlled probe signal. Biomed. Signal Process. Control **52**, 1–13 (2019). ISSN 1746-8094
3. Akhtar, M.T., Nishihara, A.: Automatic tuning of probe noise for continuous acoustic feedback cancelation in hearing aids. In: 24th European Signal Processing Conference (EUSIPCO), pp. 888–892. IEEE (2016)
4. Anand, A., Kar, A., Swamy, M.N.S.: An improved CLMS algorithm for feedback cancellation in hearing aids. Appl. Acoust. **129**, 417–426 (2018). https://doi.org/10.1016/j.apacoust.2017.09.002
5. Bustamante, D.K., Worrall, T.L., Williamson, M.J.: Measurement and adaptive suppression of acoustic feedback in hearing aids. In: IEEE International Conference on Acoustics, Speech and Signal Processing (ICASSP), pp. 2017–2020 (1989)
6. Cevallos-Larrea, P.F., Frota, S.M., Ichinose, R.M., Tierra-Crillo, C.J.: Characterization of inter-stimulus interaction in the multiple auditory steady-state responses at high sound levels. J. Acoust. Soc. Am. **148**, 1852 (2020). https://doi.org/10.1121/10.0002114
7. Chung, K.: Challenges and recent developments in hearing aids: part I. Speech understanding in noise, microphone technologies and noise reduction algorithms. Trends Amplif. **8**(3), 83–124 (2004)
8. Chung, K.: challenges and recent developments in hearing aids: part II. Feedback and occlusion effect reduction strategies. Trends Amplif. **8**(4), 125–164 (2004)
9. Eldeeb, R.: Variable step-size adaptive algorithms for acoustic echo cancellation in hands-free portable devices. Carleton University (2012)
10. Freedb, D.J.: Adaptive feedback cancellation in hearing aids with clipping in the feedback path. J. Acoust. Soc. Am. 1618–1626 (2008)
11. Guo, M., Jensen, S., Jensen, J.: Evaluation of state-of-the-art acoustic feedback cancellation systems for hearing aids. AES: J. Audio Eng. Soc. **61**, 125–137 (2013)
12. Hao, Z., Cui, Z., Yue, S., Wang, H.: 2-D median filter-based impulsive noise reduction in multi-frequency phase-sensitive demodulation of electrical impedance tomography. IEEE Trans. Instrum. Measure. **69**, 54 (2019)
13. Hashemgeloogerdi, S., Bocko, M.F.: Adaptive feedback cancellation in hearing aids based on orthonormal basis functions with prediction-error method based pre-whitening. IEEE/ACM Trans. Audio Speech Lang. Process. (2020)
14. Jayanthi, G., Parthiban, L.: Estimation of SNR based adaptive-feedback equalizers for feedback control in hearing aids. Mitteilungen Klosterneuburg J. **69**(12), 2–10 (2019)
15. Jayanthi, G., Parthiban, L.: Acoustic feedback cancellation in efficient hearing aids using genetic algorithm. Scalable Comput.: Pract. Experience (SCPE) **21**(1), 115–125 (2020a). https://doi.org/10.12694/scpe.v21i1.1630
16. Jingjing, Z.: Variable step size LMS algorithm. Int. J. Future Comput. Commun. **1**(4), 389–391 (2012)
17. Kates, J.M.: Feedback cancellation in hearing aids: results from a computer simulation. IEEE Trans. Signal Process. **39**(3), 553–562 (1991)
18. Kar, A., Anand, A., Ostergaard, J., Jensen, S., Swamy, M.N.S.: Mean square performance evaluation in frequency domain for an improved adaptive feedback cancellation in hearing aids. Signal Process. **157** (2018). https://doi.org/10.1016/j.sigpro.2018.11.003
19. Kaya, Ö.I., Soysal, B.: Variable step-size constant modulus algorithm employing fuzzy logic controller. Wireless Pers. Commun. **54**, 237–250 (2010)
20. Levitt, H., Dugot, R.S., Kopper, K.W.: Programmable digital hearing aid system, U.S. Patent 4 731 850 (1980)

21. Li, Y., Liu, Z., Liuv, Z.P., Liu, T.: High-speed electromagnetic train wheel inspection using a Kalman-model-based demodulation algorithm. IEEE Sens. J. **19**(16), 6833–6843 (2019). https://doi.org/10.1109/JSEN.2019.2912225
22. Lopez, A.: Comparative study of analog and digital hearing aids. Dissertation Submitted to Louisiana State University and Agricultural and Mechanical College, May 2020
23. Nordqvist, P.: Sound classification in hearing instruments. Doctoral Thesis, Royal Institute of Technology, Stockholm (2004)
24. Pradhan, S., George, N., Albu, F., Nordholm, S.: Two microphone acoustic feedback cancellation in digital hearing aids: a step size-controlled frequency domain approach. Appl. Acoust. 132 (2017). https://doi.org/10.1016/j.apacoust.2017.11.015
25. Rani, S., Rani, S.: Design and implementation of adaptive filtering algorithm using NLMS having different targets. Int. J. Eng. Tech. Res. (IJETR) **3**(2), 145–148 (2015)
26. Schepker, H.: Robust feedback suppression algorithms for single- and multi-microphone hearing aids. Dissertation Submitted to the University of Oldenburg, Germany (2017)
27. Spriet, A., Doclo, S., Moonen, M., Wouters, J.: Feedback control in hearing aids. In: Springer Handbook of Speech Processing, pp. 979–1000 (2008). https://doi.org/10.1007/978-3-540-49127-9_48
28. Vaseghi Saeed, V.: Advanced Digital Signal Processing and Noise Reduction, 4th edn. John Wiley & Sons, Ltd., c_2008 (2008). ISBN: 978-0-470-75406-1
29. Wu, L., Qiu, X., Guo, Y.: A generalized leaky FXLMS algorithm for tuning the waterbed effect of feedback active noise control systems. Mech. Syst. Signal Process. **106**, 13–23 (2018). https://doi.org/10.1016/j.ymssp.2017.12.021
30. Zadeh, L.A.: Fuzzy sets. Inf. Control **8**, 338–353 (1965)

Retrieval of Erroneous Information by Adopting a Novel Way Using Fuzzy Logic

A. Neeraja and B. Amudhambigai

Abstract Recovering an error in message transmission is always an important parameter of communication. Amidst the retrieval, it is also necessary to retrieve the original message, when two or more codewords exhibit the same characteristics. Taking this notion as the prime concern, in this paper, an attempt has been made to find out the exact codeword that is transmitted with the aid of fuzzy logic and relative weight of fuzzy codewords.

Keywords Fuzzy hamming weight of fuzzy codewords · Fuzzy hamming distance and maximum likelihood decoding of fuzzy codewords

Mathematics Subject Classification 68P99 · 03B52.1

1 Introduction

Transmission and receival of messages through various channels play a major role in communication. Though communication can be achieved through various mediums. The study of such forms and modes of communication was proposed by Shannon [1] that was later established in several works [2–7]. But it is also necessary that only accurate messages are sent and received. Whenever the original message is changed due to errors, a new message is received by the receiver. This new message leads to miscommunication as this was not intended to be sent. A most likely method to retrieve the original message that was sent by the sender is the maximum likelihood decoding method [8], which recovers the original codeword with the aid of Hamming distance. Some methods and applications of maximum likelihood decoding can be seen in [9–11]. This concept is now combined with fuzzy logic proposed by Zadeh [12], which opens up the additional advantage of having accurate degree of association of each codewords with the others. This accuracy is achieved by using the

A. Neeraja (✉) · B. Amudhambigai
Department of Mathematics, Sri Sarada College for Women, Salem, Tamil Nadu 636016, India

© The Author(s), under exclusive license to Springer Nature Singapore Pte Ltd. 2022

S. R. Kannan et al. (eds.), *Fuzzy Mathematical Analysis and Advances in Computational Mathematics*, Studies in Fuzziness and Soft Computing 419,
https://doi.org/10.1007/978-981-19-0471-4_18

notion of relative weight as proposed in [13]. Fuzzy logic has always been an exclusive branch of Mathematics which provides authentic solutions even in unpredictable situations. Since errors in message transmission can lead to a dilemma about the error, it is necessary, we are not caught amidst uncertainties about the correct message. Giving a membership for each and every codeword taken in consideration provides a differentiation of codewords in the first place and hence we can be more authentic about out final result. The implementation of fuzzy logic always provides a precised result between the intervals [0, 1], thereby enabling us to arrive at a quicker conclusion based on the membership value (in this article, the relative weight).

This paper is organized as follows. Section 1 consists of introduction and preliminaries. In Sect. 2, basic definitions required for the study are given, and finally in Sect. 3, an algorithm is framed which deduces the originally sent codeword with a numerical example, and finally, conclusion is given.

1.1 Preliminaries

In this section, the basic definitions required for this paper are given.

Definition 1.1. [13] A q-ary code is a set of sequences of symbols where each symbol is chosen from a set $F_q = \{\lambda_1, \lambda_2, \ldots, \lambda_q\}$ of q distinct elements.

Definition 1.2. [13] A *binary code* is a sequences of 0_s and 1_s which are called codewords.

Definition 1.3. [13] Let $\left(F_q^n\right)$ denotes the set of all ordered n-tuples $a = a_1, a_2, \ldots a_n$, where each $a_i \in F_q$. The elements of F_q^n are called *vectors or words.*

Definition 1.4. [13] The weight $w(x)$ of a vector x in F_2^n is defined to be the number of non-zero entries of x.

Definition 1.5. [13] Suppose x is a codeword of C. If $w(x) = w_1, w_2, \ldots, w_k$ are defined to be the positions of 1_s in x, then $w_1 + w_2 + ... + w_k$ are called relative weight of codeword x.

Since 11…1 is a codeword of C, then its relative weight is

$$1 + 2 + ... + n = \frac{n(n+1)}{2}$$

Thus, this weight $1 + 2 + 3 + \cdots + n$ is called the maximum relative weight of codeword x of C.

Definition 1.6. [13] The relative weight *rate* of a codeword x in $(F_2)^n$ is denoted by $J(x)$, and it is defined by

$$J(x) = (w(x))/(\text{Maximum Relative Weight})$$

Definition 1.7. [14] The exclusive OR is a basic computer operation denoted by XOR or $\oplus$, which takes two individual $\beta \in \{0, 1\}$ and $\beta' \in \{0, 1\}$ and yields.

$$\beta \oplus \beta' = \begin{cases} 0 \text{ if } \beta \text{ and } \beta' \text{ are same} \\ 1 \text{ if } \beta \text{ and } \beta' \text{ are different} \end{cases}$$

Definition 1.8. [12] Let X be a space of points. A fuzzy set A in X is characterized by a membership function $f\_A(x)$ which associates with each point in X a real number in the interval [0, 1], with the value of $f\_A(x)$ at x representing the grade of membership of x in A.

Definition 1.9. [12] Let X be a space of points. A fuzzy relation in X is a fuzzy set in the product space X x X.

Definition 1.10. [12] An *n-ary fuzzy relation* in X is a fuzzy set in the product space X x X X … x X. Such relations have membership function of the form $f_A(x_1, \ldots x_n)$ where $x_i \in X, \quad i = 1, \ldots, n$. For binary relations, the composition of two fuzzy relations A and B denoted by $B \circ A$ and it is defined as a fuzzy relation in X whose membership function is related to those of A and B by

$$f_{B \circ A}(x, y) = \text{Sup}_v \text{Min}[f_A(x, v), f_B(v, y)]$$

Definition 1.11. [13] Let C be a code. The function $J : C \to [0, 1]$ is said to be a fuzzy code if it satisfies the following conditions:

1. $J(x \oplus y) \geq \min\{J(x), J(y)\}$
2. $J(-x) = J(x)$
3. $J(x \otimes y) \leq \max\{J(x), J(y)\}$, for all $x, y \in C$

2 Some Basic Definitions [15]

In this section, initially, the notions of fuzzy Hamming weight ($\mathcal{FHW}$), fuzzy Hamming distance ($\mathcal{FHD}$), and maximum likelihood decoding of fuzzy codewords ($J(\mathcal{D}_{\mathcal{MLD}})$) are given as in [15]. These notions are differentiated from the originally proposed definitions by expressing them in terms of their relative weight.

Definition 2.1 Let $\mathfrak{C}$ be a code and $\{C_1, C_2, \ldots, C_n\}$ be the collection of codewords in $\mathfrak{C}$. Let $J(\mathfrak{C}) = \{J(C_1), J(C_2), \ldots, J(C_n)\}$ be the respective collection of fuzzy codewords associated with $\mathfrak{C}$. The fuzzy Hamming weight (briefly $\mathcal{FHW}(C_l)$) of any codeword $C_l, \quad 1 \leq l \leq n$ in $\mathfrak{C}$ is a function from $\mathfrak{C} \to I = [0, 1]$, and it is defined as the number of non-zero entries in the codeword C_l of $\mathfrak{C}$ expressed along with its relative weight.

Definition 2.2 Let $\mathfrak{C}$ be a code and $\{C_1, C_2, \ldots, C_n\}$ be the collection of codewords in $\mathfrak{C}$. Let $J(\mathfrak{C}) = \{J(C_1), J(C_2), \ldots, J(C_n)\}$ be the respective collection of fuzzy

codewords associated with $\mathfrak{C}$. The fuzzy Hamming distance (briefly $\mathcal{FHD}(C_i, C_j)$) between two codewords C_i and C_j, $(i \neq j,\ 1 \leq i, j \leq n)$ in $\mathfrak{C}$ is a function from $\mathfrak{C} \to I = [0, 1]$, and it is defined as the number of places of the vectors by which the two codewords differ expressed along with its relative weight.

Definition 2.3 The lower bound of a fuzzy code $J(\mathfrak{C})$ (denoted by $\mathcal{LB}\, J(\mathfrak{C})$) is the function (or operator) $\mathcal{FHD}$: $\mathfrak{C} \to I = [0, 1]$, and it is defined as the least fuzzy Hamming distance between any two fuzzy codewords in $J(\mathfrak{C})$.

2.1 Maximum Likelihood Decoding of Fuzzy Codewords [15]

Whenever there is a disturbance in the medium on which a message is sent, it is possible to have an **error**. Due to this error, the original codeword, that is sent, gets changed and a new codeword reaches the receiver. This new codeword is called the **transmitted codeword**. The principle of maximum likelihood decoding in fuzzy codes compares the fuzzy Hamming distance of the transmitted fuzzy codeword with the original fuzzy codewords. Among this, the original fuzzy codeword that gives the minimum fuzzy Hamming distance with the transmitted fuzzy codeword is identified to be the error rectified fuzzy codeword. Thus, we have the following Definition 2.4.

Definition 2.4 Let $\mathfrak{C}$ be a code and $\{C_1, C_2, \ldots, C_n\}$ be the collection of codewords in $\mathfrak{C}$. Let $J(\mathfrak{C}) = \{J(C_1), J(C_2), \ldots, J(C_n)\}$ be the respective collection of fuzzy codewords associated with $\mathfrak{C}$. Let the transmitted codeword be C_j, such that $\mathrm{C}_j \notin \mathfrak{C}$. Then, the maximum likelihood decoder (briefly $\big(J(\mathcal{D}_{\mathcal{MLD}})\big(C_i, C_j\big)\big)\big)$ between every pair $\big(C_i, C_j\big)$ $(1 \leq i \leq n)$ of fuzzy codewords is a function from $\mathfrak{C} \to I = [0, 1]$, and it is defined as

$$\big(J(\mathcal{D}_{\mathcal{MLD}})\big(C_i, C_j\big)\big) = \bigwedge_{i=1}^{n} \big[\mathcal{FHD}\big(C_i, C_j\big)\big]$$

for all $C_i \in \mathfrak{C}$ $(i = 1, 2, \ldots, n)$ and $C_j \notin \mathfrak{C}$, such that $C_i \neq C_j$.

Definition 2.5 Let the fuzzy codewords be transmitted to the receiver and during the transmission owing to the disturbances, some relative weights of the fuzzy codewords are erased and a blank space is received by the receiver instead of the relative weights. These blank spaces are called the fuzzy erasures.

Based on the maximum likelihood decoding of fuzzy codewords and fuzzy erasures, we now propose the following equivalent conditions:

Proposition 2.6 Let $\mathfrak{C}$ be a code and $\{C_1, C_2, \ldots, C_n\}$ be the collection of codewords in $\mathfrak{C}$. Let $J(\mathfrak{C}) = \{J(C_1), J(C_2), \ldots, J(C_n)\}$ be the respective collection of fuzzy codewords associated with $\mathfrak{C}$. Then, the following statements are equivalent:

1. For the fuzzy code $J(\mathfrak{C})$, $\mathcal{LB}\ J(\mathfrak{C})) \geq 2/n$, where "$n$" is the maximum relative weight of the collection of fuzzy codewords in $J(\mathfrak{C})$.
2. If $\mathcal{LB}\ J(\mathfrak{C})) = x/n$, such that "$x$" is odd, then $J(\mathfrak{C})$ can correct $(x-1)/2n$ errors.
3. If "e" denotes the errors in transmission, then the fuzzy code $J(\mathfrak{C})$ can detect e/n errors only if $x/n \geq (e+1)/n$, where x/n is the lower bound of $J(\mathfrak{C})$.
4. The fuzzy code $J(\mathfrak{C})$ can correct $(x-1)/n$ fuzzy erasures, where x/n is the lower bound of $J(\mathfrak{C})$.

Proof The proof for the proposition is given in [15]

3 An Algorithm for Finding the Transmitted Codeword to be Retrieved by the Receiver

In this section, the algorithm for retrieving the original transmitted codeword sent by the sender is given followed by an example.

Consider a collection of codewords in a code $\mathfrak{C}$. From this collection, one codeword is sent as a message to another person. But due to some disturbances, the original message is trampled and the receiver gets another message, which he is unable to comprehend. Thus, the error in transmission is identified and it is aimed to find out which message was actually sent by the sender.

3.1 Procedure for Message Retrieval

Let $\mathfrak{C} = \{C_1, C_2, \ldots, C_n\}$ be the collection of codewords. Let $C_b \in \mathfrak{C}$ $(1 \leq b \leq n)$ be the transmitted codeword and let $\mathcal{C}$ be the received codeword such that $\mathrm{C} \notin \mathfrak{C}$. We now find the originally sent codeword as follows:

Step 1: Separate the collection of codewords in $\mathfrak{C}$ as $\mathfrak{C}_1, \mathfrak{C}_2, \mathfrak{C}_3, \ldots,$ such that $\mathfrak{C}_1 = \{C_{11}, C_{12}, \ldots, C_{1n}\}$, where each codeword $C_{1i}(1 \leq i \leq n)$ has the same number of non-zero entries (weight) and so on.

Step 2: Compute the value of each $\mathcal{FHD}\ \big(C_{ij}, C\big),\ \ (1 \leq i, j \leq n)$. Since the codewords are grouped based on their weights, any two codewords in $\mathfrak{C}_i\ \ (i = 1, 2, \ldots, n)$ will have the same fuzzy Hamming distance. Thus, it is not necessary to find the value of $\mathcal{FHD}\ \big(C_{ij}, C\big),\ \ (1 \leq i, j \leq n)$ for all C_{ij} in $\mathfrak{C}_i$.

Step 3: Since by Definition 2.4, we choose the codeword that gives the least fuzzy Hamming distance with the transmitted codeword, we now select the collection with the minimum value of $\mathcal{FHD}\ \big(C_{ij}, C\big)$ which gives us the $(J(\mathcal{D}_{\mathcal{MLD}}))\big(C_{ij}, C\big),\ \ (1 \leq i, j \leq n)$ and this is the collection containing the originally transmitted codeword.

Step 4: Compute the direct sum of each member of the selected collection of codewords with the remaining members of the collection. For example, if $\mathfrak{C}_i = \{C_{i1}, C_{i2}, C_{i3}, C_{i4}\}$ is the selected collection, the direct sum is computed as

$\oplus$	C_{i1}	C_{i2}	C_{i3}	C_{i4}
C_{i1}	$C_{i1} \oplus C_{i1}$	$C_{i1} \oplus C_{i2}$	$C_{i1} \oplus C_{i3}$	$C_{i1} \oplus C_{i4}$
C_{i2}	$C_{i2} \oplus C_{i1}$	$C_{i2} \oplus C_{i2}$	$C_{i2} \oplus C_{i3}$	$C_{i2} \oplus C_{i4}$
C_{i3}	$C_{i3} \oplus C_{i1}$	$C_{i3} \oplus C_{i2}$	$C_{i3} \oplus C_{i3}$	$C_{i3} \oplus C_{i4}$
C_{i4}	$C_{i4} \oplus C_{i1}$	$C_{i4} \oplus C_{i2}$	$C_{i4} \oplus C_{i3}$	$C_{i4} \oplus C_{i4}$

Step 5: The corresponding relative weight of each of the above entry after computing the direct sum is found and they are tabulated.
Step 6: In a similar way, the direct product of each member of the selected collection of codewords with the remaining members of the collection is found out as shown below:

$\otimes$	C_{i1}	C_{i2}	C_{i3}	C_{i4}
C_{i1}	$C_{i1} \otimes C_{i1}$	$C_{i1} \otimes C_{i2}$	$C_{i1} \otimes C_{i3}$	$C_{i1} \otimes C_{i4}$
C_{i2}	$C_{i2} \otimes C_{i1}$	$C_{i2} \otimes C_{i2}$	$C_{i2} \otimes C_{i3}$	$C_{i2} \otimes C_{i4}$
C_{i3}	$C_{i3} \otimes C_{i1}$	$C_{i3} \otimes C_{i2}$	$C_{i3} \otimes C_{i3}$	$C_{i3} \otimes C_{i4}$
C_{i4}	$C_{i4} \otimes C_{i1}$	$C_{i4} \otimes C_{i2}$	$C_{i4} \otimes C_{i3}$	$C_{i4} \otimes C_{i4}$

Since, the definition of a fuzzy code revolves around the computation of direct sum and direct product between the codewords, this computation ensues the fuzzification between them.

Step 7: Again the corresponding relative weight of each of the above entry after computing, the direct product is found and they are tabulated.
Step 8: The composition of the relative weights between the relative weights of the direct sum and direct products in steps 5–7 is computed using the formula for composition of two fuzzy relations A and B denoted by $B \circ \mathrm{A}$ and given by

$$f_{B \circ A}(x, y) = \mathrm{Sup}_v \mathrm{Min}[f_A(x, v), f_B(v, y)]$$

Step 9: From the resulting matrix, find the sum of the relative weights along each row and column. The sum of relative weights along each row is the row sum and the sum of relative weights along each column is the column sum.
Step 10: Each row sum is added to its corresponding column sum and their final value is tabulated. Let this be the score for each codeword.
Step 11: The codeword that obtains the maximum score is the required codeword.

Numerical Example

Suppose that, a manufacturing firm produces heavy load machines and dispatches them to all parts of the country. During a particular dispatch to an industry, the machines get faulty due to a fatal accident. Some machines had become gravely deficient in their performing efficiency, while some are moderately deficient and few are slightly deficient. It is not possible for the firm to take back all the machines as it will cause them a major loss. So the industry agrees to take few machines and return the others.

Due to the accident, there are certain changes in the characteristics of these machines and hence, they are now graded based on certain parameters such as productivity, quality control, accuracy in end products, productivity duration, and they obtain a score "1" for each parameter if the output is satisfactory and a score "0" if the output is not satisfactory and they are then formed as separate codewords.

Let $\mathfrak{C} = \{1100, 1000, 0100, 0110, 1101, 0011, 1110, 0111, 0001, 0101, 0010, 1011\}$ be the respective scores obtained by the machines after initial verification. A good machine has all the above mentioned parameters in the satisfactory level; hence, the score of an efficient machine will always be 1111 and none of the machines in $\mathfrak{C}$ has this score so we proceed to the next steps.

Step 1: Separating the collection based on their weights, we have $\mathfrak{C}_1 = \{1000, 0100, 0001, 0010\}$, $\mathfrak{C}_2 = \{1100, 0110, 0011, 0101\}$, and $\mathfrak{C}_3 = \{1110, 1011, 1101, 0111\}$.

Step 2: Based on the program given in Sect. 2, we now compute $\mathcal{FHD}$ between the codewords. For example, in the collection $\mathfrak{C}_1$, $(J(\mathcal{D}_{\mathcal{MLD}}))(1000, 1111)$ is computed as follows: Here, the length of the codewords is 4. Hence, the maximum relative weight is 10. Now, the number of vectors by which 1000 and 1111 is 3 and hence by Definition 2.2, $\mathcal{FHD}(1000, 1111) = 3/10$.

Computing in the same way we have, for the collection $\mathfrak{C}_1$, $\mathcal{FHD}(1000, 1111) = 3/10$, $\mathcal{FHD}(0100, 1111) = 3/10$, $\mathcal{FHD}(0001, 1111) = 3/10$, and $\mathcal{FHD}(0010, 1111) = 3/10$. In a similar way, $\mathcal{FHD}(1100, 1111) = \mathcal{FHD}(0110, 1111) = \mathcal{FHD}(0011, 1111) = \mathcal{FHD}(0101, 1111) = 2/10$ and $\mathcal{FHD}(1110, 1111) = \mathcal{FHD}(1011, 1111) = \mathcal{FHD}(1101, 1111) = \mathcal{FHD}(0111, 1111) = 1/10$.

Step 3: Based on the values obtained in Step 2, the fuzzy Hamming distance between the respective codewords of $\mathfrak{C}_1$, $\mathfrak{C}_2$, $\mathfrak{C}_3$ and the transmitted codeword is 3/10, 2/10, 1/10, respectively.

Thus, $(J(\mathcal{D}_{\mathcal{MLD}})) = \wedge[1/10, 2/10, 3/10]$; hence, $\mathfrak{C}_1$, $(J(\mathcal{D}_{\mathcal{MLD}})) = 1/10$.

Thus, the industry takes all the machines from the collection $\mathfrak{C}_3$. Among these machines in $\mathfrak{C}_3$, the industry has to now select one particular machine which will produce more products than the rest of the machines. Since the fuzzy Hamming distance between the codewords in $\mathfrak{C}_3$ and 1111 is the same, we proceed with the following steps to find the best machine.

Step 4: The direct sum between each member of $\mathfrak{C}_3$ is now computed. Thus, we have

$\oplus$	1110	1011	1101	0111
1110	0000	0101	0011	1001
1011	0101	0000	0110	1100
1101	0011	0110	0000	1010
0111	1001	1100	1010	0000

Step 5: The relative weights of the resulting codewords are as follows:

$\oplus$	1110	1011	1101	0111
1110	0	6/10	7/10	5/10
1011	6/10	0	5/10	3/10
1101	7/10	5/10	0	4/10
0111	5/10	3/10	4/10	0

Step 6: The direct product between each member of $\mathfrak{C}_3$ is computed as shown below:

$\otimes$	1110	1011	1101	0111
1110	1110	1010	1100	0110
1011	1010	1011	1001	0011
1101	1100	1001	1101	0101
0111	0110	0011	0101	0111

Step 7: The relative weights of the codewords obtained in Step 6 are now tabulated.

$\otimes$	1110	1011	1101	0111
1110	6/10	4/10	3/10	5/10
1011	4/10	8/10	5/10	7/10
1101	3/10	5/10	7/10	6/10
0111	5/10	7/10	6/10	9/10

Step 8: The composition of the relative weights obtained in Steps 5 and 7 is now found out.

$$\begin{pmatrix} 0 & 6/10 & 7/10 & 5/10 \\ 6/10 & 0 & 5/10 & 3/10 \\ 7/10 & 5/10 & 0 & 4/10 \\ 5/10 & 3/10 & 4/10 & 0 \end{pmatrix} \circ \begin{pmatrix} 6/10 & 4/10 & 3/10 & 5/10 \\ 4/10 & 8/10 & 5/10 & 7/10 \\ 3/10 & 5/10 & 7/10 & 6/10 \\ 5/10 & 7/10 & 6/10 & 9/10 \end{pmatrix}$$

The entry at the first row and first column of the resulting matrix (say c $_{11}$) after performing the composition is computed as shown below:

$$\begin{aligned} c_{11} &= \vee[\wedge(0, 6/10), \wedge(6/10, 4/10), \wedge(7/10, 3/10), \wedge(5/10, 5/10)] \\ &= \vee[0, 4/10, 3/10, 5/10] \\ &= 5/10 \end{aligned}$$

Similarly,

$$\begin{aligned} c_{12} &= \vee[\wedge(0, 4/10), \wedge(6/10, 8/10), \wedge(7/10, 5/10), \wedge(5/10, 7/10)] \\ &= \vee[0, 6/10, 5/10, 5/10] \\ &= 6/10 \end{aligned}$$

In the same way, the remaining values are computed and thus, we have

$$\begin{pmatrix} 0 & 6/10 & 7/10 & 5/10 \\ 6/10 & 0 & 5/10 & 3/10 \\ 7/10 & 5/10 & 0 & 4/10 \\ 5/10 & 3/10 & 4/10 & 0 \end{pmatrix} \circ \begin{pmatrix} 6/10 & 4/10 & 3/10 & 5/10 \\ 4/10 & 8/10 & 5/10 & 7/10 \\ 3/10 & 5/10 & 7/10 & 6/10 \\ 5/10 & 7/10 & 6/10 & 9/10 \end{pmatrix}$$

$$= \begin{pmatrix} 5/10 & 6/10 & 7/10 & 6/10 \\ 6/10 & 5/10 & 5/10 & 5/10 \\ 6/10 & 5/10 & 5/10 & 5/10 \\ 5/10 & 4/10 & 4/10 & 5/10 \end{pmatrix}$$

$$= \begin{pmatrix} 0.5 & 0.6 & 0.7 & 0.6 \\ 0.6 & 0.5 & 0.5 & 0.5 \\ 0.6 & 0.5 & 0.5 & 0.5 \\ 0.5 & 0.4 & 0.4 & 0.5 \end{pmatrix}$$

Step 9: Thus, the row sum (RS) and column sum (CS) of these relative weights and the addition of each row sum to its column sum are now computed as shown below. The row sum (RS) of the first row is given by $0.5 + 0.6 + 0.7 + 0.6 = 2.4$

The column sum (CS) of the first column is given by $0.5 + 0.6 + 0.6 + 0.5 = 2.2$

Step 10: The row sum (RS) is now added to its column sum (CS) and thus, we get RS + CS = 2.4 + 2.2 = 4.6.

In the same way, the remaining values are computed and tabulated below:

Row sum (RS)	Column sum (CS)	RS + CS
2.4	2.2	4.6
2.1	2	4.1

(continued)

(continued)

Row sum (RS)	Column sum (CS)	RS + CS
2.1	2.1	4.2
1.8	2.1	3.9

Step 11: Thus, the highest value of RS + CS corresponds to 4.6 and the codeword that lies in the first row and first column is 1110; thus, the industry chooses the machine which has the codeword representation 1110.

4 Conclusion

It is always necessary that whenever people are presented with varied options to choose, they end up choosing the best one. Thus, this paper elucidates the method of retrieving the correct parameter with the aid of relative weights of codewords and fuzzy logic, whose implementation gives the most accurate degree of association of each parameter taken into consideration. The future work includes the merging of the notions of maximum likelihood decoding and unique decipherability of fuzzy codewords in the diction of foreign languages. This would help in detecting the errors or mismatched messages in a foreign language more faster, thereby helping in identifying the errors more clearly.

References

1. Shannon, C.E.: A mathematical theory of communication. Bell Syst. Tech. J. **27**(379–423), 623–656 (1948)
2. Bose, R.: Information Theory, Coding Theory and Cryptography. McGraw Hill Education (India) Pvt. Ltd. (2008)
3. Hamming, R.W.: Error detecting and error correcting codes. Bell Syst. Tech. J. **29**, 147–160 (1950)
4. Adams, S.S.: Introduction to Algebraic Coding Theory (2008)
5. Guruswami, V., Rudra, A., Sudan, M.: Essential Coding Theory (2019)
6. Trappe, W., Washington, L.C.: Introduction to Cryptography with Coding Theory, 2nd edn. Pearson Education, Inc. (2006)
7. Lindell, Y.: Introduction to algebraic coding theory (2010)
8. David Forney, Jr G.: Convolutional codes II. Maximum-likelihood decoding. Inf. Control **25**, 222–266 (1974)
9. Caiafa, C.F., Barraza, N.R., Proto, A.N.: Maximum likelihood decoding on a communication channel. XI Reunion de Trabajo en Procesamiento de la Informacion y Control (2007)
10. Goodman, R.M.F.: Towards the maximum-likelihood decoding of long convolutional codes. In: Algebraic Coding Theory and Applications. International Centre for Mechanical Sciences (Courses and Lectures). Springer, Berlin, Heidelberg (1979)
11. Guruswami, V., Vardy, A.: Maximum-Likelihood Decoding of Reed-Solomon Codes is NP-hard (2004)

12. Zadeh, L.A.: Fuzzy sets. Inf. Control **8**, 338–353 (1965)
13. Ozkan, A., Mehmet Ozkan, E.: A different approach to coding theory. Pak. J. Appl. Sci. **2**(11), 1032–1033 (2002)
14. Hoffstein, J., Pipher, J., Silverman, J.H.: An Introduction to Mathematical Cryptography. Springer (2008)
15. Neeraja, A., Amudhambigai, B.: A novel way of detecting and correcting transmitted errors using fuzzy logic. J. Phys.: Conf. Ser. (2021)

Author Index

A
Amsaveni, D., 1
Amudhambigai, B., 255
Ayyappan, G., 189

B
Balaji, P., 127

D
Deepana, R., 163

E
Edwin Antony Raj, M., 67, 111

G
Geetha Sivaraman, 67, 111
Gowthami, R., 189

H
Hong, Tzung-Pei, 81

J
Jayanthi, G., 237
Jethruth Emelda Mary, L., 91

K
Kalyani Desikan, 209
Kavitha, M., 81
Kiruthika, C., 163
Kiruthikaswari, R., 91

L
Latha Parthiban, 237
Loganathan, D., 137

M
Madhumidha, R., 181
Mohamed Salih Mukthar, M., 33
Muthuperumal, S., 43

N
Nandhini, R., 1
Narasimhan, D., 181, 209
Natarajan, C., 99
Neeraja, A., 255

P
Padmaja, K., 221

R
Rajadurai, P., 99, 181
Rajasekar, R., 43
Ramathilagam, S., 33
Ramesh, A., 127
Rushi Kumar, B., 221

S
Santosh Kumar Satapathy, 137

© The Editor(s) (if applicable) and The Author(s), under exclusive license to Springer Nature Singapore Pte Ltd. 2022

S. R. Kannan et al. (eds.), *Fuzzy Mathematical Analysis and Advances in Computational Mathematics*, Studies in Fuzziness and Soft Computing 419,
https://doi.org/10.1007/978-981-19-0471-4

Saravanan, R., 55

Senthil Arumugam, A., 81

Shanmugavelan, S., 99

Sundararaman, M., 181

V

Valliathal, M., 55
Venkatachalapathy, M., 43
Venkatesh, S., 99
Vignesh, R., 209
Vijayabalaji, S., 127
Vishnukumar, P., 67, 111